Twenty First Edition

Photovoltaics International

THE TECHNOLOGY RESOURCE FOR PV PROFESSIONALS

ISFH Emitter technology options for industrial PERC solar cells with up to 20.3% conversion efficiency

Fraunhofer ISE Electrically conductive adhesives: An emerging interconnection technology for high-efficiency solar modules

ISC Konstanz The status and future of industrial n-type silicon solar cells

Hanwha Q Cells PV product quality makes all the difference

Wright Williams & Kelly CIGS manufacturing: Promises and reality

Third Quarter, September 2013

www.pv-tech.org

Photovoltaics International Twenty First Edition 2013

Photovoltaics International

Published by:
Solar Media Ltd.,
Trans-World House, 100 City Road, London
EC1Y 2BP, UK
Tel: +44 (0) 207 871 0122
Fax: +44 (0) 207 871 0101
E-mail: info@pv-tech.org
Web: www.pv-tech.org

Publisher: David Owen

Head of Content: Ben Willis
Deputy Head of Content: John Parnell
Commissioning Editor: Adam Morrison
Sub-Editor: Steve D. Brierley
Senior News Editor: Mark Osborne
Senior Editor: Nilima Choudhury
Reporters: Andy Colthorpe, Lucy Woods
Editorial Consultant: Graham Anderson
Design: Tina Davidian
Production: Daniel H Brown, Viki Hämmerle

Sales Director: David Evans
Account Managers: Adam Morrison,
Graham Davie

The cover image is a SEM image of a cross section of a 20.3%-efficient PERC solar cell.

Image courtesy Institute for Solar Energy Research Hamelin (ISFH), Emmerthal, Germany.

Printed by Buxton Press
Photovoltaics International
Twenty First Edition
Third Quarter 2013
Photovoltaics International is a quarterly journal published in February, May, August and November.

Distributed in the USA by Mail Right International, 1637 Stelton Road B4, Piscataway, NJ 08854.

ISSN: 1757-1197

USPS Information
USPS Periodical Code: 025 313

Periodicals Postage Paid at
New Brunswick, NJ
Postmaster: Send changes to:
Photovoltaics International,
Solar Media Ltd., C/o 1637 Stelton
Road, B-4, Piscataway, NJ 08854, USA

Foreword

There have been encouraging signs in recent months of changing fortunes for PV equipment suppliers after a difficult period of consolidation. Shipment figures, actual and forecast, have in many instances seen an upswing, as booming markets in Japan, China and the US continue to drive demand, even as some European markets continue to dwindle.

It's probably too early to call the beginnings of a new PV technology buy cycle, but it seems more a case of 'when' rather than 'if' now, and analysts have pointed to mid-2014 as the likely point when supply and demand will be in some kind of equilibrium. Clearly the implication of this is that if demand continues to rise beyond this point, supply will have to keep up, so manufacturers will have to invest in new capacity.

This means that now is a crucial period for upstream decision makers to select the tools, materials and processes that will be used in their factories when the next buy cycle begins. At Photovoltaics International we strive to provide the most up to date, independent and authoritative information to top engineers and PV manufacturers to help them make more informed purchasing decisions. This and future editions of the journal will provide invaluable guidance on emerging technologies and trends.

In this issue, the Institute for Solar Energy Research investigates which of the currently available concepts for next-generation passivated emitter and rear cells (PERC) technology show the most promise (p.44).

Meanwhile, Fraunhofer Institute for Solar Energy Systems researchers outline the deployment of electrically conductive adhesives as interconnectors in high-efficiency cells (p.27). Their paper describes the basic principles of this emerging technology and offers insights into the performance of different materials available on the market.

And a team from Hanwha Q Cells look at the key question of quality in PV equipment and how much effort manufacturers are actually going to in living up to the promises they make about their products (p.91). They conclude that true quality can only be achieved if it is sought in every process along the value chain.

From our discussions with industry colleagues, it is evident that some of the gloom of recent years is beginning to lift. But no one is under an illusion that there are hard yards still to be made. We will be at EU PVSEC in Paris at the beginning of October, and our editorial team looks forward to meeting you there to hear your stories as you make that journey.

Ben Willis
Head of Content
Solar Media Ltd

Photovoltaics International

Photovoltaics International's primary focus is on assessing existing and new technologies for "real-world" supply chain solutions. The aim is to help engineers, managers and investors to understand the potential of equipment, materials, processes and services that can help the PV industry achieve grid parity. The Photovoltaics International advisory board has been selected to help guide the editorial direction of the technical journal so that it remains relevant to manufacturers and utility-grade installers of photovoltaic technology. The advisory board is made up of leading personnel currently working first-hand in the PV industry.

Editorial Advisory Board

Our editorial advisory board is made up of senior engineers from PV manufacturers worldwide. Meet some of our board members below:

Gary Yu, Senior Vice President, Operations

Mr. Yu served as Trina Solar's Vice President of Manufacturing since May 2007 and in July 2010 was promoted to the position of Senior Vice President of Operations. Mr. Yu has 17 years' manufacturing management experience in semiconductor-related industries. Before joining Trina Solar, he was Managing Director of Wuxi Lite-On Technology, an LED assembly company based in China. Prior to Wuxi Lite-On Technology, he served as a Director of Manufacturing for 1st Silicon Sdn. Bhd. in Malaysia, prior to which he worked at Macronix International, a semiconductor integrated device manufacturer in Taiwan. Mr. Yu has a master's degree in Industrial Engineering and Management from National Chiao Tung University in Taiwan and a bachelor's degree in Chemical Engineering from Tunghai University.

Takashi Tomita, Senior Executive Fellow, Sharp Solar

Takashi Tomita has been working at Sharp for 34 years and is widely recognised as a fore-father of the solar industry in Japan. He was responsible for setting up Sharp's solar cell manufacturing facilities in Nara and silicon production in Toyama. Takashi's passion for solar power has led him to hold numerous posts outside of his roles at Sharp, including: Vice Representative at the Japan Photovoltaic Industry Association; Committee Member of Renewable Energy Portfolio Standard of METI; Adviser Board Member of Advanced Technology of Nara; Visiting Professor of Tohoku University; Adviser of ASUKA DBJ Partners (JAPAN) and Adviser of Global Catalyst Partners (US).

Dr. Peng Heng Chang, CEO, Motech Industries, Inc.

Dr. P.H. Chang was elected CEO of Motech in March 2010. Dr. Chang has over 30 years of experience in management at multinational technology companies and in-depth knowledge in Materials Engineering. Prior to joining Motech, Dr. Chang was VP of Materials Management and Risk Management, VP of Human Resources and Senior Director of Materials Management at Taiwan Semiconductor Manufacturing Co. (TSMC); VP of Administration at Worldwide Semiconductor Manufacturing Co. and Professor of Materials Science and Engineering at National Chiao Tung University in Hsinchu, Taiwan. Dr. Chang also worked for Inland Steel Co. and Texas Instruments in the US prior to 1990. He received his Ph.D. degree in materials engineering from Purdue University in 1981.

Professor Eicke R. Weber, Director of the Fraunhofer Institute for Solar Energy Systems ISE in Freiburg

Professor Eicke R. Weber is the Director of the Fraunhofer Institute for Solar Energy Systems ISE in Freiburg. Weber has earned an international reputation as a materials researcher for defects in silicon and III-V semiconductors such as gallium arsenide and gallium nitride. He spent 23 years in the U.S. in research roles, most recently as Professor at the University of California in Berkeley. Weber is also the Chair of Applied Physics, Solar Energy, at the University of Freiburg, and during his career has been the recipient of several prestigious awards including the Alexander von Humboldt Prize in 1994, and the German Cross of Merit on ribbon in June 2006.

Dr. Zhengrong Shi, Executive Chairman and Chief Strategy Officer, Suntech

Dr. Zhengrong Shi is founder, CEO and Chairman of the board of directors of Suntech. Prior to founding Suntech in 2001, he was a Research Director and Executive Director of Pacific Solar Pty., Ltd., the next-generation thin-film technology company, before which he was a Senior Research Scientist and leader of the Thin Film Solar Cells Research Group in the Centre of Excellence for Photovoltaic Engineering at the University of New South Wales in Australia. Dr. Shi holds 11 patents in PV technologies and is a much-published author in the industry. His work has earned him such accolades as "Hero of the Environment" (TIME magazine 2007) and "Corporate Citizen of the Year" at the China Business Leaders Awards 2007. A member of the NYSE advisory board, Dr. Shi has a Bachelor's degree in optical science, a Master's degree in laser physics and a Ph.D. in electrical engineering.

Dr. Sam Hong, President and COO of Neo Solar Power

Dr. Hong has more than 30 years of experience working in the solar energy industry. He has served as the Research Division Director of Photovoltaic Solar Energy Division at Industry Technology Research Institute (ITRI), a research organization that serves to strengthen the technological competitiveness of Taiwan, and Vice President and Plant Director of Sinonar Amorphous Silicon Solar Cell Co., which is the first amorphous silicon manufacturer in Taiwan. In addition, Dr. Hong was responsible for Power Subsystem of ROCSAT 1 for the Taiwan National Space Program. Dr. Hong has published three books and 38 journal and international conference papers, and is a holder of seven patents. Dr. Hong was the recipient of Outstanding Achievement Award from the Ministry of Economic Affairs, Taiwan, and was recently elected as chairman of the Taiwan Photovoltaic Industry Association.

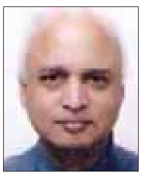

Dr. G. Rajeswaran, President and CTO of Moser Baer Photovoltaic Ltd

Raj served as President and CTO of Moser Baer Photovoltaic Ltd. from July 2007 until October 2008, since which time he has been Group CTO for all the Moser Baer business units and holder of the CEO function for launching new businesses. He spent 22 years with Eastman Kodak Company as the Vice President of Advanced Development & Strategic Initiatives, where he managed Kodak's Japan display operations including technology & business development in Japan, Taiwan, Korea and China. He has also served as Vice President and on the board of SK Display Corporation, and worked in technology development with Brookhaven National Laboratory. Raj has a Ph.D., an M.Tech. and a B.E. in electrical engineering. A much-published author, speaker and patent holder, Raj is a member of the Society for Information Display (SID) and has chaired several international conferences in the field of OLEDs.

inter**solar**
connecting solar business

The World's Leading Exhibition Series for the Solar Industry

3,000 exhibitors | 100,000 visitors | Most international solar event series with b2b focus | Meet the decision makers who are shaping the solar market | Stay informed about the latest technological innovations | Get connected at exclusive networking events | Meet renowned speakers at the world-class conferences | Benefit from the events in the world's key solar markets

SEPT 18–20 2013
www.intersolar.net.br

NOV 12–14 2013
www.intersolar.in

MAR 26–28 2014
www.intersolarchina.com

JUNE 04–06 2014
www.intersolar.de

JULY 08–10 2014
www.intersolar.us

INTERSOLAR SOUTH AMERICA | INTERSOLAR INDIA | INTERSOLAR CHINA | INTERSOLAR EUROPE | INTERSOLAR NORTH AMERICA

Contents

74

87

108

Fab & Facilities

Production scale is the key to China's PV manufacturing boom.

Scale bucks low labour costs

Production scale rather than low labour costs has driven China's boom in manufacturing PV modules, according to a joint report released today by the National Renewable Energy Laboratory and the Massachusetts Institute of Technology. Low labour costs and generous government subsidies have often been cited as the main reasons for China's dominance in PV manufacturing, views which formed the basis of the SolarWorld trade challenge that resulted in US trade levies on Chinese PV imports last year. The report's authors used a Minimum Sustainable Price (MSP) for monocrystalline silicon solar panels to predict factory location decisions. MSP estimates the long-term market-clearing price for the product assuming competitive equilibrium, or the minimum price of modules that will provide an adequate rate of return for a company and sustain growth without subsidies. Scale and supply-chain advantages were found to account for the majority of a Chinese factory's MSP advantage.

Full capacity facilities

Sharp near full capacity at UK solar module assembly plant

Sharp's European PV module manufacturing operations, based in Wrexham, UK are running at near full nameplate capacity of 400MW due to demand across Europe in the residential market, according to the company.

The announcement is in stark contrast to Sharp's decision only a year ago to consolidate its European sales and marketing operations from Germany to London, UK and local news reports that the Wrexham plant was laying off workers due to weak demand and being uncompetitive with Chinese competitors.

The announcement that its Wrexham plant is running at near full capacity is the first public statement the European operation of the company has announced in over 12 months.

Source: Sharp

Sharp's UK module plant is near full capacity.

Panasonic reaches full capacity at 300MW Malaysian module solar plant

Panasonic Corporation said it had started full-scale production of its 'HIT' PV modules at its new integrated facility in Malaysia.

The plant has an initial nameplate capacity of 300MW. The company noted that the majority of modules were being shipped to Japan to meet booming installations.

The plant located in Kulim Hi-Tech Park, in the state of Kedah started production in December 2012.

Technology upgrades

Improving technology not materials to drive down Chinese solar costs: GTM

Improving technology not the falling cost of materials will be the dominant factor in the ongoing fall in costs of Chinese module manufacturers, according to a report by GTM Research.

GTM claims that Chinese manufacturers will be able to produce modules at a cost of US$0.36 per Watt by 2017 and has provided more details on how they could get there.

They have already achieved a 54% decrease in manufacturing costs since 2010. GTM found that the majority of this came from the falling cost of materials caused by an oversupply with polysilicon responsible for 54% of the total reductions and other materials contributing a further 26%.

Source: SolarWorld

SolarWorld to close Hillsboro wafer operations for technology upgrades.

SolarWorld to close Hillsboro wafer operations for technology upgrades

Having gone through a major financial restructuring, SolarWorld is starting to tackle its issues on competitive manufacturing, with a round of technology upgrades and new product introductions.

At the core is upgrading its multicrystalline ingot/wafer production plants in Germany and the US, including lowering cost production, a key problem the company had in competing with Chinese producers that had both the scale and claimed lowest production, causing almost all wafer production in Europe to cease.

In its efforts to upgrade processes, SolarWorld said in its first-half year interim financial report that its wafer operations in Hillsboro, Oregon would close at the end of August, 2013 for upgrades to processes.

First Solar to manufacture new crystalline silicon line

First Solar will start a 100MW manufacturing line for crystalline silicon cells for the residential distributed market from the end of next year with production scaling from 2015.

In May this year, the leader in thin-film CdTe acquired the lower-cost, high efficiency crystalline silicon start-up founded in 2009 by Denis de Ceuster after 12 years at Sunpower.

By 2017, distributed residential and commercial generation is expected to account for more than half of the market, a lucrative, growing market that is more suited to higher efficiency crystalline technologies than thin film, which typically requires larger installation areas.

Celestica gains TÜV Rheinland PTL approval of PV lab in Toronto (image)

In an effort to be able to support the manufacture of better PV products and certification for outsourcing customers, third-party manufacturer, Celestica has opened a PV testing lab in Toronto, Canada.

Celestica's solar lab has been audited and approved by TÜV Rheinland PTL to provide tests for a variety of PV standards, including UL-1703 / ULC-1703 and IEC-61215 /IEC-61730.

The company said that the lab would be operated independently within the Total Quality Management System at Celestica to ensure the integrity of test procedures and results.

Joint ventures

First Solar buys GE's CdTe thin-film IP and forms business partnership

GE has decided to cancel plans to ramp its own cadmium telluride (CdTe) thin-film operations in Aurora, Colorado, instead selling the intellectual property portfolio to CdTe leader, First Solar.

First Solar has issued 1.75 million shares of common stock as part of the transaction, while GE will retain the shares for at least three years.

As part of the deal, GE Global Research will collaborate on future CdTe solar technology development with First Solar as well as teaming up on commercial levels that include purchasing and branding First Solar's modules for future global GE PV power plants. Collaboration will also include power plant equipment, such as PV central inverters, controls, balance of plant and ownership of utility-scale systems.

GE went back to basics a year ago by temporarily halting the roll out of module production and refocus on R&D to boost module efficiencies and lower production costs to better compete with the likes of First Solar and a number of CIGS start-ups. First Solar will be increasing its R&D expenditure by US$75 million to accommodate the collaboration with GE.

Canadian Solar to partner on 60MW module plant in Indonesia

To benefit from a new feed-in tariff (FiT) system to be introduced in Indonesia, Canadian Solar is planning to partner with local PV module manufacturer, PT Swadaya Prima Utama, on a proposed 60MW plant.

The companies signed a memorandum of understanding to evaluate the opportunity. Canadian Solar hopes if the joint venture is successful it will provide a strong position for participating in the new FiT and provide flexibility to meet global demand.

Source: Canadian Solar

Canadian Solar is partnering on a 60MW module plant in Indonesia.

Reports: Suntech Wuxi could be merged with rival

Reports suggest a deal is in the making that could see Suntech Power Holdings' bankrupt subsidiary rescued by the involvement of a rival Chinese PV manufacturer and several state-owned enterprises in Wuxi, China.


Source: Aleo Solar

Solar manufacturers to increase investment for first time in three years: IHS.

Suntech Wuxi is allegedly in talks with five enterprises over separate deals to provide a much needed cash injection, with the company having debts of around US$1.75 billion.

The Wuxi regional government is said to be actively participating and reportedly said that creditors, which included numerous Chinese banks would have to take a cut on loans or face higher losses.

An official was also quoted as ruling out a liquidation of the company. Based on a deal being struck with a possible Chinese rival, a cash injection would be part of deal, suggesting a merger is on the cards

Business news focus

SolarWorld to close wafer operations as part of major financial restructure

SolarWorld is starting to tackle its manufacturing competitive issues with a round of technology upgrades and new product introductions.

At the core is upgrading its multicrystalline ingot/wafer production plants in Germany and the US, including lower cost production, a key problem the company had in competing with Chinese producers that had both the scale and claimed lowest production costs that has seen almost all wafer production in Europe cease.

In its efforts to upgrade processes, SolarWorld said in its first-half year interim financial report that its wafer operations in Hillsboro, Oregon would close at the end of August, 2013 for upgrades to processes.

Only R&D activities in relation to monocrystalline wafers would continue. SolarWorld's production plants in the US and Germany made operating losses in the first-half of the year of €30 million and €43 million respectively.

Former LDK subsidiary put back on the market

The former LDK subsidiary LDK Hefei is to be sold by the local Chinese government affiliate that purchased it earlier this year.

The Hefei High-Tech Industrial Development Zone Social Service Company paid a reported RMB120 million (US$19.6 million) for LDK Hefei in April.

According to a statement posted on the website of the Hefei Bidding Centre, which will act as the middle man in the deal, LDK Hefei is on the market for RMB 330 million (US$53.9 million). The company's net assets as of 31 May 2013 were appraised at RMB326 million (US$53.2 million). LDK's Hefei solar cell manufacturing facility had a capacity of 2.2GW when it started production in 2011.

The company took an estimated loss of US$80 million when it sold the plant as part of the LDK Hefei sale to the local government affiliate.

Funding and investment

Solar manufacturers to increase investment for first time in three years: IHS

Solar manufacturers will increase their expenditure for the first time in three years as they look to meet demand from emerging economies, according to IHS. Capital expenditure, including investment in production and manufacturing operations, fell by 72% in 2012 and is expected to fall a further 36% this year.

A new report by IHS predicts that in 2014 it will rise by 30% to US$3 billion. In 2011 the industry spent US$12.9 billion but the overcapacity in the market has seen this figure nosedive to a low of US$2.3 billion in 2013.

The expected recovery is likely to be led by the rising demand for PV in emerging markets, which appear to have spurred on the financial recovery of some manufacturers, who can now look to reinvest that money.

Brazilian state announces incentive programme for renewable energy producers

A renewable energy incentive programme has been launched in the Brazilian state of Minas Gerais, by the state governor, Alberto Pinto Coelho.

The scheme, named 'Energia de Minas,' will include tax breaks for investors building modules, inverters and solar plants. This will be in conjunction with incentives for involvement in other forms of renewable energy.

Although financial details of the scheme have yet to be revealed, 'Energia de Minas' could also involve assistance from the local state-owned bank Banco de Desenvolvimento de Minas Gerais.

A local company, Companhia Energetica Integrada, is already building a 3MW solar park in the state and Tecnometal, Brazil's first solar panel maker, has apparently demonstrated an interest in investing in Minas Gerais.

In the balance: The social costs and benefits of PV

Carol Olson, Energy Research Centre of the Netherlands (ECN), Petten, The Netherlands

ABSTRACT

For more than a decade, the growth in PV markets surpassed expectations. Then, in 2012, the European market declined for the first time compared with the previous year. As policymakers' support for PV hesitates over the costs to society of this technology, it is timely to take an overview of the social costs and benefits, also referred to as the 'external costs', of PV electricity. In this article, these costs are put into perspective vis-à-vis those associated with conventional electricity-generating technologies. The external costs of electricity can be broken down into: 1) the environmental and health costs; 2) the costs of subsidies and energy security; and 3) the costs for grid expansion and reliability. Included in these costs are the increased insurance, health, social and environmental costs associated with damages to health, infrastructure and environment, as well as tax payments that subsidize producers of electricity or fuels, their markets and the electricity infrastructure. A life cycle assessment (LCA) of the environmental impact is used in the quantification of the associated environmental and health costs. Because the environmental footprint of PV electricity is highly dependent on the electricity mix used in PV module fabrication, the environmental indicators are calculated for PV electricity manufactured using different electricity mixes, and compared with those for the European electricity mix (UCTE), and electricity generated by burning 100% coal or 100% natural gas. In 2012$, coal electricity requires 19–29¢/kWh above the market price, compared with 1–1.6¢/kWh for PV manufactured with 100% coal electricity. The sum of the subsidies, avoided fossil-fuel imports and energy security, and the economic stimulation associated with PV electricity deployment, amounts to net external benefits. Integrating high penetrations of renewables, with the same reliability as we have today, appears to be fully feasible and within the cost horizons of the current activities of system operators.

Background

PV modules convert sunlight into electricity and operate for decades without emitting any greenhouse gases at all. But energy, with its associated carbon footprint, is intrinsic to the materials used to produce a PV module. In addition, energy (usually including a significant amount of conventional electricity) is directly used in PV module manufacturing and installation, as well as in its de-installation and recycling at the end of its life. This energy, which is invested in a PV module over its lifetime, is usually 'paid back' by the energy generated over about one year's operation of that module ('energy payback time'), or roughly 1/25th of the module's lifetime. A life cycle assessment (LCA) of a PV module considers the energy use, greenhouse gas emissions and other environmental impacts of the module from the manufacturing phase, through installation and operation, to the end-of-life and recycling stage.

One might fully accept the idea that a PV module does not emit greenhouse gases over its operation, but wonder whether it really makes sense for society to invest money and energy to switch from mostly conventional electricity production to a much greater amount from renewables. Given the current state of the world, it is urgent to address both the emission of greenhouse gases and the economy. It is therefore instructive to analyze what the costs and benefits are for society in opting for PV electricity, or electricity from renewable energy sources in general, as compared with conventional electricity-generating technologies. Costs which are not included in the market price of a saleable item are called 'external costs'. For electricity, external costs can be categorized into: 1) environmental and health costs; 2) costs associated with subsidies and energy security; and 3) costs for grid expansion and reliability. Included in these costs are the increased insurance, health, social and environmental costs associated with damage to health, infrastructure and the environment, as well as tax payments that subsidize producers of electricity or fuels, their markets and the electricity infrastructure.

In this article, an LCA of the environmental impact of PV electricity is presented and compared with that of conventional electricity. Because the environmental footprint of PV electricity is highly dependent on the electricity mix used in PV module fabrication [1], the environmental indicators are calculated for PV electricity manufactured using different electricity mixes, and compared with those for the European electricity mix (UCTE) and electricity generated by burning 100% coal or 100% natural gas. The environmental indicators are then used to quantify the associated environmental and health costs. The recent monetarization of these impacts is discussed, and compared with the findings of earlier studies.

Next, the global energy subsidies in 2011 and the energy subsidies in Germany over the past decades are reviewed. The amounts spent on subsidies to stimulate renewable energy deployment are compared with the savings on fossil fuel imports, and other economic effects of a stimulated industry sector. The security of a renewable energy supply is also explored.

Finally, the costs for grid expansion and grid reliability are considered. There are various motivations for grid expansion, some of which are not related to renewable energy generation. While a cost analysis of grid expansion is beyond the scope of this article, an examination of a current grid development plan suggests that a new estimate, with the interests of the future electricity mix and market in mind, may be required. Some recent studies are included to put into perspective the costs for achieving a very reliable electricity supply with a high penetration of renewable energy sources.

Wafer thickness	180µm
Cell size	156mm × 156mm
Module size	60 cells
Glass	single
Frame	yes
Roof mounting	Schletter
Inverter	2.5kW
Module efficiency	14.4%
Degradation	0.7%/yr
Performance ratio	0.8
Lifetime	30yrs
Irradiation	1700kWh/m^2/yr

Table 1. Key parameters associated with a PV system.

Methods

An LCA evaluates the environmental impact of a product or service over its lifetime. This analysis follows the guidelines set out in the international standard ISO 14040, which describes the principles and framework for LCA, as well as the methodology for LCA of PV electricity by the IEA [2]. The software used in this analysis is Simapro 7.3 with the ecoinvent 2.2 database, and the ReCiPe method for calculating a range of environmental indicators [3]. The carbon footprint is a measure of the emissions of greenhouse gases (in kg of CO_2 equivalents), effective over a period of 100 years, using the GWP100a method as defined by the Intergovernmental Panel on Climate Change (IPCC) in 2007 [4].

Data and key parameters

In order to calculate the environmental impact of 1kWh electricity over the lifetime of the generation source, data are required for each stage in the life cycle. Most of the data are supplied by the ecoinvent database, one of the world's leading international databases for life cycle studies. A kWh of electricity generated by coal or natural gas, or produced with the European electricity mix, can be readily calculated using the ecoinvent database. However, recent (2011) data on the energy and material use and processing of PV modules are not yet available in the ecoinvent database. This set of data has been compiled at ECN and was used to calculate the environmental profile of currently available PV modules. The key parameters of typical polysilicon PV modules manufactured in 2011 are given in Table 1.

A 12.4kWp PV system, mounted on-roof, with cabling and inverter, is taken as a typical PV system for a small to mid-size commercial enterprise. Electricity directly from the module is considered to be comparable to electricity from the power plant.

The environmental profile of electricity from three different PV modules is calculated: 1) one fabricated using electricity produced by 100% coal generation in European (UCTE) power plants; 2) another one manufactured using the average European (UCTE 2000) electricity mix (47% conventional thermal, 37% nuclear, 16% hydro); and 3) a third one made using hydropower in the production of the silicon feedstock, and natural gas electricity in the manufacturing of the cell and module. The manufacturing techniques, based on recent (2011) processes, of the three PV modules are in every other way identical. The environmental profile of natural gas electricity and the UCTE electricity mix is also calculated, and all the results are normalized to electricity generated with coal, in order to put them into perspective. The electricity from hard coal, natural gas and the UCTE mix is representative of average European plants in 2000 or 2001, as specified in the ecoinvent 2.2 database. In 2008 the UCTE mix consisted of 56% thermal (a mix of coal and gas technologies), 28% nuclear, 10% hydro and 7% other renewable energy sources.

Environmental impact

Greenhouse gases and air pollutants

Roughly 30% of the CO_2 emissions in Europe and the USA [5] are contributed by the power sector and are a major cause of global warming. These emissions lead to changes in the climate, including more frequent and more energetic weather events, rises in sea level, river flooding, heat waves and droughts, as well as changes in agriculture [6].

> "Roughly 30% of the CO_2 emissions in Europe and the USA are contributed by the power sector and are a major cause of global warming."

The air pollutant emissions by 1kWh electricity from multicrystalline silicon PV modules (19, 38 or 39g CO_2 eq) compared with electricity derived from burning gas (620g CO_2 eq), coal (1020g CO_2 eq), and the UCTE mix (506g CO_2 eq) are shown in Fig. 1. The emissions of greenhouse gases contributing to climate change (kg CO_2 eq) from PV modules manufactured with 100% coal electricity are double those from PV modules manufactured with hydro power and natural gas electricity, but are still 96% less than the emissions of electricity generated by coal. Coal electricity is also a leading cause of mercury emissions that may be inhaled or ingested by humans, causing neurological damage and contributing to the human toxicity indicator. Non-methane volatile organic compounds (NMVOCs) are organic compounds (e.g. benzene) that typically have compounding long-term health effects. Many are carcinogens. Particulate matter is suspended in air as an aerosol, and is associated with lung cancer and respiratory disease. Emissions of sulphur oxides lead to acid rain, which affects the biology of soil and vegetation and accelerates degradation of buildings and structures. The emissions calculated here are the average emissions of UCTE coal plants in 2000. Between 2000 and 2006, SO_2 emissions have decreased on average by ~40% in up-to-date coal plants, but 70% of coal plants in Europe are over 20 years old [7,8].

The results for the formation of photochemical oxidants and particulates and for terrestrial acidification follow the same pattern: the PV module made using hydro and natural gas electricity produces electricity with only ~2–3% of the impact per kWh of coal. The PV modules made with UCTE electricity (~50% fossil fuel) and with 100% coal electricity have twice the impact of the cleaner PV module (~6–7.5% of coal electricity). Electricity generated with natural gas provides 60% of the greenhouse gas emissions of coal, 36% of the volatile organic compounds (VOC), 15% of the particulates and 14% of the acidification. UCTE electricity presents the same level of human toxicity as coal electricity, but only 50% of the greenhouse gas emissions, 42% of the VOCs, 50% of the particulates and 47% of the acidification.

The UCTE electricity mix consists of almost a third nuclear generation, which is the reason for the high level of human toxicity in Fig. 1 and for the much greater amount of ionizing radiation in Fig. 2.

Water depletion and eutrophication

Water depletion and eutrophication (Fig. 3) are two critical issues for water management, now and in the future. Water depletion is a measure of the water withdrawn for use, and accounts for the water intake (which may damage ecosystems), the consumption (which reduces water availability) and the discharged water (which may present water quality issues). The eutrophication, or the accumulation of reactive nitrogen in the environment, is a leading cause of water quality impairment, and a serious threat to the health of marine systems. Both coal and, to a lesser extent, natural gas contribute to marine eutrophication. Water depletion for coal electricity is calculated to be 2682 litres/MWh, which is consistent with recent estimates for pulverized coal plants [9]. UCTE electricity uses 4300 litres/MWh, and natural gas, 2114 litres/MWh. The water demand of the thermal generation of electricity using coal or natural gas dwarfs the demand of PV electricity (575 litres/MWh for PV fabricated with coal or UCTE, and 474 litres/MWh for PV made with gas and hydro).

"Although PV plants require some water over the life cycle, they offer the advantage of requiring little or no water for operation."

During recent warm, dry summers (2003, 2006 and 2009), several thermoelectric (fossil fuel and nuclear) plants in Europe were forced to reduce production because of a lack of cooling water. Recent analysis shows that the electricity supply from thermoelectric plants is vulnerable to climate change [10]. Although PV plants require some water over the life cycle, they offer the advantage, in terms of energy security, of requiring little or no water for operation.

Transformation of land

The transformation of natural land, as well as the occupation of urban and agricultural land, is large for hard coal because of the mining and infrastructure. Electricity from natural gas requires about three times as much transformation of natural land as coal or UCTE electricity as a result of the requirements for gas pipelines (Fig. 4).

Compared with coal electricity (per kWh), PV uses 86–89% less water, occupies or transforms over 80% less land and presents ~95% lower toxicity to humans; it also contributes 92–97% less to terrestrial acidification, 97–98% less to marine eutrophication and 96–98% less to climate change.

Monetarization of health and environmental impacts

The external costs of electricity have been discussed in political

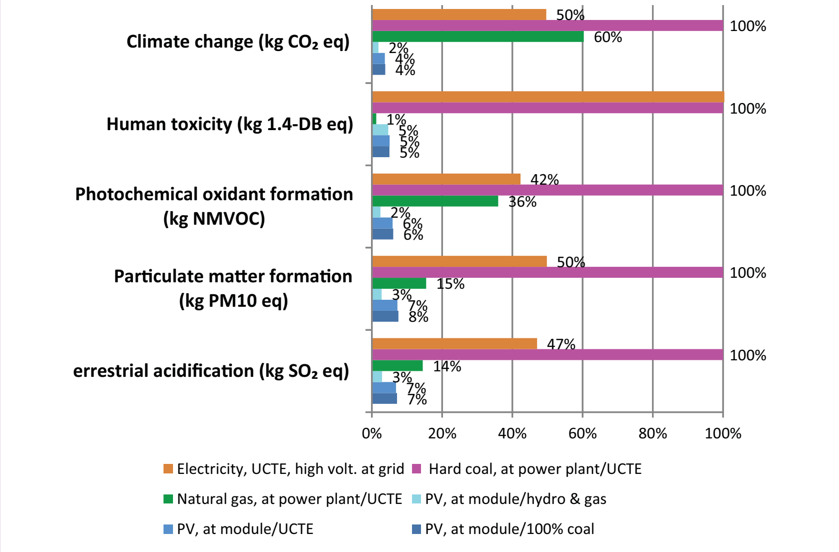

Figure 1. Comparison of air pollutant emissions of electricity produced by PV, natural gas, and the UCTE mix, at power plant, relevant to climate change (kg CO_2 eq), human toxicity (kg 1.4 dichlorobenzene (DB)), reactive organic pollutants (kg non-methane volatile organic compounds (NMVOCs)), and atmospheric particulate matter loading (kg of particulate matter smaller than ~10µm (PM10)), normalized to the impacts of hard coal electricity.

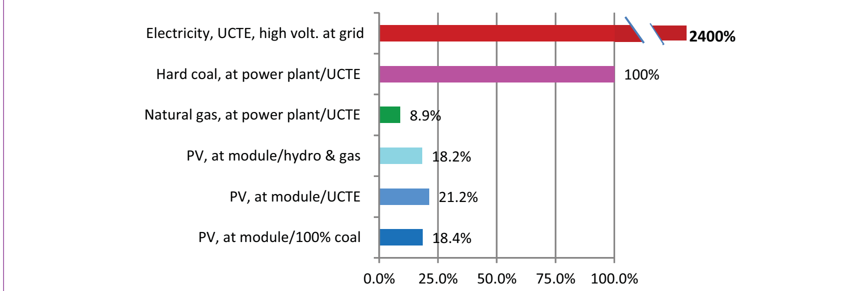

Figure 2. Comparison of the ionizing radiation emitted over the life cycle of various electricity generation sources.

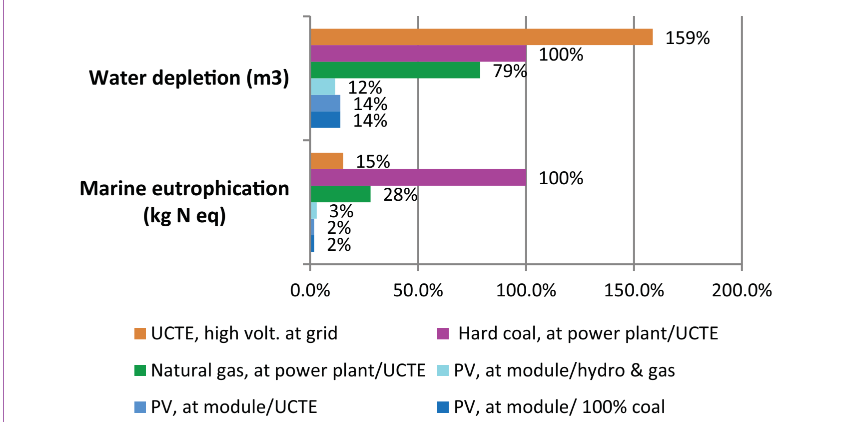

Figure 3. Comparison of water depletion and marine eutrophication by various electricity generation sources.

and scientific contexts for about 20 years. A very comprehensive, though finally inconsistent and incomplete, exercise quantifying energy-related externalities in Europe was done in the ExternE project [11], which continued through the NEEDS and CASES projects. The most recent (2010) set of results from the early methodology of ExternE estimates the total external costs for coal between 2.5 and 3¢/kWh (2008$) [12]. A more recent (2011) appraisal of these costs, carried out by Epstein et al. [13] at Harvard's School of Public Health, valued the environmental and health costs of coal electricity in the range of 18–27¢/kWh (2008$). This disparity of a factor of ten arises out of three fundamental differences in the bases of the evaluations: 1) the value placed on human morbidity; 2) the adequacy of the medical evaluation of the health and environmental damage; and 3) the appropriate and updated valuation of climate change. ExternE uses a much lower valuation (~50%) of human life than Epstein, who uses the value of statistical life most commonly used by the US Environmental Protection Agency. ExternE also uses outdated estimates of health and environmental impacts. Epstein gives a more complete epidemiology of air pollution, including particulates, and of the toxicity of heavy metals, such as mercury, relying on recent medical studies.

Finally, ExternE and its successors put an incredibly low value on the impact of climate change: an effective social cost of carbon of €2/tonne CO_2 [11]. The idea behind putting a price on CO_2 emissions was to stimulate industry and utilities to invest in clean electricity. When the price of CO_2 plummeted to €4/tonne last year, E.on CEO Johannes Teyssen proclaimed that the CO_2 market was a failure [13]. At this price, coal power plants are the most competitive, and even gas power plants can no longer stay in business [14]. E.on has also called for a minimum CO_2 price to be set, so that the market can begin to function as intended. The absolute minimum carbon price is considered to be about €20/tonne, as evidenced by the UK's carbon 'floor' price, the minimum CO_2 price set by the UK government in April 2013, with the plan that it will go up to €35/tonne by 2020 [15,16]. For the social cost of carbon, Epstein [13] uses values of US$30/tonne (€23/tonne) or US$100/tonne (€78/tonne) (low and high in Table 2).

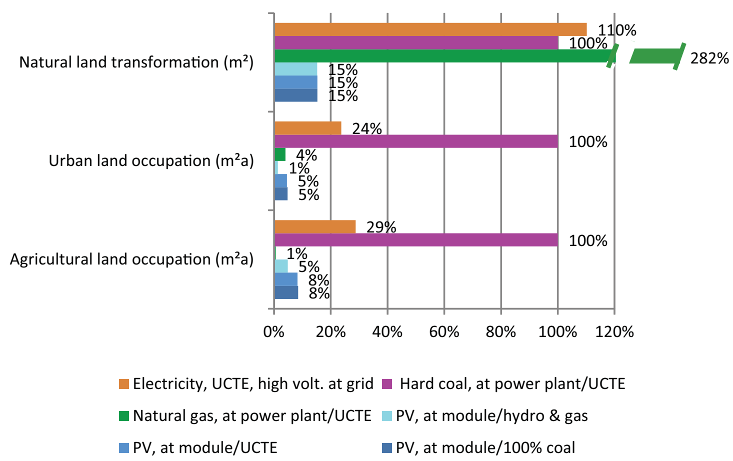

Figure 4. Land occupation and transformation for electricity (kWh) from PV, natural gas and coal, and the UCTE mix.

Before 2006, external cost studies of electricity did not take into account the magnitude of the costs of climate change. Then Nicolas Stern [17] changed that with his report stating that, if no action is taken, climate change will cost annually between 5–20% of the global GDP. A 2011 study, based on the social cost of carbon in Stern's work (US$85/tonne CO_2), estimated the cost of the impact of global greenhouse gas emissions to be US$4.5 trillion in 2008 (8% of GDP), with an expected rise to US$28.6 trillion in 2050 [18].

> "Climate change is contributing to the frequency and magnitude of extreme weather events, causing the losses from these events to steadily grow."

A validation of the increased valuation of climate change costs is the observation by the insurance industry in recent years that climate change is contributing to the frequency and magnitude of extreme weather events, causing the losses from these events to steadily grow. In 2012 the ten costliest natural catastrophes worldwide amounted to US$131bn in losses [19]. Total losses from natural catastrophes worldwide are approaching US$1 trillion annually, as contrasted with a norm 30 years ago of less than US$400bn/year [14]. The IPCC states in a 2012 report [20]: "Loss estimates

	Coal [¢/kWh]		% impact of PV	PV/coal [¢/kWh]	
Category	Low	High		Low	High
Climate change	3.15	10.55	3.8	0.12	0.40
Human toxicity	4.69	6.08	5	0.23	0.30
NMVOC+PM+SO_2	9.31	9.31	6.9	0.64	0.64
Land+AML	0.45	0.61	15	0.07	0.09
Coal transport	0.09	0.09	5	0.00	0.00
Total	17.69	26.64		1.07	1.44

Table 2. Monetarization of the environmental and health impact of 1kWh of electricity from coal compared with 1kWh of electricity from a PV module manufactured with 100% coal electricity, as per Epstein et al. [13]. Categories include: non-methane volatile organic compounds (NMVOCs) + particulate matter (PM) + sulphur oxide emissions (SO_2), and land transformation + abandoned mine lands (AML).

are lower bound estimates because many impacts, such as loss of human lives, cultural heritage, and ecosystem services, are difficult to value and monetarize, and thus they are poorly reflected in estimates of losses. Impacts on the informal or undocumented economy as well as indirect economic effects can be very important in some areas and sectors, but are generally not counted in reported estimates of losses." The estimate of roughly half a trillion dollars for the cost of extreme weather reveals that the order of magnitude for the costs of climate change must be at least in the trillions of dollars annually, which is consistent with Epstein et al., but not with the earlier methodology.

The methodology for costing damages from global warming is still evolving but the trend clearly indicates that climate change is much more expensive than originally thought. Indeed, insurers are currently re-evaluating their risk and business models in order to accommodate the new 'normal' of climate change events [21].

By using the methodology of Epstein et al., the external environmental and health costs can be estimated for PV manufactured with 100% coal electricity. Because the lion's share of the environmental impact of PV is associated with the electricity used to produce it, it is more consistent to compare 1kWh of electricity generated from PV manufactured using 100% coal electricity with 1kWh of electricity generated from coal.

Epstein et al. [13] assign monetary values (¢/kWh) for each impact category associated with the life cycle of coal, summarized here in the 'coal' columns of Table 2. The relative impact of PV ('% impact of PV' in Table 2) is taken from the environmental indicators for PV as a percentage of those for coal, as reported in Figs. 1-4. If the monetarization of Epstein et al. [13] is used, an estimate of the external environmental and health costs for a PV module manufactured exclusively with 100% coal electricity may be determined. This leads to an estimate of less than 1.5¢/kWh for the environmental costs for a PV module manufactured with 100% coal electricity, compared with 18–27¢/kWh for electricity generated from coal (2008$).

Subsidies

As pointed out by Chang [22]: "Virtually all of today's rich countries used protectionism and subsidies to promote their infant industries ... The computer, semiconductors, aircraft, internet and biotechnology industries have all been developed thanks to subsidized R&D from the US government." The energy sector, in both the USA and Europe, is no exception. It is important to look at subsidies across the energy sector to put into context subsidies for renewable energy sources in general, and for PV in particular.

The IMF estimates that subsidies for fossil fuels took US$1.9 trillion out of the global economy in 2011, or 2.5% of global GDP, on an annual basis [23]. The figure for directly subsidizing fossil fuel use in 2011 was US$523bn (or ~25% of the total), compared with US$88bn subsidies for all renewable energy sources [24]. The other ~75% is attributable to the accompanying costs of environmental, health and infrastructure damages paid by taxpayer money (Fig. 5).

One example of a national renewable energy source subsidy is the feed-in tariff associated with the German Renewable Energy Law (EEG), which stimulated the growth of PV installations so that in 2012 PV generated 5% of German electricity. The feed-in tariff is funded by electricity users (but not large industrial electricity users) through a surcharge that appears on their electricity bills. The proceeds go to renewable electricity 'producers', the majority of whom are residential customers. From its inception, the feed-in tariff was designed so that the assistance would taper off to zero as the feed-in tariff converged to the market price of electricity as a function of the market growth in renewable energy. Fig. 6 gives an overview of the subsidies paid out by the German government from 1970 to 2012 [25].

The contribution that German electricity users pay to subsidize renewable energy rose from 3.592ct/kWh in 2012 to 5.277ct/kWh in 2013, constituting an increase of 46.9%. For an average household (3,500kWh/yr), electricity customers are paying about €185 total (or €84/person) during 2013, to finance a cleaner society and a new business sector with the associated jobs [26]. According to Claudia Kemfert, the Director of the Energy, Transportation and Environment Unit at the German Institute for Economic Research in Berlin, the cost of renewable energy is really quite small, i.e. about 2.3% of the average household's consumption expenditure – a lot less than the high prices of gasoline and heating, since the price of fossil fuels has been rising and will continue to rise [27].

Federal Environment Minister Peter Altmaier (Christian Democratic Union) and Federal Economics Minister Philipp Rösler (Free Democratic Party) have brought attention to the

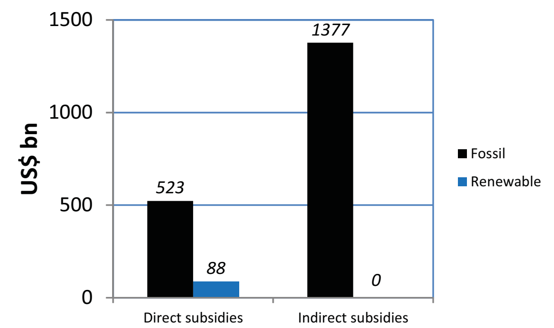

Figure 5. IMF statistics of annual global energy subsidies. The direct fossil fuel subsidies are concentrated in developing countries, while the indirect fossil fuel subsidies are predominately in the developed countries [19].

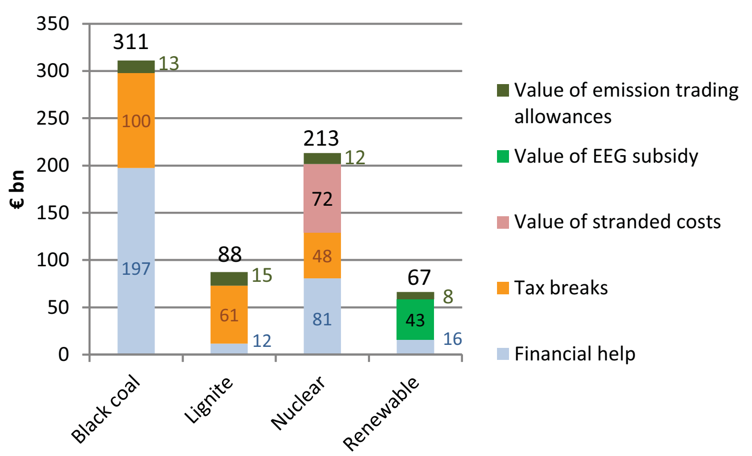

Figure 6. German government subsidies 1970–2012 in €bn (real) [21].

idea that the costs for the renewable energy transition are too high, and that renewable installations need to be slowed down significantly or stopped [28]. Altmaier has alarmed audiences with the claim that the energy transition will cost €1 trillion. However, economic analyses that take into consideration the cost of avoided fossil fuel imports, and avoided environmental damage among other related effects, do not substantiate the idea that renewable electricity is more expensive than fossil fuel electricity [29].

The main costs and benefits of the energy transition can be identified by looking at an economic analysis of the renewable energy expenditures for 2011, as shown in Fig. 7 [30]. In 2011 Germans paid, via the Renewable Energy Law, €11bn to install new renewable energy systems. For this price they received almost €60bn in economic and environmental benefits; in addition, 14,200 jobs were created in 2011, bringing the renewable energy employment to a total of 381,600 direct and indirect jobs (Fig. 7) [26].

Fuel imports and energy security

The political and economic potential risks and uncertainties of importing fossil fuels from outside Europe are continuously assessed in order to determine the security of Europe's energy supply (Fig. 8) [31]. A recent working paper of the European Commission discusses Europe's deteriorating security of energy supply [32]. "The EU currently imports more than 50% of its energy: more than 80% of the oil and more than 60% of the gas. If the current trends continue, import levels could reach more than 70% of the EU overall energy needs by 2030" [28]. The increased share of renewable energy will take some demand pressure off the fossil fuel supply, slowing down price escalation and increasing the EU's energy independence.

Compared with conventional energy, renewable energy is more economically and politically secure because fuel imports and dependencies are avoided, and the associated money does not leave the borders of the country. Furthermore, renewable deployment is associated with net job creation [33] – a stabilizing economic factor. Available studies show that job creation associated with renewable energy deployment is significant and occurs along the entire value chain, e.g. in manufacturing, sales, engineering, installation and administration. This means that countries which do not manufacture renewable energy products will still have a net job increase in the downstream parts of the value chain.

> "Compared with conventional energy, renewable energy is more economically and politically secure."

The costs that German society paid in 2011 through the EEG surcharge (€10.9bn) are almost balanced by the savings on fossil fuel imports alone (€7.1bn). The presence of renewable energy in the energy market brings down the cost of peak electricity (the merit order effect (€4.6bn)). Just these two factors more than offset the costs, and there is still a list of other benefits on top of that. Consequently, the net economic results of subsidies, fossil fuel imports and energy security are net external benefits.

Costs for grid expansion, control and balancing

In Fig. 7 (relating to the case of renewable energies in Germany in 2011), the costs for renewable energy (€10.9bn) include the direct renewable energy system costs (€10.6bn), electricity transaction costs (€0.3bn, or ~3% of the total costs) and the costs for control and balancing as well as grid expansion (most PV systems are connected to the low or medium voltage grid and do not require the kinds of additional transmission line that offshore wind requires).

Allocating the costs for grid expansion to PV, and to renewable energy sources in general, is complicated by several different factors. The ten-year plan of ENTSOE [34] sets out an ambitious and expensive blueprint for transforming Europe's transmission grid. The three motivations that it addresses are: 1) security of supply; 2) renewable energy integration; and 3) internal market integration, with the latter deemed the most important [34]. The security of supply aspect also relates to necessary upgrades to the ageing infrastructure, which were not performed over the past decades [35]. As there is little incentive in the liberalized energy market for investment in the common energy infrastructure, an investment shortfall has accumulated. The current need for investment in the electricity grid infrastructure because of insufficient investment in the past should not automatically be allocated to new electricity generators. Indeed, transparent and detailed information

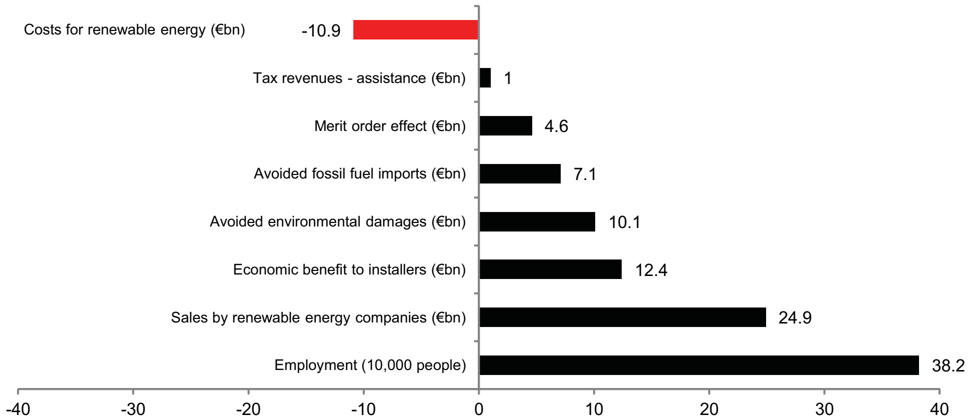

Figure 7. Economic analysis of the costs and benefits of the Renewable Energy Law in 2011, carried out by the German Federal Ministry for the Environment, Nature Conservation and Nuclear Safety. In 2011 14,200 more jobs were created, bringing the total number of renewable energy jobs to 381,600.

over what costs are really necessary in terms of infrastructure should be put out in the public domain. Furthermore, this information should be separated from the costs for a market structure whose benefit to customers is debatable.

ENTSOE's development plan currently allocates more than 60% of the investments to internal market integration in accordance with, and building on, the current energy market design [31]. However, the energy market is currently designed for conventional generators, and is against flexible renewable generators [36]. Considering that the energy market will need to evolve with the inevitable increase of renewables, the large investment in this energy market design should not be accepted without question.

Questions have been raised about the costs (which include the costs for balancing and reserve capacities) for assuring the reliability of integrating large amounts of renewables. Recent studies [37,38] demonstrate that the same high level of reliability as at present can be achieved on an hourly basis throughout the year, for the estimated electricity demand for the year 2050, with more than 50% renewable generation (TWh); this 'transition' scenario would offer savings of US$83bn over 40 years compared with the 'business as usual' (BAU) scenario. Those studies also demonstrate that the idea that 'every MW of renewable capacity requires a MW of fossil fuel generation capacity to back it up' is a misconception. The transition scenario requires 20% extra capacity, whereas 30% extra capacity is required by the BAU scenario.

The US National Renewable Energy Laboratory (NREL) has also produced a study which shows that balanced electricity from 80% renewables is feasible for the USA in 2050 [39]. The cost was found to be comparable to other possible energy scenarios (including combinations of renewable, nuclear and low-emission fossil fuels).

The experiences of system operators such as the Xcel Energy subsidiary Public Service Company of Colorado (PSCo) and the Electric Reliability Council of Texas (ERCOT) are also relevant. PSCo has had well over 50% wind at times, and ERCOT has over 10GW wind. ERCOT's calculations for the total cost of integrating wind in 2011 came out to about US$0.50/MWh, or a modest ~1.3% of the energy value [40]. ERCOT explains that its efficient dispatch of wind is a result of state-of-the-art forecasting, five-minute dispatch intervals, the advantages of a large geographic area, and the ability to use 'non-spinning reserves' to cover the risk

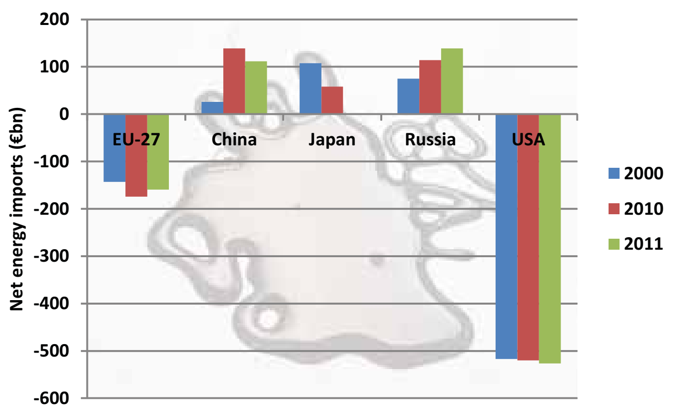

Figure 8. EU-27 and the USA dependency on imports of coal, lignite, oil and gas (2011 data for Japan were not available).

of insufficient generating capacity [35]. 'Non-spinning reserves' means that they can obtain electricity by turning on generation sources with a fast start-up, or by balancing imports and exports to retain more electricity to cover demand.

This kind of flexible, short-interval dispatch is what is necessary for low-cost integration of large penetrations of renewable energy sources. In February 2013 the California Independent System Operator (CAISO) and PacifiCorp (a utility ranging over six western states in the USA) signed a memorandum of understanding to create an energy imbalance market in 2014. This will create the sort of market structure for enabling flexible, short-interval dispatch. NREL anticipates that this market will save US$150–300m per year over current operations, as well as allowing low-cost integration of a high percentage of renewables [41,42].

Instances of high penetrations of renewables are increasingly occurring in Europe. Redes Energéticas Nacionais (REN), Portugal's grid operator, reported that 70% of the country's electricity was generated by renewable energy sources in the first quarter of 2013 [43].

The cost of integrating renewables clearly depends on the abilities of the system operator to operate flexibly, with short-interval dispatch, and to share reserve generation across a broader region. It may be that many system operators have to update their operations to rise to the inevitable challenge of high penetrations of renewables; the solutions some utilities and operators have found to achieve this apparently come with cost savings, rather than cost burdens. Detailed cost pictures for integrating renewables necessarily depend upon the system operator, and this is beyond the scope of this paper. However, the adaptation to the future electricity supply based on very large penetration of renewables appears to lie within the choice of business model and operations of the system operators.

Renewable energy is a solution for mitigating the deteriorating energy supply, for bringing down greenhouse gas emissions, for avoiding the economic drain of importing fossil fuels from third countries, and for stimulating the creation of jobs. Integrating high penetrations of renewables, with the same reliability as we have today, appears to be totally feasible and within the cost horizons of current operations. It therefore does not need to be considered an external cost burden for distributed renewable generators.

Conclusions

The social, economic and environmental value of PV specifically, and renewable energy in general, is especially relevant today. Two indicators, one social and one environmental, are emblematic for the state of the world in 2013: income inequality and the atmospheric level of CO_2. The first indicator is highlighted in the World Economic Forum's 2013 Global Risk Report. Severe income disparity, or inequality of wealth and income, is identified as one of the direst risks in 2013, and a symptom of the continued stress on the global economic system [44]. The OECD also recently published a report showing that the first three years of the financial crisis markedly increased income inequality worldwide: from 2007 to 2010 the inequality in income from work and capital increased as much as in the previous twelve years [45]. That report cautions that, given the current sluggish recovery, with less spending capability of the middle classes, this trend may spiral downwards.

The social and economic benefits of investing in renewable energy, and PV specifically, include not having to send increasing sums of money for fossil fuels to third countries, which increases energy security and creates jobs and renewable energy products and markets, as well as lower wholesale electricity prices. The costs paid in 2011 by German society through the EEG surcharge (€10.9bn) are almost balanced by the savings on fossil fuel imports alone (€7.1bn). The presence of renewable energy in the energy market brings down the cost of peak electricity on account of the merit order effect (€4.6bn). These two factors alone more than offset the costs, and there is additionally a list of other benefits on top of that. The combination of subsidies, avoided fossil fuel imports and energy security therefore results in net external benefits.

"Switching to renewable energy sources is the single most effective measure that can be taken to slow the acceleration of CO_2 levels in the atmosphere."

The second indicator – the atmospheric level of CO_2 – has just passed the 400ppm mark; CO_2 added to the atmosphere and oceans stays around for thousands of years. Thus climate changes forced by CO_2 depend primarily on cumulative emissions, making it progressively more and more difficult to avoid further substantial climate change [46]. Switching to renewable energy sources is the single most effective measure that can be taken to slow the acceleration of CO_2 levels in the atmosphere. As Ralph Keeling [43], from the Scripps Institute of Oceanography, says: "It mainly comes down to how much we continue to rely on fossil fuels for energy." PV electricity contributes 96–98% less greenhouse gases than electricity from 100% coal, and 92–96% less compared with the European electricity mix. Furthermore, compared with coal electricity, PV electricity over its lifetime uses 89–86% less water, occupies or transforms over 80% less land, and presents ~95% lower toxicity to humans; it also contributes 92–97% less to terrestrial acidification and 97–98% less to marine eutrophication. The economic consequences are expressed as the environmental and health external costs, which, for a PV module manufactured with 100% coal electricity, is 1–1.5¢/kWh compared with 18–27¢/kWh for electricity from coal (2008$). In 2012$, coal electricity requires an extra 19–29¢/kWh, compared with 1–1.6¢/kWh for PV manufactured with 100% coal electricity. For households this is yet another economic burden that may be avoided by using renewable electricity.

The final reservations about integrating high amounts of renewable energy into the grid appear to be resolvable, as more and more evidence mounts showing that it is indeed feasible to do so. Integrating high penetrations of renewables, with the same reliability as we have today, appears to be totally feasible and within the cost horizons of current operations of the system operators. It therefore does not need to be considered an external cost burden for distributed renewable generators. If the goal of policymakers is to improve the health and welfare of society, then they need not hesitate in supporting PV and other renewable energy sources.

Acknowledgements

This work was carried out in the framework of the European Project PV Parity (Contract No. IEE/10/307/SI2.592205). Funding was provided by the European Commission and the Dutch Ministry of Economic Affairs, Agriculture and Innovation.

References

[1] De Wild Scholten, M. 2011, "Environmental profile of PV mass production: Globalization", *Proc. 26th EU PVSEC*, Hamburg, Germany.

[2] IEA 2011, "Methodology of life cycle assessment for photovoltaic electricity", Report IEA-PVPS T12-03:2011 [http://www.iea-pvps.org/fileadmin/dam/public/report/technical/rep12_11.pdf].

[3] Goedkoop, M. 2012, "ReCiPe 2008", Report for the Dutch Ministry of Housing, Spatial Planning and the Environment (VROM) [http://www.lcia-recipe.net/].

[4] Working Group I 2007, "Global warming potentials", Contribution to the fourth assessment report of the Intergovernmental Panel on Climate Change [http://www.ipcc.ch/publications_and_data/ar4/wg1/en/tssts-2-5.html].

[5] Eurostat 2011, "Energy, transport and environment indicators" [http://epp.eurostat.ec.europa.eu/cache/ITY_OFFPUB/KS-DK-11-001/EN/KS-DK-11-001-EN.PDF].

[6] European Environmental Agency 2012, "Climate change, impacts and vulnerability in Europe 2012" [http://www.eea.europa.eu/publications/climate-impacts-and-vulnerability-2012].

[7] Ito, O. 2011, "Emissions from coal fired power generation", IEA Workshop on High Efficiency, Low Emissions Coal Technology Roadmap [http://www.iea.org/media/workshops/2011/cea/Ito.pdf].

[8] Drake, F.-D., "Investment in coal-fired power generation", IEA/NEA Joint Workshop on Power Generation Investment in Liberalized Electricity Markets [https://www.oecd-nea.org/ndd/investment/session3/Drake.pdf].

[9] Martin, A.D. 2012, "Water footprint of electric power generation: Modeling its use and analyzing options for a water-scarce future" [http://sequestration.mit.edu/pdf/AnnaDelgado_Thesis_June2012.pdf].

[10] van Vliet, M. 2012, "Vulnerability of US and European electricity supply to climate change", *Nature Climate Change*, Vol. 2, pp. 676–681.

[11] Krewitt, W. 2002, "External costs of energy – Do the answers match the questions? Looking back at 10 years of ExternE", *Energy Policy*, Vol. 30, pp. 839–848.

[12] Markandya, A., Bigano, A. & Porchia, R. (Eds.) 2010, *The Social Costs of Electricity*. Northampton, MA, USA: Edward Elgar Publishing.

[13] Epstein, P. et al. 2011, "Full cost accounting for the life cycle of coal", *Ann. N.Y. Acad. Sci.*, Vol. 1219, pp. 73–98.

[14] Chestney, N. 2012, "POLL-analysts cut EU, UN carbon forecasts" [http://www.pointcarbon.com/news/reutersnews/1.2087144].

[15] Pilita Clark, P. & Tighe, C. 2013, "UK business attacks EU carbon move", *Financial Times* (April 17) [http://www.ft.com/intl/cms/s/0/652c2932-a77d-11e2-9fbe-00144feabdc0.html#axzz2XEEkWTDp].

[16] HM Revenue & Customs 2013, "Carbon price floor" [http://www.hmrc.gov.uk/climate-change-levy/carbon-pf.htm].

[17] Stern, N. 2006, "Stern review: The economics of climate change", Executive Summary [http://webarchive.nationalarchives.gov.uk/+/http:/www.hm-treasury.gov.uk/media/4/3/Executive_Summary.pdf].

[18] United Nations Environment Programme Finance Initiative & Principles for Responsible Investment 2011, "Universal ownership: Why environmental externalities matter to institutional investors" [http://www.unpri.org/files/6728_ES_report_environmental_externalities.pdf].

[19] Munich Re Touch 2012, Annual Statistics [http://www.munichre.com/touch/naturalhazards/en/natcatservice/annual_statistics.aspx].
[20] IPCC 2012, "Summary for policymakers", in *Managing the Risks of Extreme Events and Disasters to Advance Climate Change Adaptation. A Special Report of Working Groups I and II of the Intergovernmental Panel on Climate Change*, Field, C.B. et al. (Eds.). Cambridge and New York: Cambridge University Press, pp. 3–21 [http://ipcc-wg2.gov/SREX/images/uploads/SREX-SPM_FINAL.pdf].
[21] McHale, C. & Leurig, S. 2012, "Stormy future for U.S. property/casualty insurers [https://www.ceres.org/resources/reports/stormy-future/view].
[22] Chang, H-J. 2011, *23 Things They Don't Tell You about Capitalism*. London: Penguin Books.
[23] IMF 2013, "Energy subsidy reform: Lessons and implications" [http://www.imf.org/external/np/pp/eng/2013/012813.pdf].
[24] IEA 2013, "Tracking clean energy progress 2013" [http://www.iea.org/publications/TCEP_web.pdf].
[25] Greenpeace & BWE 2012, "Was Strom werklich kostet" [http://www.greenpeace-energy.de/uploads/media/Stromkostenstudie_Greenpeace_Energy_BWE.pdf].
[26] German Federal Ministry for Family Affairs, Senior Citizens, Women and Youth 2004, "Families in Germany, facts and figures" [http://www.bmfsfj.de/RedaktionBMFSFJ/Broschuerenstelle/Pdf-Anlagen/Brosch_C3_BCre-Familie-im-Spiegel-englisch,property=pdf,bereich=,sprache=de,rwb=true.pdf].
[27] Hockenos, P. 2013, "The battle over electricity" [http://energytransition.de/2013/04/the-battle-over-electricity/].
[28] Enkhardt, S. 2013, "Germany: Severe renewable energy cuts planned" [http://www.pv-magazine.com/news/details/beitrag/germany--severe-renewable-energy-cuts-planned_100010216/#ixzz2Sb82NmzK].
[29] Green Budget Germany 2013, "Die Kosten der Energiewende – Wie belastbar ist Altmaiers Billion?" [http://www.foes.de/pdf/2013-03_Kurzanalyse_Energiewendekosten_Billion.pdf].
[30] Federal Ministry for the Environment, Nature Conservation and Nuclear Safety 2012, "Renewable energy sources in figures – National and international development" [http://www.erneuerbare-energien.de/fileadmin/Daten_EE/Dokumente__PDFs_/broschuere_ee_zahlen_en_bf.pdf].
[31] Eurostat 2012, "Energy, transport and environment indicators" [http://epp.eurostat.ec.europa.eu/cache/ITY_OFFPUB/KS-DK-12-001/EN/KS-DK-12-001-EN.PDF].
[32] European Commission Staff Working Paper 2012, "Renewable energy: A major player in the European energy market", 271 final [http://eur-lex.europa.eu/LexUriServ/LexUriServ.do?uri=SWD:2012:0149:FIN:EN:PDF].
[33] International Renewable Energy Agency (IRENA) 2012, "Renewable energy – Jobs status, prospects & policies" [http://www.irena.org/DocumentDownloads/Publications/RenewableEnergyJobs.pdf].
[34] ENTSOE 2012, "Ten-year network development plan 2012", p. 48 [https://www.entsoe.eu/major-projects/ten-year-network-development-plan/tyndp-2012/].
[35] European Commission 2011, "Connecting Europe: The energy infrastructure for tomorrow" [http://ec.europa.eu/energy/mff/facility/doc/2012/connecting-europe.pdf].
[36] Neuhoff, K. 2011, "Opening the electricity market to renewable energy: Making better use of the grid" [http://www.diw.de/documents/publikationen/73/diw_01.c.375862.de/diw_econ_bull_2011-01-4.pdf].
[37] Vitolo, T. et al. 2013, "Meeting load with a resource mix beyond business as usual", *Synapse Energy Economics*, April 17 [http://www.civilsocietyinstitute.org/media/pdfs/20130417Meeting%20Load%20with%20a%20Resource%20Mix%20Beyond%20Business%20as%20Usual%20-%20FINAL.pdf].
[38] Keith, G. et al. 2011, "Toward a sustainable future for the U.S. power sector: Beyond business as usual 2011" [http://www.synapse-energy.com/Downloads/SynapseReport.2011-11.CSI.BBAU-2011.11-037.pdf].
[39] NREL 2012, "Renewable electricity futures study" [http://www.nrel.gov/analysis/re_futures/].
[40] Ahlstrom, M. 2013, "A market perspective on forecast value", WindLogics [http://www.uwig.org/slcforework/Ahlstrom-Session1.pdf].
[41] Baak, J. 2013, "CAISO and PacifiCorp agreement paves way for lower cost solar integration" [http://www.renewableenergyworld.com/rea/news/article/2013/02/caiso-and-pacificorp-agreement-paves-way-for-lower-cost-solar-integration].
[42] Milligan, M. et al. 2012, "Examination of potential benefits of an energy imbalance market in the Western interconnection", NREL Report [http://www.westgov.org/PUCeim/documents/drftNRELba.pdf].
[43] REN 2013, "Renewables supply 70% of domestic consumption of electricity in Q1" [http://www.ren.pt/media/comunicados/detalhe/renovaveis_abastecem_cerca_de_70__do_consumo_nacional_de_eletricidade_no_1__trimestre/?culture=en-GB].
[44] World Economic Forum 2013, "Global risks 2013" [http://www3.weforum.org/docs/WEF_GlobalRisks_Report_2013.pdf].
[45] OECD 2011, "Crisis squeezes income and puts pressure on inequality and poverty" [http://www.oecd.org/els/soc/OECD2013-Inequality-and-Poverty-8p.pdf].
[46] National Oceanic and Atmospheric Administration (NOAA) 2013, "Carbon dioxide at NOAA's Mauna Loa Observatory reaches new milestone: Tops 400 ppm" [http://research.noaa.gov/News/NewsArchive/LatestNews/TabId/684/ArtMID/1768/ArticleID/10061/Carbon-Dioxide-at-NOAA%e2%80%99s-Mauna-Loa-Observatory-reaches-new-milestone-Tops-400-ppm.aspx].

About the Author

Carol Olson received a Ph.D. in physics from Imperial College, London, in 2003. After joining ECN in 2006, she carried out research in the areas of thin-film PV and characterization of silicon solar cells. Dr. Olson currently manages projects relating to life cycle assessment of photovoltaic products and processing lines, as well as those relating to sustainability of PV. She participates in the EPIA sustainability working group and in the IEA-PVPS Task 12 on PV environmental health and safety activities.

Enquiries

Dr. Carol L. Olson
Solar Energy
Energy Research Centre of the Netherlands
Westerduinweg 3
1755LE Petten
The Netherlands

Tel: +31 88 515 48 56
Fax: +31 88 515 82 14
Email: olson@ecn.nl

Materials

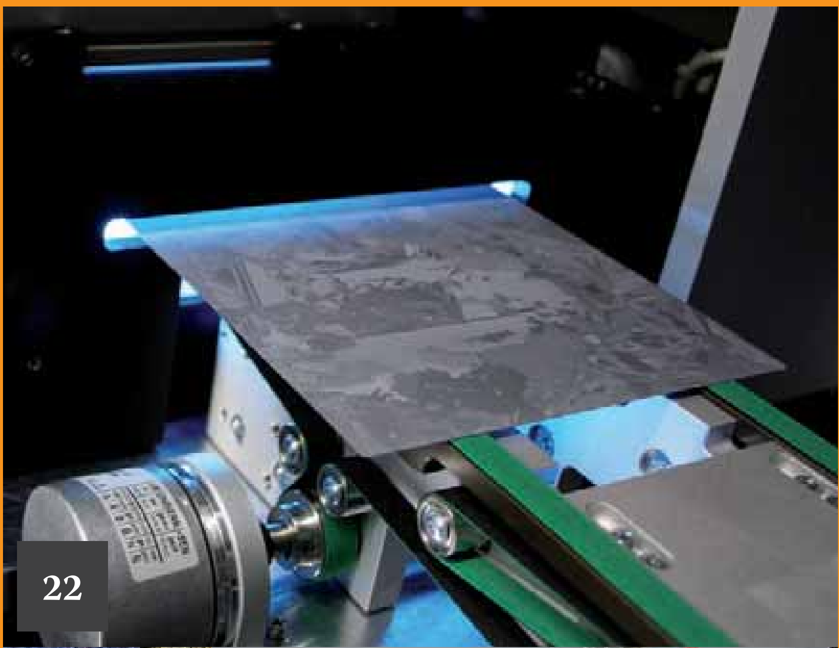

Suntech's Chinese suppliers ISRA Vision cites signs of solar business recovery in upstream sector

Leading machine vision systems specialist, ISRA Vision, has hinted at further PV equipment acquisitions and a whiff of recovery in equipment enquiries within the PV sector in reporting third quarter financial year results.
Having acquired GP Solar GmbH in May, ISRA Vision said that it was assessing further acquisition targets within the PV sector as it positions itself with an increasingly broad product offering to capitalise on the next technology and capacity buy-cycle. An acquisition could occur this year, or in 2014, the company said. Its Surface Vision segment targets the glass manufacturing sector, which saw revenues increase slightly in the first three quarters to €48.0 million. Overall, the company still expects full-year revenue to be in the range of €100 million.

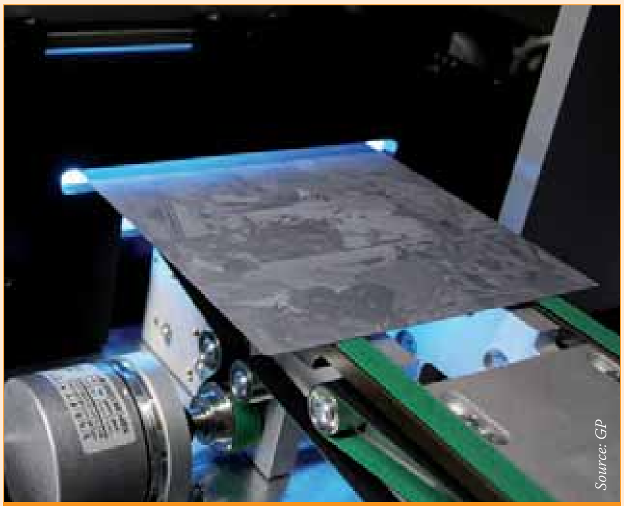

ISRA Vision is considering buyouts following GP solar acquisition.

Polysilicon

GCL-Poly blames losses on polysilicon price dumping; wafer sales up 21%

China's largest polysilicon and solar wafer producer GCL-Poly said in a financial statement that there were only three to five polysilicon producers still in production in China, but supply appeared to be beginning to fall short of demand.

GCL-Poly Energy Holdings reported a group loss of HK$917.3 million (US$118.2 million) or the first-half of 2013, citing polysilicon price dumping from major overseas rivals, after recently announcing a profit warning.

The company reported its solar business segment sales for the first six months of the year reached HK$7,647 million (US$985.9 million) and a segment loss of US$184.3 million.

GCL-Poly said it sold 8,472MT of polysilicon and 3,858MW of solar wafers in the period, a decrease of 6.0% for polysilicon but an increase of 21.1% for solar wafers.

Daqo to expand polysilicon production as costs targeted at US$14/kg

Stabilizing polysilicon prices and recent technical upgrades to its polysilicon production facilities are behind Daqo New Energy's plan to boost production in the second-half of the year in a bid to reach production costs as low as US$14/kg.

Gongda Yao, chief executive of Daqo, said: "In the second quarter of 2013, our Xinjiang polysilicon facilities continued to contribute positive cash flow. In April, we successfully conducted several technical improvement projects which reduced our production cost below US$16/kg, which is significantly lower than our original target of us$20/kg. We expect our Xinjiang facilities to generate positive operating income in the third quarter of 2013. We are also making great effort to maximize our capacity in Xinjiang. We plan to expand our capacity in Xinjiang to 6,150 MT by the end of 2013. By achieving that, we expect that we can reduce our cost to the level of US$14/kg at that time."

However, to achieve lower production costs and reduce operating losses, Daqo said that it was closing its polysilicon facility in Wanzhou it would move polysilicon equipment to its Xinjiang facilities.

The company said the relocation would result in impairment charges of US$158.4 million.

Hemlock sues GET over breach of polysilicon supply deal

Solar polysilicon manufacturer Hemlock Semiconductor has filed a US$737 million lawsuit against Green Energy Technology (GET) over an alleged breach of a long-term supply agreement.

Hemlock claims GET, a Taiwan-based wafer manufacturer, defaulted on a down payment relating to a contract the two companies agreed in 2011 and failed to place orders it had committed to under the same deal.

According to court papers, Hemlock Semiconducter agreed to supply GET with polysilicon manufactured at its plant in Michigan, US, up to 2020.

In return GET agreed to pay a US$81.5 million advance payment in installments. But after making its first payment, Hemlock alleges GET failed to make six subsequent monthly installments, amounting to US$46,047,500 – claims Hemlock says GET later acknowledged in correspondence.

Hemlock claims GET also defaulted on an installment in January 2013 worth US$16.3 million.

In addition to failing to meet its advance payment obligations, Hemlock maintains GET failed to order and pay for certain quantities of product it had agreed to purchase in 2013.

Source: Hemlock Semiconductor

Hemlock Semiconductor is suing GET over supply contract breach.

As a result Hemlock terminated its supply agreement with GET on 13 August, demanding payment of all amounts under the contract, totalling US$737,235,429.17.

OCI to postpone South Korea polysilicon plant expansion

South Korean polysilicon manufacturer OCI has shelved plans to expand one of its production lines.

In a regulatory filing, the company said it had postponed US$100 million plans to expand production at its Gunsan plant, citing ongoing uncertainties in the solar market. The expansion would have increased plant capacity by 10,000 tonnes.

Technology not materials to drive down Chinese solar costs: GTM

Improving technology not the falling cost of materials will be the dominant factor in the ongoing fall in costs of Chinese module manufacturers, according to a report by GTM Research.

GTM claims that Chinese manufacturers will be able to produce modules at a cost of US$0.36 per Watt by 2017 and has provided more details on how they could get there.

They have already achieved a 54% decrease in manufacturing costs since 2010. GTM found that the majority of this came from the falling cost of materials caused by an oversupply with polysilicon responsible for 54% of the total reductions and other materials contributing a further 26%.

New REC bonds incentivise investors on split plans oversubscribed

Renewable Energy Corporation (REC) announced a new US$110 million convertible bond offer and a partial repurchase offer of existing bonds as it looked to appease investors.

The company announced in July that it would split its PV module and polysilicon production into two separate companies. On 13 August REC announced the new US$110 million convertible bond offer was oversubscribed and is now closed.

REC has been given 57% anti-dumping tariff by Chinese authorities, the largest of all polysilicon producers, while having the lowest costs due to its FBR technology.

According to research note Citigroup, the company's bondholders were likely to resist attempts to expose a new standalone REC Silicon arm to these tariffs.

The company announced the new convertible bond loan will mature in 2018 and will offer the partial repurchase and exchange of the existing 2014 convertible bond and the partial repurchase of the 2014, 2016 an 2018 bond loans. The separation of the company is subject to the approval of an extraordinary general meeting of the company and also of its bondholders.

Source: REC

REC has announced a US$110 million to appease investors as it plans to split.

Wafers

Solargiga sales boosted by supply deal with Sharp

Monocrystalline product supplier, Solargiga Energy Holdings, reported a 68.9% increase in revenue for the first half of 2013, compared to the same quarter a year ago as demand from Sharp for N-type mono-wafers and modules increased due to the booming Japanese market.

Solargiga recently signed a new supply agreement with Sharp, including 370MW third-party N-type mono-modules. The company reported revenue of RMB818.94 million (US$133.8 million) for the first six-months of 2013, up 68.9% from RMB484.959 million in the same period a year ago.

Sales to Japan continued to be its major revenue stream, totalling around US$83.6 million in the first-half of the year, up from US$23.3 million in the first-half of 2012. Sales of ingots/wafers to Taiwan also increased significantly from the same period a year ago, reaching US$20.5 million, compared to US$4.6 million in the first-half of 2012.

Sales to Spain and Germany dropped significantly in the first-half of 2013, while wafer sales to the UK, stopped completely in 2012 as well as to the US.

Solargiga said that it would be increasing the proportion of production and sales of N-type products, claiming its high-performance N-type wafer generated conversion efficiencies of 22-23%.

ReneSola posts 32.8% increase in sales on record shipment volume

Despite raising second quarter 2013 shipment guidance significantly, ReneSola exceeded the figure and reported record shipment volume of wafers and modules totalling 849.3MW.

The company previously expected total solar wafer and module shipments to be in the range of 760MW to 770MW, compared to its previously guided range of between 700MW to 720MW. ReneSola guided third quarter solar wafer and module shipments to be in the same range as originally expected for the second quarter of 730MW to 750MW.

The company reported net revenues in the second quarter of US$377.4 million, an increase of 32.8% from US$284.2 million in the prior quarter.

However, ReneSola guided revenue for the third quarter of 2013 to be in the range of US$360 million to US$380 million with a gross margin in the range of 7% to 9%, slightly higher than the 7.3% gross margin reported for the second quarter of 2013.

As a result of the increased sales and shipments in the second quarter, the company reiterated its recently revised shipment forecast to be between 2.8GW to 3.0GW, compared to its previously guided range of 2.7GW to 2.9GW.

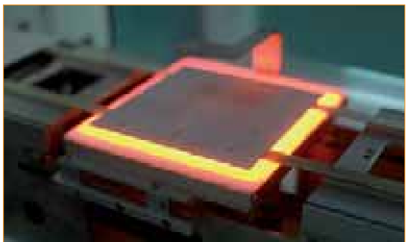

Source: ReneSola

ReneSola posts 32.8% increase in sales on record shipment volume.

Silicor secures new funding to fuel growth

Solar silicon provider Silicor has announced that it has secured new investment as it looks to expand its manufacturing operations.

The company has raised US$6 million from existing investor Hudson Clean Energy Partners and has appointed the asset management and investment firm Robert W. Baird to help raise additional capital.

Silicor is currently in advanced development work at several sites for a new solar silicon manufacturing plant capable of producing 16,000 tonnes annually.

The company claims it is the lowest-cost producer of high-quality solar silicon and expects increasing demand for its products as cell, wafer and module manufacturers look to continue lowering costs.

SunEdison's polysilicon and wafer operations made loss in first half of 2013

SunEdison plans to spin-off and IPO its polysilicon and wafer operations, which could net the company around US$250 million.

However, in an SEC filing, SunEdison revealed that its SunEdison Semiconductor Inc division, including its polysilicon and wafer operations, made a first-half year loss of US$21.4 million on net sales of US$471.3 million.

Revenue for the full year 2012 was US$927.4 million, down from US$1.05 billion in 2011. In a separate SEC filing the same day, SunEdison said that its cancelled silicon tetrachloride (TCS) supply agreement with Evonik Industries for its shuttered semiconductor polysilicon plant in Italy will now result in a €7.68 million penalty charge to be paid to Evonik.

The IPO proceeds are expected to be used for building PV power plants, while its SunEdison Semiconductor spin-off will use a range of banks for credit facilities.

The company later said its project pipeline remained strong, it expected total project completions in 2013 to be between 75-105MW.

Metallization pastes

DEK Solar and Yingli Green team on solar cell metallization R&D

Screen printing specialist, DEK Solar is to collaborate with leading PV module manufacturer, Yingli Green Energy, on next-generation metallization technology.

The companies held a signing ceremony on the 9 August. The collaboration will include DEK Solar supplying, at no cost, one of its 'Apollo' metallization lines, which will be used for ongoing research on silver paste usage and cost reductions at Yingli Green.

Source: GIGASOLAR

DEK Solar is to partner with Yingli Green team on metallization R&D.

Applied Nanotech eyes efficiency record after signing R&D agreement

Materials IP developer Applied Nanotech has signed an R&D agreement with Sichuan Yinhe Chemical Co (YHCC) and thin silicon manufacturer Solexel.

YHCC has the exclusive rights to Applied Nanotech's solar ink and paste technology and will produce the 1000 tonnes of the materials at a new plant in Sichuan Province.

The deal will see the technology commercialised in the cells of California-based Solexel.

The company achieved a world record of 20.62% efficiency from a 156x156 mm full-square solar cell using its low cost ultra thin epitaxial silicon film and porous silicon lift-off technology. Now the trio are eying improvement to raise this efficiency to 22%.

Product Reviews

Scifiniti

Scifiniti's 'SmartWafer' technology reduces high purity silicon usage by more than 90%

Product Outline: US start-up, Scifiniti, is developing a low-cost 'SmartWafer' that is claimed to enhance the performance and significantly lower the cost of silicon-based products.

Problem: To enable the continued cost reduction and growth of solar energy, the largest opportunity in the value chain is to dramatically decrease the cost of the silicon wafer. SmartWafer has been engineered specifically for solar cell manufacturing, unlike traditional wafers that have been adapted from the semiconductor industry.

Solution: SmartWafer uses a thin, deposited, high-quality silicon layer on a conductive substrate, offering the same form-factor as a standard wafer and enabling a 'drop-in' replacement. Cell and module manufacturers can use the SmartWafer without any changes to existing processes or purchase new capital equipment. The company estimates that high purity silicon usage is reduced by more than 90% and provide improved yields from reduced wafer breakage rates when compared to conventional wafers. The wafers comprise a 30 micrometer high-quality multicrystalline silicon active layer, on top of a 170 micrometer low cost substrate for mechanical support. Scifiniti notes that a silicon layer of 30 to 50 microns with effective light trapping has the same conversion efficiency as a conventional wafer of 160-180 microns.

Applications: : Solar-grade wafers.

Platform: SmartWafers comprise a 30 micron, high-quality multicrystalline silicon active layer. Along with the SmartWafer, Scifiniti has developed a number of new technologies, including an inline continuous deposition system, a crystallization system and advanced semi-grade ceramic processes.

Availability: Sampling only.

ISRA

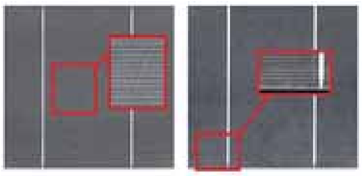

ISRA Vision's SOLARSCAN-MICRO-D provides inline wafer crack detection

Product Outline: ISRA Vision's SOLARSCAN-MICRO-D is a non-contact inline on-the-fly inspection system for the detection of micro-cracks in processed solar cells. The wafer segment accounts for about 60% of the total module processing costs incurred, therefore error-free production quality lowers cost.

Problem: The biggest challenge in PV production is the detection of defects within wafers. These so-called micro-cracks can occur in every production step and increase breakage rates dramatically. Shipment of wafers, handling during processing and processing itself can trigger cracks or micro- cracks in wafers and cells.

Solution: The inspection solutions offered by GP Solar a subsidiary of ISRA Vision detect defects in as-cut wafers, rear side prints as well as in finished solar cells and reduce production downtime and eliminate breakage sources. Most of the damaged material can be sorted out by means of optical systems. Micro cracks within finished solar cells, however, cannot be detected with standard systems. For this application the system SOLARSCAN-MICRO-D provides a solution. It is a non-contact inline on-the-fly inspection system for the detection of micro cracks in processed solar cells. Its innovative technology works independent from grain boundaries, variations of electronic material properties. As a result it delivers exact information on the position, shape and size of the cracks.

Applications: Micro crack detection of defects hidden within the bulk of the wafer.

Platform: The MICRO-D extends the range of applications as it can also handle the incoming control for module manufacturers. In addition, a stand-alone system for grading cells by quality is already available with the 'TEST-UNIT' tool.

Availability: Currently available.

Linde Gases

Linde and LiSEC team to provide anti-reflection glass coating technology to boost module performace

Product Outline: Linde Gases, a division of the Linde Group, has developed the 'S-COAT,' claimed to be a cost effective anti-reflection (AR) coating technology which significantly increases light transmission values and resultant energy yields of PV modules.

Problem: Solar module manufacturers are under pressure to optimize costs. An economical solution for effectively improving energy yields without changing solar cell processes provides significant advantages from both a capital and operating expenditure viewpoint, as compared to competing technologies.

Solution: Together with LiSEC, an Austrian based global company specializing in glass processing lines, Linde Gases Division has developed the new anti-reflection solar glass coating technology to deliver light transmission gains of around 3% on average – and up to 3.5% in peak conditions – as compared to identical glass substrates without such a coating. The patented coating process involves applying a specially developed water-based chemical mixture onto the glass surface using an inert gas spraying technology, and results in a glass surface finish of controlled porosity, maximising light transmission.

Applications: Anti-reflection coating for solar glass.

Platform: S-COAT can be installed into existing glass processing lines and operates at speeds up to 15 metres per minute, meaning no loss to productivity. After the coating is applied, the glass sheets are tempered to create a highly damage and wear resistant finish for the solar module.

Availability: Currently available.

Electrically conductive adhesives: An emerging interconnection technology for high-efficiency solar modules

Torsten Geipel & **Ulrich Eitner**, Fraunhofer Institute for Solar Energy Systems ISE, Freiburg, Germany

Fab & Facilities
Materials
Cell Processing
Thin Film
PV Modules
Power Generation
Market Watch

ABSTRACT
Electrically conductive adhesives (ECAs) are an alternative interconnection technology especially suited to high-efficiency cell concepts with new contact structures. This paper describes the basic principles of this emerging interconnection technology and discusses the different material types on the market. Mechanical and electrical characterization methods for conductive adhesives are also presented. Results are included from peel tests, volume and contact resistivity measurements, metallographic investigations, dynamic mechanical analysis and differential scanning calorimetry. Finally, a novel simulation approach for the cure kinetics of ECAs and arbitrary temperature profiles is briefly described and demonstrated by an example of an epoxy adhesive cure.

Introduction

Although soldering is currently the standard interconnection technology for crystalline solar module manufacturing because of its relatively low cost and proven long-term reliability, electrically conductive adhesives (ECAs) have gained increasing attention as an alternative [1]. On the one hand, ECA is a lead-free and flux-free technology, and an adhesive can be processed at lower temperatures (120–180°C), which therefore imposes less thermomechanical stress on the cells than soldering. Moreover, ECA is usually a flexible and compliant material that can absorb and reduce mechanical stress caused by the different thermal expansion coefficients of the module components.

> "ECA is a lead-free and flux-free technology."

On the other hand, the cost of ECA is an important concern because of the high silver content in the glues that is still necessary for achieving a reasonable electrical performance. However, ECA manufacturers are currently making significant progress in driving down costs of the material, and in increasing mechanical strength while maintaining reliability. Although it has been shown by many other researchers and producers that modules fabricated with ECA can withstand IEC certification tests [2–4], there are still open questions regarding the long-term stability and degradation mechanisms of the material. The cost and the lack of long-term experience of ECA are the key factors that still limit its wider use in module manufacturing.

Despite these concerns, ECA is a key technology for emerging new high-efficiency cell concepts. The most prominent example is the metal-wrap-through (MWT) solar cell together with the module integration based on conductive backsheets [5]. MWT solar cells have both contacts on the rear side, so the busbars on the sunny side can be omitted, increasing efficiency and reducing material consumption. For the interconnection of the cells, the backsheet of the module contains a structured metal layer, comparable to a circuit board in microelectronics, where the cells are glued with ECA. The glue is cured together with the cross-linking of the encapsulation material during a standard lamination process.

Another high-performance concept comes from Sanyo, which was the first company to industrialize crystalline heterojunction solar cells and modules. The efficiency of these high-performance cells exceeds 20% [6]. Since they contain temperature-sensitive layers such as amorphous silicon and a transparent conductive oxide, the use of ECA is one possible solution for a low-temperature interconnection [7].

ECA can also be used as a substitute for the front-side busbar [8]. The busbars are omitted in the screen-printing process during solar cell fabrication, and a standard ribbon is directly glued to the grid during the interconnection process in the module fab. Eliminating the screen-printed busbar has the advantage of improved efficiency because of better passivation of the front side, but most importantly saves roughly 40% of the front-side silver paste.

This paper will begin with a brief overview of the fundamental principles of conductive adhesives. A selection of relevant characterization techniques will then be discussed. In the last section the focus will be on the cure kinetics of ECA; a modelling approach will be demonstrated, along with a presentation of the results of a simulation.

Fundamentals of conductive adhesives

Components: polymers and filler

ECAs are basically polymers that are filled with electrically conductive particles. ECAs are usually viscous pastes of monomers or pre-polymers that cross-link when they are exposed to heat to form a solid polymer. The adhesives are applied to the components by printing or dispensing techniques, and the curing is carried out by using furnaces, heating plates, thermodes or infrared lamps.

> "ECAs are basically polymers that are filled with electrically conductive particles."

The polymer matrix provides cohesion (internal strength) of the material and adhesion to the surfaces to be bonded. Interestingly, the fundamentals of adhesion are still a field of debate. Many theories exist, such as chemical bonding, physical interlocking, diffusion and physical adsorption (especially by Van der Waals forces), with the latter being the most widely accepted [9,10].

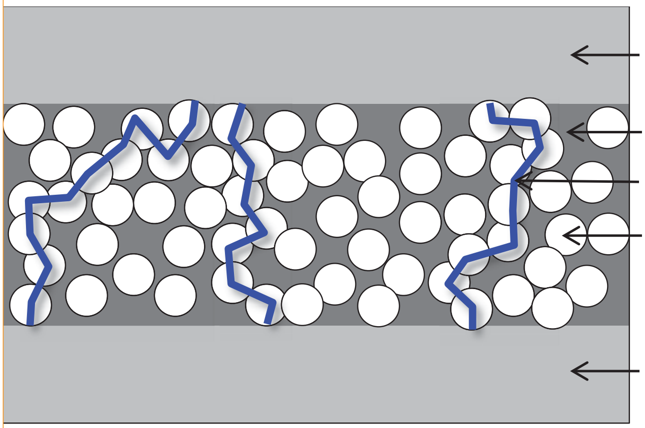

Figure 1. Schematic of a cross section of a conductive adhesive, showing how electrical paths are formed as a result of the internal contact of the filler particles.

The filler particles inside the adhesive form an electrically conductive network once the quantity is high enough to reach the so-called percolation threshold (see Fig. 1). They can be of different materials and can have various shapes and sizes, such as spheres or flakes. A 'typical' conductive adhesive is based on an epoxy polymer and contains silver flakes with 35–40 vol% and a diameter of 1–10µm. Additional components are diluting and curing agents as well as lubricants [11].

Types of conductive adhesive

Conductive adhesives for solar cell applications can be distinguished in respect of their conduction mechanism (isotropic, anisotropic) or polymer base (epoxies, acrylates, silicones).

Isotropic conductive adhesives

Isotropic conductive adhesives (ICAs) are presently the dominant type on the market. After curing, the conductivity is equally high in all directions; this is achieved by a large fraction of metal particles well above the percolation threshold. As one-component products they come pre-mixed in syringes of different sizes, frozen at –40°C. However, users also have the option to obtain the two components separately and take care of the proper mixing in their own fab, a process which requires sophisticated mixing equipment. If the user chooses the deep-frozen syringes, appropriate cooling equipment must be provided and the limited shelf life (usually six to twelve months) taken into account. Beyond expiration, particles can sink down and clog; in addition, the viscosity increases and makes the adhesives practically useless for automated equipment.

ICAs are relatively simple to process using printing or dispensing equipment and a curing step which does not require additional bonding pressure except from the fixation of the component or ribbon to the contact pad.

Anisotropic conductive adhesives

The characteristic of anisotropic conductive adhesives (ACAs) is that the current flows in one direction. Since only 0.5–5 vol% conductive particles are needed, this type of adhesive has considerable cost-saving potential.

Prominent ACAs come as conductive tapes, but paste-type products are also available. Tapes have the advantage of being clean in their application. However, they require special bonding conditions, usually at temperatures of 180°C with simultaneous pressure application of 2MPa for 10 sec [12], which may not only limit throughput but also cancel out the advantage of being a low-stress interconnection technology.

Solder-filled adhesives can also be put into this category [13]. They have the potential to be completely silver-free and almost compatible with existing module manufacturing equipment, for example a stringer used at low temperatures as a first curing step and a laminator for a final cure. Of course, modifications to the stringer are necessary in order to allow it to dispense or print the adhesive.

Epoxies

The characteristic feature of the cure reaction of epoxies is a polyaddition of components A (resin) and B (hardener) to a solid polymer. This is the most common polymer base for ECAs.

The curing time of epoxy-based ECAs ranges from 1.5 min to 10 min at 150°C. In the authors' experience, in tests the peel strength of the fully cured material is in the range of 0.2–1N/mm. Epoxies have stable properties at temperatures of up to 180–200°C and have a relatively high resistance to water and chemical attacks [14].

Acrylates

Acrylates as monomers have a particular chemical structure in that there exists a carbon–carbon double bond. This bond is cleaved by radicals during the cure reaction, resulting in the creation of new valences where the same kind of monomers can join and form the polymer network. Since only one kind of monomer is involved, the reaction is called polymerization.

The cure time at 150°C takes just a few seconds, which makes this polymer base an ideal candidate for solder replacement from a process point of view. However, acrylates are less temperature resistant, with a limitation of about 100°C [9].

Silicones

Silicones contain silicon–oxygen bonds instead of carbon chains. They are categorized as polycondensation adhesives, although silicones exist that can also be formed without the creation of a by-product.

At 150°C the cure time of silicones is in the range of 10–15 min, demonstrating a good compatibility with standard lamination times. Silicones have outstanding temperature stability, displaying high elasticity in a wide temperature range of at least –40°C to 200°C. Resistance to environmental attacks is claimed to be high [14].

Material characterization

Numerous methods are available for the mechanical and electrical characterization of conductive adhesives [15–17]. The focus here will be on the following methods: peel test, volume and contact resistance, metallography and dynamic mechanical analysis. For studying the cure reaction, the modelling procedure is based on differential scanning calorimetry experiments.

Peel test

Quality control incorporating the peel test for solar cell interconnections was reported by Wirth [18] in 2010. The foundation of the peel test is DIN EN 50461 [19]; the test was performed at a constant speed of 1mm/s and an angle of 90 degrees.

> "A major concern is the typically low peel strength of conductive adhesives compared with soldering."

A major concern expressed by industry is the typically low peel strength of conductive adhesives compared with soldering. The reason is that peel stress is a highly localized stress and adhesives are polymers with naturally lower toughness than metals, resulting in lower resistance to peeling. Moreover, adhesives are highly filled with particles that cannot contribute to the cohesive strength of the adhesive layer. Nevertheless, some adhesives, such as glue A shown in Fig. 2, are able to achieve the criterion of 1N/mm. Despite the above-mentioned drawback, other mechanical characteristics of ECAs – for example higher compliance and flexibility – may be advantageous from a long-term perspective and should not be neglected.

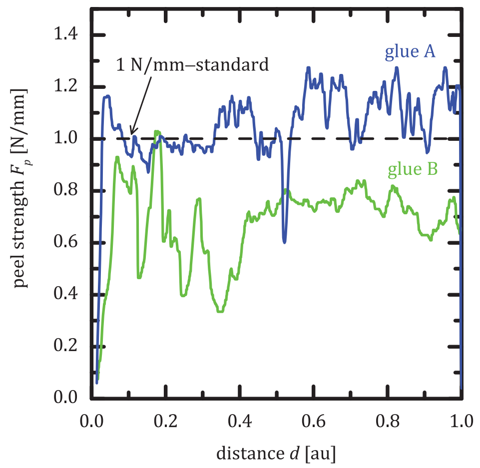

Figure 2. Peel strength of conductive adhesives.

Volume and contact resistivity

The volume resistance of ECAs is determined in accordance with MIL-STD-883H [20]. A cured adhesive track of defined dimensions is prepared on a glass slide. The resistance is determined by a four-point-probe measurement. The volume resistivity ρ_v can be calculated using the formula:

$$\rho_v = R_v \frac{w \cdot th}{l} \quad (1)$$

where R_v = measured resistance, w = width, th = thickness and l = length of the adhesive track.

The volume resistivity of some conductive adhesives is given in Fig. 3; it can be seen that the difference is not very distinct. Epoxies A and B are standard isotropic adhesives with ~80 wt% Ag-content and have the lowest resistance among the tested ECAs. As expected, a greater resistance can be observed for an epoxy with a low Ag content. The acrylate and silicone also have relatively high Ag contents but show higher resistances or stronger variations, which could be caused by the polymer base.

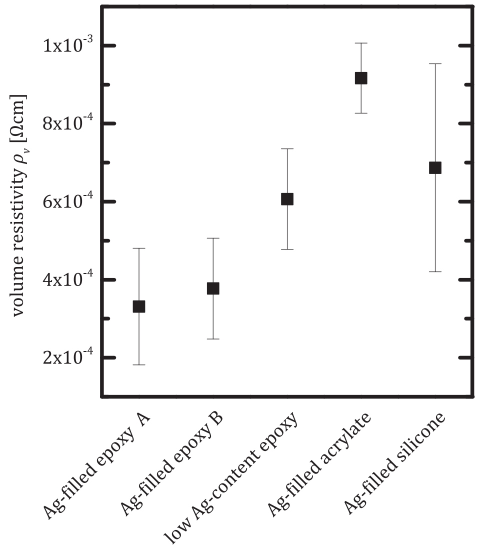

Figure 3. Volume resistivity of ECAs (error bars depict the standard deviation of the set of measurements).

The contact resistivity of a conductive adhesive joint can be determined by the transfer length method (TLM) [21,22]. Ribbons have to be attached perpendicularly to the busbar at successively increasing distances. The resistance between adjacent contacts is determined using a four-point-measurement and then plotted against the distance. The intercept of the linear fit to the measurements with the y-axis is equal to the contact resistance R_c multiplied by two.

The contact resistivity (or specific contact resistance) can be calculated by:

$$\rho_c = R_c L_T Z \quad (2)$$

where L_T = transfer length and Z = length of the contact if a rectangular contact area is assumed.

Contact resistivities for three different glues and various ribbon coatings glued on the busbar can be seen in Fig. 4. Adhesive A is a silver-filled isotropic epoxy and works best on Ag finishes. The contact resistivity for the Ag-coated ribbon is even in the range of that corresponding to a soldered contact. It can be seen that using adhesive B on a SnAg coating leads to a contact resistance that is greater by an order of magnitude. Glue C with SnAg ribbons yields the highest contact resistivity. According to the glue manufacturer, the reason for this is that the ribbon material is not ideally suited to this type of glue.

Contact resistance is typically the dominant electrical loss factor for ECA joints and thus is of particular importance for modules built with ECA. As can be seen in Fig. 4, contact resistance strongly depends on surface metals; glue manufacturers are usually aware of which substrates the glue can be used on. In this test, initial resistance is lowest on Ag- and Cu-finished surfaces. For cost-reduction purposes it may seem reasonable to use bare Cu or Sn-coated ribbons instead of Ag, but those can lead to resistance increases due to oxidation and/or galvanic corrosion during outdoor exposure. Some adhesive manufacturers sell formulations having stable contact resistance on Sn and OSP-treated Cu, which is especially important for the MWT conductive backsheet concept that uses OSP-treated Cu circuitry on the backsheet foil.

Metallography

The inspection of cross sections by using metallographic methods gives an insight into the joint integrity

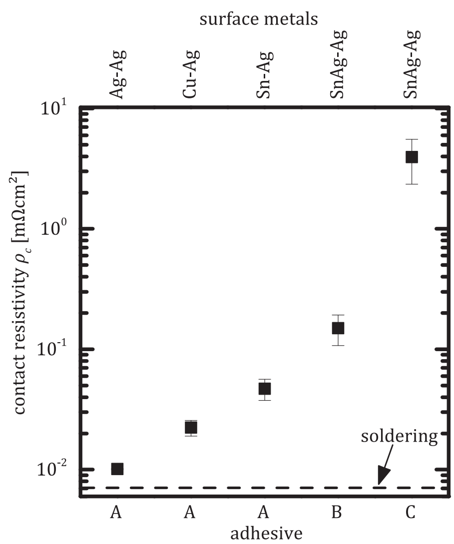

Figure 4. Contact resistivities for conductive adhesives on different ribbon coatings and front-side busbar (error bars depict the standard deviation of the set of measurements).

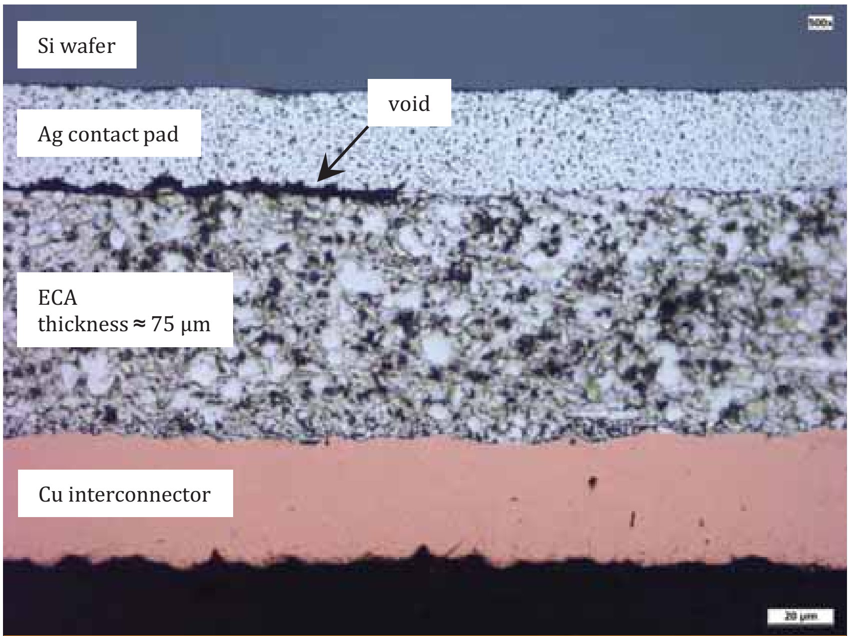

Figure 5. Cross section (500× magnification) of a conductive adhesive bond prepared with metallographic methods. A narrow void is visible between the ECA and the contact pad.

and the morphological structure of the adhesive bond. Metallographic preparation techniques require several cutting and polishing steps [23]. A polished cross section of a conductive adhesive bond of an MWT cell with a copper interconnector can be seen in Fig. 5. Important information – such as bond line thickness, voids, cracks and morphological structure of the glue – can be obtained using this technique.

Dynamic mechanical analysis

To study the mechanical bulk properties of polymers, dynamic mechanical analysis (DMA) can be used [24]. In DMA a sinusoidal force is applied to a bulk sample of an adhesive, and the resulting deformation and phase shift of the material are measured. The storage modulus E', the loss modulus E'' and the damping factor tan δ at various temperatures and frequencies can be calculated from the response. The storage modulus is a measure of the elasticity of the material, whereas the loss modulus is related to the energy that is dissipated in the bulk of the material. The damping factor is an indicator of the material's ability to lose energy through molecular rearrangements and internal friction.

> "DMA is extremely sensitive to material transitions and therefore ideally suited to studying the glass transition of ECAs."

DMA is extremely sensitive to material transitions and therefore ideally suited to studying the glass transition of ECAs. Figs. 6 and 7 show the DMA data for two different ECAs measured in tension mode at 1Hz. The glass transition temperature T_g, determined here as the peak of the tan δ curve, is considerably different for both adhesives: while the T_g of adhesive A is 31°C, for adhesive B it is 113°C. This means that adhesive A can be either soft ($E' < 1000$MPa) or rigid, depending on the operating temperature of the module. Adhesive B, however, will always be rigid within the relevant temperature range. This may give rise to concern about the reliability of the module when the mechanical properties are changing according to the temperature conditions.

Cure kinetics

Curing is an exothermal reaction, and in order to obtain kinetic information about the conductive adhesive the generated heat can be measured using differential scanning calorimetry (DSC) [25]. This method is used in polymer science primarily for investigating phase transitions, such as melting point, glass transition and crystallization.

The partial heat $Q_p(t)$ can be determined by partially integrating the heat flow, as measured by DSC, over time t. If this is then divided by the total generated heat Q_t, information about the degree of cure α over time can be obtained:

$$\alpha(t)=\frac{Q_p(t)}{Q_t} \tag{3}$$

Around 15mg of a typical isotropic silver-filled epoxy was dispensed into sample pans made of aluminium, which were then hermetically sealed. Sample and reference were quickly brought to an isothermal temperature and held until the reaction was finished. Fig. 8 shows $\alpha(t)$ curves for various constant temperatures. It takes eight minutes to fully cure the adhesive at 120°C, but the reaction can be speeded up to under a minute if 170°C is used instead. The large process window and flexibility in curing conditions of most adhesives is one of the major advantages of this technology.

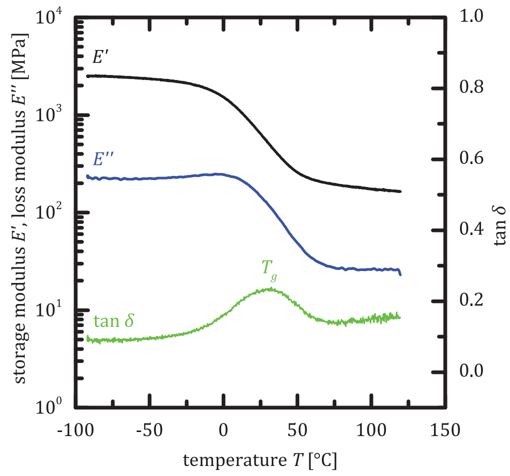

Figure 6. DMA measurement of adhesive A at 1Hz.

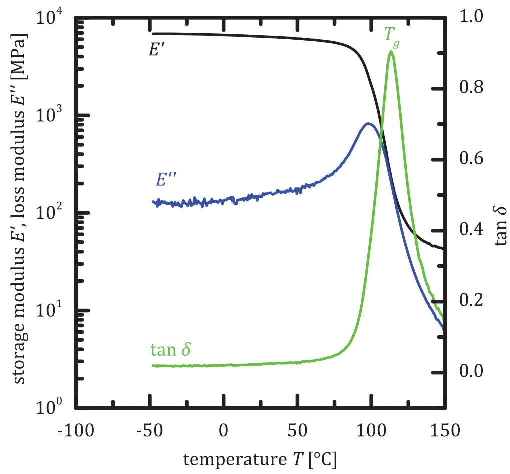

Figure 7. DMA measurement of adhesive B at 1Hz.

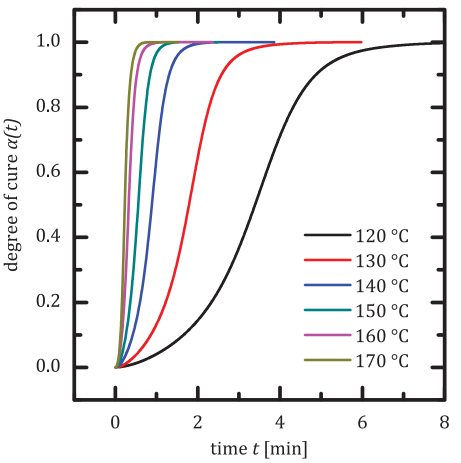

Figure 8. Degree of cure of a conductive adhesive at various constant temperatures.

"The large process window and flexibility in curing conditions of most adhesives is one of the major advantages of this technology."

Curing is a new process step in module fabrication and having control over it is essential in order to ensure reliable interconnections. A model, along with a simulation tool to calculate the cure kinetics for an epoxy ECA and arbitrary temperature profiles, has recently been developed [26,27]. The steps are: 1) establish the model; 2) identify the model parameters with dynamic DSC measurements of the used ECA; and 3) solve the equations numerically.

The model is based on the general rate law, the Arrhenius relationship and an autocatalytic reaction model:

$$\frac{d\alpha}{dt} = A\exp\left(-\frac{E}{RT}\right)\left[\alpha^{m}(1-\alpha)^{n}\right] \qquad (4)$$

where $d\alpha/dt$ = conversion rate, A = pre-exponential factor, E = activation energy, T = absolute temperature, α = degree of cure, and m, n = exponents of the reaction model.

The task is to find values for the parameters A, E, m and n, a procedure for which has been extensively described by Geipel and Eitner [26]. Simulation results of the cure kinetics of a conductive epoxy, for example, are shown in Fig. 9. The temperature profile, represented as the dashed black line, was used as an input. The red curve shows the degree of cure, as calculated using the given temperature profile. The blue line corresponds to a simulation of an isothermal cure at 150°C; the blue squares on this curve show experimental data from the isothermal cure, highlighting the satisfactory accuracy of the model.

If the isothermal cure is compared with the temperature profile cure, one may conclude that the latter, containing an extended ramp-up phase, takes significantly longer (7 min) than the former (2 min) at comparable set temperatures. Thus, knowing the actual time needed to fully cure the adhesive is extremely helpful for process optimizations in the fab.

Conclusions

Conductive adhesives are an alternative interconnection technology well suited to high-efficiency cell concepts with new contact structures, while offering low thermomechanical stress

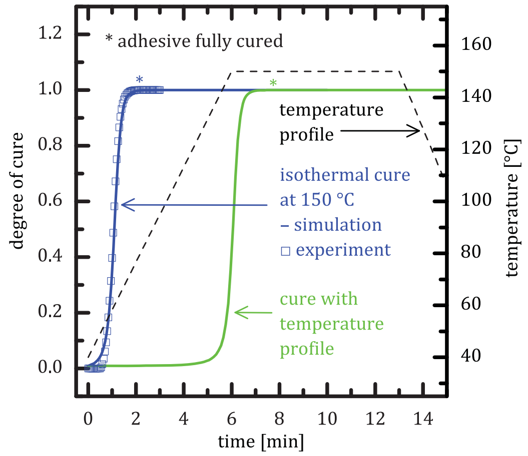

Figure 9. Simulated degree of cure with an arbitrary temperature profile, along with both simulation and experimental data of an isothermal cure at 150°C for comparison.

and high flexibility. To guarantee module reliability for 25+ years, ECAs and the involved processes have to be thoroughly understood using characterization techniques and methods common in PV and well established in polymer science.

This article has discussed a selection of mechanical and electrical methods for determining the relevant characteristics of ECAs, such as peel strength, volume and contact resistance, morphology, glass transition temperature and cure kinetics. The most important findings are summarized as follows.

It was shown that the peel strength of ECAs can reach 1N/mm; work is currently ongoing to further improve this.

The electrical losses of ECA bonds are dominated by contact resistivity, and particular attention must be given to the compatibility of the surface metals. Ag demonstrated the lowest resistivity of typically 0.01–0.1mΩcm^2, which is in the range of that of a soldered contact. Cu, Sn and SnAg yielded significantly higher resistivities (> 0.1mΩcm^2), and the compatibility with an adhesive must be investigated for each specific case. However, if not protected from moisture, all non-noble metals – Sn and Cu for example – during long-term testing are prone to oxidation and/or galvanic corrosion, which can dramatically increase the resistance.

By metallographic investigations it was observed that the most common filler shapes are flakes and spheres with a diameter of 1–10µm. Moreover, the existence of voids is a concern in terms of the adhesive bond quality having an impact on mechanical and electrical performance losses.

Additionally, DMA measurements were carried out in order to investigate the bulk properties of adhesives. Wide variations in glass transition temperature were seen among the adhesives. An interesting question for further discourse is how these differences in mechanical characteristics with regard to the module's operating temperature range can affect reliability.

> "ECA is a technically interesting, reliable and even cost-competitive interconnection technology for high-efficiency solar modules."

Finally, a model was established and used to simulate the degree of cure over time for any given temperature profile for an epoxy ECA. The actual curing time using a specific heating device is usually longer than that for an ideal isothermal cure at a comparable set temperature. In the authors' opinion, ECA is a technically interesting, reliable and even cost-competitive interconnection technology for high-efficiency solar modules.

References

[1] Beier, B. et al. 2001, "Electrical conductive adhesives: A novel reliable method for interconnecting crystalline silicon solar cells", *Proc. 17th EU PVSEC*, Munich, Germany, pp. 812–815.

[2] Bennett, I. et al. 2007, "Low-stress interconnection of solar cells", *Proc. 22nd EU PVSEC*, Milan, Italy, pp. 2674–2678.

[3] Späth, M. et al. 2011, "Hetero-junction module technology", *Proc. 26th EU PVSEC*, Hamburg, Germany, pp. 3121–3124.

[4] Zemen, Y. et al. 2011, "Innovative and gentle interconnection technique for high efficiency c-Si solar cells and cost-of-ownership-analysis (COO)", *Proc. 26th EU PVSEC*, Hamburg, Germany, pp. 3125–3132.

[5] Lamers, M. et al. 2012, "17.9% Metal-wrap-through mc-Si cells resulting in module efficiency of 17.0%", *Prog. Photovolt.: Res. Appl.*, Vol. 20, No. 1, pp. 62–73.

[6] Mishima, T. et al. 2011, "Development status of high-efficiency HIT solar cells", *Solar Energy Mater. & Solar Cells*, Vol. 95, No. 1, pp. 18–21.

[7] Scherff, M.L.D. et al. 2006, "10 × 10 cm^2 HIT solar sells contacted with lead-free electrical conductive adhesives to solar cell interconnectors", *Proc. 4th IEEE WCPEC*, Waikoloa, Hawaii, USA, pp. 1384–1387

[8] Schneider, A. et al. 2012, "Conductive gluing as interconnection technique towards solar cells without front busbars and rear pads", *Proc. 27th EU PVSEC*, Frankfurt, Germany, pp. 335–339.

[9] Adams, R.D. (Ed.) 2005, *Adhesive Bonding: Science, Technology and Applications*, Cambridge: Woodhead Publishing Limited.

[10] Habenicht, G. 2009, *Kleben: Grundlagen, Technologien, Anwendungen*, Berlin, Heidelberg: Springer.

[11] Chunduri, S.K. 2011, "Sticky and cool", *Photon International*, No. 11, pp. 158–165.

[12] Kopeček, R. et al. 2010, "Aluminium rear emitter large area n-type Cz-Si solar cells for industrial application", *Proc. 25th EU PVSEC*, Valencia, Spain, pp. 2381–2386.

[13] Eom, Y.-S. et al. 2010, "Electrical interconnection with a smart ACA composed of fluxing polymer and solder powder", *ETRI J.*, Vol. 32, No. 3, pp. 414–421.

[14] Habenicht, G. 2008, *Kleben - erfolgreich und fehlerfrei: Handwerk, Praktiker, Ausbildung, Industrie*, Wiesbaden: Vieweg+Teubner.

[15] Eitner, U. et al. 2012, "Characterization of electrically conductive adhesives", *Energy Procedia*, Vol. 27, pp. 676–679.

[16] Hinz, I. et al. 2012, "Characterization of electrical conductive adhesives (ECA) for the photovoltaic-industry", *Proc. 27th EU PVSEC*, Frankfurt, Germany,

pp. 3474–3478

[17] Li, Y., Wong, C. & Lu, D. 2009, "Characterizations of electrically conductive adhesives", in *Electrical Conductive Adhesives with Nanotechnologies*, New York, Dordrecht, Heidelberg, London: Springer, pp. 81–120.

[18] Wirth, H. 2010, "Tabbing-stringing quality control challenges", *Photovoltaics International*, 9th edn.

[19] DIN 2007, "Solar Cells – Datasheet information and product data for crystalline silicon solar cells", DIN EN 50461.

[20] U.S. Department of Defense 2010, "Test Method Standard – Microcircuits", MIL-STD-883H.

[21] Berger, H.H. 1972, "Contact resistance and contact resistivity", *J. Electrochem. Soc.*, Vol. 119, No. 4, pp. 507–514.

[22] Schroder, D.K. 2006, "Contact resistance and Schottky barriers", in *Semiconductor Material and Device Characterization*, Hoboken, New Jersey: John Wiley & Sons, pp. 127–184.

[23] Eberlein, D., Schmitt, P. & Voos, P. 2011, "Metallographic sample preparation of soldered solar cells", *Practical Metallography*, Vol. 48, No. 5, pp. 239–260.

[24] Menard, K.P. 2008, *Dynamic Mechanical Analysis: A practical introduction*, Boca Raton, London, New York: CRC Press.

[25] Li, L. & Morris, J.E. 1999, "Curing of isotropic electrically conductive adhesives", in *Conductive Adhesives for Electronics Packaging*, Port Erin, Isle of Man: Electrochemical Publications Ltd., pp. 99–116.

[26] Geipel, T. & Eitner, U. 2013, "Cure kinetics of electrically conductive adhesives for solar cell interconnection", *IEEE J. Photovolt.*, Vol. 3, No. 4.

[27] Geipel, T. & Eitner, U. 2013, "Cure kinetics of electrically conductive adhesives", *Energy Procedia* [forthcoming].

About the Authors

Torsten Geipel received the Diploma degree in information system technology from the Technical University of Dresden in Germany. His diploma thesis concerned 2D simulation methods for silicon solar cells. From 2008 to 2011 Torsten worked on cell and module characterization and reliability testing in the Department of Research and Development at the module and system manufacturer Solon SE in Berlin. He joined the Photovoltaic Modules group at Fraunhofer ISE in November 2011 as a doctoral student, studying electrically conductive adhesives.

Ulrich Eitner studied technical mathematics at the University of Karlsruhe (TH). From 2006 to 2011 he worked in the field of thermomechanics of PV modules at the Institute for Solar Energy Research Hamelin (ISFH) and obtained his Ph.D. from the University of Halle-Wittenberg in 2011. Dr. Eitner has been managing the Photovoltaic Modules group at Fraunhofer ISE since 2011.

Enquiries

Torsten Geipel
Fraunhofer Institute for Solar Energy Systems ISE
Heidenhofstrasse 2
79110 Freiburg
Germany

Tel: +49 761 45885023
Email: torsten.geipel@ise.fraunhofer.de
Website: www.ise.fraunhofer.de

Progress in n-type monocrystalline silicon for high efficiency solar cells

Joel Kearns and **Bo Li**, SunEdison, Inc.

ABSTRACT

Future high efficiency silicon solar cells are expected to be based on n-type monocrystalline wafers. Cell and module photovoltaic conversion efficiency increases are required to contribute to lower cost per watt peak and to reduce balance of systems cost. Past barriers to adoption of n-type silicon cells by a broad base of cell and module suppliers include the higher cost to manufacture a p-type emitter junction and the higher cost of the n-type mono silicon crystal. Technologies to reduce the cost of manufacturing the p-type emitter by diffusion or implantation of boron are being developed in the industry. To reduce the cost and improve further the quality of n-type mono silicon crystal, SunEdison has developed a continuous Czochralski (CCZ) crystal pulling process, based on the technology of Solaicx, acquired in 2010. This CCZ technique allows production of a crystal with much greater resistivity uniformity, with a lower incorporation rate of lifetime-reducing metals impurities, and allows crystal oxygen to be selected independent of production batch size. CCZ is expected to reduce n-type crystal cost below that of current p-type mono crystal.

Advantages of silicon as a solid state material

Silicon, although an indirect band-gap element, has several advantages which have made it the primary material for semiconductor and photovoltaic applications. It is made into a conductor by measured addition of a small amount of electronic impurities, such as boron. It exhibits an acceptable (indirect) band-gap, carrier mobility, bulk minority carrier lifetimes and other electronic properties. It grows a very stable native oxide, allowing the protection and passivation of interfaces. Silicon crystals can be grown threading "dislocation-free" (DF) in large sizes (meters in length and up to 450mm in diameter). The fact that single crystals can be grown threading DF enables the agglomeration of chemical and native point defects into specific bulk micro-defects not possible in materials possessing dislocations. Some of these defects can be advantageous in semiconductor manufacturing (oxygen defects used for internal/intrinsic gettering of process-added impurities) and some unwanted (oxygen clusters and precipitates which are physical recombination centers, reducing lifetime). Silicon is abundant; it is the second most common element in the Earth's crust, bound in silicates. The cost of the purified raw material – solar or electronic grade polysilicion – is relatively low and can be bought in high purity in large volumes. Finally, silicon technology for solar cell materials benefits from over 50 years, sustained investment in research and development by the semiconductor silicon industry.

Monocrystalline silicon wafers show very high minority carrier lifetimes compared to multicrystalline wafers, due to the absence of grain boundaries, dislocations, electrical-active decorated metals on those structural defects and excessive background metals; these defects in multicrystalline silicon reduce photovoltaic conversion efficiency due to the many types and large density of carrier recombination centers.

Advantages of n-type monocrystalline silicon

The champion silicon photovoltaic conversion efficiencies, without stacked multi-junctions or concentrators, have been demonstrated on n-type Heterojunction with Intrinsic Thin layer (HIT) and inter-digitated back contact (IBC) cells [1, 4, 6]. In 2013, Panasonic produced a record 24.7% cell conversion efficiency using its HIT architecture on a thin (98 um) cell with a surface area of 101.8 cm^2 [2]. Panasonic's 2013 production cell efficiency, using a similar earlier generation architecture, has been independently estimated as 21.6%. In 2012, Sunpower demonstrated 24.2% using its third generation "Maxeon" IBC cell, and offers modules with up to 20% efficiency [3, 6]. An IBC cell must be fabricated using silicon wafers with a large minority carrier diffusion length, for all the charge carriers to reach the emitter, since the p-n junction is deliberately located at the rear of the cell.

N-type silicon exhibits a stable, high minority carrier lifetime [6, 17]. Diffusion lengths of minority carriers (holes) in n-type silicon are much higher than for electrons in p-type silicon. N-type silicon does not exhibit light induced degradation seen in p-type silicon, allowing increased values of stabilized cell efficiency. Light induced degradation (LID) is an immediate, light activated reduction in material bulk minority carrier lifetime leading to lower photovoltaic conversion efficiency. LID has been shown to be a strong function of boron and oxygen concentration [5]; in p-type silicon, boron is the impurity deliberately added to provide electrical resistivity. In p-type monocrystalline silicon, the initial conversion efficiency can be reduced by 0.5-3% (relative) by LID, due to the boron and oxygen defect effect on lifetime. Since the reduction is to a value of lifetime set by the boron-oxygen defect concentration in the crystal, as advanced devices are made which allow higher initial lifetimes due to reduced surface recombination, the decrease due to LID is even more evident. N-type silicon avoids this condition as no appreciable concentration of boron is present (oxygen concentration may be the same as for p-type ingot).

N-type silicon exhibits a higher lifetime tolerance for most common bulk metallic impurities (e.g., Fe) [6, 9]. Tolerance for Co and W was also demonstrated. This led to an early expectation that n-type mono silicon would be relatively impervious to metals addition, but this is not accurate. Certain impurities and defects can decrease lifetime in n-type silicon (e.g., Cr). Cr can affect n-type cell efficiencies at concentrations as low as 10^{10} atoms/cm^3 [16]. Cu can also strongly reduce the lifetime of n-type silicon, similar

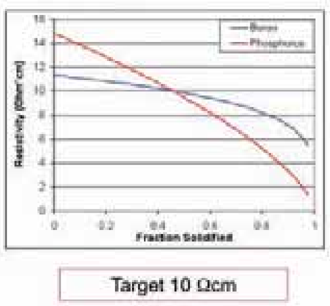

Figure 1: Calculated Crystal Resistivity Distribution for Boron and Phosphorous Doped crystal grown by Czochralski technique

to its effect on p-type silicon [15] So n-type silicon is resistant to some common metals, but not all metals.

The *International Technology Roadmap for Photovoltaics* predicts n-type mono-crystalline material to reach ~10% of the total Si solar module market by the year 2015, and over 30% by 2023 [8]. This roadmap predicts a substantial shift from p-type to n-type mono-Si within the mono-Si material market [8]. Past barriers to adoption of n-type silicon cells by a broad base of cell and module suppliers include the higher cost to manufacture a p-type emitter junction and the higher cost of the n-type mono silicon crystal. Technologies to reduce the cost of manufacturing the p-type emitter by diffusion or implantation of boron are being developed in the industry [1].

Crystal growth technology defines the cost of the n-type crystal

The Czochralski (CZ) method of crystal pulling is used to economically produce large amounts of dislocation-free, single orientation ('mono') silicon for photovoltaic conversion applications. Most of this crystal is p-type, doped with boron. In the CZ method, a single crystal of silicon is grown by pulling a seed of the desired crystal orientation from the melt contained in a fused silica crucible. The CZ method is a batch process in that a crystal is pulled from a single crucible charge; the crucible is used once and is discarded after use. To increase yield per crystal growth operation and reduce unit crystal growth cost, strategies such as larger starting charge sizes or pulling several crystals sequentially from a single crucible after 'recharging' the melt with additional polysilicon, have been employed in high volume, large-scale production. However, a disadvantage of recharging the melt can be that unwanted impurities can build up in the residual melt between recharges, due to macro-segregation. These impurities can lead to a variety of lifetime-reducing recombination centers that degrade solar cell efficiency.

The crystals are grown in the shape of right circular cylinders. To convert them to the 'pseudo-square' shape needed for solar cells, the crystals are cut from a circular to a roughly square cross section shape, and the roughly 27% mass 'wings' of the original crystal are diverted as recycle silicon for future mono crystal growing or to cast multi-crystalline silicon ingots. The wings are not directly used in making the cell on the wafers sliced from the crystal. They are recycled and offset ~27% by mass the need for virgin polysilicon, contributing to lower cost of the combined polysilicion plus crystal conversion cost.

Unique challenges of n-type silicon crystal

Phosphorous is used as the n-type crystal dopant, just as it is for semiconductor device processing. During CZ crystal growth, phase diagram partition segregation of phosphorous will lead to a wide range of resistivity along the crystal length and from wafer to wafer. Figure 1 calculates and compares the resistivity distribution down the length of two CZ crystals both nominally targeted at 10 ohm-cm, one crystal p-type (boron dopant) and the other crystal n-type (phosphorous dopant). While the ratio of seed-end resistivity to tail-end resistivity for a boron doped crystal will often be slightly less than 1.8, the ratio for a phosphorous doped crystal can be 7. How detrimental this is depends on the base resistivity specification upper and lower limits for the particular device – that is, how much electrical properties are changed because of the value of base resistivity. Since there is always some error in the dopant concentration produced in the crystal – from measurement error of the dopant or polysilicon amount, variation in the crucible shape from suppliers, etc. – there is additional variation introduced from crystal to crystal. Yingli Solar reported that in high volume manufacturing, new necessary procedures had to be implemented to minimize the yield loss from resistivity non-uniformity along the length of the n-type crystals [18].

This large range of resistivity is therefore also in the 'wings' slabbed from the crystal sides as waste from making the pseudo-square shaped ingot from the crystal. If the wings possess varying resistivity down their length, they must be carefully matched to similar resistivity sections for recycling and use in future n-type crystal growth runs; the amount of dopant to add in that run will depend on the amount of dopant already introduced in the form of recycled wings. This need to match and bin resistivity of the recycled material adds cost to the growth of n-type crystals. The n-type wings cannot be used as source poly for p-type multicrystalline ingots, or the ingots may be compensated; the n-type wings must be recycled for n-type mono growing, or roughly 27% more virgin polysilicon must be added to offset the lost wings.

Oxygen is an unavoidable chemical impurity in CZ-grown monosilicon crystals; the oxygen is introduced from dissolution of the fused silica crucible which holds the molten silicon during growth. In addition to generating LID in p-type crystal, high oxygen concentrations combined with particular but common crystal growing conditions can encourage oxygen atoms to cluster in the silicon. This leads to nano-scale microstructures, which act as charge carrier recombination centers. If oxygen concentration is high enough in the starting crystal, and cell temperatures high enough during cell manufacture on the wafers, the oxygen clusters can form with silicon a secondary silicon-oxide phase with a defined boundary, which again acts as a carrier recombination centre. Both of these types of defects would trap charges, reducing lifetime and diffusion length. Although this oxygen behavior is not unique to n-type, the recombination centres it produces can have a profound effect on the normally high lifetime n-type material, dramatically reducing the lifetime after specific cell processing steps. To preclude this, the n-type silicon may have to be grown using more complex CZ techniques, or the higher oxygen sections of crystals screened out for device use and recycled as feedstock, lowering first pass crystal yield. Both of these increase costs compared to p-type silicon grown by CZ technique.

Continuous CZ to produce n-type crystal

Continuous CZ (CCZ) can produce near-uniform resistivity mono wafers [11]. CCZ can provide quasi-steady state heat and mass transfer conditions during pulling, and produce multiple crystals during a single operation, by continuously adding polysilicon and electronic impurities during the crystal growth itself. Macroscopic crystal axial

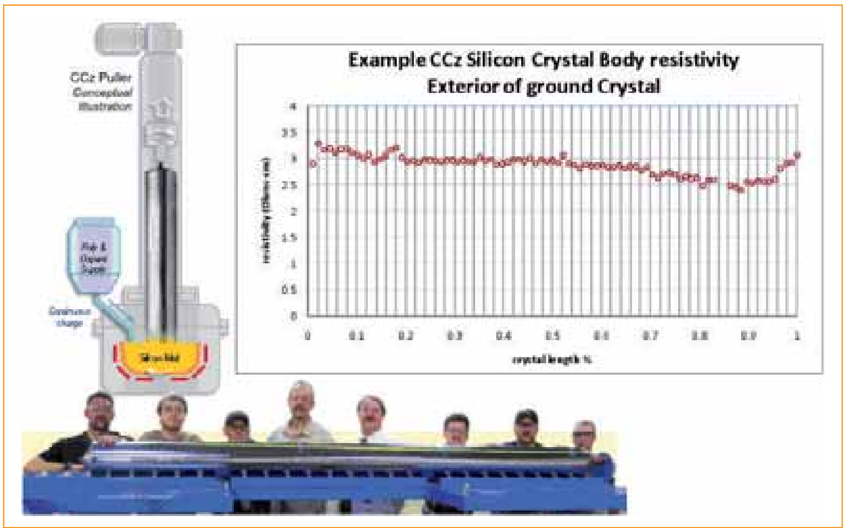

Figure 2: Crystal grown by Continuous Czochralski Technical, notional pulling process, and measured within crystal axial resistivity uniformity.

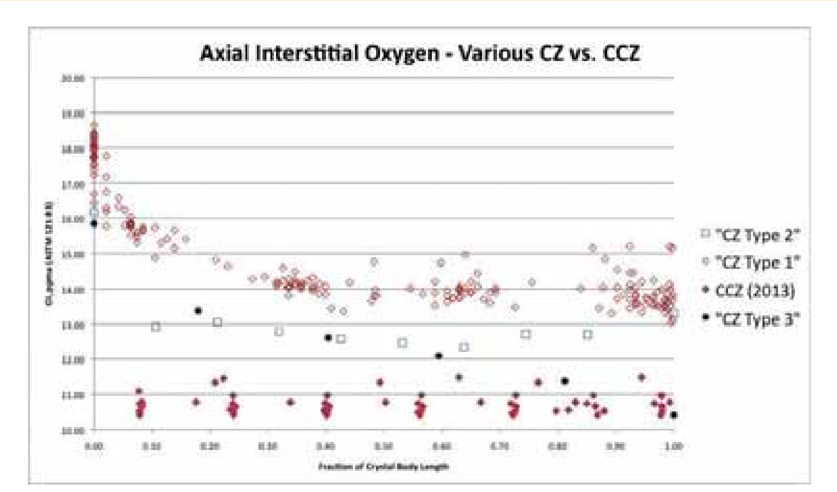

Figure 3: Measured axial crystal interstitial oxygen comparing CCZ to various CZ methods.

impurity variation is inherent in the CZ 'batch' growth process due to macro-segregation phenomena during normal freezing conditions. By continuously controlling charging of both polysilicon and dopant via CCZ, the resistivity is directly controlled.

Bulk chemical inhomogeneities in crystals grown by the conventional CZ method are a direct result of phase partitioning combined with the melt volume reduction during crystal growth. The CCZ method can be used to reduce the production cost of crystals as wells as to grow crystals under quasi-steady heat and mass transport conditions, leading to quasi-uniform structural and chemical defect distributions. The CCZ process can be designed to lead to a much slower build-up of impurities than sequential melt replenishment. It has been shown that a lower impurity build-up, and greater axial uniformity of impurities incorporated, can be achieved by the CCZ method when compared to either the conventional or sequential multiple crystal growth CZ methods [11, 12].

For more than 55 years, CCZ has been an anticipated silicon manufacturing breakthrough [10]. Research at all major silicon manufacturers (i.e., MEMC, Motorola, SEH, Siltronic, Toshiba) plus by the US government, Russia and numerous universities, did not generate a high volume manufacturing CCZ process. Several promising crystal growing configurations were generated, but were not demonstrated to have the cost or repeatability for high volume manufacturing [13,14]. However, a production-scale CCZ process has been demonstrated and is being implemented by SunEdison [11, 12]. Figure 2 shows a representative long crystal generated by the CCZ process, as well as the level resistivity along a crystal body length [11, 17]. Figure 3 shows the oxygen exhibited by CCZ process compared to representative CZ crystals grown for solar application [12].

For n-type solar cell crystal substrate, there are several benefits of the CCZ approach for n-type mono-silicon [11,12]:

1. Metered dopant/polysilicon introduction during crystal growth allows for 'uniform' axial resistivity for both p-type and n-type and improves crystal manufacturing yield (particularly for dopants with segregation coefficients <<1, such as Phosphorous). There are fewer 'bins' of solar cell power output and cell efficiency, in those cases where power or efficiency is greatly influenced by the value of base resistivity.

2. It can prevent a gradual build-up of unwanted impurities (i.e. C, metals); metals are a major determiner of lifetime.

3. The oxygen concentration can be decoupled from crucible size and crystal diameter, and relatively low oxygen concentrations obtained over long crystal lengths without use of a magnet to change the molten silicon flow conditions.

4. Many long body crystals are produced from each CCZ production run, spreading out cost per run for specialized or unusual consumables.

5. The crystal/ingot length is determined by 'height of building' (length of pull chamber) instead of crucible and hot zone and puller tank size. This allows longer crystals (and more wafers) to be made in a run without increasing the size and cost of the consumables or the production equipment.

6. The continuous supply of fresh polysilicon during body growth allows modification (shortening) of the sequential charge-melt-stabilize-grow-remove cycle for crystals.

7. Constant melt height maintains targeted bulk crystal growth conditions. The process can be designed to maximize crystal body pull speed for higher crystal productivity.

8. Quasi steady-state distribution of bulk micro-defects in the crystal can be realized from the quasi stead growing conditions. The majority of crystal length can cooled under similar conditions, which should lead to similar grown-in micro-defects in wafers produced from each crystal.

Conclusion

It is likely that solar cell architectures will migrate from 'traditional' p-type Al back-surface field (BSF) cells to more advanced p-type cells and ultimately to n-type cells, due to cost/watt-peak reductions needed for modules and the independent impact on balance-of-systems economics. This increased efficiency should be particularly beneficial to residential installations. One barrier to adoption of n-type high efficiency cells is the cost of n-type mono crystal. CCZ is being developed or implemented by several companies to enable a large supply of n-type Si for high efficiency Si cells. This will allow avoidance of crystal yield loss from both resistivity extremes due to axial phosphorous segregation as well as high oxygen concentration. It will also potentially reduce the number cell bins, when that binning is influenced by the base resistivity. CCZ can enable more uniform material properties and reduced wafer costs.

There are several different technical approaches to CCZ being implemented by different equipment makers and wafer suppliers. The specific CCZ technical approach will determine if productivity is high and conversion cost is low enough to be implemented for solar PV applications, but it is likely that at least one approach will be successful.

References

[1] A. Lanterne, S. Gall, Y. Veschetti, R. Cabal, F. Miles, M. Coig and A. Tauzin, PVTC 2013, Aix en Provence, France.

[2] Panasonic Press Release, "Panasonic HIT Solar Cell Achieves World's Highest Conversion Efficiency of 24.7% at Research Level", February 12, 2013. Retrieved from http://panasonic.co.jp/corp/news/official.data/data.dir/2013/02/en130212-7/en130212-7.html.

[3] Sunpower document 001-65754RevA, 2011.

[4] P. Cousins, Proceedings 36th IEEE Photovoltaic Specialists Conference, Hawaii (2010).

[5] K. Bothe, J. Schmidt, and R. Hezel, Proc. 29th IEEE Photovoltaic Specialists Conference, New Orleans, LA, (IEEE New York 2002), 194.

[6] I. G. Romijn, J. Anker, A. Burgers, A. Gutjahr, B. Heurtault, M. Koppes, E. Kossen, M. Lamers, D. Saynova and C. Tool, presented at China PV Technology International Conference (CPTIC), 20-22 March 2013, Shanghai, China.

[7] S. Glunz, Proceedings 2nd WCPEC Vienna, Austria 1998, 1343.

[8] *International Technology Roadmap for Photovoltaic*, Fourth Edition, March 2013, www.itrpv.net.

[9] D. Macdonald and L. Geerligs, *Applied Physics Letters 92 (2008)*, 4061.

[10] G. W. Rusler, *United States Patent 2892739*, June 30, 1959.

[11] J. Kearns, J. Holzer, R. Nandan, J. Binns and E. Good, "N-type Mono CZ Silicon: Continuous Czochralski Silicon for high efficiency n-type solar cells", presented at the 23rd Workshop on Crystalline Silicon Solar Cells & Modules: Materials and Processes, Breckenridge, Colorado, July 28 2013.

[12] J. Kearns, J. Holzer and R. Nandan, "Continuous Czochralski Silicon for high efficiency n-type solar cells", presented at the 19th American Conference on Crystal Growth and Epitaxy, Keystone, Colorado, July 23, 2013.

[13] N. Ono, M. Kida, Y. Arai and K. Sahira, J. Electrochemical Society, 140, 7 (1993) 2101.

[14] C. Wang, H. Zhang, T. Wang and T. Ciszek, *Journal of Crystal Growth 250* (2003) 209-214.

[15] K. Stewart, A. Cuevas, D. Macdonald and J. Williams, Proc. 11th Workshop on crystalline silicon solar cell materials and processes, Estes Park,Colorado, 2001, 212–215.

[16] J. Schmidt, 22nd European Photovoltaic Solar Energy Conference, 3-7 September 2007, Milan, Italy

[17] Capital Markets Day Presentation, SunEdison, 13 March 2013.

[18] Faye Li, Yingli Solar, High Efficiency Low Cost N-Type Si Solar Cell In Mass Production, nPV workshop, 2012, Amsterdam

About the Authors

Joel Kearns is Vice President for Solar R&D and directs SunEdison's work in crystal growth for solar. He worked at NASA and SUMCO after his Masters degree from Worcester Polytechnic Institute, and is working on his Ph. D. He authored 12 papers and 4 patents for crystal growth.

Bo Li is currently the General Manager of Solar Cells at SunEdison. He was the Cell Technology Director at SunEdison. Prior to that, Bo spent 6 years at SunPower Corporation as an Engineering Manager and Cell Technologist Principal developing high efficiency (23+%) cost effective interdigitated back contact solar cell. Bo started his professional career in semiconductor industry, where he designed, developed and commercialized bottom anti-reflective coatings that enabled industry's 65nm, 45nm technology and beyond. He has a total of 30 US/International patents and patent applications relating to semiconductor materials and processes as well as solar cell and module.

Enquiries

Joel Kearns
Sunedison, Inc.
501 Pearl Drive (City of O'Fallon)
St. Peters, Missouri 63376 USA
1-636-474-5367
joelkearns@sunedison.com or
bli@sunedison.com

Cell Processing

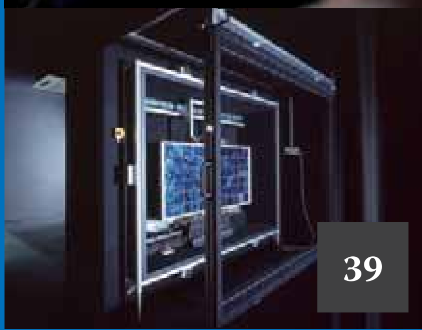

First Solar to manufacture China Sunergy cells achieve conversion efficiency record of 20.26%

China Sunergy has announced its monocrystalline solar cells reached a record 20.26% efficiency during pilot research and development with the record certified by the Fraunhofer Institute for Solar Energy Systems (Fraunhofer ISE), the largest solar research centre in Europe. China Sunergy claims the new record breaking cell is the result of a combination of breakthroughs with its previous cells, Waratah and QSAR. Using a new design structure with normal wafers, China Sunergy was given ISE certification as the leading conversion level amongst Chinese PV companies. The company plans for mass commercial production of the new high-efficiency cell to start by the end of next year and has installed a 70MW capacity production line. The high-efficiency cell surpasses the benchmark of 20% conversion efficiency, set by development guides by the state council for China's photovoltaic industry, in July 2013.

China Sunergy cells have achieved a conversion efficiency record of 20.26%.

Cell efficiencies

Hareon Solar reveals PERC and IBC cells developments

Hareon Solar Technology has demonstrated new technological developments for both Passivated Emitter and Rear Cells (PERC) and Interdigitated Back Contact (IBC) solar cells.

Hareon Solar noted that its IBC-based cell used a novel process to reduce costs, yet claimed a peak cell efficiency of 19.6%. IBC cells are expected to provide conversion efficiencies of over 24%. Its 'Andes' series solar cell, which employed highly passivated rear surface to minimize loss, was reported to have achieved batch average efficiency of 19.9%. Hareon Solar's Andes cells were said to be in pilot production.

JA Solar monocrystalline cells top 20% conversion efficiency.

Source: JA Solar

JA Solar monocrystalline cells top 20% conversion efficiency

Chinese solar cell producer JA Solar's new p-type monocrystalline silicon ('mono-Si') solar cells have surpassed a conversion effiency of 20%, as verified by the PV calibration lab at the Fraunhofer Institute for Solar Energy Systems (Fraunhofer ISE), Freiburg, Germany.

According to JA Solar, this puts the company's new range of solar cells, trade-named PERCIUM, at the forefront of industry efficiency standards for industrial size solar cells that use p-type mono-Si wafers. JA Solar aims to integrate PERCIUM cells into commercial module assembly lines for mass production.

The company also reported a record cell efficiency of 18.3% for a standard (156x156 mm2) multicrystalline solar cell, verified by Yangzhou Opto-Electrical Products Testing Institute in China.

Solar3D touts leap forward in cell design

PV start-up Solar3D has claimed the use of an unspecified "thinner" silicon wafer substrate in prototyping its technology has achieved improved cell efficiency of 10% above its 25% cell efficiency claimed in 2012. The results have not been verified by a third party.

The start-up also claimed that its 3D cell had a wider angle of light capture than previous designs, boosting low-light operation beyond existing cell designs.

Taiwan boon

Taiwan cell producers the only beneficiaries of trade war, says report

According to Taiwan-based research firm, EnergyTrend, Taiwan-based solar cell producers shipped 3.2GW of cells in the first half of 2013 on the back of anti-dumping duties against China in the US and EU.

EnergyTrend said 16% of the worldwide solar cell shipments in the first half of 2013 came from Taiwanese producers. Taiwanese PV cell shipments grew by 6.7% compared to H1 2012.

EnergyTrend said that Taiwanese solar cell producers benefited from the anti-dumping duties but also from the higher cell efficiencies they offer compared to their Chinese competitors as well as offering PID-free products.

Hareon Solar to build 300MW solar cell plant in Taiwan

In late July, a potential shift by Chinese PV manufacturers to avoid anti-dumping duties in the US and EU as well as in India included the move by Hareon Solar to build a 300MW solar cell plant in Taiwan.

The China-based company signed a memorandum of understanding with Mascotte Holdings, which acquired polysilicon start-up, Sun Mass Energy, last year. Sun Mass Energy is using a proprietary 'hydrogen-assist-reductive-combustion' process for producing polysilicon, claimed to reduce costs to around US$12/kg.

Neo Solar Power monthly sales pass US$67.2 million following DelSolar merger

The merger of Taiwan-based solar cell producer Neo Solar Power (NSP) and Delsolar was successfully completed on May 31.

The merged companies fall under the Neo Solar Power Corporation name but will have two seats on its board occupied by Delta Electronics executives.

The merger and continued strong demand for solar cells pushed Neo Solar Power's monthly sales past NT$2 billion (US$67.2 million) in August 2013. NSP stated as the merger went ahead that the company's order visibility extended to Q3 2013.

Business news focus

Amtech continues to reduce headcount to weather solar equipment drought

Specialist equipment supplier Amtech continues to reduce staffing levels as one of a series of measures aimed at reducing costs. The company reported FY third quarter 2013 sales of US$10.4 million, including US$6.5 million in its solar segment. The company incurred non-cash inventory write-downs of US$4.4 million and a stock compensation expense of US$1.6 million. Net loss for the quarter was US$12.1 million.

Centrotherm photovoltaics ends bankruptcy but loses CEEG contract

In early June, Centrotherm Photovoltaics successfully restructured the company under insolvency proceedings, securing around 900 jobs.

Ulm District Court in Germany approved the company's insolvency plan, enabling the company to operate independently once again. Subsidiaries Centrotherm Thermal Solutions and Centrotherm Si-Tec, are also expected to have proceedings halted.

Creditors have agreed a debt-for-equity swap and will hold a majority share in the company. The company said that the restructuring has also secured its stock market listing, central to creditors potentially recouping debts completely.

Centrotherm said it would continue to allocate expenditure to focus on next-generation R&D.

Low solar sales continue at BTU International

Thermal processing equipment specialist, BTU International reported second quarter 2013 sales of $14.2 million, up 35.6% compared to $10.5 million in the preceding quarter, due primarily due to sales in the electronics industry. However, the company noted it had few solar sector sales in the quarter as overcapacity remained.

Manz expects record growth year without solar equipment sales contribution

The strategy to diversify from dependence on sectors such as solar is proving to be a success for equipment supplier Manz AG.

Manz reported record quarterly sales of €87.9 million and guided full-year sales to the highest in its history of between €250 million to €260 million.

However, the solar segment accounted for only 1.2% of the company's order backlog, while the high-growth in its Display division was said to be the main driver of sales growth during the first six months of 2013.

SEMI PV equipment book-to-bill showed historic lows in first quarter 2013

According to the SEMI PV manufacturing equipment supplier book-to-bill survey, which last posted findings in early July, orders and sales remained at unprecedentedly low levels in the first quarter of 2013.

In the first quarter of 2013, SEMI, said that worldwide billings declined to US$291 million, a 41% decline from the prior quarter and 58% below the same quarter a year ago.

Worldwide bookings for the first quarter dropped to US$174 million, 17% below the previous quarter and 71% lower than the first quarter of 2012.

The long down-cycle for equipment sales is apparent with it being the eighth consecutive quarter when the book-to-bill ratio stayed below parity and stood at 0.60 in the first quarter of 2013.

Manz expects record growth year without solar equipment sales contribution.

Upstream recovery

Asia-based solar cell customer qualifies Invetac's ion implant tool

Specialist PV equipment manufacturer, Intevac said it had successfully qualifiedits 'ENERGi' ion implantation production system that was announced and shipped in the first quarter of 2013 to an unidentified large solar cell manufacturer based in Asia. Invetac stated that the unidentified manufacturer is a Tier 1 producer.

The ENERGi ion implant system is said to employ a continuous flux ion source system that offers a replacement for diffusion based POCl3 doping systems, while providing doping for improved emitter profiles boosting cell efficiencies.

The tool was said to have a throughput of 2,400 wafers per hour for both P- and N-type wafers.

Meyer Burger cites turning point in PV equipment orders

Major equipment supplier Meyer Burger reported a better than expected order intake over a six week period this summer, citing it as a "turning point in customer behaviour."

Meyer Burger said that it expected customers to start making new capital investments in wafer, cell and module manufacturing lines during the second half of 2013 and continuing to develop in 2014. As a result, Meyer Burger expects increasing levels of orders and sales.

Meyer Burger also noted that it expected to sign order contracts for its heterojunction solar cell processing equipment as well as further orders for its 'SmartWire' connection technology that would include the purchase of integrated production lines.

DuPont reports increasing PV materials demand

Reduced silver consumption and lower silver prices meant DuPont's Electronics & Communications division reported an 18% decline in second quarter 2013 sales of US$653 million.

However, the company reported that on a sequential basis, total segment volumes increased by about 10% on higher PV installations, notably in China, and broad-based demand improvements, which were said to continue in the second half of the year.

DuPont said that in the third quarter, earnings would continue to improve from the second quarter, despite expected price declines for silver, which are being passed directly to customers, especially in the PV industry.

SoLayTec installs first two production ALD tools in Asia

In a rare move in the current low of capital spending and meager signs of a technology buy cycle, PV equipment specialist SoLayTec has installed its first two mass production ALD (Atomic Layer Deposition) tools at high-efficiency solar cell manufacturers based in Asia. Names and financial details were not disclosed.

SoLayTec said that the new orders took the tally of 'InPassion' ALD tool, for depositing Al2O3 in mass production deliveries to eight, making the company the current market leader of spatial ALD technology used in the PV industry.

ACT Aurora Control Technologies bags another evaluation project

Inline measurement systems start-up ACT Aurora Control Technologies said it had entered into a new evaluation agreement for its Decima tool.

The company will be working with an unidentified solar cell equipment supplier on the Decima's measurement and control capabilities of various emitter formation processes.

The equipment supplier was said to be a leading provider of coating and thermal processing equipment.

RENA and Tempress Systems win 100MW advanced cell line contract from US-based Nexolon

Wafer producer Nexolon, which plans to invest more than US$115 million to become a major US-based PV module manufacturer has selected the n-PASHA Alliance (RENA, ECN and Tempress Systems) to provide its advanced n-type solar cell technology for bi-facial module production.

The n-PASHA Alliance has won a 200MW turnkey equipment and process order, which will be organized in two 100MW phases for Nexolon's facility Texas.

Nexolon America plans to generate over 400 jobs at the new manufacturing plant.

China drives increased materials demand for DuPont.

Product Reviews

3D-Micromac

3D-Micromac's PERC cell process offers improved price to performance ratio

Product Outline: 3D-Micromac has developed a novel, highly productive laser system for opening the rear sides of PERC cells. Innovative on-the-fly technology makes it possible to achieve an improved cost-benefit ratio. The system is modular, combinable with different laser-source technologies and achieves a typical efficiency increase of up to one percentage point.

Problem: PERC cells are photovoltaic cells made of crystalline silicon having special, optimized rear-side passivation. A PERC cell's rear side is completely coated with a non-conductive, dielectric SiOx/SiN or AlOx/Sin layer. The task is to open this layer with the aid of point or line patterns using lasers without damaging the underlying silicon in order to later apply a metal layer for contacting.

Solution: 3D-Micromac relies on its 'on-the-fly' technology, which is claimed to offer the highest productivity with an excellent price-performance ratio, leading to an increase in cell efficiency. The productivity advantage is due to the handling and individual positioning procedures of the cells, which are eliminated. The cells are instead transported under the laser source on a conveyor belt, which renders alignment stops superfluous. The integrated optics automatically compensates for the cells' relative motion and scribes exactly the desired pattern into the cell's sensitive rear side.

Applications: PERC cell passivation.

Platform: The system is being initially offered as a stand-alone variant; however it can also be completely integrated into existing production automation. The structuring platform from 3D-Micromac is also suitable for processing of selective-emitter, MWT, and EWT cells.

Availability: Already available.

BTU International

BTU's SinTerra metallization firing furnace designed for low-cost production

Product Outline: BTU International has launched its new 'SinTerra' metallization firing furnace that offers outstanding value by providing high-performance heating and cooling technologies. SinTerra delivers the lowest cost of ownership with industry-leading uptime, unmatched process repeatability and competitive pricing, according to the company.

Problem: PV cell manufacturers remain under tremendous pressure to wring cost out of their manufacturing lines while increasing efficiency. Very fast ramp rates are required to optimize contact formation on silicon wafers. Rapid ramp rates are constantly pushing for faster belt speed, which in turn drives the overall length of the firing furnace. Uptime, reliability and cost of ownership are also becoming increasingly important.

Solution: The contact firing and metallization application is used in the manufacturing of silicon solar cells. The final step is performed in the metallization furnace. The metallization furnace actually integrates four process steps into one tool: drying to remove the last solvent, burnout to remove the binder, firing to form the electrical contact and finally the cool down. SinTerra, the latest technology for metallization drying and firing from BTU, was designed to meet that challenge, with superior thermal performance, including fast ramp rates, all while enabling lower cost manufacturing through high uptime and high throughput.

Applications: Silicon solar cell contact firing and metallization.

Platform: SinTerra is claimed to have the best-in-class uptime/reliability (98%) coupled to the lowest cost and short lead-times due to being manufactured in China. The system employs fast spike heating and convection cooling for process repeatability.

Availability: April 2013 onwards.

Heraeus

'SOL202' from Heraeus offers 45% less silver content in back-side tabbing

Product Outline: Heraeus Photovoltaics Business Unit is featuring its low silver content back-side tabbing pastes for conventional c-Si solar cells, the SOL202 Series. The back-side tabbing paste is said to contain 45% less silver than previous versions while providing 18% better adhesion, according to the company.

Problem: Silver remains a high-expense item in solar cell manufacturing, forcing PV cell manufacturers to look for ways to reduce usage, while retaining silver's inherent qualities.

Solution: The SOL202 Series enables the back-side tabbing of a string of cells using Ag conductor paste for mono and multicrystalline silicon wafers. SOL202 requires less paste per cell than previous generations and maintains the advantage of printability ease and excellent cell adhesion. The paste is co-fireable with back-side aluminum and front-side silver pastes. SOL202 is a Pb and Cd free material that has excellent solderability in both lead and lead-free solders, according to the company. This reduction in silver usage, combined with excellent performance, will assist solar cell manufacturers in reducing their cells' cost per watt.

Applications: Solar cell back-side tabbing process.

Platform: Typical properties include a viscosity of 70–130 kcps and solderability of 96.5Sn/3.0Ag/0.5Cu. Guidelines may vary based on manufacturing process. Drying in an IR dryer with set points of 250–300°C in less than 20 seconds or 150°C for 10 minutes in circulated air oven.

Availability: July 2013 onwards.

Emitter technology options for industrial PERC solar cells with up to 20.3% conversion efficiency

Thorsten Dullweber[1], Helge Hannebauer[1], Christopher Kranz[1], Rene Hesse[1], Sabrina Wyczanowski[1], Vikram Bhosle[2], Chris Dubé[2], Katrin Weise[3], Franck Delahaye[3], Oliver Doll[4], Ingo Kohler[4], Rolf Brendel[1] & Franck Delahaye[3]

[1] Institute for Solar Energy Research Hamelin (ISFH), Emmerthal, Germany
[2] Applied Materials, Varian Semiconductor Equipment, Gloucester, Massachusetts, USA
[3] RENA GmbH, Freiburg, Germany
[4] Merck KGaA, Darmstadt, Germany

ABSTRACT

Passivated emitter and rear cells (PERC) are considered to be a next generation of industrial solar cells, and several companies have already started pilot production. The much-reduced rear-surface recombination in PERC cells requires improvements to the front side, for example the emitter, in order to further increase the conversion efficiency in the future. This paper presents an evaluation of the emitter technologies of three industrially applicable PERC cell concepts: 1) with an ion-implanted emitter, 2) with a chemically polished rear surface, and 3) with a selective emitter formed by gas phase etch-back (GEB). The results are compared with a reference high-efficiency $POCl_3$-diffused PERC cell. The three industrial PERC concepts utilize lean industrially applicable process flows which reduce the phosphorus concentration at the wafer surface. Accordingly, when compared with the $POCl_3$-diffused emitter, the ion-implanted and GEB emitters obtain significantly lower emitter saturation current densities of 40 to 60fA/cm^2 for emitter sheet resistances of 90 to 130Ω/sq. When applied to large-area PERC cells with screen-printed metal contacts, the ion-implanted and GEB emitter cells demonstrate up to 10mV higher open-circuit voltages than the $POCl_3$-diffused reference PERC cell, and achieve conversion efficiencies of 20.0 and 20.3%, respectively. The next steps in further increasing the efficiency are outlined.

Introduction

The passivated emitter and rear cell (PERC) concept was first published in 1989 [1] as a high-efficiency laboratory-type solar cell. PERC solar cells have since been intensively evaluated and optimized by industry and research institutes as a next-generation silicon solar cell concept for mass production. Several companies have already announced the pilot production of PERC solar cells [2–5], and efficiencies of up to 21.0% have been demonstrated for large-area PERC cells with screen-printed contacts [6]. Excellent rear-surface recombination velocities below 150cm/s have been reported, demonstrating the high-efficiency potential of industrial PERC cells [7,8].

Because of the much-reduced carrier recombination at the rear side of PERC cells, the phosphorus emitter now requires further optimization for conversion efficiencies beyond 21.0% to be achieved in the future. To keep production costs low, however, improvements in emitter technology have to be realized using a very lean process flow and as few extra process steps as possible. In recent years, a lot of effort has already been dedicated to optimizing the phosphorus emitter, in particular with respect to selective emitters [9–14], which are applicable to PERC cells as well.

> "The phosphorus emitter now requires further optimization for conversion efficiencies beyond 21.0% to be achieved in the future."

Four different PERC process flows which yield almost identical rear sides, but result in four different phosphorus emitters, are investigated and compared in this paper:

1. **Ref. PERC:** ISFH reference PERC process flow employing a homogeneously $POCl_3$-diffused 70Ω/sq. emitter and a planar rear side obtained by a protection layer.
2. **I^2-PERC:** PERC process flow where the emitter is formed by phosphorus ion implantation (I^2) and subsequent annealing.
3. **Polished PERC:** PERC process flow where the rear side is chemically polished after texturing and $POCl_3$-diffusion. The rear polish and subsequent wet cleaning slightly etch back the emitter.
4. **GEB PERC:** PERC process flow where the very reactive gas phase of a modified polishing process is used to form a selective emitter via gas phase etch-back (GEB).

Whereas the reference PERC process serves as a high-efficiency baseline process, the other three PERC process flows are designed to reduce the front-surface phosphorus concentration and hence potentially reduce the emitter saturation current density, allowing higher conversion efficiencies. At the same time, these three industrial PERC process flows incorporate very lean process sequences with the aim of targeting industrial mass production. The emitter doping profiles and saturation current densities, as well as the *I-V* parameters and quantum efficiencies of the resulting PERC solar cells, are reported in this paper.

The PERC process flows and emitter technologies investigated

Boron-doped Cz wafers of size 156×156mm^2 with a resistivity of 2–3Ωcm and a starting thickness of 190µm are used for all PERC process flows. The four process flows, shown in Table 1, differ in their emitter formation and rear-surface preparation. Process steps which impact the emitter formation are highlighted in green. All four PERC process flows, however, apply the same initial wafer cleaning, alkaline texturing, SiN_x front-surface passivation, AlO_x/SiN_y rear-surface passivation, laser contact opening (LCO), screen printing of Ag front (print-on-print) and Al rear metal contacts, and firing profile, as indicated by the process steps highlighted in blue in Table 1. The resulting PERC cell structures are shown schematically in Fig. 1. An overview of each of the four different PERC process flows of Table 1 and Fig. 1, with an emphasis on the emitter formation, is given next.

A) Ref. PERC: reference PERC cells with rear protection layer

The process flow for the reference PERC solar cells is described in detail by Dullweber et al. [7]. Before texturing and $POCl_3$ diffusion, a dielectric protection layer is deposited on the rear side of the wafer, resulting in a planar and non-diffused rear side. A homogeneously doped emitter with a sheet resistance of about 60Ω/sq. measured after diffusion is applied. Because of the subsequent wet cleaning (PSG and dielectric etch, cleaning before rear passivation), the emitter is etched back slightly, which increases the emitter sheet resistance to a final value of around 70Ω/sq. A 10nm-thick atomic layer deposited (ALD) AlO_x layer is applied to the rear side. A plasma-enhanced chemical vapour deposition (PECVD) SiN_y capping layer is then deposited on top of the AlO_x passivation layer at the rear in order to improve both the optical reflectivity and the surface passivation quality.

The emitter is covered with a PECVD SiN_x anti-reflective coating. To form local line openings, the dielectric layer stack at the rear is locally ablated by LCO [7,15]. Line contacts were chosen instead of point contacts, since the former facilitate the formation of a deep and uniform local Al-BSF [16]. The Ag front contacts are deposited by a print-on-print (PoP) screen-printing process, resulting in a finger width of around 60µm [17]. The Al rear contact is formed by full-area Al screen printing of a commercially available Al paste designed for local rear contacts. In total, 11 process steps are necessary for this reference PERC process flow, resulting in the PERC solar cell shown schematically in Fig. 1 (left).

B) I^2-PERC: PERC solar cells with ion-implanted phosphorus emitter

As an alternative to $POCl_3$ diffusion, emitter formation by ion implantation is evaluated; see Dullweber et al. [18] for a detailed description of the I^2-PERC process flow. A single-

A: Ref. PERC	B: I^2-PERC	C: Polished PERC	D: GEB PERC
Wafer cleaning	Wafer cleaning	Wafer cleaning	Wafer cleaning
Rear protection layer	*Rear protection layer*		
Texturing	Texturing	Texturing	Texturing
Phosphorus diffusion	Ion implantation	Phosphorus diffusion	Phosphorus diffusion
PSG + dielectric etch	Anneal		Front: etch barrier
	Front: SiN_x	Rear: Polish	Polish + GEB
Rear: AlO_x/SiN_y	*Rear: dielectric etch*	Rear: AlO_x/SiN_y	Rear: AlO_x/SiN_y
Front: SiN_x	Rear: AlO_x/SiN_y	Front: SiN_x	Front: SiN_x
Rear: laser ablation	Rear: laser ablation	Rear: laser ablation	Rear: laser ablation
Ag screen printing	Ag screen printing	Ag screen printing	Ag screen printing
Al screen printing	Al screen printing	Al screen printing	Al screen printing
Co-firing	Co-firing	Co-firing	Co-firing
11 steps	12 (10) steps	10 steps	11 steps

Table 1. Process flows of the reference PERC cell (A), as well as the three industrially applicable PERC cell concepts with ion-implanted emitter (B), chemically polished rear surface (C) and selective emitter by gas phase etch-back (GEB) (D). The 'green' process steps impact the emitter formation, whereas the 'blue' process steps are identical for all four PERC process flows.

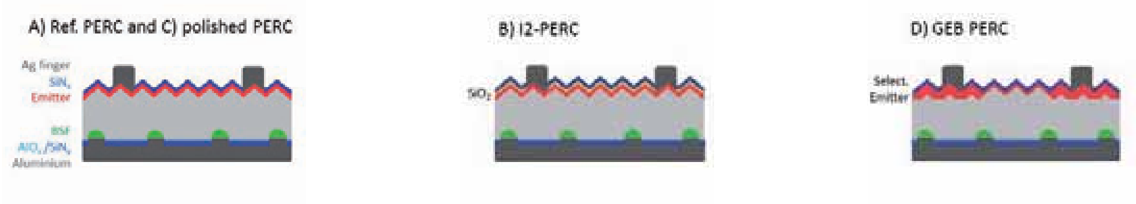

Figure 1. Schematic cross sections of the four PERC cells resulting from the different process flows in Table 1.

sided texturing of the front side is obtained by using a rear protection layer, which is later removed in the process flow. The phosphorus emitter is ion implanted using an implanter similar to the Applied Materials Solion tool [13]. Afterwards, the crystal damage caused by the ion implantation is annealed in a high-temperature step, which activates the phosphorus doping, resulting in an emitter sheet resistance of around 65Ω/sq. A thin thermal oxide is then grown in the furnace as part of the anneal, providing surface passivation of the emitter. A SiN_x anti-reflective coating is deposited on the front side, and the dielectric layer on the wafer rear side is then removed. Next, the AlO_x/SiN_y passivation stack is deposited on the wafer rear side. The LCO and the screen printing of the front and rear contacts is performed as described above for the reference PERC process flow.

The resulting PERC solar cell is shown schematically in Fig. 1 (centre); this cell differs from the reference PERC cell in its emitter doping profile and SiO_2/SiN_y front-surface passivation. A future option for a very lean process flow with industrial manufacturing in mind is to skip the rear protection layer and apply a single-sided alkaline texturing or a chemical rear polish after double-sided texturing as in the polished PERC cell (described in the next section). This would allow the dielectric etch (later in the process flow) to also be skipped, so that only 10 steps in total would be required for the PERC cell processing.

C) Polished PERC: PERC solar cells with polished rear side

The process flow for the polished PERC cell is described in detail by Kranz et al. [19]. After double-sided alkaline texturing, the emitter is formed by $POCl_3$ diffusion, resulting in an emitter sheet resistance of 45Ω/sq. after diffusion. The RENA InPilot tool is then used to take off about 5µm of silicon from the rear surface by single-sided wet chemical polishing; this removes the rear-side emitter and smooths the rear surface. After the polishing step, a cleaning sequence is carried out prior to depositing the AlO_x/SiN_y rear passivation layer. The polishing process, and even more so the subsequent wet cleaning, slightly etch back the emitter, which increases the emitter sheet resistance from the initial 45Ω/sq. to around 65Ω/sq. The passivation of the rear and front surfaces, the LCO and the screen printing of the front and rear contacts are performed as described

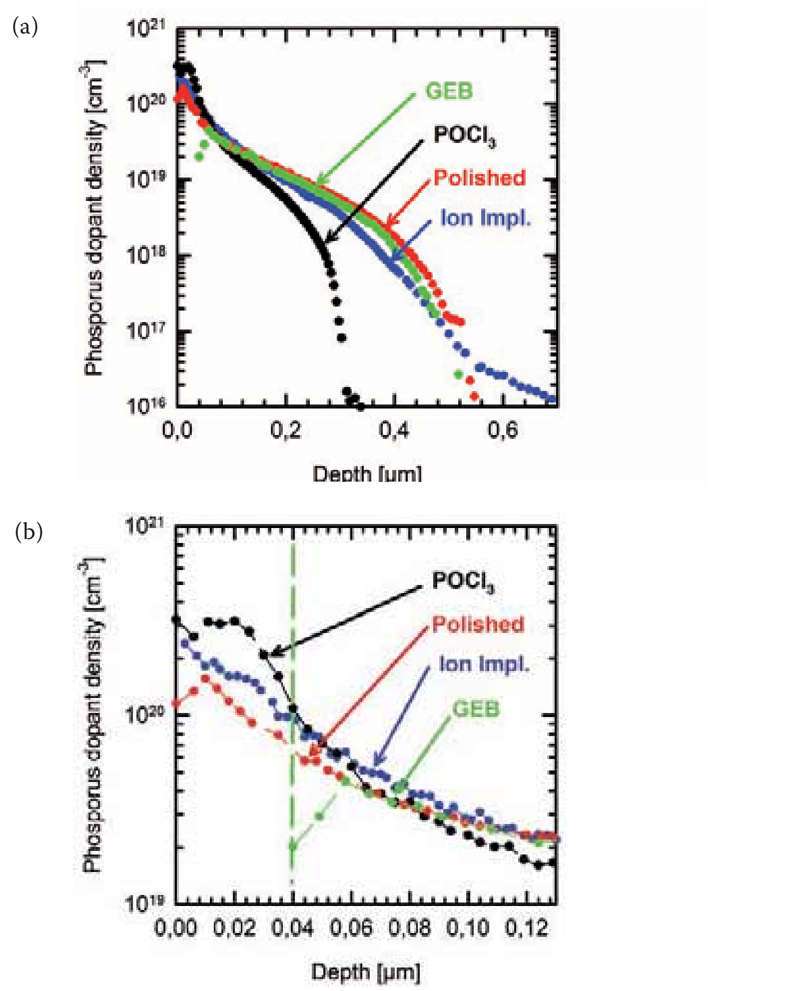

Figure 2. (a) Doping profiles of the ion-implanted phosphorus emitter (65Ω/sq.), the emitter after polishing (65Ω/sq.) and the gas phase etch-back (GEB) emitter (90Ω/sq., shifted by 40nm) measured by ECV profiling. The doping profile of the $POCl_3$-diffused emitter (70Ω/sq.) is included as a reference. (b) Close-up of the front surface in Fig. 2(a). The dashed green line denotes the removal of around 40nm of silicon by the GEB process. The lower concentration of surface phosphorus of the GEB, polished and implanted emitters compared with the $POCl_3$ emitter is the main reason why the J_{0e} (see Fig. 3) values are lower and the V_{oc} values are higher (see Table 2).

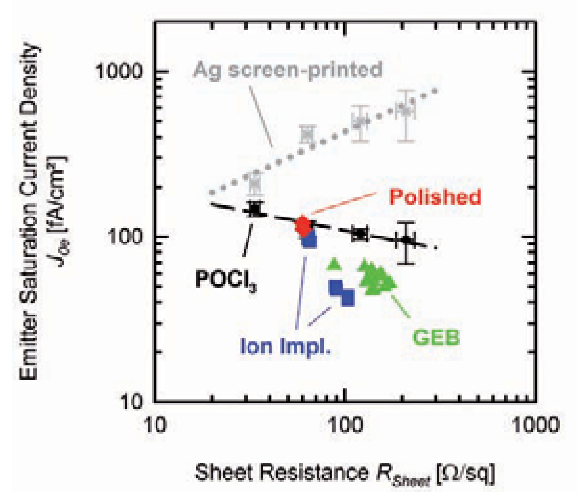

Figure 3. Emitter saturation current density of homogeneously $POCl_3$-diffused emitters with Ag screen-printed contacts (grey), as well as a SiN_x surface passivation (black) [21]. The emitter saturation current densities of the GEB (green) and ion-implanted (blue) emitters are significantly lower than for $POCl_3$-diffused emitters with the same sheet resistance.

earlier for the reference PERC process.

This very lean PERC process flow requires just 10 process steps. The schematic cross section of the resulting PERC solar cell is basically identical to the reference PERC cell in Fig. 1 (left). However, the rear surface of the polished PERC cell is slightly rougher, and the doping profile of the emitter is different from that of the reference PERC cell.

D) GEB PERC: PERC solar cells with selective emitter formed by gas phase etch-back

See Hannebauer et al. [20] for an in-depth description of the novel selective emitter process for GEB PERC cells. The wafers are double-sided textured and double-sided $POCl_3$ diffused, with an emitter sheet resistance of 45Ω/sq. Using an inkjet printer, an etch barrier (barrier material provided by Merck) is printed on the front side of the wafer in areas where the front Ag fingers will later also be screen printed. The printed etch barrier width is around 600µm, which is subject to further reduction and optimization.

The rear side is then polished using the RENA InPilot tool, and the emitter is thereby simultaneously etched back on the front side in between the etch barrier fingers by the reactive gas phase of the polish bath. In contrast with the previously described polished PERC process, the polish recipe is adjusted in order to obtain a much more reactive gas phase which removes about 30 to 40nm of the phosphorus emitter on the front side while wet chemically polishing and removing about 8µm of silicon on the rear side. The cleaning after the polish removes the etch barrier.

The final emitter sheet resistances are about 90Ω/sq. in between the etch barrier fingers (later SiN_x passivated), and about 45Ω/sq. below the etch barrier (later Ag screen printed). The passivation of the rear and front surfaces, the LCO and the screen printing of the front and rear contacts are carried out as described earlier for the reference PERC process. Compared with the polished PERC cells, the GEB PERC process flow requires just one additional process step (etch barrier deposition) to form a selective emitter instead of a homogeneously doped emitter. Fig. 1 (right) shows a schematic drawing of the GEB PERC solar cell with selective emitter.

Emitter doping profiles and saturation currents

The doping profiles are obtained by electrochemical capacitance-voltage (ECV) measurements of planar test wafers which have been processed in a very similar way to that of the corresponding PERC solar cells. Fig. 2(a) shows the resulting doping profiles; the 70Ω/sq. $POCl_3$ emitter of the reference PERC cell is shown in black and serves as a reference. The doping profile of the 90Ω/sq. GEB emitter is almost identical to that of the polished PERC cell, since in both cases a 45Ω/sq. $POCl_3$ diffusion is applied. However, around 40nm of the front surface of the emitter has been removed by the GEB; accordingly, the ECV profile of the GEB emitter is shifted by 40nm in Figs. 2(a) and (b). The doping profile of the 65Ω/sq. ion-implanted emitter after annealing has a depth of around 0.55µm, which is comparable to that for the GEB and polished PERC emitters.

Fig. 2(b) shows a close-up of the first 0.1µm in Fig. 2(a) so that the significantly different phosphorus concentrations at the front surface can be observed. As can be seen, the GEB 90Ω/sq. emitter is etched back by approximately 40nm, resulting in the lowest phosphorus surface concentrations of $5\times10^{19}cm^{-3}$. The doping profile of the polished PERC emitter shows a front phosphorus concentration of around $1.5\times10^{20}cm^{-3}$, despite the strong 45Ω/sq. $POCl_3$ diffusion. This is achieved by the aggressive wet cleaning after the rear polishing, which partly etches the emitter front surface. The ion-implanted emitter indicates a low phosphorus concentration of around $2\times10^{20}cm^{-3}$ of the front as well, which is achieved by a suitable combination of implant and annealing parameters. In this case, the diffusion mechanism follows a 'limited source behaviour' according to Fick's laws of diffusion, which allows a reduction in the surface concentration of phosphorus, as opposed to the typically 'unlimited source behaviour' of $POCl_3$ diffusion, which maintains the concentration at the surface.

To assess the electrical performance of the different emitters, the emitter saturation current density J_{0e} is measured by quasi-steady-state photoconductance (QSSPC) of suitable test structures using float zone wafers with resistivities of about 200Ωcm. The GEB, polished and ion-implanted emitters are processed in the same way as the corresponding PERC cells, including a textured surface passivated by SiN_x.

> "The superior performance of the ion-implanted and GEB emitters is due to the significantly lower front-surface phosphorus concentration."

Measurements taken after firing are shown in Fig. 3. The black data points represent the reference $POCl_3$ emitter for different sheet resistances and are taken from Hannebauer et al. [21]. The grey data points, labelled 'Ag screen-printed', refer to J_{0e} measurements by dynamic infrared lifetime mapping (DILM) of Ag screen-printed contacts on $POCl_3$-diffused emitters with different sheet resistances, as published in Hannebauer et al. [21]. For sheet resistances of 90 to 130Ω/sq. in particular, the ion-implanted and GEB emitters yield significantly lower J_{0e}

PERC type	Emitter technology	Emitter doping	η [%]	V_{oc} [mV]	J_{sc} [mA/cm²]	FF [%]
Ref. PERC	$POCl_3$	H, 70Ω/sq.	20.0	649	38.1	80.9
I²-PERC	Ion implantation	H, 65Ω/sq.	20.0	659	38.7	78.3
Polished PERC	$POCl_3$	H, 65Ω/sq.	20.2	655	38.0	81.0
GEB PERC	GEB	SE, 90/45Ω/sq.	20.3*	660	38.3	80.3

*Independently confirmed by ISE CalLab

Table 2. Solar cell parameters of the best PERC solar cell of each process flow, measured under standard testing conditions (H = homogeneously doped; SE = selective emitter).

values of 40 to 60fA/cm^2, compared with 90fA/cm^2 for the $POCl_3$-diffused emitter. The superior performance of the ion-implanted and GEB emitters is due to the significantly lower front-surface phosphorus concentration, as shown in Fig. 2(b), resulting in fewer inactive phosphorus atoms which could act as recombination centres. For the polished PERC cells, however, the J_{0e} values of around 110fA/cm^2 are comparable to the current densities for $POCl_3$-diffused emitters of the same sheet resistance.

PERC solar cells

Table 2 shows the *I-V* parameters of the best performing PERC cells of the four PERC cell process flows described earlier. The reference PERC cell demonstrates a conversion efficiency η of 20.0%, whereas the polished and GEB PERC cells yield conversion efficiencies of 20.2% and 20.3% respectively. The benefit of the selective emitter of the GEB PERC cell can be seen in the high open-circuit voltage V_{oc} of 660mV and good short-circuit density J_{sc} of 38.3mA/cm^2. The I^2-PERC cell achieves 20.0% conversion efficiency and high V_{oc} and J_{sc} values; the fill factor *FF*, however, is significantly lower than for the other PERC cells. It has to be considered, though, that the I^2-PERC cell has been produced using an older process, with respect to the rear-surface passivation and front-side metallization, than in the case of the other three PERC cells, which have been created using the latest process at ISFH. If the latest process is applied to the I^2-PERC cells, the conversion efficiency is expected to be around 20.2%.

Another option for further increasing the conversion efficiency of I^2-PERC cells is to apply a selective emitter by putting a shadow mask in the ion beam, a technique which requires no additional process step [12]. Moreover, it should be mentioned that the GEB PERC cells stem from only the fourth batch ever of cells processed using this novel selective emitter concept. The etch barrier still has improvement potential with respect to the barrier width and the etch resistance. Efficiencies higher by at least 0.2% abs. are therefore expected with an optimized GEB PERC cell process in the future.

“Efficiencies higher by at least 0.2% abs. are expected with an optimized GEB PERC cell process in the future.”

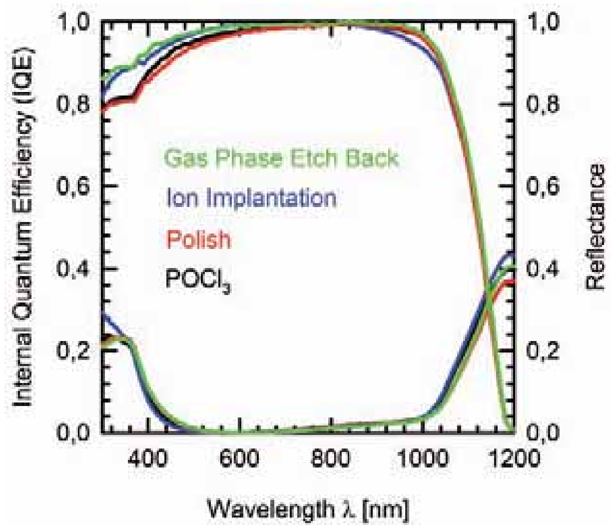

Figure 4. IQE (top) and reflectance (bottom) measurements of the GEB PERC cell, the I^2-PERC cell, the polished PERC cell and the reference PERC cell ($POCl_3$) in Table 2. The improved IQE in the blue-wavelength regime of the GEB and I^2-PERC cells compared with the reference PERC cell is in accordance with the lower J_{0e} values shown in Fig. 3. The slightly lower IQE of the I^2-PERC cell in the infrared-wavelength regime is due to the older rear-passivation process.

To compare the performance of the different phosphorus emitters, the internal quantum efficiency (IQE) and reflectance of the four PERC cells of Table 2 were measured. As can be seen in Fig. 4, the GEB PERC and the I^2-PERC cells show a significantly improved blue-wavelength IQE compared with the reference PERC cell. Accordingly, the lower J_{0e} values of the ion-implanted emitter and the GEB emitter compared with the $POCl_3$ emitter in Fig. 3 translate into a higher blue-wavelength IQE, and hence into higher V_{oc} and J_{sc} values, as shown in Table 2.

Fig. 4 also indicates that the IQE of the I^2-PERC cell is slightly lower in the infrared regime around 1000nm wavelength; this is caused by the older rear-passivation process and is not related to the emitter formation. The IQE of the polished PERC cell is almost identical to that of the reference PERC cell, despite the different types of $POCl_3$ diffusion used in the process flows. The wet chemical etch-back of the emitter of the polished PERC cell therefore compensates for the stronger $POCl_3$ diffusion. Furthermore, in the red-wavelength regime the IQEs of the GEB and polished PERC cells are comparable to the IQE of the reference PERC cell, which proves that the rear polish is sufficient to allow an excellent rear-surface passivation.

Conclusions

Emitter technologies of three industrially applicable PERC cell concepts have been evaluated, including ion-implanted emitter, chemically polished rear surface, and selective emitter by GEB. The results were compared with a high-efficiency reference PERC cell. The three industrial PERC concepts employ lean industrially applicable process sequences which reduce the phosphorus concentration at the wafer surface.

“When applied to PERC cells, the ion-implanted and GEB emitters achieve conversion efficiencies of up to 20.3%.”

The ion-implanted and GEB emitters consequently obtain significantly reduced emitter saturation current densities of 40 to 60fA/cm^2 for emitter sheet resistances of 90 to 130Ω/sq. When applied to PERC cells, the ion-implanted and GEB emitters demonstrate up to 10mV higher open-circuit voltages than the $POCl_3$-diffused reference PERC cell and achieve conversion efficiencies of up to 20.3%. The potential for further increases in efficiency has been discussed.

Emitter technology options for industrial PERC solar cells with up to 20.3% conversion efficiency

Thorsten Dullweber[1], Helge Hannebauer[1], Christopher Kranz[1], Rene Hesse[1], Sabrina Wyczanowski[1], Vikram Bhosle[2] & Chris Dubé[2], Katrin Weise[3] & Franck Delahaye[3], Oliver Doll[4], Ingo Kohler[4], Rolf Brendel[1]

[1] Institute for Solar Energy Research Hamelin (ISFH), Emmerthal, Germany
[2] Applied Materials, Varian Semiconductor Equipment, Gloucester, Massachusetts, USA
[3] RENA GmbH, Freiburg, Germany
[4] Merck KGaA, Darmstadt, Germany

ABSTRACT

Passivated emitter and rear cells (PERC) are considered to be a next generation of industrial solar cells, and several companies have already started pilot production. The much-reduced rear-surface recombination in PERC cells requires improvements to the front side, for example the emitter, in order to further increase the conversion efficiency in the future. This paper presents an evaluation of the emitter technologies of three industrially applicable PERC cell concepts: 1) with an ion-implanted emitter, 2) with a chemically polished rear surface, and 3) with a selective emitter formed by gas phase etch-back (GEB). The results are compared with a reference high-efficiency $POCl_3$-diffused PERC cell. The three industrial PERC concepts utilize lean industrially applicable process flows which reduce the phosphorus concentration at the wafer surface. Accordingly, when compared with the $POCl_3$-diffused emitter, the ion-implanted and GEB emitters obtain significantly lower emitter saturation current densities of 40 to 60fA/cm^2 for emitter sheet resistances of 90 to 130Ω/sq. When applied to large-area PERC cells with screen-printed metal contacts, the ion-implanted and GEB emitter cells demonstrate up to 10mV higher open-circuit voltages than the $POCl_3$-diffused reference PERC cell, and achieve conversion efficiencies of 20.0 and 20.3%, respectively. The next steps in further increasing the efficiency are outlined.

Introduction

The passivated emitter and rear cell (PERC) concept was first published in 1989 [1] as a high-efficiency laboratory-type solar cell. PERC solar cells have since been intensively evaluated and optimized by industry and research institutes as a next-generation silicon solar cell concept for mass production. Several companies have already announced the pilot production of PERC solar cells [2–5], and efficiencies of up to 21.0% have been demonstrated for large-area PERC cells with screen-printed contacts [6]. Excellent rear-surface recombination velocities below 150cm/s have been reported, demonstrating the high-efficiency potential of industrial PERC cells [7,8].

Because of the much-reduced carrier recombination at the rear side of PERC cells, the phosphorus emitter now requires further optimization for conversion efficiencies beyond 21.0% to be achieved in the future. To keep production costs low, however, improvements in emitter technology have to be realized using a very lean process flow and as few extra process steps as possible. In recent years, a lot of effort has already been dedicated to optimizing the phosphorus emitter, in particular with respect to selective emitters [9–14], which are applicable to PERC cells as well.

> "The phosphorus emitter now requires further optimization for conversion efficiencies beyond 21.0% to be achieved in the future."

Four different PERC process flows which yield almost identical rear sides, but result in four different phosphorus emitters, are investigated and compared in this paper:

1. **Ref. PERC:** ISFH reference PERC process flow employing a homogeneously $POCl_3$-diffused 70Ω/sq. emitter and a planar rear side obtained by a protection layer.

2. **I^2-PERC:** PERC process flow where the emitter is formed by phosphorus ion implantation (I^2) and subsequent annealing.

3. **Polished PERC:** PERC process flow where the rear side is chemically polished after texturing and $POCl_3$-diffusion. The rear polish and subsequent wet cleaning slightly etch back the emitter.

4. **GEB PERC:** PERC process flow where the very reactive gas phase of a modified polishing process is used to form a selective emitter via **g**as phase **e**tch-**b**ack (GEB).

Whereas the reference PERC process serves as a high-efficiency baseline process, the other three PERC process flows are designed to reduce the front-surface phosphorus concentration and hence potentially reduce the emitter saturation current density, allowing higher conversion efficiencies. At the same time, these three industrial PERC process flows incorporate very lean process sequences with the aim of targeting industrial mass production. The emitter doping profiles and saturation current densities, as well as the *I-V* parameters and quantum efficiencies of the resulting PERC solar cells, are reported in this paper.

The PERC process flows and emitter technologies investigated

Boron-doped Cz wafers of size 156×156mm^2 with a resistivity of 2–3Ωcm and a starting thickness of 190µm are used for all PERC process flows. The four process flows, shown in Table 1, differ in their emitter formation and rear-surface preparation. Process steps which impact the emitter formation are highlighted in green. All four PERC process flows, however, apply the same initial wafer cleaning, alkaline texturing, SiN_x front-surface passivation, AlO_x/SiN_y rear-surface passivation, laser contact opening (LCO), screen printing of Ag front (print-on-print) and Al rear metal contacts, and firing profile, as indicated by the process steps highlighted in blue in Table 1. The resulting PERC cell structures are shown schematically in Fig. 1. An overview of each of the four different PERC process flows of Table 1 and Fig. 1, with an emphasis on the emitter formation, is given next.

A) Ref. PERC: reference PERC cells with rear protection layer

The process flow for the reference PERC solar cells is described in detail by Dullweber et al. [7]. Before texturing and $POCl_3$ diffusion, a dielectric protection layer is deposited on the rear side of the wafer, resulting in a planar and non-diffused rear side. A homogeneously doped emitter with a sheet resistance of about 60Ω/sq. measured after diffusion is applied. Because of the subsequent wet cleaning (PSG and dielectric etch, cleaning before rear passivation), the emitter is etched back slightly, which increases the emitter sheet resistance to a final value of around 70Ω/sq. A 10nm-thick atomic layer deposited (ALD) AlO_x layer is applied to the rear side. A plasma-enhanced chemical vapour deposition (PECVD) SiN_y capping layer is then deposited on top of the AlO_x passivation layer at the rear in order to improve both the optical reflectivity and the surface passivation quality.

The emitter is covered with a PECVD SiN_x anti-reflective coating. To form local line openings, the dielectric layer stack at the rear is locally ablated by LCO [7,15]. Line contacts were chosen instead of point contacts, since the former facilitate the formation of a deep and uniform local Al-BSF [16]. The Ag front contacts are deposited by a print-on-print (PoP) screen-printing process, resulting in a finger width of around 60µm [17]. The Al rear contact is formed by full-area Al screen printing of a commercially available Al paste designed for local rear contacts. In total, 11 process steps are necessary for this reference PERC process flow, resulting in the PERC solar cell shown schematically in Fig. 1 (left).

B) I^2-PERC: PERC solar cells with ion-implanted phosphorus emitter

As an alternative to $POCl_3$ diffusion, emitter formation by ion implantation is evaluated; see Dullweber et al. [18] for a detailed description of the I^2-PERC process flow. A single-

A: Ref. PERC	B: I^2-PERC	C: Polished PERC	D: GEB PERC
Wafer cleaning	Wafer cleaning	Wafer cleaning	Wafer cleaning
Rear protection layer	*Rear protection layer*		
Texturing	Texturing	Texturing	Texturing
Phosphorus diffusion	Ion implantation	Phosphorus diffusion	Phosphorus diffusion
PSG + dielectric etch	Anneal		Front: etch barrier
	Front: SiN_x	Rear: Polish	Polish + GEB
Rear: AlO_x/SiN_y	*Rear: dielectric etch*	Rear: AlO_x/SiN_y	Rear: AlO_x/SiN_y
Front: SiN_x	Rear: AlO_x/SiN_y	Front: SiN_x	Front: SiN_x
Rear: laser ablation	Rear: laser ablation	Rear: laser ablation	Rear: laser ablation
Ag screen printing	Ag screen printing	Ag screen printing	Ag screen printing
Al screen printing	Al screen printing	Al screen printing	Al screen printing
Co-firing	Co-firing	Co-firing	Co-firing
11 steps	12 (10) steps	10 steps	11 steps

Table 1. Process flows of the reference PERC cell (A), as well as the three industrially applicable PERC cell concepts with ion-implanted emitter (B), chemically polished rear surface (C) and selective emitter by gas phase etch-back (GEB) (D). The 'green' process steps impact the emitter formation, whereas the 'blue' process steps are identical for all four PERC process flows.

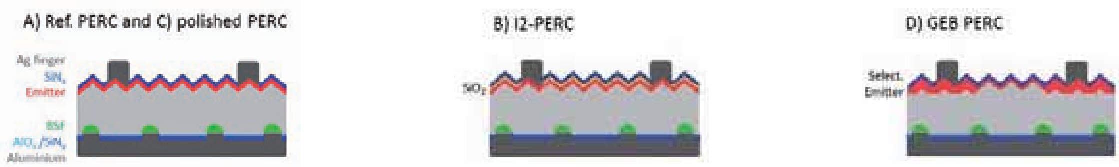

Figure 1. Schematic cross sections of the four PERC cells resulting from the different process flows in Table 1.

sided texturing of the front side is obtained by using a rear protection layer, which is later removed in the process flow. The phosphorus emitter is ion implanted using an implanter similar to the Applied Materials Solion tool [13]. Afterwards, the crystal damage caused by the ion implantation is annealed in a high-temperature step, which activates the phosphorus doping, resulting in an emitter sheet resistance of around 65Ω/sq. A thin thermal oxide is then grown in the furnace as part of the anneal, providing surface passivation of the emitter. A SiN_x anti-reflective coating is deposited on the front side, and the dielectric layer on the wafer rear side is then removed. Next, the AlO_x/SiN_y passivation stack is deposited on the wafer rear side. The LCO and the screen printing of the front and rear contacts is performed as described above for the reference PERC process flow.

The resulting PERC solar cell is shown schematically in Fig. 1 (centre); this cell differs from the reference PERC cell in its emitter doping profile and SiO_2/SiN_y front-surface passivation. A future option for a very lean process flow with industrial manufacturing in mind is to skip the rear protection layer and apply a single-sided alkaline texturing or a chemical rear polish after double-sided texturing as in the polished PERC cell (described in the next section). This would allow the dielectric etch (later in the process flow) to also be skipped, so that only 10 steps in total would be required for the PERC cell processing.

C) Polished PERC: PERC solar cells with polished rear side

The process flow for the polished PERC cell is described in detail by Kranz et al. [19]. After double-sided alkaline texturing, the emitter is formed by $POCl_3$ diffusion, resulting in an emitter sheet resistance of 45Ω/sq. after diffusion. The RENA InPilot tool is then used to take off about 5μm of silicon from the rear surface by single-sided wet chemical polishing; this removes the rear-side emitter and smooths the rear surface. After the polishing step, a cleaning sequence is carried out prior to depositing the AlO_x/SiN_y rear passivation layer. The polishing process, and even more so the subsequent wet cleaning, slightly etch back the emitter, which increases the emitter sheet resistance from the initial 45Ω/sq. to around 65Ω/sq. The passivation of the rear and front surfaces, the LCO and the screen printing of the front and rear contacts are performed as described

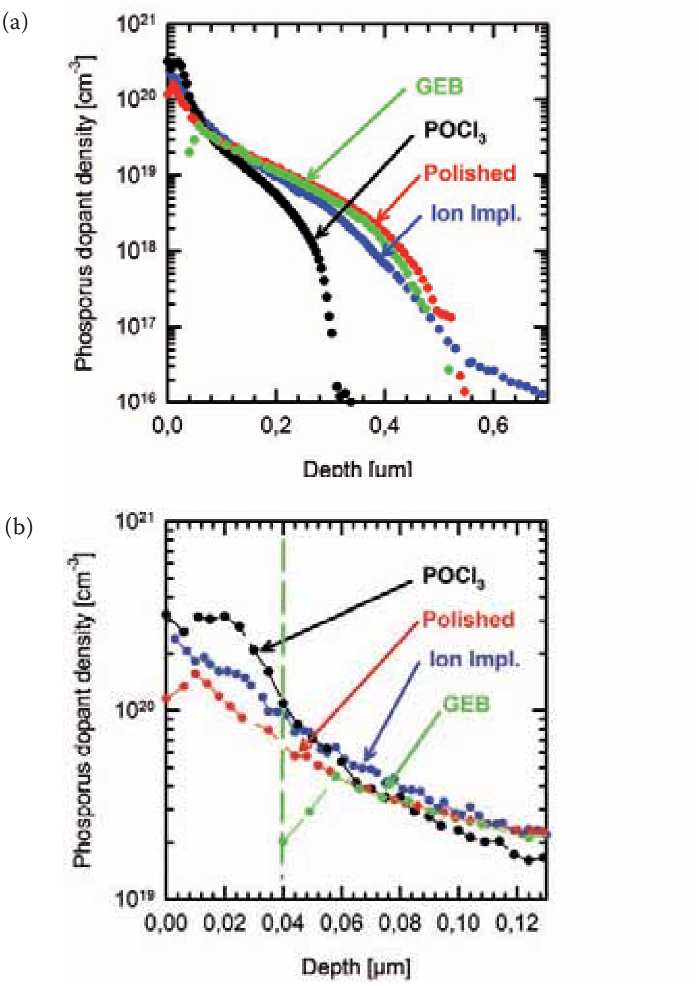

Figure 2. (a) Doping profiles of the ion-implanted phosphorus emitter (65Ω/sq.), the emitter after polishing (65Ω/sq.) and the gas phase etch-back (GEB) emitter (90Ω/sq., shifted by 40nm) measured by ECV profiling. The doping profile of the $POCl_3$-diffused emitter (70Ω/sq.) is included as a reference. (b) Close-up of the front surface in Fig. 2(a). The dashed green line denotes the removal of around 40nm of silicon by the GEB process. The lower concentration of surface phosphorus of the GEB, polished and implanted emitters compared with the $POCl_3$ emitter is the main reason why the J_{0e} (see Fig. 3) values are lower and the V_{oc} values are higher (see Table 2).

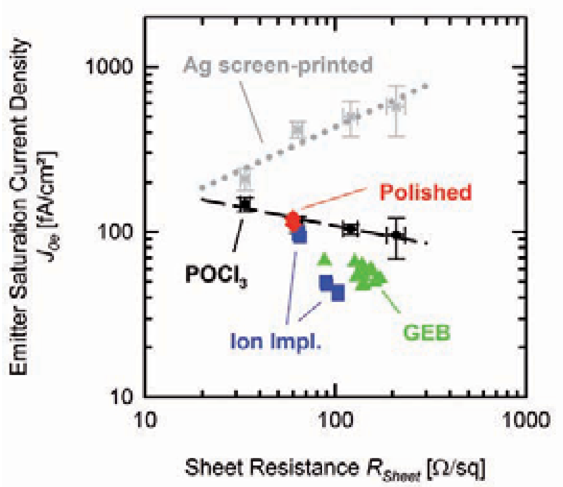

Figure 3. Emitter saturation current density of homogeneously $POCl_3$-diffused emitters with Ag screen-printed contacts (grey), as well as a SiN_x surface passivation (black) [21]. The emitter saturation current densities of the GEB (green) and ion-implanted (blue) emitters are significantly lower than for $POCl_3$-diffused emitters with the same sheet resistance.

earlier for the reference PERC process.

This very lean PERC process flow requires just 10 process steps. The schematic cross section of the resulting PERC solar cell is basically identical to the reference PERC cell in Fig. 1 (left). However, the rear surface of the polished PERC cell is slightly rougher, and the doping profile of the emitter is different from that of the reference PERC cell.

D) GEB PERC: PERC solar cells with selective emitter formed by gas phase etch-back

See Hannebauer et al. [20] for an in-depth description of the novel selective emitter process for GEB PERC cells. The wafers are double-sided textured and double-sided $POCl_3$ diffused, with an emitter sheet resistance of 45Ω/sq. Using an inkjet printer, an etch barrier (barrier material provided by Merck) is printed on the front side of the wafer in areas where the front Ag fingers will later also be screen printed. The printed etch barrier width is around 600µm, which is subject to further reduction and optimization.

The rear side is then polished using the RENA InPilot tool, and the emitter is thereby simultaneously etched back on the front side in between the etch barrier fingers by the reactive gas phase of the polish bath. In contrast with the previously described polished PERC process, the polish recipe is adjusted in order to obtain a much more reactive gas phase which removes about 30 to 40nm of the phosphorus emitter on the front side while wet chemically polishing and removing about 8µm of silicon on the rear side. The cleaning after the polish removes the etch barrier.

The final emitter sheet resistances are about 90Ω/sq. in between the etch barrier fingers (later SiN_x passivated), and about 45Ω/sq. below the etch barrier (later Ag screen printed). The passivation of the rear and front surfaces, the LCO and the screen printing of the front and rear contacts are carried out as described earlier for the reference PERC process. Compared with the polished PERC cells, the GEB PERC process flow requires just one additional process step (etch barrier deposition) to form a selective emitter instead of a homogeneously doped emitter. Fig. 1 (right) shows a schematic drawing of the GEB PERC solar cell with selective emitter.

Emitter doping profiles and saturation currents

The doping profiles are obtained by electrochemical capacitance-voltage (ECV) measurements of planar test wafers which have been processed in a very similar way to that of the corresponding PERC solar cells. Fig. 2(a) shows the resulting doping profiles; the 70Ω/sq. $POCl_3$ emitter of the reference PERC cell is shown in black and serves as a reference. The doping profile of the 90Ω/sq. GEB emitter is almost identical to that of the polished PERC cell, since in both cases a 45Ω/sq. $POCl_3$ diffusion is applied. However, around 40nm of the front surface of the emitter has been removed by the GEB; accordingly, the ECV profile of the GEB emitter is shifted by 40nm in Figs. 2(a) and (b). The doping profile of the 65Ω/sq. ion-implanted emitter after annealing has a depth of around 0.55µm, which is comparable to that for the GEB and polished PERC emitters.

Fig. 2(b) shows a close-up of the first 0.1µm in Fig. 2(a) so that the significantly different phosphorus concentrations at the front surface can be observed. As can be seen, the GEB 90Ω/sq. emitter is etched back by approximately 40nm, resulting in the lowest phosphorus surface concentrations of $5\times10^{19}cm^{-3}$. The doping profile of the polished PERC emitter shows a front phosphorus concentration of around $1.5\times10^{20}cm^{-3}$, despite the strong 45Ω/sq. $POCl_3$ diffusion. This is achieved by the aggressive wet cleaning after the rear polishing, which partly etches the emitter front surface. The ion-implanted emitter indicates a low phosphorus concentration of around $2\times10^{20}cm^{-3}$ of the front as well, which is achieved by a suitable combination of implant and annealing parameters. In this case, the diffusion mechanism follows a 'limited source behaviour' according to Fick's laws of diffusion, which allows a reduction in the surface concentration of phosphorus, as opposed to the typically 'unlimited source behaviour' of $POCl_3$ diffusion, which maintains the concentration at the surface.

To assess the electrical performance of the different emitters, the emitter saturation current density J_{0e} is measured by quasi-steady-state photoconductance (QSSPC) of suitable test structures using float zone wafers with resistivities of about 200Ωcm. The GEB, polished and ion-implanted emitters are processed in the same way as the corresponding PERC cells, including a textured surface passivated by SiN_x.

"The superior performance of the ion-implanted and GEB emitters is due to the significantly lower front-surface phosphorus concentration."

Measurements taken after firing are shown in Fig. 3. The black data points represent the reference $POCl_3$ emitter for different sheet resistances and are taken from Hannebauer et al. [21]. The grey data points, labelled 'Ag screen-printed', refer to J_{0e} measurements by dynamic infrared lifetime mapping (DILM) of Ag screen-printed contacts on $POCl_3$-diffused emitters with different sheet resistances, as published in Hannebauer et al. [21]. For sheet resistances of 90 to 130Ω/sq. in particular, the ion-implanted and GEB emitters yield significantly lower J_{0e}

PERC type	Emitter technology	Emitter doping	η [%]	V_{oc} [mV]	J_{sc} [mA/cm^2]	FF [%]
Ref. PERC	$POCl_3$	H, 70Ω/sq.	20.0	649	38.1	80.9
I^2-PERC	Ion implantation	H, 65Ω/sq.	20.0	659	38.7	78.3
Polished PERC	$POCl_3$	H, 65Ω/sq.	20.2	655	38.0	81.0
GEB PERC	GEB	SE, 90/45Ω/sq.	20.3*	660	38.3	80.3

*Independently confirmed by ISE CalLab

Table 2. Solar cell parameters of the best PERC solar cell of each process flow, measured under standard testing conditions (H = homogeneously doped; SE = selective emitter).

values of 40 to 60fA/cm^2, compared with 90fA/cm^2 for the $POCl_3$-diffused emitter. The superior performance of the ion-implanted and GEB emitters is due to the significantly lower front-surface phosphorus concentration, as shown in Fig. 2(b), resulting in fewer inactive phosphorus atoms which could act as recombination centres. For the polished PERC cells, however, the J_{0e} values of around 110fA/cm^2 are comparable to the current densities for $POCl_3$-diffused emitters of the same sheet resistance.

PERC solar cells

Table 2 shows the *I-V* parameters of the best performing PERC cells of the four PERC cell process flows described earlier. The reference PERC cell demonstrates a conversion efficiency η of 20.0%, whereas the polished and GEB PERC cells yield conversion efficiencies of 20.2% and 20.3% respectively. The benefit of the selective emitter of the GEB PERC cell can be seen in the high open-circuit voltage V_{oc} of 660mV and good short-circuit density J_{sc} of 38.3mA/cm^2. The I^2-PERC cell achieves 20.0% conversion efficiency and high V_{oc} and J_{sc} values; the fill factor *FF*, however, is significantly lower than for the other PERC cells. It has to be considered, though, that the I^2-PERC cell has been produced using an older process, with respect to the rear-surface passivation and front-side metallization, than in the case of the other three PERC cells, which have been created using the latest process at ISFH. If the latest process is applied to the I^2-PERC cells, the conversion efficiency is expected to be around 20.2%.

Another option for further increasing the conversion efficiency of I^2-PERC cells is to apply a selective emitter by putting a shadow mask in the ion beam, a technique which requires no additional process step [12]. Moreover, it should be mentioned that the GEB PERC cells stem from only the fourth batch ever of cells processed using this novel selective emitter concept. The etch barrier still has improvement potential with respect to the barrier width and the etch resistance. Efficiencies higher by at least 0.2% abs. are therefore expected with an optimized GEB PERC cell process in the future.

"Efficiencies higher by at least 0.2% abs. are expected with an optimized GEB PERC cell process in the future."

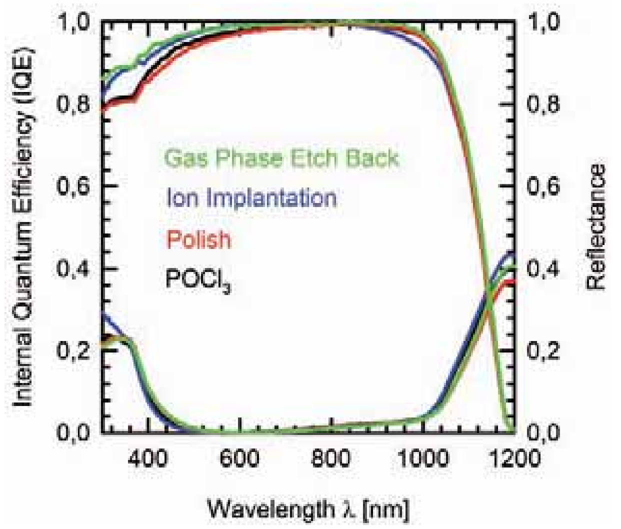

Figure 4. IQE (top) and reflectance (bottom) measurements of the GEB PERC cell, the I^2-PERC cell, the polished PERC cell and the reference PERC cell ($POCl_3$) in Table 2. The improved IQE in the blue-wavelength regime of the GEB and I^2-PERC cells compared with the reference PERC cell is in accordance with the lower J_{0e} values shown in Fig. 3. The slightly lower IQE of the I^2-PERC cell in the infrared-wavelength regime is due to the older rear-passivation process.

To compare the performance of the different phosphorus emitters, the internal quantum efficiency (IQE) and reflectance of the four PERC cells of Table 2 were measured. As can be seen in Fig. 4, the GEB PERC and the I^2-PERC cells show a significantly improved blue-wavelength IQE compared with the reference PERC cell. Accordingly, the lower J_{0e} values of the ion-implanted emitter and the GEB emitter compared with the $POCl_3$ emitter in Fig. 3 translate into a higher blue-wavelength IQE, and hence into higher V_{oc} and J_{sc} values, as shown in Table 2.

Fig. 4 also indicates that the IQE of the I^2-PERC cell is slightly lower in the infrared regime around 1000nm wavelength; this is caused by the older rear-passivation process and is not related to the emitter formation. The IQE of the polished PERC cell is almost identical to that of the reference PERC cell, despite the different types of $POCl_3$ diffusion used in the process flows. The wet chemical etch-back of the emitter of the polished PERC cell therefore compensates for the stronger $POCl_3$ diffusion. Furthermore, in the red-wavelength regime the IQEs of the GEB and polished PERC cells are comparable to the IQE of the reference PERC cell, which proves that the rear polish is sufficient to allow an excellent rear-surface passivation.

Conclusions

Emitter technologies of three industrially applicable PERC cell concepts have been evaluated, including ion-implanted emitter, chemically polished rear surface, and selective emitter by GEB. The results were compared with a high-efficiency reference PERC cell. The three industrial PERC concepts employ lean industrially applicable process sequences which reduce the phosphorus concentration at the wafer surface.

"When applied to PERC cells, the ion-implanted and GEB emitters achieve conversion efficiencies of up to 20.3%."

The ion-implanted and GEB emitters consequently obtain significantly reduced emitter saturation current densities of 40 to 60fA/cm^2 for emitter sheet resistances of 90 to 130Ω/sq. When applied to PERC cells, the ion-implanted and GEB emitters demonstrate up to 10mV higher open-circuit voltages than the $POCl_3$-diffused reference PERC cell and achieve conversion efficiencies of up to 20.3%. The potential for further increases in efficiency has been discussed.

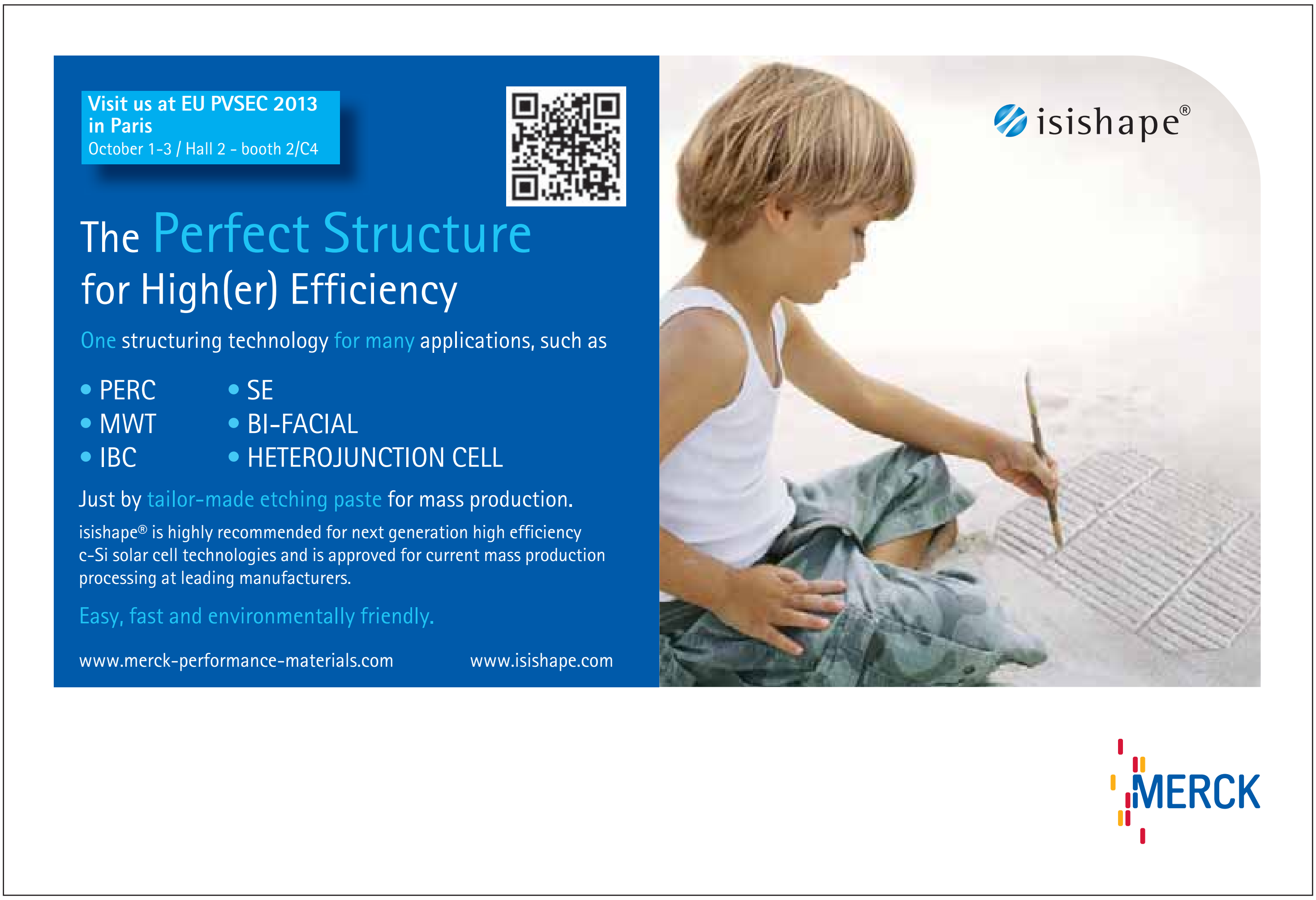
Visit us at EU PVSEC 2013
in Paris
October 1-3 / Hall 2 - booth 2/C4
The Perfect Structure
for High(er) Efficiency
One structuring technology for many applications, such as
• PERC
• MWT
• IBC
• SE
• BI-FACIAL
• HETEROJUNCTION CELL
Just by tailor-made etching paste for mass production.
isishape® is highly recommended for next generation high efficiency c-Si solar cell technologies and is approved for current mass production processing at leading manufacturers.
Easy, fast and environmentally friendly.
www.merck-performance-materials.com
www.isishape.com
isishape®
MERCK


THE
WET PROCESSING
COMPANY
RENA
RENA PERC Technology
› 20 % efficiency for mono
› 18 % efficiency for multi
• rear side polishing
• rear side passivation with InPassion ALD Al_2O_3 – typical layer thickness 5 nm
• rear side laser contact opening
More at www.rena.com

Acknowledgements

We thank our colleagues at ISFH for their support in the processing of the solar cells. This work was funded in part by the German Federal Ministry for the Environment, Nature Conservation and Nuclear Safety within the HighScreen R&D project and by our industry partners Singulus Technologies, RENA, Heraeus, Solar World and Applied Materials.

References

[1] Blakers, A.W. et al. 1989, "22.8% efficient silicon solar cell", *Appl. Phys. Lett.*, Vol. 55, p. 1363.

[2] Klöter, B. et al. 2013, "Current status of high-efficiency Q.ANTUM technology at Hanwha Q.Cells", *Proc. 39th IEEE PVSC*, Tampa, Florida, USA [in press].

[3] Zhao, J. 2013, "A 20% efficient PERC type cell and prospects for the future of high efficiency cell technologies", *Proc. 39th IEEE PVSC*, Tampa, Florida, USA [in press].

[4] Xia, Z. et al. 2013, "Rear side dielectrics choices in PERC solar cells", *Proc. 39th IEEE PVSC*, Tampa, Florida, USA [in press].

[5] Weber, T. et al. 2013, "High volume pilot production of high efficiency PERC solar cells – analysis based on device simulation", *Proc. 4th SiliconPV Conf.*, Hamelin, Germany [in press].

[6] Lachowicz, A. et al. 2012, "NO_x-free solution for emitter etch-back", *Proc. 27th EU PVSEC*, Frankfurt, Germany, p. 1846.

[7] Dullweber, T. et al. 2012, "Towards 20% efficient large-area screen-printed rear-passivated silicon solar cells", *Prog. Photovolt.: Res. Appl.*, Vol. 20, pp. 630–638.

[8] Lai, J.H. et al. 2011, "Large area 19.6% efficient rear passivated silicon solar cells with local Al BSF and screen printed contacts", *Proc. 37th IEEE PVSC*, Seattle, Washington, USA, pp. 1929–1932.

[9] Haverkamp, H. et al. 2008, "Minimizing the electrical losses on the front side: Development of a selective emitter process from a single diffusion", *Proc. 33rd IEEE PVSC*, San Diego, California, USA, pp. 430–433.

[10] Antoniadis, H. et al 2010, "All screen printed mass produced silicon ink selective emitter solar cells", *Proc. 35th IEEE PVSC*, Honolulu, Hawaii, USA, pp. 1193–1196.

[11] Köhler, J.R. et al. 2009, "Laser doped selective emitters yield 0.5% efficiency gain", *Proc. 24th EU PVSEC*, Hamburg, Germany, pp. 1847–1850.

[12] Jäger, U. et al. 2009, "Selective emitter by laser doping from phosphorus silicate glass", *Proc. 24th EU PVSEC*, Hamburg, Germany, pp. 1740–1743.

[13] Dubé, C.E. et al. 2011, "High efficiency selective emitter cells using patterned ion implantation", *Energy Procedia*, Vol. 8, pp. 706–711.

[14] Hahn, G. 2010, "Status of selective emitter technology", *Proc. 25th EU PVSEC*, Valencia, Spain, pp. 1091–1096.

[15] Gatz, S. et al 2012, "Analysis and optimization of the bulk and rear recombination of screen-printed PERC solar cells", *Energy Procedia*, Vol. 27, pp. 95–102.

[16] Müller, J. et al. 2011, "Contact formation and recombination at screen-printed local aluminum-alloyed silicon solar cell base contacts", *IEEE Trans. Electron. Dev.*, Vol. 58, No. 10, pp. 3239–3245.

[17] Hannebauer, H. et al. 2013, "Record low Ag paste consumption of 67.7 mg with dual print", 4th Metalliz. Worksh., Constance, Germany [in press].

[18] Dullweber, T. et al. 2013, "Ion-implanted PERC solar cells with Al_2O_3/SiN_x rear passivation", *Proc. 4th SiliconPV*, Hamelin, Germany [in press].

[19] Kranz, C. et al. 2013, "Wet chemical polishing for industrial type PERC solar cells", *Proc. 4th SiliconPV*, Hamelin, Germany [in press].

[20] Hannebauer, H. et al. 2013, "Gas phase etch back: A new selective emitter technology for high-efficiency PERC solar cells", *Proc. 28th EU PVSEC*, Paris, France [forthcoming].

[21] Hannebauer, H. et al. 2012, "Analysis of the emitter saturation current density of industrial type silver screen-printed front contacts", *Proc. 27th EU PVSEC*, Frankfurt, Germany, p. 1360.

About the Authors

Thorsten Dullweber received his Ph.D. from the University of Stuttgart, Germany, in 2002. From 2001 to 2009 he worked as a project leader at Siemens, Infineon and Qimonda. Since 2009 he has led the R&D solar cell production processes group at ISFH, focusing on process and efficiency improvements of industrial-type screen-printed silicon solar cells.

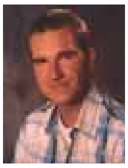

Helge Hannebauer studied technical physics at the Leibniz University of Hanover from 2005 to 2009. For his diploma thesis at ISFH he studied the optimization of screen-printed solar cells. He started his Ph.D. degree in 2010, also at ISFH, with a focus on advanced screen printing and selective emitters.

Christopher Kranz received his diploma degree in physics from the University of Münster (WWU) in 2011, after which he began a Ph.D. programme at ISFH in the R&D group for solar cell production processes. He currently carries out research on screen-printed solar cells with passivated emitter and rear side.

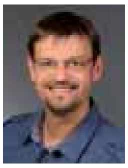

Rene Hesse studied engineering at the University of Applied Sciences in Brandenburg/Havel. Since receiving his diploma degree in 2007, he has worked as an R&D engineer at ISFH, with a focus on screen printing.

Sabrina Wyczanowski joined ISFH in 2008 as a technical assistant. She is responsible for the RENA InPilot tool at ISFH, including the development of improved chemical polishing processes. She is also in charge of processing PERC solar cells within different R&D projects at ISFH.

Vikram Bhosle received his Ph.D. in materials science and engineering in 2007 from North Carolina State University, USA. His thesis work was related to novel transparent conducting oxide for optoelectronic and photovoltaic devices. He has been with Varian Semiconductor Equipment/ Applied Materials since 2011, working on the development of ion implantation and processing for high-efficiency solar cells.

Chris Dubé has B.S. and Ph.D. degrees in chemistry and an M.S. in electrical engineering. He started his career in photovoltaics at Mobil Solar Energy Corporation (1982–1992), followed by Evergreen Solar (2004–

2009). Since 2009 he has been with Varian Semiconductor Equipment/Applied Materials, developing and promoting ion implantion for solar cell processing.

Katrin Weise studied electrical engineering at the University of Paderborn from 2003 to 2008. She then worked in the PV department at Stiebel Eltron on the industrialization of the RISE EWT solar cell concept that was developed at ISFH. In 2011 she joined the R&D department of RENA GmbH as a process engineer for wet chemical smoothening processes.

Dr. Oliver Doll heads the R&D labs of Structuring Solutions within the chemicals business sector of Merck KGaA, Germany. He holds a Ph.D. in the field of inorganic and analytical chemistry.

Dr. Ingo Koehler is head of R&D and technical marketing of Structuring Solutions at Merck KGaA, Germany. Since 2007 he has contributed to numerous publications on c-Si PV cell performance. He holds a Ph.D. in the field of semiconductor and solid-state physics and is a member of the scientific advisory board of Fraunhofer ISE PV-TEC, Germany.

Prof. Rolf Brendel is the scientific director of ISFH. He received his Ph.D. in materials science from the University of Erlangen, for which he researched infrared spectroscopy. In 2004 he joined the Institute of Solid State Physics of the Leibniz University of Hanover as a full professor. His main research focuses on the physics and technology of crystalline silicon solar cells.

Franck Delahaye studied process technology. In 1999 he started PV activities at RENA. He worked on various PV technologies and invented wet processing applications like single side etching. At present he is product manager in the solar division of RENA.

Enquiries

Thorsten Dullweber
Institute for
Solar Energy Research Hamelin
(ISFH)

Am Ohrberg 1
31860 Emmerthal
Germany

Tel: +49-5151-999-638
Fax: +49-5151-999-400
Email: t.dullweber@isfh.de

The status and future of industrial n-type silicon solar cells

Cell Processing

Radovan Kopecek & **Joris Libal**, ISC Konstanz, Konstanz, Germany

ABSTRACT

According to the ITRPV (International Roadmap for PV), a large fraction of future solar cells will be n-type and rear-contact cells with the highest efficiencies and fabricated using low-cost processes. As the standard p-type silicon solar cell in mass production is completely optimized and has therefore reached its cost limit, it is currently very difficult for new solar cell concepts to be cost effective from the outset when introduced into production. Consequently, in the current market situation, the introduction of new solar cell concepts to the market is not straightforward. The only way to achieve this is to use the fully adapted standard processes employed in today's manufacturing lines and only upgrade them with a few industrially approved process steps – such as laser ablation and boron diffusion – in order to implement low-cost device structures with stable efficiencies well above 20%. This paper gives an overview of n-type cell concepts already present on the market and of promising technologies ready for pilot production; the latter were summarized and discussed at the 3rd nPV workshop in April 2013 in Chambéry, France. The consequences for module manufacturing, as well as for measurement techniques and for requirements in respect of new standardization for cell and module characterization, will also be discussed.

Introduction

In the last 10 years, the PV industry has had to survive three large crises: the feedstock crisis in 2005–2008, the world financial crisis in 2008–2009, and, the most difficult one so far, the large overcapacity of wafer, cell and module producers beginning in 2011. The last one is the most difficult so far and still ongoing; because of consolidation, only the fittest companies and most cost-effective technologies are surviving it.

Fig. 1 shows schematically the known learning curve for PV module prices. The plummet in price is due to sales that are close to, or even below, production costs in the struggle for survival. In 2013, module prices have now fallen to €0.50/Wp on average, so that – apart from the downstream players – actually nobody in the PV business today is making a profit. The period after 2014 is expected to be characterized by a continuous but slow decrease in module manufacturing cost, with the module price stabilizing for a certain time, enabling manufacturers to restore some profit margins. At the same time, balance of system cost is expected to experience a stronger cost reduction, resulting in an overall decrease in the cost of the installed PV system. Compared with the boom period lasting until 2011, characterized by continuous expansion of production capacities all along the value chain, it is now much more difficult to introduce new technologies to the market as the capability of cell producers to invest in the future drops to zero because of the lack of liquidity and of the persisting overcapacity.

At the moment, however, the situation is slightly improving, and the concepts that were popular two or three years ago are gaining interest again, because, after the crises, high-level companies have to be prepared to distinguish their products from standard mass-produced p-type products. This is possible by, for example, introducing n-type technologies that – thanks to the stable and high efficiencies – will enable a significant step forwards regarding the reduction in the cost of electricity (€/kWh) generated by PV.

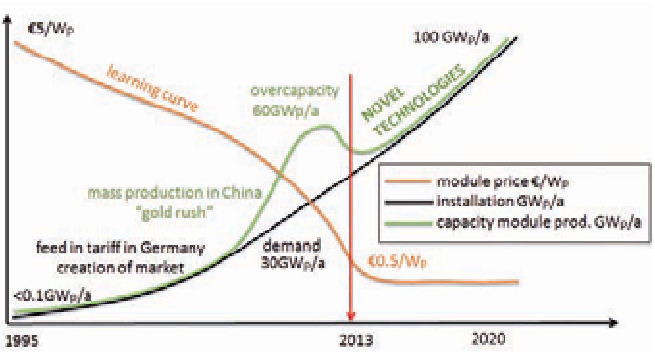

Figure 1. The development of demand, production capacity and module prices over the years and a forecast for the future.

> "The trend is moving towards ion-implanted cells, rear-contacted cells or n-type processes."

In order to significantly exceed 20% efficiency, the trend is moving towards ion-implanted cells, rear-contacted cells or n-type processes. Actually the combination of these three technologies will result in the most cost-effective and powerful device – an ion-implanted, n-type, rear-contacted interdigitated back-contact (IBC) cell with a potential efficiency greater than 23% in mass production. Provided that low-cost processes will be available, the addition of surface passivation by a-Si layers will further enhance the efficiency potential.

In the next section, the challenges and chances for the industrial implementation of n-type solar cell concepts will be considered. This will be followed by an overview of existing technologies, with a focus on diffused screen-printed devices; the specific requirements such devices have regarding suitable *I-V* measurements will be examined. Finally, useful advanced module technologies will be summarized and the future of n-type PV discussed.

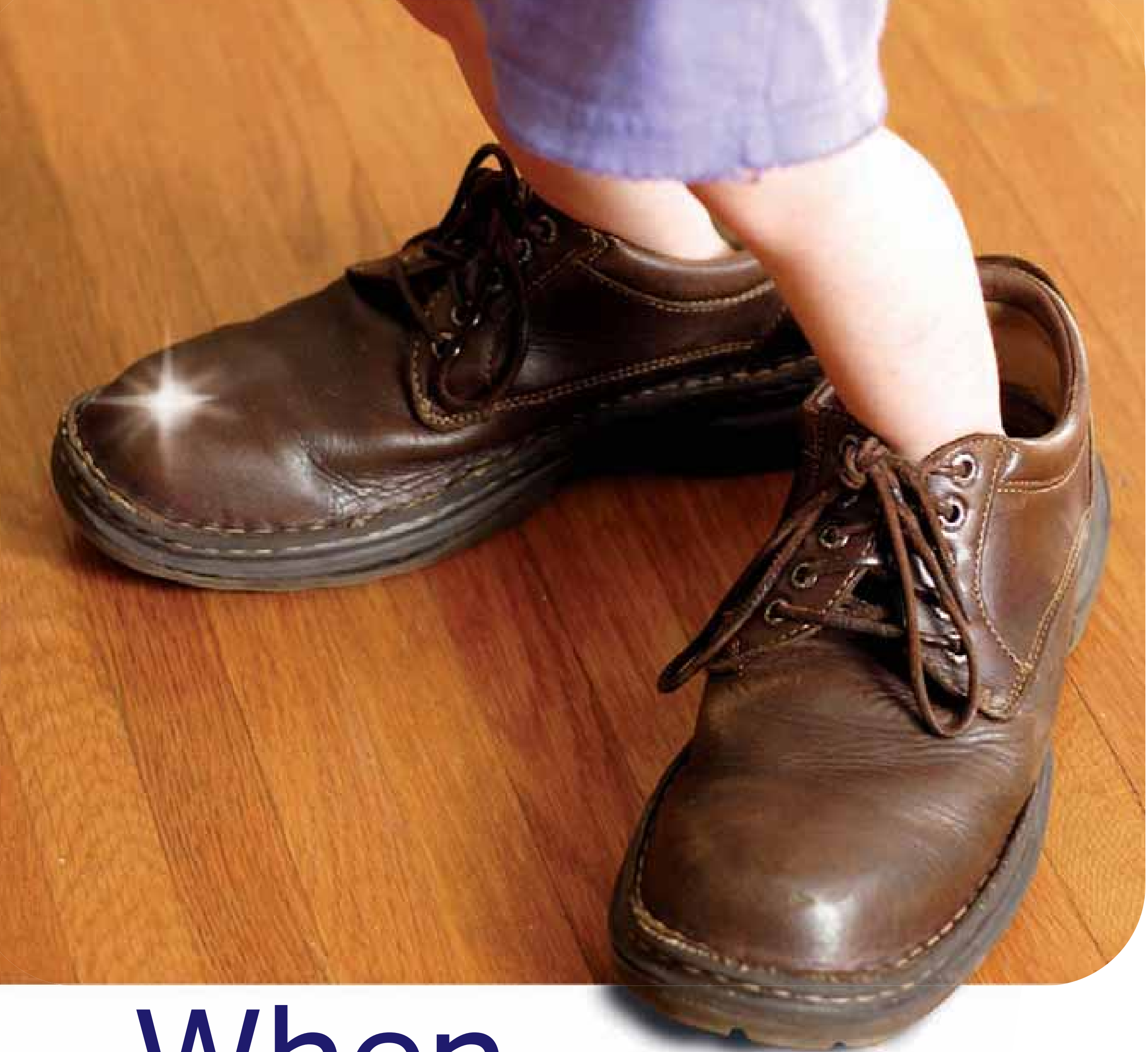

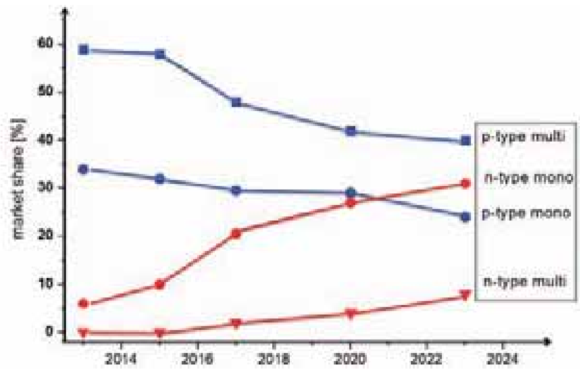

Figure 2. Predicted market share of various Si PV technologies according to ITRPV [2]. The data have been simplified as follows: 'p-type multi' includes 'p-type multi' and 'p-type high-performance mc-Si', while 'p-type mono-like' has been included in 'p-type mono'.

Challenges and chances for n-type cells

Challenges

- Wafer availability and price
- Homogeneous boron diffusion
- Silver consumption
- Dependence on few paste manufacturers

As regards the challenges for n-type PV technology in becoming the leading technology – not only from an efficiency point of view, but also in terms of production cost – an important issue up until now has been the higher sales price of n-type Cz-Si wafers than that of p-type Cz-Si wafers. One reason for this price gap is that certain n-type cell concepts currently implemented in industrial production require a very narrow resistivity range; in addition, some of them require wafers with rather high minority-charge carrier lifetimes (e.g. HIT – heterojunction with intrinsic thin amorphous layer). As the strong segregation effect of P in silicon leads to a larger resistivity distribution within the n-type Si crystal than within B-doped p-type silicon, the requirement of a wafer specification with a narrow resistivity range decreases the wafer production yield and consequently increases wafer cost.

Another important factor is today's small market share of n-type solar cells that prevents n-type Si crystal and wafer producers from benefiting from economy of scale on the same level as p-type manufacturers currently do. As more and more n-type-based cell manufacturing lines are expected to enter into production in the short and mid term (see section 'A look into the crystal ball'), the increasing production volume of n-type wafers will help to close the price gap. Recent news, such as the announcement by Comtec Solar of the construction of a 1GW/year n-type mono ingot and wafer plant in Malaysia (production start in January 2014 [1]), confirms this trend. In addition, upcoming crystal growth techniques, such as continuous Cz-Si pulling (CCz-Si by MEMC/SunEdison – technology from Solaixc, and HiCz by GTAT – technology from Confluence Solar) not only have the potential to enable production of monocrystalline Cz-Si at the cost of cast multicrystalline silicon, but also intrinsically feature the same production cost for n-type doping as for p-type doping, because of the narrow resistivity range the techniques allow for both types.

> "The market share of p-type mono and multi is expected to decrease, while n-type mono particularly will strongly increase."

The ITRPV [2] expects n-type mono to quadruple its market share from today's 5% to 20% in 2017, and to further increase it to 30% in 2023. Fig. 2 clearly shows this trend: the market share of p-type mono and multi is expected to decrease, while n-type mono particularly will strongly increase and, together with p-type multi, will dominate the Si PV market.

Another feature of almost all n-type cell concepts is the fact that the p^+-doped regions are formed by a boron diffusion and not by alloying of Al as in the case of a standard p-type Al back-surface-field (BSF) cell. Consequently, new types of screen-printing metal paste are required that, on the one hand, provide a low contact resistance when applied to the B-doped silicon, and, on the other hand, feature a good electrical conductivity when printed as fingers on, for example, the front-side B-emitter of a bifacial n-type cell. New types of paste for this purpose (in general Ag pastes with a small amount of Al) are now commercially available; however, further developments are required in order to allow the efficiency potential of screen-printed n-type Si solar cells to be fully exploited (see section 'The status of diffused and screen-printed solar cells'), and to reduce the Ag content of these p^+-contacting pastes. Initially, the need for this additional Ag/Al paste causes a greater Ag consumption per cell, leading to an increased Ag cost compared with standard p-type cells. Apart from reducing the Ag content of the pastes, reducing the quantity of paste used for the formation of the busbars, or even eliminating them completely (see section 'Module interconnection'), will significantly reduce the Ag consumption for n-type cells. If the increasing gap between n- and p-type cells in terms of stabilized efficiency is also taken into account, the Ag consumption in g/Wp (and consequently the cost in €/Wp) will further improve in favour of n-type cells.

Chances

- Higher efficiency potential (light-induced degradation (LID), metallic impurities, temperature stability)
- Higher energy harvest (higher sensitivity to low light intensity, bifaciality)

The challenges highlighted earlier are all being tackled by research institutes and companies involved in n-type solar cell process development; n-type technology therefore offers two important advantages, namely a higher *stabilized* efficiency and an increased energy harvest (more kWh/kWp) potential.

> "IBC and the HIT cell concepts both achieve the highest efficiency when using n-type Si wafers instead of p-type."

The potential for higher efficiency is based on the fact that the IBC and the HIT cell concepts – cell designs that are capable of achieving much higher efficiencies than any standard cell design – both achieve the highest efficiency when using n-type Si wafers instead of p-type. A high module efficiency reduces the costs related to the balance of system (BOS) of a PV installation. Consequently, if high efficiency does not come at the price of high module production cost, the cost of the installed PV system can be reduced. It is also important to stress that with increasing market share of n-type, the consideration of *stabilized* efficiency will gain more and more importance. Within the first few weeks after their installation in the field, standard p-type modules lose, because of LID, up to 2–3% of the P_{mpp} value at which they have been sold to the customer. As p-type-based PV modules nowadays represent more than 95% of the PV module market (or nearly 100% when considering just the 'standard' price segment), customers in the current situation have no alternative but to accept this initial power loss. As soon as more n-type-based modules not prone to LID become available, the LID susceptibility of p-type modules, from the point of view of the end-user, will translate into a higher module price (€/Wp) or into a lower energy yield and thus a higher cost of the electricity generated by the modules.

As pointed out and discussed in more detail in the section 'The need for additional measurement standards for bifacial structures', most n-type cells are intrinsically bifacial and can achieve an increased energy yield (kWh/kWp) both in monofacial (standard) and in bifacial module configurations.

Overview of n-type technologies

A comprehensive overview of n-type technologies can be found in Kopecek & Libal [3] – only the most important n-type cell concepts will be summarized here.

The very first solar cell, the 'Bell Solar battery' [4] created in 1954, was actually fabricated using an n-type Cz-Si wafer. The p^+- and n^+-doped regions, as well as the electrodes, were all located on the rear side of the cell in an interdigitated geometry: this was the first n-type IBC cell. Since then, the IBC concept has been used by many R&D groups in order to obtain record efficiencies using manufacturing process steps in the laboratory. Today, the IBC cells and modules produced by SunPower feature a module energy conversion efficiency of 21.5%, which is the highest among commercially available crystalline silicon PV modules. However, because of the rather complex process sequence, the production cost (€/Wp) is significantly higher than that of c-Si mainstream PV technology.

In second place in the efficiency ranking of commercial solar modules is another n-type concept: the HIT solar cell from Sanyo, now commercialized by Panasonic. In addition to the advantages of n-type cells described earlier in this paper, because of the heterojunction and the resulting high open-circuit voltages, the reduction of P_{mpp} with increasing module temperature is low for the HIT concept. Consequently, HIT modules can achieve a significantly higher energy yield (kWh/kWp) than standard crystalline silicon modules. Factors that have up until now contributed to a higher price (€/Wp) than standard PV technology are first – as already mentioned above – the need for very high quality wafers in order to take advantage of the excellent surface passivation by the amorphous silicon layer and thus to fully exploit the potential of the HIT concept, particularly in terms of open-circuit voltage, and, second, the high level of cleanliness of the wafers required during the HIT process sequence, which increases the cost for wet chemical cleaning steps.

For a long time, the HIT and IBC concepts (both meanwhile achieving over 23% cell efficiency in mass production) have been the only n-type cell concepts in industrial production – each concept being produced by a single manufacturer only. In 2009 Yingli started to industrially implement and further develop the n-Pasha cell developed by ECN. This bifacial n-type cell – with a boron-diffused front-side emitter, phosphorus-diffused BSF and

Company/Institute	Country	Name	Bifacial cell structure	Technology	Efficiency [%]	Reference
Yingli	China	PANDA	H-pattern	Diffused, SP	19.5	[7]
ECN	Netherlands	n-Pasha	H-pattern	Diffused, SP	20	[8]
INES	France	NN	H-pattern	Diffused, SP	20	[9]
ISC Konstanz	Germany	BiSoN	H-pattern	Diffused, SP	20	[10]
PVG Solutions	Japan	NN	H-pattern	Diffused, SP	20	[11]
Suniva	USA	NN	H-pattern	Implanted, SP	20	[12]
LG Electronics	Korea	Neon	H-pattern	Implanted, SP	20.5	[13]
Bosch Solar	Germany	iBiN	H-pattern	Implanted, SP	20.5	[14]
Hareon	China	NN	IBC	Diffused, SP	20	[15]
Samsung	Korea	NN	IBC	Implanted, SP (metal glass)	20.5	[16]
ISC Konstanz	Germany	ZEBRA	IBC	Diffused, SP	21	[17]

Table 1. Diffused and ion-implanted 6″ industrial n-type solar cells from different companies/institutes with screen-printed (SP) metallization and with two different geometries, both having a bifacial characteristic. (Efficiency values are rounded to 0.5% abs., as different measuring conditions were applied.)

metal finger grid on the front and rear sides – is commercially available in Yingli's PANDA modules.

The so-called PhosTop concept [5] is another category of n-type cells that is noteworthy. From the manufacturing point of view, it is the simplest n-type cell concept: the same process sequence as for standard p-type BSF solar cells is applied to n-type wafers to obtain an n-type solar cell with a rear-side Al-alloyed emitter and a phosphorus-diffused front-surface field (FSF). The particular advantage of the PhosTop cell concept is the fact that a standard p-type cell-manufacturing line can be used without the need for any significant equipment modifications. There are two reasons why this type of cell has not yet been implemented in industry: first, the rear Al emitter must be completely closed, so no Ag/Al pads can be located on the rear side and consequently standard soldering for interconnecting the cells within the module is not possible; second, being a rear emitter cell, this cell design requires rather high-quality wafer material with high minority-charge carrier lifetimes, making it difficult to achieve the lowest production cost. In addition, as various authors (for example Schmiga et al. [6]) have shown by numerical simulations, even when applying more-advanced techniques, such as a selective FSF, the potential of an industrially viable PhosTop cell with full Al rear emitter is limited to around 20%. Ultimately, because of the limited efficiency potential, it seems that today's higher cost of n-type wafers and the additional investment required for the module manufacturing line are not offset by the slightly higher module power output using the PhosTop cell design.

The status of diffused and screen-printed solar cells

In the authors' opinion, diffused and screen-printed n-type solar cells have the greatest potential to be cost efficient, as they rely on the standard p-type process which has been optimized in mass production. Many companies and institutes are therefore working intensively on such solar cells with two-sided contact geometry (similar to the Yingli PANDA cell) and with the IBC cell structure (similar to ZEBRA cell of ISC Konstanz).

Table 1 summarizes the solar cell concepts which have been presented, for example at the nPV workshops [7] and other PV conferences such as the EU PVSEC and IEEE PVSC, in recent years. The table shows that all solar cell concepts have efficiencies of about 20%, with the highest (21%) being achieved by the ZEBRA concept from ISC Konstanz. As ion implantation is beginning to enter the p-type solar cell market, and seems to be (in some cases) also cost efficient, some of the listed n-type concepts have implanted emitters as well.

It is obvious that these solar cells are limited by one of the process steps, which in this case is screen printing. The most important drawback is the recombination beneath the AgAl contacts to the B emitter. Measurements before screen-printing metallization show implied open-circuit voltages (V_{oc}), for example for the ZEBRA concept, of around 700mV, which is then reduced by 40–50mV to an actual V_{oc} of about 655mV because of metal-induced recombination (MIR) [18]. In order to increase the voltage, a deeper diffusion would be preferable, a softer metallization needs to be done, or something similar to passivated contacts has to be adapted in combination with screen-printed contacts. Efficiencies well above 22% would then be feasible for the IBC approach.

It is important that a more detailed measurement standard be agreed on: at the moment the kind of measurement chuck to be used for standardized measurements has not been defined. This topic will be discussed in the next section.

The need for additional measurement standards for bifacial structures

Bifacial solar cells are still thought to be only interesting to an exclusive niche market and are also considered to be very costly. Both of these impressions are false, since 90% of n-type cell concepts are bifacial anyhow (or can easily be made as such) as shown in Fig. 3. This opens up the possibility of using bifacial devices in bifacial modules and benefiting from the additional albedo (as glass–glass modules are now cheaper and demonstrate longer lifetimes). However, bifacial devices in standard monofacial modules also offer additional advantages, which have been demonstrated very effectively by Bosch [19] and LG [20] in high-power 60-cell modules, with P_{mpp} exceeding 300W.

Since the cells are bifacial and demonstrate higher efficiency, other measuring standards are needed: capacity effects begin to play an important role, and the conductivity and reflectivity of the measuring chuck will have a large influence on measurements, even if taken in monofacial mode (no additional light from the rear). Such devices can be also measured in bifacial mode, but this would be an article in itself, as there are many possibilities and challenges for such characterization. This topic will therefore only be touched on very briefly in the next section. Fig. 4 shows schematically what such measurements look like, with 1 sun 1.5AM applied to the front side. The amount of albedo collected by the rear in Fig. 4(a) depends on the nature of the surroundings; the chuck used in Fig. 4(b) depends on the kind of backsheet that is planned to be included in the module.

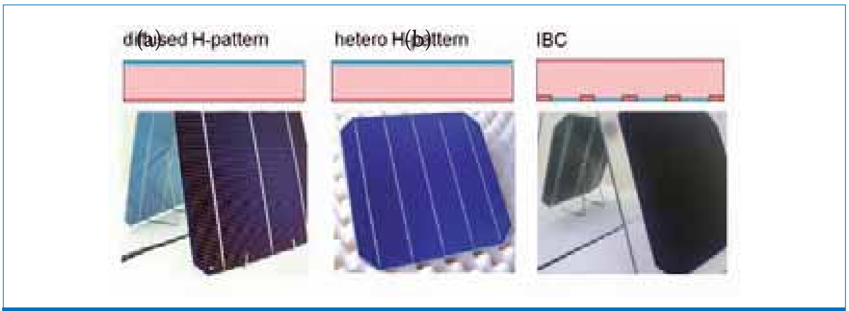

Figure 3. Cross sections and images of the most prominent n-type solar cells. Since both sides always have an emitter or a BSF/FSF, and as none of the sides has a fully metallized surface, the solar cells can be made bifacial.

"Other measuring standards are needed: capacity effects begin to play an important role, and the conductivity and reflectivity of the measuring chuck will have a large influence."

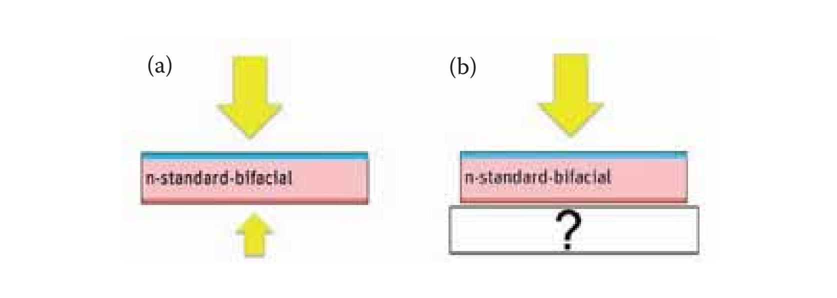

Figure 4. Schematic of the illumination of a bifacial cell in (a) bifacial and (b) monofacial modes. The unknown features are the illumination from the rear and the choice of chuck.

Bifacial measurements of bifacial devices

Bifacial modules (glass transparent backsheet or glass–glass) with effective bifacial devices inside offer a huge potential for greater kWh harvesting. Because n-type devices are moving towards bifacial anyway, and thin glass is becoming more cost effective, the bifacial effect will surely be widely used in many installations in the future. Of course, the more reflective the ground or the surroundings, the more productive the bifacial effect: white flat roofs and installations on sand are therefore very good applications for boosting yearly power output without requiring any tracking.

Fig. 5(a) shows two possible ways of measuring bifacial cells in bifacial mode: 1) with one light source, two mirrors and filters (top); and 2) two light sources (bottom). The measured power gain is shown in Fig. 5(b) for different light intensities coupled into the rear side of a cell. When installations on sand are considered (reflectance of 40%), a power increase of 35% is expected; this means that standard 260Wp 60 6″ cell modules would have a performance similar to 350Wp modules (which actually do not exist at the moment). Such installations would be a good way of reducing the total system cost.

Monofacial measurements of bifacial devices

Like bifacial measurements, for which many measuring standards have to be agreed on, monofacial measurements can be also very complex, since other effects have to be considered as for standard solar cell measurements. The most important questions are:

1. What must the pulse length of the light flash be?
2. How should the chuck property be chosen (considering reflectivity and conductivity)?

In some cases, in order not to suffer from capacity effects, the flash pulse length even has to be chosen above 200ms, when V_{oc} is around 720mV (HIT and IBC). Otherwise, capacity effects of the measured solar cells will lead to inaccurate measurements of the efficiency. This must be checked before measurements are taken.

The properties of the chuck play an important role as shown in Fig. 6, where the internal quantum efficiency (IQE) is indicated for standard and bifacial p-type cells measured on a black chuck and on a white (reflective) chuck. A difference at long wavelengths between 1000 and 1200nm is clearly visible in the bifacial solar cells measurements taken on black and on white chucks. This is obviously due to the reflection of the chuck, leading to higher J_{sc} in the case of the reflective chuck.

Bosch Solar Energy has measured its n-type bifacial solar cells at FhG ISE using two different chucks depicted schematically in Fig. 7(a). The corresponding calibrated measurements are shown in Fig. 7(b) [21]. The measurement on the black, non-conductive chuck led to a cell efficiency below 20%, whereas for the reflective, conductive chuck it was above 20%. Bosch therefore proposed to use a white, non-conductive chuck in order to approximate the situation in the module where there is a rear side with a white backsheet. In this case the resulting efficiency would be 20.1%, as the current and voltage can be taken from the reflective chuck; however, since the fill factor *FF* in this situation is overestimated, the value for that has to be taken from the non-conductive chuck. Because such measurements are close to the module properties, the cell-to-module losses can easily be quantitatively estimated.

Assembly of n-type modules

Module interconnection

Just as with standard p-type cells, n-type cells with contacts on the front and rear sides, such as BiSoN and n-Pasha, can be interconnected by the soldering of copper ribbons – usually using fully automated tabber-stringer machines. The use of electrically conductive adhesives (ECAs) instead of soldering for connecting the ribbons to the cell is currently undergoing intense study, and this method can be applied to p-type as well as n-type cells. Gluing the ribbons has the advantage

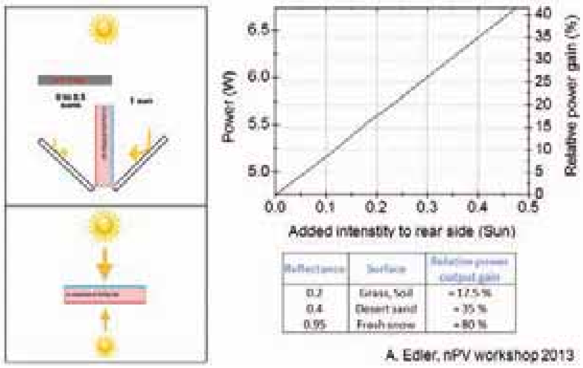

Figure 5. (a) Possible bifacial measurement modes. (b) Power gain as a function of rear albedo.

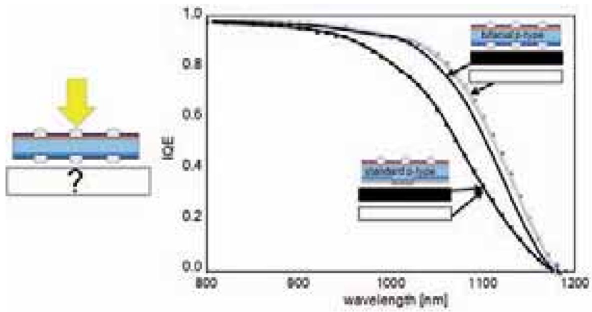

Figure 6. IQE for a bifacial p-type cell, measured with a black and a white chuck, and the same measurements for a standard p-type solar cell with full Al rear contact. The gain in short-circuit current J_{sc} for the bifacial cell, when using a white chuck, results from reflected light of wavelengths from 1000 to 1200nm.

(a)

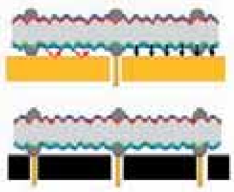

(b)

Chuck	Jsc [mA]	Voc [mV]	FF [%]	eta [%]
Golden*	39.12	647.5	79.47	20.13
Black*	38.69	647.1	79.35	19.86
Combined	39.12	647.5	79.35	20.10
Δ	1.1%	<0.1%	0.2%	1.2%

(*ISE CalLab measurements)

Figure 7. (a) The reflective conductive chuck (top) and the black (non-reflective) and non-conductive chuck (bottom) used for measuring Bosch's n-type bifacial solar cells. (b) Measurements of these cells taken at FHG ISE [21].

of significantly reducing the formation of microcracks in the cells, especially when using wafers of thickness below 150µm – a thickness predicted by the latest ITRPV [2] from 2017 onwards.

The interconnection of back-contact cells can be accomplished using two different approaches. The first possibility is the use of conductive backsheets (CBSs) in combination with ECA for the interconnection. The CBS uses a known concept from the production of printed-circuit boards and is a laminate consisting of three functional layers:

1. Close to the cells, an isolating layer with openings for contacting the cells to the second layer.

2. A thin (e.g. 0.35mm) copper or aluminium layer, where the conductors for the two polarities are electrically isolated and structured in such a way as to create a series connection of the cells within the module.

3. An external layer made of polymeric materials (e.g. Tedlar), whose purpose is to protect the module under all possible climatic conditions in order to guarantee a long module lifetime.

The back-contact cells are glued using ECA to the conductive backsheet (with a layer of encapsulant inserted in between). The large cross section of the copper conductors (only 0.35mm thick, but with a width in the cm range) allows very low series resistances, leading to a reduced cell-to-module power loss. This technology is already in use on an industrial level for p-type metal-wrap-through (MWT) module assembly and can be directly applied to n-type MWT and IBC cells.

The second interconnection possibility is the soldering of copper ribbons using modified tabber-stringer machines (e.g. available from Komax). To reduce the additional mechanical stress and excessive bowing of the cells due to the fact that soldering takes place only on the rear sides of the cells, a soft ribbon (low yield strength) should be used. Another option for reducing the occurrence of microcracks is again the use of ECA instead of soldering. An important advantage of using standard ribbons for interconnection instead of CBS is that, in combination with a transparent backsheet, the bifaciality of the n-type cells can also be exploited at the module level, leading to a significantly increased energy yield (kWh/kWp(front)) and thus a reduced levelized cost of energy (LCOE – €/kWh).

An innovative module interconnection technique that can be applied to p-type as well as n-type cells is the NICE technology [22] from Apollon Solar: besides eliminating the encapsulant, this technology also replaces the backsheet by a glass pane. Such a glass–glass module has two advantages: first, it can be used in bifacial configurations; second, the replacement of standard backsheets by glass provides the best protection against climatic impact, allowing module lifetime guarantees exceeding 30–35 years.

Cell encapsulation

Apart from NICE technology, all n-type cell technologies have two important requirements with respect to the encapsulants. First, the encapsulant must be chemically compatible with the metal pastes used for cell fabrication as well as with the ECA. Second, advanced n-type cell concepts, in particular IBC cells, feature an excellent spectral response in the short-wavelength range (300–400nm); in order to transfer this efficiency increase to the final module, highly UV-transparent encapsulants are necessary. Promising candidates for meeting these requirements are ionomers, polyolefines and liquid silicone. Moreover, certain polyolefines have demonstrated a resistance to PID, for example when used in n-type ZEBRA modules [23]. When considering back-contact cells, the front-side encapsulant in any case can be thinner than in standard modules, leading to increased light transmission and reduced cost.

A look into the crystal ball: the future of n-type solar cells

As already noted, for many years the highest-efficiency c-Si solar cells have been processed on n-type silicon. New, lower-cost processes under development are being reported by many companies, such as Samsung, Suniva, Top Cell and Hareon among others. LG and Bosch, for instance, have demonstrated monofacial modules with 60 solar cells (6″ large) yielding P_{mpp} > 300Wp using bifacial n-type solar cells with H-pattern metallization on both sides. This result is in part a consequence of the additional advantage of reflection of the white Tedlar into the rear of the cell, leading actually to cell-to-module gains of up to 2% rel. Recently the construction of a 1GW n-type wafer factory in Malaysia was announced [1], and the n-Pasha consortium have begun planning a 100MW line in the USA for Nexolon [24].

> "More and more n-type technologies will enter the PV market in the coming years."

The authors are confident that in the light of the steady improvement of the screen-printing pastes for n-type devices, the mass production of n-type wafers, the continuous progress in improving industrial processes for B-emitter formation, and, in particular, the high and stable efficiencies and high-energy yields, more and more n-type technologies will enter the PV market in the coming years. Since technologies that are based on established industrial process steps – as in the case of, for example, the ZEBRA IBC cell by ISC Konstanz – will substantially benefit from these developments, ISC Konstanz plans to transfer the ZEBRA technology to industrial production in 2014.

A new era of PV has begun in which adapted solutions for PV cells and modules will be introduced into the market, guaranteeing the lowest possible LCOEs and the longest module lifetimes for the respective applications. Manufacturers will thereby be given the opportunity to diversify their products away from the mass-produced commodity products such as the n-type technologies discussed in this article or through, for example, desert modules for hot and harsh climate conditions [25].

References

[1] PV-Tech.org, June 27, 2013, "Comtec Solar starts construction of 1GW N-type mono wafer plant in Malaysia" [http://www.pv-tech.org/news/comtec_solar_starts_construction_of_1gw_n_type_mono_wafer_plant_in_malaysia].

[2] SEMI PV Group Europe 2013, "International technology roadmap for photovoltaic (ITRVP): Results 2012", 4th edn (March) [http://www.itrpv.net/Reports/Downloads/].

[3] Kopecek, R. & Libal, J. 2012, "Switch from p to n", *pv magazine*, Issue 06.

[4] Chapin, D.M. et al. 1954, "A new

silicon p-n junction photocell for converting solar radiation into electric power", *J. Appl. Phys.*, Vol. 25, pp. 676–677.
[5] Hacke, P. et al. 2004, "Efficiency optimization of the n+/n/p+ 'Phostop' cell", *Proc. 19th EU PVSEC*, Paris, France, p. 1292.
[6] Schmiga, C. et al. 2010, "Optimisations of industrial n-type silicon solar cells with aluminium-alloyed rear emitter by means of 2D numerical simulation", *Proc. 25th EU PVSEC*, Valencia, Spain, p. 2280.
[7] Li, F. 2012, "High efficiency low cost n-type Si solar cells in mass production", nPV Workshop, Amsterdam, the Netherlands [http://www.nPV-workshop.com].
[8] I. Romijn, I. 2012, "Industrial implementation of efficiency improvements in n-type solar cells and modules", *Proc. 27th EU PVSEC*, Frankfurt, Germany, p. 533.
[9] Veschetti, Y. et al. 2013, "High efficiency on large area n-type Si bifacial solar cells", nPV Workshop, Chambéry, France [http://www.nPV-workshop.com].
[10] Edler, A. et al. 2013, "BiSoN: Bifacial industrial solar cell on n-type", nPV Workshop, Chambéry, France [http://www.nPV-workshop.com].
[11] Ishikawa, N. 2012, "Industrial production of high efficiency and high bifaciality solar cells", bifi PV Workshop, Konstanz, Germany [www.bifiPV-workshop.com].
[12] Tao, Y. et al. 2013, Fully ion-implanted and screen-printed 20.2% efficient front junction silicon cells on 239cm^2 commercial n-type CZ substrate", *Proc. 39th IEEE PVSC*, Tampa, Florida, USA.
[13] LG Solar [http://www.lg-solar.com/].
[14] Böscke, T.S. et al. 2013, "Fully ion implanted n-type cells – A contender for industrial cells with >20.5% efficiency", *Proc. 39th IEEE PVSC*, Tampa, Florida, USA.
[15] Dong, J. et al. 2013, "High efficiency full back contacted cells using industrial processes", *Proc. 39th IEEE PVSC*, Tampa, Florida, USA.
[16] Lee, E. et al. 2013, "Metallic glass: A new approach of solar cell electrode for high efficiency Si-solar cell", *Proc. 39th IEEE PVSC*, Tampa, Florida, USA.
[17] Halm, A. et al. 2012, "The ZEBRA cell concept – Large area n-type interdigitated back contact solar cells and one-cell modules fabricated using standard industrial processing equipment", *Proc. 27th EU PVSEC*, Frankfurt, Germany, p. 567.
[18] Edler, A. et al. 2012, "On the metallization losses of bifacial n-type silicon solar cells", *Proc. 27th EU PVSEC*, Frankfurt, Germany, p. 1429.
[19] Bosch Solar Energy 2013, "Bosch presents innovative photovoltaic and storage solutions", Press Release [http://www.bosch-presse.de/presseforum/details.htm?txtID=6113&locale=en].
[20] PV-Tech.org, September 12, 2012, "SPI 2012: The 300W module club expanding" [http://www.pv-tech.org/news/spi_2012_the_300_watt_module_club_expanding].
[21] Lossen, J. et al. 2012, "Increased energy yield for Bosch's n-type solar cells in bifacial application", bifi PV Workshop, Konstanz, Germany [www.bifiPV-workshop.com].
[22] Podewils, C. 2010, "A late bloomer", *Photon International* (October).
[23] Halm, A. 2013, "Reducing cell to module losses for n-type IBC solar cells with state of the art consumables and production equipment", nPV Workshop, Chambéry, France [http://www.nPV-workshop.com].
[24] PV-Tech.org, June 19, 2013, "Order focus: RENA and Tempress Systems win 100MW advanced cell line contract from US-based Nexolon" [http://www.pv-tech.org/news/order_focus_rena_and_tempress_systems_win_100mw_advanced_cell_line_contract].
[25] PV-Tech.org, July 23, 2013, "ISC Konstanz and Technical University of Berlin open desert module test facility in Egypt" [http://www.pv-tech.org/news/isc_konstanz_and_technical_university_of_berlin_open_desert_module_test_fac].

About the Authors

Radovan Kopecek, one of the founders of ISC Konstanz, has been working at the institute as a full-time manager and researcher since January 2007, and is currently the leader of the Advanced Solar Cells Department. Dr. Kopecek has also been teaching the basics of PV at the DHBW in Friedrichshafen since 2012. He received his Master of Science from Portland State University (Oregon, USA) in 1995, and then obtained his Diploma in physics at the University of Stuttgart in 1998. He completed his Ph.D. in 2002 in Konstanz, with a dissertation topic of thin-film silicon solar cells.

Joris Libal works at ISC Konstanz as a research engineer, focusing on business development and technology transfer in the areas of high-efficiency n-type solar cells and innovative module technology. He received a Diploma in physics from the University of Tübingen and a Ph.D. in the field of n-type crystalline silicon solar cells from the University of Konstanz. Dr. Libal has been involved in R&D along the entire value chain of crystalline silicon PV for more than 10 years, having held various positions at the University of Konstanz, at the University of Milano-Bicocca and, more recently, as an R&D manager with the Italian PV module manufacturer Silfab SpA.

Enquiries

ISC Konstanz
Rudolf-Diesel-Straße 15
78467 Konstanz
Germany

Tel: +49-7531-36 18 3-22
Email: radovan.kopecek@isc-konstanz.de

EU PVSEC 2013

28th European PV Solar Energy Conference and Exhibition

Parc des Expositions Paris Nord Villepinte

Conference 30 Sep - 04 Oct 2013

Exhibition 01 Oct - 03 Oct 2013

The most important international platform for exchange between PV industry, research, finance, politics and the related sectors

EU PVSEC at a glance

Benefits from multiple synergies

- Top international Industry Exhibition
- World's leading PV Conference
- Parallel Events on selected topics as: PV role in the electricity market
  Photovoltaic systems performance
  Materials for innovation

The gathering of the global PV Community

- Business-to-Business
- Business-to-Science
- Business-to-Industries

More information

www.photovoltaic-exhibition.com
www.photovoltaic-conference.com
facebook.com/EUPVSEC
twitter.com/EUPVSEC

With the support of UNESCO's Natural Sciences Sector

WCRE – World Council for Renewable Energy

Cost-effective and reliable Ni/Cu plating for p- and n-type PERx silicon solar cells yielding efficiencies above 20.5%

Richard Russell[1], Loic Tous[1], Riet Labie[1], Monica Aleman[1], Filip Duerinckx[1], Jurgen Bertens[2], Takeshi Horiuchi[3] & Jozef Szlufcik[1]

[1] imec, Leuven, Belgium
[2] Meco Equipment Engineers BV, Drunen, The Netherlands
[3] Hitachi Chemical Co Ltd, Chikusei, Japan

ABSTRACT

This paper presents the status of imec's work on the use of copper for the main conductor as an alternative to screen-printed silver front contacts in solar cells. This work is motivated not only by the limitations that Ag screen-printed contacts have regarding solar cell efficiency (high contact shading, limited line conductivity, and poor contact resistance to moderately doped emitters), but also by the PV industry's desire to reduce Ag usage for reasons of cost. Despite the potential advantages of Ni/Cu contacts, their commercialization has been limited because of increased process complexity and doubts over the €/Wp advantage and long-term reliability. These three factors all depend on the specific process and toolset and are discussed in this paper. A relatively simple process sequence is described that uses industrial pilot-line tools and consists of: 1) defining the front-contact pattern by ps-UV laser ablation; 2) self-aligned plating of the contacts using Ni/Cu/Ag; and, finally, 3) sintering in N_2 for nickel silicidation. The process sequence is applied to 15.6×15.6cm^2 p-type CZ-Si PERC (passivated emitter and rear cell) solar cells with 120Ω/sq. homogeneous emitters; average cell efficiencies of 20.5% are achieved over more than 100 cells. Cost analysis results are then discussed, indicating that this Ni/Cu process sequence has a lower cost/piece than equivalent screen-printed PERC cells while also providing ~0.5% abs. higher cell efficiency. Thermal-cycling and damp-heat reliability data that meet extended (1.5×) IEC 61215 criteria for single-cell laminates and small modules are reported. The improved efficiency potential of applying this metallization sequence to rear-junction n-type PERT (passivated emitter and rear totally diffused) cells is discussed and preliminary results are given.

Background and motivation for copper-based metallization

There is a strong motivation within the PV industry to decrease the usage of silver in cells; this is driven mainly by the desire to reduce €/Wp costs. For conventional screen-printed solar cells, silver accounts for 30–45% of the wafer-to-cell conversion cost and is the main cost element [1]. Despite efforts to reduce silver usage for front contacting in the last four or five years, this cost element has not generally been reduced in production owing to a doubling of the average yearly Ag price between 2008 and 2012. Furthermore, if the PV industry continues to grow and Ag remains the dominant metallization method, within a few years PV will be the major user of Ag and its share of total Ag production will continue to increase, putting further pressure on Ag prices (Fig. 1). It therefore seems likely that silver will remain a significant cost element for conventional solar cells for the foreseeable future.

"Copper-based metallization clearly has a potential cost advantage."

Given that copper has a similar electrical conductivity to silver but is less than a hundredth of the price per kg, copper-based metallization clearly has a potential cost advantage. However, the motivation for replacing silver with a copper-based metallization scheme is not just because of the potential cost-reduction arguments and concerns over future Ag prices: contacts based on nickel/copper provide many technological advantages which can increase cell efficiency. Ni/Cu contacts provide ~2.5× higher electrical conductivity than Ag paste, lower contact resistance at low Ns [3] and no restriction on line widths (because of the self-aligned nature of plating).

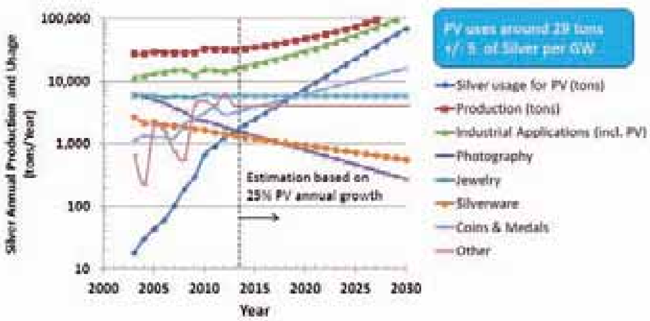

Figure 1. Worldwide annual silver production and usage by applications. (Historical data from The Silver Institute, 2013; Future prediction from Verlinden [2].)

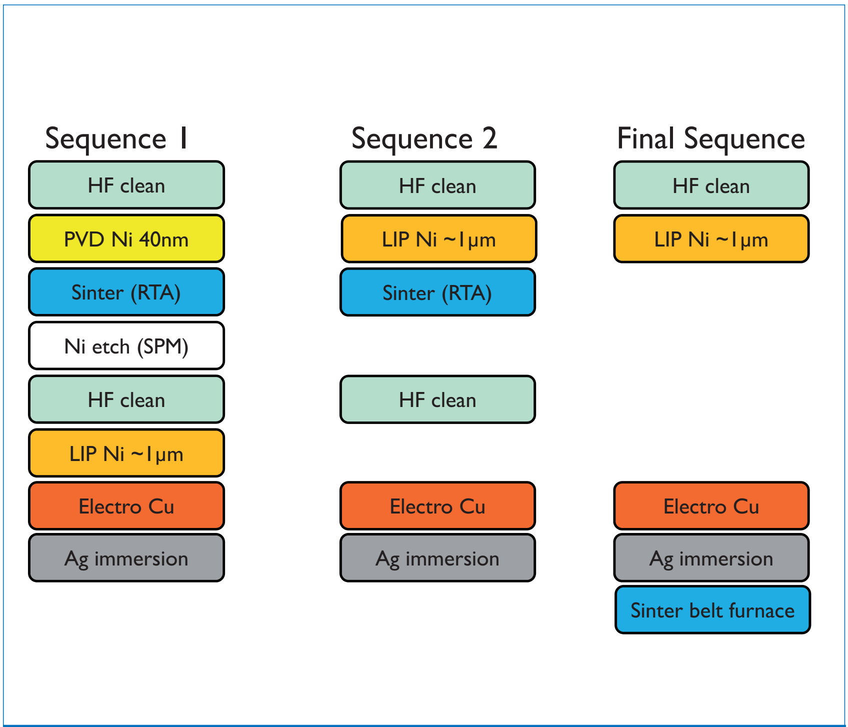

Figure 2. Metallization process evolution at imec.

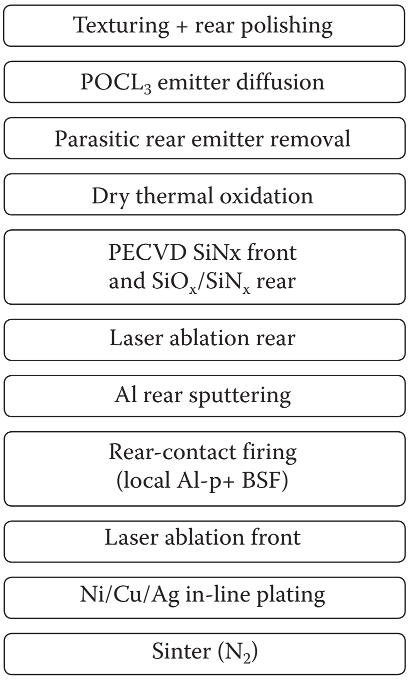

Figure 3. i-PERC cell process flow with Ni/Cu metallization.

Contacts of this type are typically sintered between 250 and 400°C, which is significantly lower than the temperature of 750–850°C required for Ag paste contacts, enabling passivation schemes degraded by high temperatures to be used as well as providing superior rear dielectric/Al reflectance in the PERC (passivated emitter and rear cell) cell since no melting of the rear Al occurs on contact formation.

Despite the potential advantages of Ni/Cu contacts, their commercialization has so far been limited, with the notable exception of BP Solar between the years 1992 and 2008 [4]. Reasons for the limitation include the increased process complexity and the availability of suitable low-cost production techniques and tools. In BP Solar's process, cells were laser grooved and subsequently nickel plated, sintered to form nickel silicide for low contact resistance and contact adhesion, then copper plated and a thin layer of Ag deposited for solderability. Although this metallization process provided highly conductive, low contact resistance metallized fingers with low shading, the downside from the point of view of production was that it relied on electroless Ni and Cu plating, with the process flow being interrupted by Ni sintering between plating steps. The low plating rate (compared with typical electroplating) of the electroless plating solutions created an undesirably large amount of work-in-progress. Electroless plating solutions have the reducing agent in the electrolyte and need to be well controlled, and require frequent dosing and bath changing, which leads to significant waste disposal costs. Even though some development work in copper electroplating was carried out in 2004 [5,6], the process was not introduced into production at BP Solar, one issue being the suitability of available production equipment at the time. Despite these issues, BP Solar sold ~150MWp of modules of the Ni/Cu laser-grooved buried contact process. An early, large 1MWp installation in Toledo, Spain, commissioned in 1992 but still operational today, provides evidence that long-term reliability is possible using Cu-based metallization.

Some of the early obstacles to achieving a viable low-cost Cu metallization process have been surmounted by recent advances in plating and dielectric patterning techniques. Bias-assisted light-induced Ni/Cu plating and suitable production electroplating tools now provide increased plating rates and stable baths which can operate for long periods of time as a result of consumed metal ions being replaced from metal anodes, greatly reducing effluent treatment costs. New cost-effective patterning techniques such as laser ablation, laser doping and patterned etching have also made possible new metallization strategies which do not rely on Ag screen printing.

It is therefore not surprising that there has been a recent re-emergence of interest in copper plating. Over the last year at least six companies (Kaneka, TetraSun, Silevo, Schott Solar, Hyundai heavy industries, SunTech) have reported solar cell efficiencies of over 20% (some significantly higher) with the incorporation of Cu metallization. However, it is not achievable cell efficiencies that will trigger a major switch to copper metallization but rather the demonstration of a clear reduction in the cost of the energy produced over the lifetime of modules compared with other metallization technologies. Convincing the PV community of the possibility of long-term module reliability with Cu-based contacts may now be the biggest hurdle to overcome for the widespread introduction of Cu metallization.

Copper metallization development at imec

At imec the focus has been on investigating the cell efficiency potential, module reliability and €/Wp cost potential for Ni/Cu contacts on i-PERC cells using industrial pilot-line processing tools. Initially, sputtered Ni layers were used to guarantee good uniformity, and nickel silicidation was performed before copper plating, which, as expertise grew, progressed to a simpler Ni/Cu metallization sequence as shown in Fig. 2. The final simplified sequence has the advantage of a minimal number of process steps and allows one-stop in-line plating.

All results reported here use the

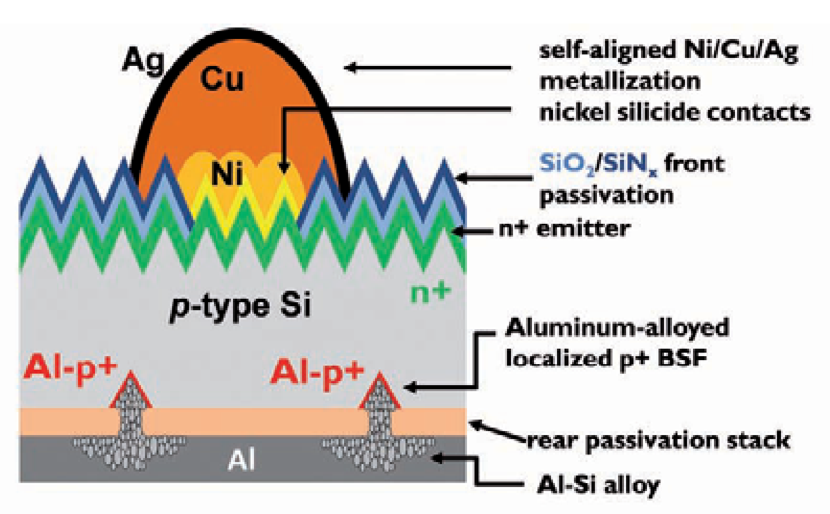

Figure 4. Cell structure of Ni/Cu i-PERC cells.

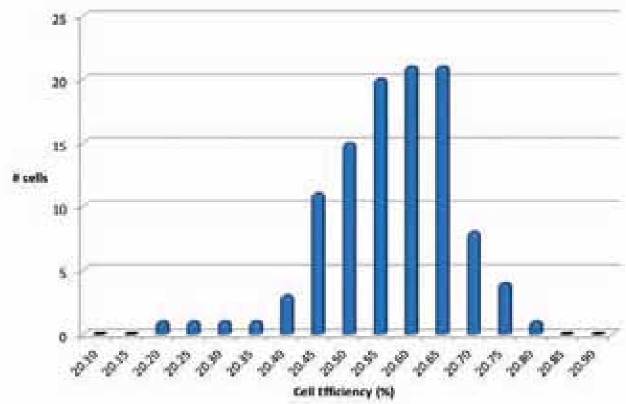

Figure 5. Cell efficiency distribution from a 109 Ni/Cu i-PERC cell run.

	J_{sc} [mA/cm^2]	V_{oc} [mV]	*FF* [%]	*Eff* [%]
Average	38.8	661.3	80.0	20.54
CoV	*0.26%*	*0.18%*	*0.25%*	*0.49%*
Best cell	39.1	663.3	80.3	20.79

Table 1. Ni/Cu i-PERC cell results for 156mm MCZ wafers (averages over 109 cells). (*CoV* = coefficient of variation = std dev/mean %.)

simplified sequence, with the Ni/Cu/Ag plating being made in an industrial pilot-line plating tool from Meco, and the final nickel silicidation step in a belt furnace from BTU; both tools have throughputs of greater than 100 6″ cells/hr. The full i-PERC process sequence using Ni/Cu metallization is shown in Fig. 3, with the final cell structure depicted in Fig. 4.

In this plating sequence Ag is still used, albeit only a 100–200nm, thin, dense layer deposited by displacement plating, adding minimal cost. Ag is preferred over, for example, Sn because the final sintering step is above the melting point of Sn. Since the cell rear remains metallic Al in this process, conventional solder tabbing is not possible in module fabrication. This is a problem which is common to many high-efficiency cell structures, but several solutions already exist, such as the use of conductive adhesives, Schmid's TinPad technology [7] sputtering additional layers, or displacement plating of a zinc layer on the Al, enabling further rear plating. The use of a non-Ag-containing conductive adhesive film from Hitachi Chemical for module tabbing is reported here.

Cell results

In 2012 imec reported top efficiencies (confirmed at Fhg-ISE Cal lab) of 20.3% on 125mm CZ-Si substrates and 20.5% on magnetic Czochralski Si (MCZ Si) [8] using the Ni/Cu i-PERC process described in Russell et al. [9].

Before the process was transferred to 156mm wafers, a power loss analysis (in mW/cm^2) gave a detailed quantification of the loss mechanisms limiting cell efficiency [10]. The analysis showed that the three main contributors lowering cell efficiency were: 1) recombination losses at V_{oc} (3.35mW/cm^2) mainly from recombination at the front metal contacts; 2) optical losses (2.99mW/cm^2) mainly from high shading and non-optimal rear reflectance; and 3) recombination losses (1.33mW/cm^2) as a result of a non-ideal diode. On the basis of this analysis, performance improvements for several process changes were estimated using PC1D, predicting that cell efficiencies greater than 21% should be feasible, as discussed in Tous et al. [10].

Several performance-improving process changes have already been incorporated into the process flow for 156mm wafers [11]. Other potential improvements – in particular, improving rear-side reflectivity and lowering rear-contact recombination by replacing local Al back-surface field (BSF) contacts with local epitaxially grown B BSF contacts – are under development, with promising results being reported [12]. Current cell efficiencies obtained at imec using MCZ-Si 156mm wafers are shown in Table 1, with a tight cell efficiency distribution as shown in Fig. 5. With only one electrically failed cell (not included), these results demonstrate a repeatable, robust Ni/Cu process capable of providing high cell efficiencies. All 109 remaining cells yielded efficiencies above 20% (average of 20.5%), with the best cell achieving 20.8%.

> "Results demonstrate a repeatable, robust Ni/Cu process capable of providing high cell efficiencies."

Adhesion and reliability data

A summary of imec's current reliability test data is presented here (more details can be found in Russell et al. [9]). Cells were made for reliability testing according to the i-PERC process flow as described. Single- and multi-cell laminates were made either by using a non-Ag-containing conductive adhesive film from Hitachi Chemical for tabbing or by conventionally soldering Sn/Ag/Pb-coated ribbons at five points along the cell length at 320°C. Note that, in order to allow some cells to be conventionally soldered, these cells had an additional 2µm-Al/40nm-Ni/150nm-Cu layer sputtered on the rear after rear-contact firing; this was necessary because in the standard i-PERC process flow the cell rear remains metallic aluminium, which cannot be soldered to by conventional means.

Pull-tab adhesion

Table 2 presents adhesion results for three cell types: 1) Ag screen-printed i-PERC cells as a control group; 2) Cu-metallized i-PERC cells; and 3) Cu-metallized i-PERC cells with an additional 2µm-Al/40nm-Ni/150nm-Cu layer sputtered on the rear to allow rear-side conventional soldering. The results in Table 2 represent averages taken over 20 or 50 measurements for the maximum 45-degree pull strength registered at a test point normalized to the metallized contact width (N/mm).

Single-cell laminates put on test

Eighteen 25×25cm^2 Tedlar/EVA/1cell/EVA/glass laminates were prepared for either thermal-cycling (−40 to 85°C) or damp-heat (85% relative humidity, 85°C) tests. Cells were pre-conditioned to approximately 5kWh/m^2 to remove any light-induced degradation before testing.

The ribbons were conventionally soldered onto cells or else connected via a non-Ag-containing conductive adhesive film technology from Hitachi Chemical. Standard Ag screen-printed cells (Ag sp/Al BSF with Ag rear busbars) tabbed by soldering and Ag screen-printed i-PERC cells (Ag sp/Al) tabbed by conductive adhesive film were included as control groups. Copper-metallized i-PERC cells had rear surfaces of either metallic Al (Cu/Al) or metallic Al/Ni/Cu/Ag (Cu/Al Ni Cu Ag) and were tabbed either using conventional soldering or via a conductive adhesive film from Hitachi Chemical. The single-cell laminates put on test are summarized in Table 3.

Multi-cell modules put on test

Two modules were made (size for 60 × 156mm cells), one for thermal-cycling and the other for damp-heat testing in accordance with IEC 61512 specifications at an external accredited test site. Within each module there were five individual cell strings consisting of eight or ten cells, each string electrically separated from the others, allowing each string to be measured individually. Four different cell-type/tabbing technology combinations were put on test, as indicated in Table 4. The cells were sister cells from the single-cell laminate tests and the same tabbing conditions were used.

Reliability test results

Summaries of the average results for copper-metallized cells and for Ag screen-printed cells are given in Tables 5 and 6 respectively.

Many of the single-cell laminates in damp-heat testing showed significant progressive J_{sc} loss dominating cell efficiency losses, particularly for the copper-plated cells. These laminates had obvious EVA discolouration and were tinted brown. As this affected both Ag- and Cu-metallized cell laminates, and no such J_{sc} loss was seen in the damp-heat Ag or Cu 10-cell string tests, the cause is believed to be related to the batch of EVA or Tedlar used for the laminates. The IEC 61215 test pass criterion is ≤5% P_{max} loss after 200 thermal cycles (−40 to 85°C) or 1000 hours damp-heat exposure (85°C, 85% relative humidity) [10]. In the tests, a total of 16 copper and 12 silver-paste metallized single/multi-cell laminates were subjected to thermal cycling (–40 to 85°C) or damp-heat ageing (85°C, 85% relative humidity). All laminates passed 300 thermal cycles or 1500 hours damp-heat exposure, which corresponds to one and a half times the IEC 61215 test specification, with no evidence of one metallization type being superior to any other. Although more complete testing is required and is planned, the results are clearly encouraging.

"All laminates passed 300 thermal cycles or 1500 hours damp-heat exposure, which corresponds to one and a half times the IEC 61215 test specification."

Estimates of the cost of ownership advantage of Ni/Cu plating

While the developed Ni/Cu-plating process certainly has the potential for yielding higher efficiencies compared with a reference screen-printing process, it can also deliver substantial advantages with regard to cost of ownership (COO). COO calculations were carried out by imec for a hypothetical PERC-type production line comparing screen-printed Ag- and Ni/Cu-plated front contacts. In both cases, the assumed output of the line was roughly 2100 cells/hour. Included in these calculations were investment costs, floor space, consumables/materials, utilities, labour, downtime and yield losses.

At first sight, the Ni/Cu-plating process appears to have a disadvantage, since it creates additional process complexity and higher capital expenses. This is clear from the fact that a Ag printer/dryer has to be replaced by a trio of systems: a laser, a plating system and a low-temperature sintering furnace. However, in terms of COO, this disadvantage is easily nullified when considering the cost of materials. Ag paste remains very expensive and this aspect is expected to become even more problematic as yearly production capacity increases in years to come. Although considerable efforts worldwide are being made to reduce the amount of Ag used per wafer [13], it is imec's belief that this is only postponing the inevitable switch to the application of Cu.

If all the cost factors mentioned above are taken into account for both metallization possibilities, an advantage of 5.5€¢/cell in favour of the Ni/Cu-plating scenario is estimated. This, however, assumes that a similar emitter is used in both cases. If an adapted emitter is necessary then the advantage can decrease to a level of 3.2€¢/cell, still clearly in favour of the plating option. This means that introducing Ni/Cu plating instead of screen printing in a production line significantly reduces not only the cost per Wp (by working on both the numerator and the denominator of the equation), but also the cost per piece as shown above. This makes Ni/Cu plating one of the few new technologies that can improve both the efficiency and the cost of the technology it aims to replace.

Cell type (front/rear)	Technology	Measurements per side	Av front [N/mm]	Av rear [N/mm]
Ag sp/Al	Conductive adhesive	20	2.5	2.9
Cu/Al	Conductive adhesive	50	2.2	3.3
Cu/Al	Standard soldering	50	2.5	N/A
Cu/Al Ni Cu	Standard soldering	20	2.0	3.5

Table 2. Summary of adhesion results for three cell types.

Cell type (front/rear)	Tabbing	Damp heat No. of cells	Thermal cycling No. of cells
Ag sp/Al BSF	Soldering	2	2
Ag sp/Al	Conductive adhesive	2	2
Cu/Al	Conductive adhesive	2	2
Cu/Al Ni Cu	Conductive adhesive	2	2
Cu/Al Ni Cu	Soldering	1	1

Table 3. Summary of single-cell laminates put on test.

Cell string type (front/rear)	Tabbing	Module 1 Damp heat No. cells in string	Module 2 Thermal cycling No. cells in string
Ag sp/Al BSF	Soldering	10	10
Ag sp/Al	Conductive adhesive	10	10
Cu/Al	Conductive adhesive	8	10
Cu/Al	Conductive adhesive	10	8
Cu/Al Ni Cu	Conductive adhesive	10	10

Table 4. Summary of strings in multi-cell modules put on test.

Ni/Cu metallization applied to n-PERT Cells

Metallization based on Ni/Cu contacts can be applied to many different cell structures. In fact imec has now started to look at applying this metallization scheme to an n-PERT (passivated emitter and rear totally diffused) cell, whose structure is shown in Fig. 6.

In the PERT cell structure, the rear side is totally diffused to form the emitter, which is then passivated by a dielectric layer and locally contacted. The plated front side remains n-type, so no modification is required to the plating process used for Ni/Cu p-type i-PERC cells. However, there are several advantages: 1) no light-induced degradation of final cell efficiencies typical of p-type wafer cells; 2) high minority-carrier diffusion lengths of n-type wafers; and 3) any defect creation during front-contact laser ablation or metal diffusion (during nickel silicidation) is kept away from the

		IEC 61215		Extended IEC 61215	
		200 thermal cycles	1000 hours damp heat	300 thermal cycles	1500 hours damp heat
Cu 1-cell laminates	Av ΔIsc	-0.1%	-2.7%	-0.5%	-2.6%
4 Hitachi adhesive	Av ΔVoc	-0.3%	1.0%	0.2%	1.1%
1 standard solder	Av ΔFF	-0.9%	0.9%	-0.8%	1.0%
	Av ΔEff	**-1.3%**	**-0.8%**	**-1.3%**	**-0.5%**
	Max ΔEff	**-2.2%**	**-4.1%**	**-2.3%**	**-4.6%**
Cu 10-cell strings	Av ΔIsc	2.9%	2.0%	2.4%	1.6%
3 Hitachi adhesive	Av ΔVoc	0.2%	1.2%	0.5%	0.4%
	Av ΔFF	-1.2%	-0.6%	-3.2%	-2.9%
	Av ΔEff	**1.9%**	**2.7%**	**-0.4%**	**-1.0%**
	Max ΔEff	**0.9%**	**0.6%**	**-1.3%**	**-2.6%**

Table 5. Summary of test results: copper-metallized cells.

		IEC 61215		Extended IEC 61215	
		200 thermal cycles	1000 hours damp heat	300 thermal cycles	1500 hours damp heat
Ag 1-cell laminates	Av ΔIsc	-0.1%	-1.2%	-0.2%	-0.9%
2 Hitachi adhesive	Av ΔVoc	0.1%	0.3%	0.2%	0.4%
2 standard solder	Av ΔFF	-0.8%	-0.7%	-0.9%	-1.1%
	Av ΔEff	**-0.8%**	**-1.6%**	**-1.0%**	**-1.5%**
	Max ΔEff	**-1.4%**	**-2.8%**	**-1.6%**	**-2.5%**
Ag 10-cell strings	Av ΔIsc	1.6%	1.7%	0.5%	1.5%
1 Hitachi adhesive	Av ΔVoc	0.2%	0.3%	0.2%	0.3%
1 standard solder	Av ΔFF	0.9%	0.5%	-0.7%	-0.4%
	Av ΔEff	**0.9%**	**2.3%**	**-0.2%**	**1.5%**
	Max ΔEff	**0.9%**	**1.8%**	**-0.2%**	**0.7%**

Table 6. Summary of test results: Ag screen-printed cells.

most sensitive part of the cell – the emitter. This should add up to higher cell efficiencies and a more robust process.

Indeed, imec's PC1D simulations [14] predict that higher cell efficiencies (>0.5% abs.) should be achievable with n-PERT cells if recombination at the front surface can be kept low. As the junction is on the cell rear in the n-PERT design, it is more sensitive to front-surface recombination compared with p-type i-PERC cells, as shown in Fig. 7.

In addition to a higher cell efficiency potential, n-PERT cells also present stronger efficiency tolerance to thinner wafers. This can be explained by the fact that if wafer thickness is decreased, minority-carrier recombination in the bulk (which is a significant recombination loss in rear-junction devices) can be reduced, balancing out optical losses from reduced photon absorption.

Initial n-PERT results on 156mm wafers look very promising [15]. A best cell efficiency of 20.7% (J_{sc} = 38.3mA/cm^2, V_{oc} = 677mV, FF = 79.8%) has already been achieved on 156mm CZ-Si wafers, with higher currents of 38.4mA/cm^2, voltages of 682mV and fill factors of 80.1% being demonstrated on other individual cells.

Summary

Strong pressure exists to decrease silver usage in solar cells in order to reduce €/Wp costs, and significant efforts have been made in this area. The benefits of reduced usage per cell, however, can be neutralized by rising Ag prices. A future scenario in which PV relies on Ag-based metallization and continues to grow significantly to become the dominant market user, creating further pressure on volatile Ag prices, is a concern.

Switching to Ni/Cu-based metallization has the potential to not only reduce costs but also provide higher cell efficiencies, benefiting both sides of the €/Wp equation. It is not surprising then that there has been a re-emergence of interest in Ni/Cu-based metallization schemes. Nevertheless, no significant switch to Ni/Cu has yet been seen: there are concerns about process complexity, realizing potential €/Wp cost reductions and long-term reliability.

A relatively simple Ni/Cu metallization process has been developed at imec which uses industrial plating techniques and tools that were not available to the earlier Ni/Cu adopters, providing more robust and cheaper processing than previously possible. When this metallization process is applied to 6″ i-PERC cells, high average cell efficiencies ~20.5% (109 cells) with a tight distribution are demonstrated. Cost calculations estimate that the metallization process is cheaper at the €/cell level than Ag screen printing, with the added benefit of higher efficiency. Reliability data show that modules made from these cells pass damp-heat and thermal-cycling IEC 61215 extended tests. While not enough to fully demonstrate the long-term reliability of imec's Ni/Cu-based metallization scheme yet, it is a good starting point, with further testing planned.

For the future, imec is applying its Ni/Cu metallization expertise to rear-junction n-type cells, as it is believed that they have a higher efficiency potential and offer increased process robustness. It is also believed that a strong focus on reliability is important, because it seems that a significant switch to Ni/Cu-based metallization, as also predicted by the ITRPV roadmap, will be inevitable, provided that concern about reliability can be replaced by confidence.

> "It seems that a significant switch to Ni/Cu-based metallization will be inevitable as long as concern about reliability can be replaced by confidence."

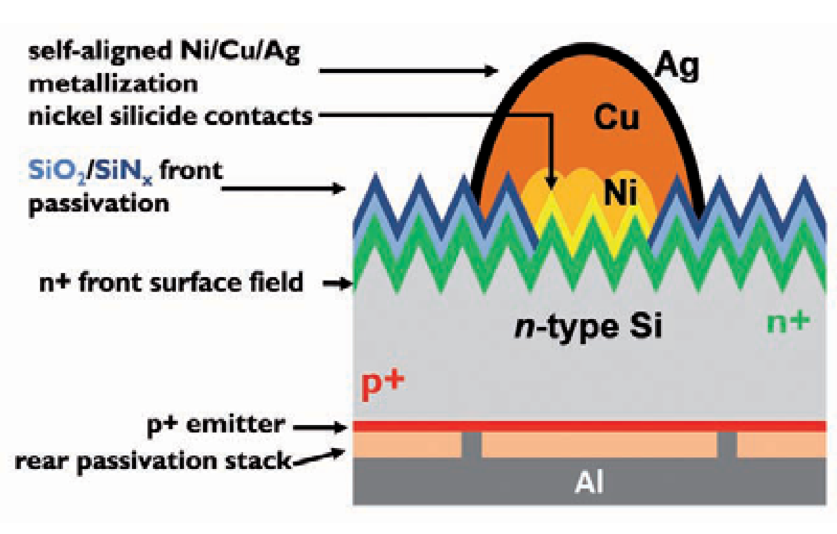

Figure 6. Cell structure of a Ni/Cu n-PERT cell.

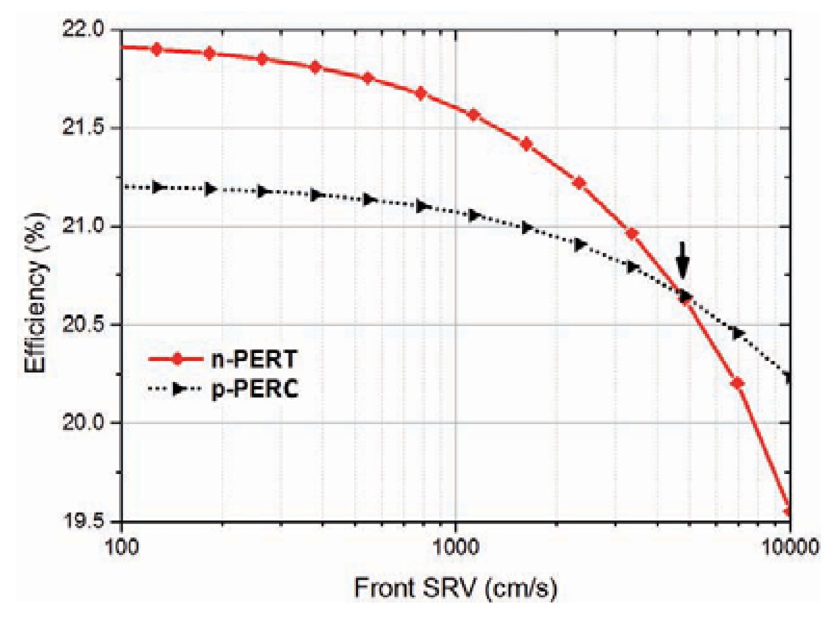

Figure 7. Simulated cell efficiencies for n-PERT and p-PERC cells as a function of front-surface recombination velocity.

References

[1] Mason, N. 2012, 7th PV Fab Managers Forum, Berlin, Germany.

[2 Verlinden, P.J. 2013, *Proc. 28th EU PVSEC*, Paris, France.

[3] Tous, L. et al. 2011, *Proc. 26th EU PVSEC*, Frankfurt, Germany.

[4] Bruton, T. et al. 2003, *Proc. 3rd WCPEC*, Osaka, Japan.

[5] Eager, S. et al. 2003, *Proc. Int. Solar Energy Soc. UK Conf.*, pp. 69–72.

[6] Eager, S. et al. 2002, *Proc. 29th IEEE PVSC*, New Orleans, Louisiana, USA, pp. 62–65.

[7] Campe, H. von et al. 2012, *Proc. 27th EU PVSEC*, Frankfurt, Germany, pp. 1150–1153.

[8] Horzel, J. et al. 2012, *Proc. 27th EU PVSEC*, Frankfurt, Germany, pp. 780–788.

[9] Russell, R. et al. 2012, *Proc. 27th EU PVSEC*, Frankfurt, Germany, pp. 538–543.

[10] Tous, L. et al. 2013, Silicon PV, Hamelin, Germany.

[11] Tous, L. et al. 2013, *Proc. 28th EU PVSEC*, Paris, France.

[12] Récaman-Payo, M. et al. 2013, *Proc. 28th EU PVSEC*, Paris, France.

[13] Muschelknautz, C. et al. 2013, 4th Metalliz. Worksh. Contact. Si Sol. Cells, Constance, Germany.

[14] Tous, L. et al. [submitted for publication].

[15] Aleman, M. et al. 2013, *Proc. 28th EU PVSEC*, Paris, France.

About the Authors

Richard Russell received a bachelor's degree in physics from the University of Exeter, England, and a master's degree in physics from the University of Dundee, Scotland. Between 1990 and 2010 he worked for BP Solar, mainly on Ni/Cu-metallized laser-grooved buried contact cells. He joined imec in 2011, where he leads copper-based metallization activities within the iPERx platform.

Loic Tous obtained his M.Sc. degree in material sciences and engineering from INSA Lyon, France, in 2009. Since 2010 he has been working towards a Ph.D. degree with imec and KU Leuven in Belgium, where he develops nickel/copper-plated contacts for the front-side metallization of industrial silicon solar cells.

Riet Labie received M.Sc. and Ph.D. degrees in materials science and engineering from KU Leuven in Belgium, in 1999 and 2007 respectively. She began working at imec in 1999 as a researcher on various topics, including electroplating and reliability of solder interconnections for packaging applications and 3D-interconnection schemes with Cu through-Si vias. She joined the silicon photovoltaics department in 2010.

Monica Aleman has been working with c-Si Solar cells since 2004, and began evaluating different schemes for the front-side metallization of p-type Si cells at Fraunhofer ISE. In 2009 she joined imec, where her research has been related to the integration of high-efficiency n-type Si cells.

Filip Duerinckx leads the iPERx platform in the silicon photovoltaics department at imec. He received his M.Sc. in engineering from KU Leuven, Belgium, in 1994, followed by his Ph.D. in 1999. His current area of interest is the performance and economic aspects of p- and n-type PERx silicon solar cells.

Jurgen Bertens obtained his bachelor's degree in physics in 1997 from the University of Fontys Eindhoven. He worked at Dimes (TU Delft) as a process engineer and joined Meco in 2001 as a process developer, working on process and equipment development for advanced metallization of crystalline silicon solar cells.

Takeshi Horiuchi obtained his bachelor's degree in chemistry in 1990 from the University of Chiba, Japan. He then began working for Hitachi Chemical, specializing in the development of thermo-setting resin. After gaining experience in ACF development for display electrode connection, he worked on conductive film (CF) development based on ACF technology for PV, as well as on PV market development.

Jozef Szlufcik received his M.Sc. and Ph.D. degrees, both in electronic engineering, from Wroclaw University of Technology, Poland. He joined imec in 1990, where he led research in low-cost crystalline silicon solar cells. From 2003 to 2012 he held the position of R&D and technology manager at Photovoltech in Belgium. He is currently the director of the silicon photovoltaics department at imec.

Enquiries

Richard Russell
imec
Kapeldreef 75
B3001 Leuven
Belgium

Tel: +32 16 28 76 68
Email: Richard.Russell@imec.be
Website: www.imec.be

Thin Film

Researchers pledge to crack open BIPV with flexible encapsulant

Germany's Fraunhofer Institute for Electron Beam and Plasma Technology, ISC and IVV are working to develop a flexible weather-resistant PV encapsulation film aimed at building-integrated PV (BIPV) applications. The aim of the project is to develop a flexible film for thin-film solar cells that offers a service lifetime of 25 years. The research bodies claim such a product would be a "key" enabling technology for BIPV and allow parts of buildings previously unusable for PV installations to be exploited for electricity generation.

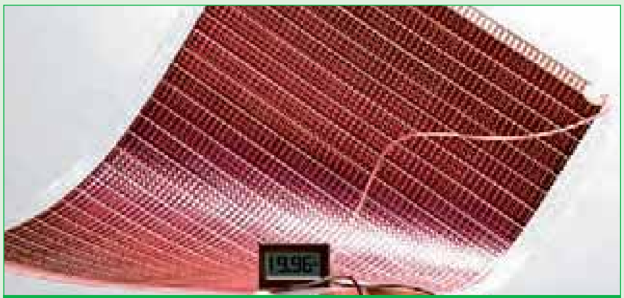

Researchers are developing a flexible BIPV encapsulant.

Cell efficiencies

TSMC Solar raises CIGS module efficiency to 15.7%

Taiwan-based TSMC Solar has pushed its CIGS thin-film module efficiency to 15.7%, up from 15.1%, only four months ago.

The new rating has been verified by TUV SUD.

TSMC Solar said that the latest improvements were achieved with existing equipment and processes, which also led to improved module temperature coefficient characteristics.

Champion CIS thin-film module at Solar Frontier verified at 14.6% conversion efficiency

Solar Frontier's latest champion CIS thin-film module has reached a conversion efficiency of 14.6%, close to values reported for mass-marketed polycrystalline silicon modules.

The PV manufacturer said the rated capacity of its 1257mm x 977mm sized module has been certified by Underwriters Laboratories Inc. (UL) at 179.8W and was produced at its Kunitomi Plant in Miyazaki, Japan.

Breakthrough efficiency set by Solliance and imec for CZTSe solar cell

With the aim of achieving 20% conversion efficiencies but with lower material costs, Solliance and imec have demonstrated a CZTSe (Cu2ZnSnSe4)-based thin-film solar cell (1x1cm2, AM1.5G) with 9.7% efficiency.

Imec's associated lab at the Hasselt University, IMOMEC, fabricated the CZTSe layers by sputtering Cu, Zn and Sn metal layers on a Molybdenum-on-glass substrate with a subsequent anneal in an H2Se containing atmosphere.

The highest efficiency said to have been obtained was 9.7%, with a maximum short circuit current of 38.9mA/cm2, an open circuit voltage of 0.41V and a fill factor of 61 percent.

The 1x1cm2 cell was produced with polycrystalline absorber layers only 1µm thick, with a typical grain size of about 1µm.

Source: Solar Frontier

Solar Frontier's latest champion CIS thin-film module has reached a conversion efficiency of 14.6%.

Liquid phase crystallisation technology promises Masdar PV 14% module efficiencies

A research and development collaboration between Helmholtz-Zentrum Berlin (HZB) and silicon thin-film manufacturer, Masdar PV, could potentially enable module efficiencies above 20%.

Research by HZB on thin-film crystalline silicon created by Liquid Phase Crystallisation (LPC) has produced an open-circuit voltage of 582 mV for c-Si on glass with the depositing of a 10µm layer of silicon.

Initially, HZB / PVcomB and Masdar PV are aiming at producing 14% module efficiencies with the LPC technology. Masdar PV plans to transfer the technology to its existing production facilities and use it on its ultra-large (5.7m^2) substrates in the future.

Technology focus

Solibro's CIGS thin-film IP changes hands within Hanergy as conversion efficiency issues loom

Hanergy Holding is transferring intellectual property (IP) rights to Solibro's copper-indium-gallium-selenium (CIGS) thin-film technology to subsidiary, Apollo Kunming.

Included in the deal is the IP from Solibro Research AB, a Swedish CIGS solar technology research and development company.

Hanergy noted that new Chinese government directives on PV manufacturers improved conversion efficiency targets, including thin-film manufacturers, would lead to further consolidation and a greater need to focus resources on R&D activities.

The company said that it would focus on more advanced thin-film technologies including nano-crystalline silicon and CIGS.

News

Stion announces improvement to its CIGS PV modules

CIGS thin-film module manufacturer Stion has announced the release of the Elevation Series STO module line which it claims adds 10W to the performance of its existing modules through a number of process improvements.

Stion claims that the module's dual glass/glass construction provides "significantly improved moisture resistance and lifetime durability over the traditional polymer based backsheets". Stion also claimed that it had achieved a record low temperature coefficient of 0.26%/degrees C.

Dyesol claims 90% initial performance retention after extended IEC 61646 test

Employing its liquid-based dye solar cell (DSC) substrate, Australian clean-tech company Dyesol claims it has surpassed the standard IEC 61646 design qualification for PV modules, without disclosing the approved testing house.

The IEC 61646 testing standard was mainly based on amorphous silicon (a-Si) technology, designed to monitor such module's performance (Pmax) capabilities under prolonged exposure to 'standard' climates.

Dysol said that its liquid-based dye solar cell (DSC) substrate maintained over 90% of initial performance after a 5000 hour cycle at 85 degrees C. The company said that the IEC 61646 standard called for 1,000 hours and 85degrees C.

Merck leads research consortium to increase dye-sensitised cell efficiency

German chemical company Merck will lead a consortium to develop high-efficiency cobalt-based dye-sensitised solar cells (DSSCs).

The German Federal Ministry of Education and Research (BMBF) will provide around €3 million (US$4 million) for project COBRA (organic cobalt-based low-cost printable large-area photovoltaics), running for three years.

Other participating companies include 3GSolar from Israel and Colour Synthesis Solutions (CSS) from the United Kingdom. Merck claims a cobalt-based redox system in a non-volatile electrolyte of the cell may be crucial. The large-area dye-sensitised solar cells are to have a projected lifetime of more than 20 years.

First Solar

First Solar and Sharp thwart global dominance of Chinese PV suppliers

NPD Solarbuzz's Module Tracker Quarterly for Q2 2013 revealed that only First Solar and Sharp were competing with Chinese PV manufacturers, with First Solar dominating in the US and India and Sharp leading rankings in Japan.

Chinese companies lead in seven of the top 10 PV regions according to shipment figures over the 12 months ending 30 June 2013.

Otherwise, the top manufacturers in all other seven regions are big Chinese names – Yingli, Trina, Canadian Solar and Suntech. Chinese manufacturers have almost universal dominance, with Yingli, Jinko Solar and Haeron Solar supplying 25% of modules to the Chinese market.

Jinko Solar leads a list of other tier one Chinese manufacturers that Solarbuzz says are gaining market share across the world, among them Renesola, JA Solar and Hanwha SolarOne.

In the emerging markets of Latin America, the Middle East and Africa, Western and Japanese suppliers provided stronger competition to Chinese manufacturers, including Conergy, Sharp, REC Solar, SolarWorld and Kyocera.

Source: First Solar

First Solar is the leading module supplier in the US.

First Solar and Ingenero form partnership to take on Australia and Asia-Pacific markets

US thin-film module manufacturer First Solar and Australian PV developer and installer Ingenero, which has experience of building small to medium-scale projects, have formed a partnership agreement aimed at serving the market in Australia and the Asia-Pacific. The two companies will target the commercial and off-grid markets.

First Solar to build 23MW of solar capacity in New Mexico

An agreement between First Solar and US regional power provider Public Service Company of New Mexico (PNM) to construct a total of 23MW of solar power generating capacity across three sites is awaiting approval by the New Mexico Public Regulation Commission.

The plants will be built with thin-film PV modules produced by First Solar, which will also provide engineering, procurement and construction (EPC) services. PNM have around half a million energy customers.

First Solar and BELECTRIC create joint venture for PV power plant projects

A joint venture firm has been created between First Solar and BELECTRIC to pursue the building of PV power plants in Europe, North Africa and the US.

PV Projects will be based in Germany and formalises a business relationship started between the companies around 10 years ago.

The companies recently collaborated in the 128MWp Templin solar power plant in Germany. Specifically in the US market, the companies will focus on smaller-scale projects below 20MW.

Residential thin film

Hanergy expands into residential solar market through UK acquisition

Chinese thin-film manufacturer Hanergy has acquired Engensa, a UK-based home energy systems provider, for an undisclosed purchase price.

The deal will enable the Chinese renewable energy company to break into the UK residential solar market and at the same time provide additional support for Hanergy's strategy to expand into the downstream market.

Credit: First Solar

CIGS suffering in a PV thin-film market in decline, says NPD Solarbuzz.

Solar Frontier goes rooftop with lightweight PV module

Japanese CIS thin-film manufacturer, Solar Frontier, is touting a new lightweight PV module for the residential rooftop market, primarily in the company's domestic market.

Dubbed 'Solacis neo', the 6.5mm-thick module is claimed by Solar Frontier to be the lightest glass substrate thin-film CIS module on the market, weighing only 8kg.

Inherently, thin-film substrates are heavier than conventional crystalline-based modules due to the use of the glass/glass format.

The frameless design is also claimed to increase flex tolerance and will be produced at Solar Frontier's Miyazaki No.2 Plant, with shipments scheduled to start in November 2013 for the Japanese residential market.

Solar Frontier is also launching a new rooftop mounting system called 'Cross One' designed for the new module as well as its current 'SF' series modules. The new mounting system is claimed to reduce by 40% the number of mounting points needed to install its modules on roofs.

Source: Solar Frontier

Solar Frontier goes rooftop with lightweight PV module.

Thin-film consolidation

CIGS suffering in a PV thin-film market in decline, says NPD Solarbuzz

According to NPD Solarbuzz, the continued competitiveness of conventional c-Si technologies and market overcapacity is taking its toll on PV thin-film market share.

The PV thin-film market was said to have peaked back in 2009 as the shortage of polysilicon and peak prices attracted investment, capacity and downstream installations, which led to a 16% global market share that year, up from only 3% in 2000.

However, NPD Solarbuzz is forecasting thin-film PV market share to continue to decline, retaining only a 7% share of new PV production during 2017.

The market research firm noted that in contrast, annual investments in new thin-film equipment exceeded US$1 billion from 2007 to 2012, due to new entrants.

SoloPower looks for investors as restructuring continues

Thin-film manufacturer SoloPower has announced it is looking for new investors as its restructuring process continues.

The company's head offices will also relocate from San Jose, California, to Portland, Oregon, where the firm's CIGS PV module plant is based.

A company statement said an agreement "in principle has been reached with its major secured creditors on a comprehensive restructuring plan as it continues to seek new strategic financing for future expansion".

First Solar sales hit by large-scale PV project slump

First Solar reported worse than expected sales for Q2 2013 while downgrading full-year revenue guidance.

The company reported that the slump in sales was due to its PV project business and a delay in selling projects.

The company reported second quarter 2013 sales of US$520 million, a 31% decline from the previous quarter. Sales have declined for two straight quarters from a fourth quarter 2012 peak of over US$1.0 billion.

First Solar had reported sales of US$957 million in the same quarter a year ago. The company lowered full-year revenue guidance from US$3.8 billion to US$4 billion to between US$3.6 billion and US$3.8 billion.

Product Reviews

3D-Micromac

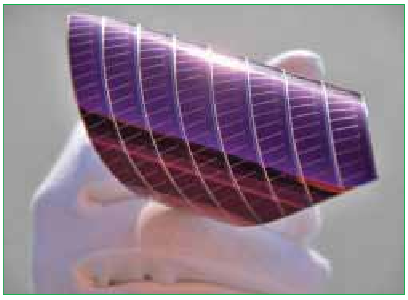

3D-Micromac's 'One-Stop-Patterning' process increases thin-film module efficiencies

Product Outline: 3D-Micromac has launched the first production equipment that can conduct the integrated series-connection of a thin-film solar module on one single platform and in one single production step. The new One-Stop-Patterning process (OSP) only structures the modules once all of the functional layers have been deposited.

Problem: Formerly, thin-film modules were structured with a laser or a mechanical unit, but after each individual layering step, cleaning steps were required,, lengthening processing times and leading to efficiency losses. Due to inaccuracies, 200 to 400 micrometre wide 'dead zones' can be formed which could not be used to produce electricity.

Solution: The OSP process is said to significantly simplify the production process. In addition, the new process prevents inaccuracies, which are caused when the substrate is positioned and aligned on different tables - an improvement which increases the efficiency of a thin-film module by up to a claimed 0.8%. The OSP process also minimizes dead zones to less than 100 micrometres, simplifies manufacturing and increases efficiency. For production, 3D-Micromac falls back upon a combined process from laser and printing technology. The company has been successfully using it in other areas of application. Used for amorphous silicon, cadmium telluride or CIGS thin-film production, the OPS system can easily be integrated into an existing production line and works on all common formats up to 1.10 by 1.30 metres.

Applications: All types of glass substrate thin-film modules.

Platform: The OSP could provide module efficiency gains of up to 0.8%.

Availability: June 2013 onwards.

First Solar

First Solar's 'Series 3' CdTe thin-film module platform offers harsh environment capability

Product Outline: First Solar has launched a new evolution of its Series 3 CdTe thin-film PV module platform. The 'Series 3 Black' is said to incorporate First Solar's latest advances in conversion efficiency as well as additional features to enhance its performance in utility-scale power plants.

Problem: According to First Solar, around 90% of PV power plants are located in hot temperature climates where module temperatures are above 25°C. Due to temperature coefficient impacts on module yields, limiting the temperature impact provides operators and owners with the best possible plant yield.

Solution: The all-black module's change in appearance results from the use of an advanced, all-black edge seal technology combined with an innovative encapsulation material that further enhances its field durability and demonstrates improvements in accelerated life testing results. Tighter scribe lines at the module edge are used. The Series 3 Black's performance in a wide range of operating environments is further validated by its new IEC 60068-2-68 'sand and dust test' certification, which measures durability in harsh desert environments, characterized by blowing abrasive sand. The Series 3 Black is expected to have module conversion efficiencies of 12.9% to 13% plus.

Applications: Industrial and utility-scale PV power plants.

Platform: The Series 3 Black module maintains all the existing IEC certifications and UL listings for the Series 3 family which enable the 1000V system designs.

Availability: Currently available.

Solar Frontier

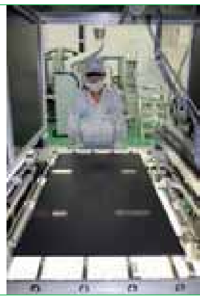

Solar Frontier super-slim thin-film module thinner than a smart phone

Product Outline: Solar Frontier will be launching its Solacis neo, the world's lightest glass substrate thin-film CIS module, which will be offered primarily in Japan on initial launch later in 2013.

Problem: With land availability a growing concern in Japan for ground mounted PV power plants, emphasis is expected to shift to commercial and residential rooftop installs. Providing a lightweight module enables a greater number of rooftop structures to be used for PV.

Solution: : Solacis neo is a slim, lightweight module using Solar Frontier's latest CIS technology. The module is just 6.5 mm thick, virtually the same as a smart-phone, and weighs only 8.0kg. This constitutes a 40% reduction in weight from previous models. The lighter weight, advanced frameless design, increased flex tolerance, all-black appearance, and overall high quality, 'Made-in-Japan' construction, make it well-suited to rooftops.

Applications: Commercial and residential rooftops, primarily in Japan.

Platform: Solar Frontier will also feature new mounting systems for residential use called 'Cross One' mounting system for Solacis neo and SF series modules respectively. The new mounting system substantially reduces the number of mounting points needed to install CIS systems on roofs, without sacrificing safety and reliability. The Cross One mounting system can cut installation time by a claimed 40%, as well as reduce the load on roofs, which means a wider range of roofs can be outfitted with solar panels.

Availability: Manufacturing of Solacis neo is expected to begin at Miyazaki No.2 Plant in October 2013, with shipments scheduled to start in November 2013.

CIGS manufacturing: Promises and reality

David Jimenez, Wright Williams & Kelly, Inc., Pleasanton, California, USA

ABSTRACT

Economic issues are the driving forces behind PV adoption. Even technological advances are measured against their impacts on cost per watt, levelized cost of energy (LCOE), and total cost of ownership for energy (TCOe™). This sixth paper in a series covering business analysis for PV processes looks at two approaches to manufacturing thin-film copper-indium-gallium-diselenide (CIGS) PV – sputtering and co-evaporation – and their potential areas for cost improvement.

The promise of CIGS [1]

In contrast to the non-crystallinity of amorphous silicon (a-Si), thin-film copper-indium-gallium-diselenide (CIGS) is a polycrystalline material consisting of small crystallites. CIGS has several characteristics that make it a valuable PV material. One is its absorption coefficient, which is among the highest for semiconductor materials: 99% of the light incident on CIGS is absorbed in the first micrometre of the device. Thus cells with a thickness of that order of magnitude are possible. Another favourable characteristic is that CIGS has one of the highest current densities of any semiconductor material, with the potential to produce high current outputs. Third, these films retain their performance properties better than most semiconductors. And last, CIGS is amenable to large-area automated production.

Efficiencies in excess of 20% have been reported for small-area experimental cells made of thin-film CIGS. A principal problem with the material is its low open-circuit voltage. However, this deficiency seems to be correctable through improving compositional uniformity by, for example, removing oxygen.

The CIG portion is usually formed on a base electrode of molybdenum (Mo), chosen for its refractory nature and good electrical conductivity. Thin-film CIGS is a p-type semiconductor and a junction is formed at the surface by deposition of a very thin layer of cadmium sulphide (CdS). This creates an n-p homojunction just inside the CIGS material, rather than a simple heterojunction. The device is completed by deposition of a transparent conducting oxide (TCO), such as zinc oxide (ZnO), on top of the junction to help collect the light-generated current. Fig. 1 shows a typical CIGS solar module cross section.

Figure 1. CIGS module cross section.

In a manner similar to the definition and monolithic integration of thin-film a-Si cells, individual CIGS cells are defined and serially interconnected via three patterning steps. The first scribe (in Mo) is performed by a laser beam, while the second and third scribes (to remove CIGS and separate the ZnO) can be performed mechanically or by laser. Again, metal foils are bonded to the first and last cells, and the module is encapsulated using a top cover glass, laminated with encapsulant.

The principle of operation of the device is similar to that of conventional crystalline silicon (c-Si) solar cells. Light is absorbed in the CIGS layer, creating free electrons and holes. The electrons diffuse in the CIGS grains until they find themselves in the electric field within the junction region, at which point they are driven into the CdS/ZnO, thereby building up a voltage between the ZnO electrode and the Mo base electrode.

Why is CIGS appealing? [2]

If you realize the initial success of First Solar, you realize that a thin-film cell having a higher efficiency than cadmium telluride (CdTe) with the potential to eliminate the toxic element cadmium would be of great interest. This major drawback has resulted in purchase restrictions on CdTe panels. In the CIGS manufacturing process, CdS is deposited in a very thin layer (30–50nm) compared with CdTe (2µm). A CIGS module therefore contains much less Cd (1/40th the amount) than a same size CdTe module. Currently, the use of CIGS instead of CdTe makes the issue of toxicity a smaller one, and it is expected that in 3–4 years CIGS manufacturers will have established a Cd-free buffer.

The benefits of CIGS modules [3] are:

- The form factor of CIGS solar cells is optimal for rigid and flexible substrates. CIGS cells can be manufactured on low-cost glass

CIGS companies	Absorber formation step method	Substrate
Q-Cells,Solibro	Co-evaporation	Monolithic on glass
Mantz-Wurth Solar	Co-evaporation	Monolithic on glass
Heliovolt	Co-evaporation	Monolithic on glass
Centrotherm	Co-evaporation	Monolithic on glass
Johanna Solar	Co-evaporation	Monolithic on glass
Miasole	Reactive sputtering	Cell based roll to roll
SoloPower	Electroplating	Cell based roll to roll
NanoSolar	Printing	Cell based roll to roll
Stion	Two-step sputtering	Monolithic on glass
AVANCIS	Two-step sputtering	Monolithic on glass
Solar Frontier	Two-step sputtering	Monolithic on glass
Bosch Solar CISTech	Two-step sputtering	Monolithic on glass
TSMC	Two-step sputtering	Monolithic on glass

Table 1. CIGS companies and absorber formation method.

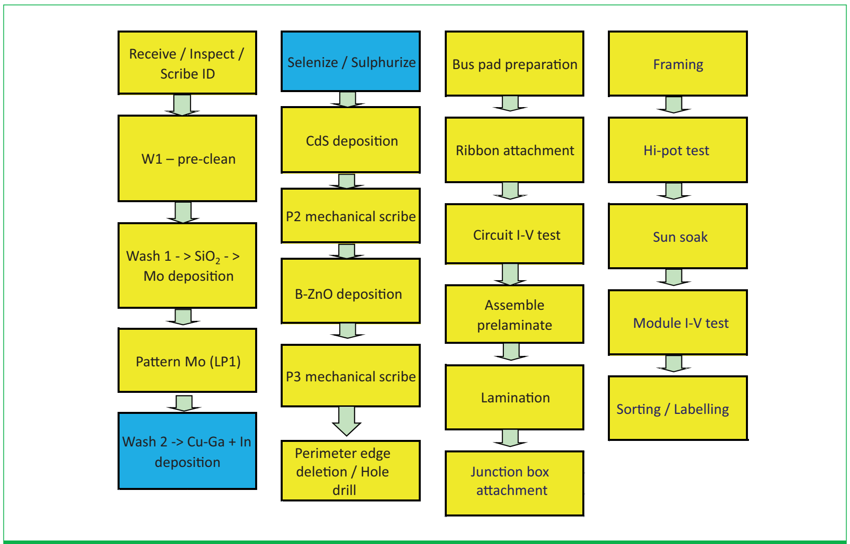

Figure 2. Sputtered CIGS process flow.

substrates, which gives access to the largest PV markets, enables use of existing mounting systems, is compatible with existing PV system infrastructure, and has the ability to dominate the building-integrated photovoltaics (BIPV) market in the future.

- CIGS yields the highest efficiency among all thin-film solar technologies. The cells can absorb over 99% of the solar spectrum and they have the highest current density. CIGS laboratory samples rank the highest in conversion efficiency among all other thin-film solar technologies.

- CIGS modules can be produced at competitive costs, even in the 100MW/year volume range with high local content, avoiding dependence on Si wafer or Si cell manufacturers.

- CIGS modules have demonstrated reliable and stable field performance for nearly 20 years.

> “CIGS yields the highest efficiency among all thin-film solar technologies.”

Today and tomorrow

Listed below is the current state of CIGS manufacturing and some short-term projections.

- 14% module efficiency in production (Manz)

- 15.7% record module efficiency (TSMC)

- Annual efficiency improvement rate in the last five years has averaged 0.4% per year – outpacing p-type c-Si in the last three years

- Energy harvest data from Manz test installations:
  - Middle East: 7% better than p-type c-Si
  - Southern Europe: 5% better than p-type c-Si
  - Southern China: 10% better than p-type c-Si

- Operating expense (OPEX) has reached CdTe levels; further efficiency improvements will result in lower OPEX ($0.50/watt-peak in 2014, $0.45/watt-peak in 2015)

- Future OPEX potential with scaled module format (1 × 1.6m^2): < $0.30/watt-peak

- Best footprint (150MW) factory building: < 1m^2/MW output

- Best headcount (all in production): < 1.5/MW output

- Lowest market entrance barrier: competitive OPEX reached at factory output of 150MW

CIGS production processes

There are two major approaches to CIGS manufacturing: 1) multi-target sputtering followed by a selenization furnace, and 2) co-evaporation. A number of companies have used, or are using, these processes, and the data used in this paper (while based on publicly available sources) are representative of the corresponding companies in Table 1.

Multi-target sputtering/selenization furnace

The process flow used in this paper is based on Fig. 2, with only the CIGS formation steps (see blue cells) being changed. The key parameters for each step (some cells in Fig. 2 represent more than one step) are shown in Table 2.

As can be seen from Table 2, the line balance for a 100MW factory is very good, with almost all tools having a 120 or 60 panel per hour throughput. It takes approximately 120 panels per hour in a 24×7 operation to approximate a 100MW factory size, given 150W per panel and utilization between 70 and 80%. Two exceptions are the selenization furnace and the TCO deposition tools.

"The co-evaporation process replaces the CIG sputtering step and the selenization furnace step with a single process step."

Co-evaporation

The second approach is based on CIGS formation using a co-evaporation tool. Referring to the previously described Fig. 2, the co-evaporation process replaces the CIG sputtering step and the selenization furnace step with a single process step utilizing all four elements required to form the CIGS film.

As can be seen by comparing Table 3 with Table 2, the co-evaporation process has eliminated one step and reduced the equipment set by 24 tools. However, the co-evaporation equipment is more expensive than the equipment it is replacing.

Step description	Tool group	Process throughput [panels/hr]	Step yield	Availability	Number of tools	Purchase capital [k$/tool]	Main materials
Receive / Inspect / Scribe ID	Scriber	120	99.10%	90.0%	1	65.0	
W1 - pre-clean	GlassWash	120	99.10%	90.0%	1	190.0	
Wash 1	MoCleaner	120	100.00%	90.0%	1	190.0	
SiO_2 -> Mo deposition	MoSputter	120	99.10%	90.0%	1	6,213.0	Moly target, silicon target
Pattern Mo (LP1)	LaserScriberP1	120	99.10%	90.0%	1	1,786.0	
Wash 2	CIGCleaner	120	100.00%	90.0%	1	190.0	
Cu-Ga + In deposition	CIGSputter	120	99.10%	90.0%	1	6,098.0	Cu-Ga target 1, Cu-Ga target 2, In target
Selenize / Sulphurize	SASFurnace	5	99.10%	90.0%	28	1,056.0	Hydrogen sulfide, hydrogen selenide
CdS deposition	Cji	60	99.10%	90.0%	2	1,462.0	Thiourea, cadmium sulphate, ammonium solution
P2 mechanical scribe	LaserScriberP2	120	99.10%	90.0%	1	1,065.0	
B-ZnO deposition	MOCVD-TCO	6	99.10%	90.0%	28	510.0	
P3 mechanical scribe	LaserScriberP3	120	99.10%	90.0%	1	1,012.0	MOCVD TCO 1, MOCVD TCO 2
Perimeter edge deletion	Laser4J	60	99.90%	90.0%	2	675.0	
Hole drill	HoleDrill	60	100.00%	90.0%	2	675.0	
Bus pad prep and clean	Cutter	60	100.00%	90.0%	2	288.0	
Ribbon attachment	RibbonAttach	60	100.00%	90.0%	2	288.0	Copper ribbon, tin solder, indium solder
Circuit I-V test	CircuitTester	60	99.90%	90.0%	2	200.0	
Front glass clean	GlassWash2	60	100.00%	90.0%	2	190.0	
Assemble pre-laminate	PLATool	60	100.00%	90.0%	2	190.0	Ethyl vinyl acetate, top glass
Lamination	Laminator	60	99.90%	90.0%	2	623.0	
Junction box attachment	JBATool	60	100.00%	90.0%	2	50.0	Pottant, junction box,
Framing	FrameTool	60	100.00%	90.0%	2	50.0	Frame
Hi-pot test	HiPot	60	100.00%	90.0%	2	100.0	
Sun soak	SSTool	60	100.00%	90.0%	2	100.0	
Module I-V test	ModuleTester	60	99.90%	90.0%	2	360.0	
Sorting / Labelling	SLTool	60	100.00%	90.0%	2	200.0	

Table 2. Sputtering/selenization input parameters.

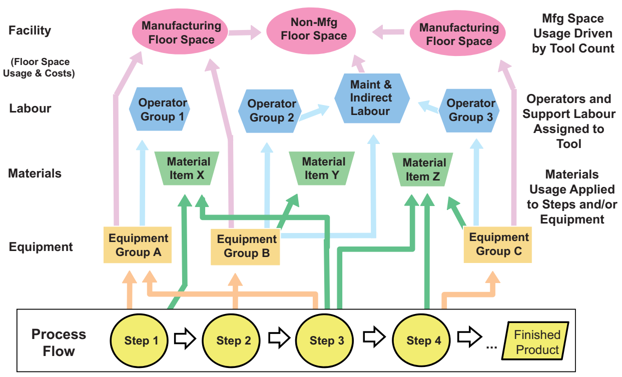

Figure 3. Activity-based resource relationships.

Case study

The case study will use cost and resource modelling to evaluate both sputtered and co-evaporated CIGS processes. Both models are based on a 100MW annual factory output. All results were generated through Wright Williams & Kelly, Inc.'s (WWK) Factory Commander® cost and resource software [4].

Cost and resource modelling history

Cost and resource modelling is a comprehensive approach to understanding a wide variety of factory-level issues. The techniques were pioneered in the 1990s by SEMATECH for integrated circuits (ICs) and by Sandia National Laboratories under the National Center for Advanced Information Components Manufacturing (NCAICM) programme for flat panel displays (FPDs). The concept was developed to initially assist these two capital-intensive industries in improving their ability to compete globally and maintain a US supply of high-tech components.

While a joint approach between SEMATECH and NCAICM was considered, substantial limitations to the SEMATECH approach known as CR/M convinced the NCAICM programme to take up a separate line of development. Core requirements such as detailed material tracking/costing, modelling of rework loops, mergers of multiple process flows, and better output reporting capabilities were among the challenges that separated SEMATECH's more limited goals from a more robust methodology that addressed both new and existing operations. Further, SEMATECH considered CR/M a strategic asset and chose to limit access to members and select suppliers. Sandia, while recognizing

Step description	Tool group	Process throughput [panels/hr]	Step yield	Availability	Number of tools	Purchase capital [k$/tool]	Main materials
Receive / Inspect / Scribe ID	Scriber	120	99.10%	90.0%	1	65.0	
W1 - pre-clean	GlassWash	120	99.10%	90.0%	1	190.0	
Wash 1	MoCleaner	120	100.00%	90.0%	1	190.0	
SiO_2 -> Mo deposition	MoSputter	120	99.10%	90.0%	1	6,213.0	Moly target, silicon target
Pattern Mo (LP1)	LaserScriberP1	120	99.10%	90.0%	1	1,786.0	
Wash 2	CIGCleaner	120	100.00%	90.0%	1	190.0	
Cu-Ga + In + Se deposition	CIGSEvaporation	25	99.10%	90.0%	5	9,000.0	Sources for Cu, In, Ga, Se
CdS deposition	Cji	60	99.10%	90.0%	2	1,462.0	Thiourea, cadmium sulphate, ammonium solution
P2 mechanical scribe	LaserScriberP2	120	99.10%	90.0%	1	1,065.0	
B-ZnO deposition	MOCVD-TCO	6	99.10%	90.0%	28	510.0	
P3 mechanical scribe	LaserScriberP3	120	99.10%	90.0%	1	1,012.0	MOCVD TCO 1, MOCVD TCO 2
Perimeter edge deletion	Laser4J	60	99.90%	90.0%	2	675.0	
Hole drill	HoleDrill	60	100.00%	90.0%	2	675.0	
Bus pad prep and clean	Cutter	60	100.00%	90.0%	2	288.0	
Ribbon attachment	RibbonAttach	60	100.00%	90.0%	2	288.0	Copper ribbon, tin solder, indium solder
Circuit I-V test	CircuitTester	60	99.90%	90.0%	2	200.0	
Front glass clean	GlassWash2	60	100.00%	90.0%	2	190.0	
Assemble pre-laminate	PLATool	60	100.00%	90.0%	2	190.0	Ethyl vinyl acetate, top glass
Lamination	Laminator	60	99.90%	90.0%	2	623.0	
Junction box attachment	JBATool	60	100.00%	90.0%	2	50.0	Pottant, junction box
Framing	FrameTool	60	100.00%	90.0%	2	50.0	Frame
Hi-pot test	HiPot	60	100.00%	90.0%	2	100.0	
Sun soak	SSTool	60	100.00%	90.0%	2	100.0	
Module I-V test	ModuleTester	60	99.90%	90.0%	2	360.0	
Sorting / Labelling	SLTool	60	100.00%	90.0%	2	200.0	

Table 3. Co-evaporation input parameters.

Thin Film

the value of the software, also understood that wider adoption would advance the technology more rapidly.

As a result, the Sandia Factory Cost Model (FCM) was developed as a 'decision tool' in order to make cost-competitive decisions regarding new manufacturing initiatives. The FCM was one of several cost-modelling tools and projects developed under the NCAICM programme. WWK acquired the intellectual property (IP) rights to Sandia's work in 1996 and commercialized FCM under the trade name Factory Commander. By using recognized standards as the basis for Factory Commander (industrial engineering, accounting, etc.), the application has proved to be robust, making it applicable to all discrete manufacturing and assembly operations, including PV.

Cost and resource models

Cost and resource models assess the resources needed – people, equipment, materials, etc. – to complete a process or task. Resources have roles, availability and costs associated with them. Cost and resource models are demand-based applications, and, to the extent possible, all resource requirements are tied to the production demand. As such, cost and resource models calculate all the resources required to meet the specified demand, typically expressed as a production schedule.

At the heart of cost and resource modelling are activities. 'Activity' is an accounting term, with the manufacturing equivalent being the process step. Each activity requires resources, and resources cost money. Activities are summed together to determine costs. Revenues are determined by the selling prices of products. By including all inflows and outflows of cash, a complete financial analysis can be performed (net present value, break-even, payback period, net cash flow, pro forma income statement, etc.) in addition to traditional industrial engineering metrics (floor space, tool counts, etc.). Four common business practices are subsets of cost and resource modelling:

1. Cost of ownership (COO) is essentially the cost of an individual activity. For a detailed discussion of the history, standards and algorithms of COO and overall equipment efficiency (OEE), see Jimenez [5].

2. Capacity analysis determines the total resources needed to meet the production demand. Typically, capacity analysis refers to equipment, but it can also include staffing, support and material needs.

3. Budgeting, including capital budgets, is a function of the capacity needs and the costs associated with meeting them.

4. Product planning, where product demand is the key driver of the resource requirements and may involve product mix variability (ramp up/ramp down).

Both SEMATECH and Sandia recognized the limitations of spreadsheets – it was a bit like taking a two-dimensional approach to a four-dimensional problem. Both chose a relational database approach to overcome the 'simple factory' limitation. This approach made it possible to account for the complex and dynamic nature of factories, with near-constant change in product volumes, product mix, yields, productivity rates (cycles of learning), process flows, step yields, material costs, labour efficiency, product value, etc. It also helped address real-world issues such as non-products run in the factory, including R&D, engineering evaluations and monitor units. There are re-entrant process flows, rework, merged process flows and sophisticated process-monitoring plans. Products can be binned into different levels and are often transformed (cells turn into modules, wafers into die, large panels of glass into small displays). Equipment can be underutilized and even pulled offline, material consumptions can vary, labour requirements can change and the price paid for any of these items can fluctuate with inflation and volume-pricing contracts.

There are outside factors – such as licensing IP, overheads and currency rates – that all impact product cost. Once these factors are identified, the cost and resource model quantifies resource requirements and allocates those resources to individual products (see Fig. 3). It should be noted that cost and resource models are deterministic and cannot explicitly estimate the dynamic aspects of production such as product queuing or work-in-process (WIP). (Estimations of dynamic measures such as WIP and cycle

Cost Categories	$ x 1000 Total Annual Cost	$/ Panel Out Unit Cost	% of Product Total	$/Watt Normalized Unit Cost	$ x 1000 Scrap Cost
Depreciation	12,664	18.996	18.7%	0.127	515
Equipment	11,245	16.868	16.6%	0.112	462
Building	1,419	2.129	2.1%	0.014	54
Operation & Maintenance	4,349	6.524	5.3%	0.036	176
Equipment	3,578	5.367	1.1%	0.008	147
Facility	771	1.157	6.4%	0.043	29
Labour	8,134	12.200	7.5%	0.081	232
Direct Labour	5,059	7.588	4.5%	0.051	146
Indirect Labour	3,075	4.613	12.0%	0.031	86
Materials & Supplies	33,882	50.823	50.0%	0.305	762
Bottom Glass	30,518	45.776	3.6%	0.024	227
Direct Process	2,418	3.627	45.0%	0.009	534
Indirect Material	947	1.420	1.4%	0.339	0
Total Production	59,029	88.543	87.1%	0.590	1,685
Product Overhead	8,749	13.123	12.9%	0.087	225
Equipment Sales Tax	8,749	13.123	12.9%	0.087	
Product Total	67,778	101.667	100.0%	0.678	1,910

Report 1. Sputtering model: product cost summary.

Process Step	Tool Group ID	Total Unit Cost ($/Panel): All Categories	Total Unit Cost ($/Panel): Cumulative Prod. Cost	Category Unit Cost ($/Panel): Equipment Depreciation	Building Depreciation	Operation & Maint.	Direct Labour	Indirect Labour	Direct Materials	Ind. Materials & Supplies	Product Overhead	Scrap Cost
Starting Material Cost :		3.627	3.627						3.627			
1 - Receive / inspect / scribe ID	Scriber	0.105	3.732	0.015	0.008	0.009	0.000	0.059	0.000	0.000	0.014	0.034
2 - W1 - Pre Clean	GlassWash	0.423	4.154	0.045	0.008	0.018	0.237	0.058	0.000	0.000	0.057	0.037
3 - Wash1	MoCleaner	0.148	4.303	0.045	0.008	0.018	0.000	0.058	0.000	0.000	0.020	0.000
3.1 - SiO2 -> Mo deposition	MoSputter	3.921	8.224	1.465	0.075	0.507	0.237	0.058	1.055	0.000	0.525	0.074
4 - Pattern Mo (LP1)	LaserScriberP1	1.039	9.262	0.421	0.033	0.152	0.237	0.057	0.000	0.000	0.139	0.083
5 - Wash2	CIGCleaner	0.147	9.410	0.045	0.008	0.018	0.000	0.057	0.000	0.000	0.020	0.000
5.1 - Cu-Ga + In deposition	CIGSputter	7.645	17.055	1.437	0.075	0.498	0.237	0.057	4.317	0.000	1.023	0.153
6 - Selenize/Sulfurize	SASFurnace	24.277	41.332	6.970	1.050	2.788	1.660	1.346	7.213	0.000	3.250	0.372
7 - CdS deposition	Cji	2.115	43.447	0.689	0.104	0.276	0.474	0.111	0.178	0.000	0.283	0.391
8 - P2 mechanical scribe	LaserScriberP2	0.778	44.225	0.251	0.033	0.098	0.237	0.055	0.000	0.000	0.104	0.398
9 - B-ZnO deposition	MOCVD-TCO	12.682	56.907	3.366	0.364	1.269	1.660	1.092	3.235	0.000	1.698	0.512
10 - P3 mechanical scribe	LaserScriberP3	0.758	57.664	0.239	0.033	0.094	0.237	0.054	0.000	0.000	0.101	0.519
11 - Perimeter edge deletion	Laser4J	1.000	58.665	0.318	0.066	0.137	0.237	0.107	0.000	0.000	0.134	0.059
11.1 - Hole Drill	HoleDrill	0.608	59.273	0.318	0.000	0.101	0.000	0.107	0.000	0.000	0.081	0.000
12 - Bus pad prep and clean	Cutter	0.429	59.701	0.136	0.055	0.073	0.000	0.107	0.000	0.000	0.057	0.000
13 - Ribbon Attach	RibbonAttach	0.997	60.698	0.136	0.000	0.043	0.000	0.107	0.578	0.000	0.133	0.000
14 - Circuit IV test	CircuitTester	0.267	60.966	0.094	0.000	0.030	0.000	0.107	0.000	0.000	0.036	0.061
14.1 - Front glass clean	GlassWash2	0.288	61.253	0.090	0.016	0.037	0.000	0.107	0.000	0.000	0.039	0.000
15 - Assemble pre-laminate	PLATool	10.458	71.711	0.090	0.000	0.029	0.000	0.107	8.833	0.000	1.400	0.000
16 - Lamination	Laminator	1.448	73.159	0.294	0.032	0.111	0.711	0.107	0.000	0.000	0.194	0.073
17 - Junction Box attachment	JBATool	5.318	78.478	0.024	0.016	0.016	0.237	0.107	4.207	0.000	0.712	0.000
18 - Framing	FrameTool	18.647	97.125	0.024	0.104	0.064	0.237	0.107	15.616	0.000	2.496	0.000
19 - Hi-pot test	HiPot	0.497	97.622	0.047	0.016	0.023	0.237	0.107	0.000	0.000	0.066	0.000
20 - Sun Soak	SSTool	0.499	98.120	0.047	0.017	0.024	0.237	0.107	0.000	0.000	0.067	0.000
21 - Module IV test	ModuleTester	0.675	98.796	0.170	0.011	0.060	0.237	0.107	0.000	0.000	0.090	0.099
22 - Sorting & Label	SLTool	0.541	99.336	0.094	0.000	0.030	0.237	0.107	0.000	0.000	0.072	0.000
23 - Packaging	Packaging	2.331	101.667	0.000	0.000	0.000	0.000	0.053	0.545	1.420	0.312	0.000
Total Unit Cost :		101.667		16.868	2.129	6.524	7.588	4.613	49.403	1.420	13.123	

Report 2. Sputtering model: unit cost per step.

Process Step / Material Item	Item Cost * ($)		Annual Quantity Used		Annual Material Cost ($ x 1000)	Material Cost per Panel ($/Panel)	Fraction of Product Material Cost (%)
Starting Material, Bottom Glass	3.3	/ Panel	732,673	Panels	2,417.8	3.627	23.92 %
5.1 - Cu-Ga + In deposition							
3 - Cu-Ga Target 1	27,000	/ unit	10.6	units	286.2	0.429	2.83 %
4 - Cu-Ga Target 2	18,600	/ unit	71	units	1,314.4	1.972	13.00 %
5 - Indium Target	28,700	/ unit	44.5	units	1,277.7	1.917	12.64 %
6 - Selenize/Sulfurize							
6 - Hydrogen Sulphide	0.09	/ litre	2,065,858	litres	185.9	0.279	1.83 %
7 - Hydrogen Selenide	1.63	/ litre	2,836,178	litres	4,623.0	6.934	45.74 %
					10,105.0	15.157	100.00 %

* Item cost includes inflation (if non-zero rate) and cost adjustment factors

Report 3. Sputtering model: material item costs.

Cost Categories	$ x 1000 Total Annual Cost	$/ Panel Out Unit Cost	% of Product Total	$/Watt Normalized Unit Cost	$ x 1000 Scrap Cost
Depreciation	14,131	21.006	18.0%	0.126	576
Equipment	12,712	18.896	2.0%	0.014	513
Building	1,419	2.109	20.0%	0.140	63
Operation & Maintenance	5,976	8.883	5.7%	0.040	248
Equipment	4,045	6.012	2.7%	0.019	163
Facility	1,931	2.871	8.4%	0.059	85
Labour	8,134	12.091	7.1%	0.081	191
Direct Labour	5,059	7.520	4.3%	0.050	129
Indirect Labour	3,075	4.571	11.5%	0.030	62
Materials & Supplies	32,736	48.663	46.3%	0.291	642
Bottom Glass	29,363	43.648	3.4%	0.024	206
Direct Process	2,418	3.594	41.5%	0.009	436
Indirect Material	955	1.420	1.4%	0.324	0
Total Production	60,977	90.642	86.2%	0.604	1,657
Product Overhead	9,776	14.531	13.8%	0.097	242
Equipment Sales Tax	9,776	14.531	13.8%	0.097	
Product Total	70,752	105.173	100.0%	0.701	1,899

Report 4. Co-evaporation model: product cost summary.

time require the use of discrete-event simulation as employed by Factory Explorer®, a commercial software package from Wright Williams &Kelly, Inc. [6].)

"Cost and resource modelling allows a new dynamic in decision-making: a virtual business model as an enabling technology."

In the midst of all of these complexities lie several challenges. First, cost and resource models need to speak multiple languages and conform to different standards. Accounting standards and nomenclature are much different from the standards and language used at the process step level (equipment and process engineering). One could therefore consider a cost and resource model as a translation vehicle that transforms technical considerations into business results, allowing engineering and finance to communicate more clearly. Cost and resource modelling allows a new dynamic in decision-making: a virtual business model as an enabling technology.

Sputtering model results

The following reports provide a summary and detailed cost analyses for the sputtering/selenization furnace case (refer to Table 2 for the input data summary). Report 1 shows the high-level cost breakdowns for capital costs, operation and maintenance, labour, materials and supplies, and overheads. The cost per panel is $101.67, with a cost per watt-peak of $0.68. It should be noted that costs presented in this paper were generated at a specific point in time and are subject to change on a continuous basis. As such, these costs should be considered on a relative basis.

Report 2 looks at the cost breakdowns for each step in the manufacturing flow, and highlights the highest cost items. The highest cost step is the selenization furnace at $24.28 per panel, with almost equal contributions from equipment costs (28 tools at $1m/tool) and direct-materials consumption. Direct materials will be examined in more detail in Report 3, later in this paper. The next-highest cost step is framing, which is the same for both models and will be ignored for the rest of the analyses. The third-highest step is TCO deposition at $12.68, again with almost equal contributions from equipment costs (28 tools at $500k/tool) and direct-materials consumption. This is also the same for both models and will be ignored for the rest of the analyses. The last item of interest is the CIG sputtering step, with a cost of $7.65 and a direct-materials contribution of $4.32.

Report 3 breaks down the material item costs, annual usage, annual costs and cost per panel. With regard to materials cost, the largest component for the CIGS formation steps is hydrogen selenide, representing $6.93 per panel, or greater than 6% of the total panel-manufacturing costs. Combined, the CIGS materials are $11.53/panel, or a little more than 11% of the total panel cost.

Co-evaporation model results

The second model is based on CIGS formation using a co-evaporation tool. The following reports provide a summary and detailed cost analyses for the co-evaporation case. Report 4 shows the high-level cost breakdowns for capital costs, operation and maintenance, labour, materials and supplies, and overhead. The cost per panel is $105.17, with a cost per watt-peak of $0.70.

"The significant difference is over $2.00 in additional equipment costs for the co-evaporation process."

Report 5 looks at the cost breakdowns for each step in the manufacturing flow and highlights the highest cost items. The highest cost step is co-evaporation at $33.80 per panel with almost equal contributions from equipment costs (five tools at $9m/tool) and direct-materials

Process Step	Tool Group ID	Total Unit Cost ($/Panel) All Categories	Cumulative Prod. Cost	Category Unit Cost ($/Panel) Equipment Depreciation	Building Depreciation	Operation & Maint.	Direct Labour	Indirect Labour	Direct Materials	Ind. Materials & Supplies	Product Overhead	Scrap Cost
	Starting Material Cost :	3.594	3.594						3.594			
1 - Receive / inspect / scribe ID	Scriber	0.121	3.715	0.015	0.003	0.009	0.000	0.076	0.000	0.000	0.017	0.033
2 - W1 - Pre Clean	GlassWash	0.468	4.183	0.044	0.003	0.018	0.259	0.076	0.000	0.000	0.067	0.038
3 - Wash1	MoCleaner	0.164	4.347	0.044	0.003	0.018	0.000	0.075	0.000	0.000	0.024	0.000
3.1 - SiO2 -> Mo deposition	MoSputter	3.925	8.272	1.451	0.030	0.502	0.259	0.075	1.046	0.000	0.561	0.074
4 - Pattern Mo (LP1)	LaserScriberP1	1.067	9.339	0.417	0.013	0.150	0.259	0.074	0.000	0.000	0.153	0.084
5 - Wash2	CIGCleaner	0.163	9.501	0.044	0.003	0.018	0.000	0.074	0.000	0.000	0.023	0.000
5.1 - Cu-Ga + In + Se deposition	CIGSEvaporatio	33.797	43.298	10.512	1.712	5.675	1.296	0.354	9.412	0.000	4.835	0.390
7 - CdS deposition	Cji	2.147	45.445	0.683	0.041	0.273	0.519	0.146	0.178	0.000	0.307	0.409
8 - P2 mechanical scribe	LaserScriberP2	0.805	46.251	0.249	0.013	0.097	0.259	0.072	0.000	0.000	0.115	0.416
9 - B-ZnO deposition	MOCVD-TCO	13.096	59.347	3.336	0.144	1.257	1.815	1.436	3.235	0.000	1.873	0.534
10 - P3 mechanical scribe	LaserScriberP3	0.785	60.132	0.236	0.013	0.093	0.259	0.071	0.000	0.000	0.112	0.541
11 - Perimeter edge deletion	Laser4J	1.025	61.156	0.315	0.026	0.136	0.259	0.141	0.000	0.000	0.147	0.061
11.1 - Hole Drill	HoleDrill	0.649	61.806	0.315	0.000	0.100	0.000	0.141	0.000	0.000	0.093	0.000
12 - Bus pad prep and clean	Cutter	0.432	62.237	0.135	0.022	0.073	0.000	0.141	0.000	0.000	0.062	0.000
13 - Ribbon Attach	RibbonAttach	1.045	63.283	0.135	0.000	0.043	0.000	0.141	0.578	0.000	0.150	0.000
14 - Circuit IV test	CircuitTester	0.308	63.591	0.093	0.000	0.030	0.000	0.141	0.000	0.000	0.044	0.064
14.1 - Front glass clean	GlassWash2	0.318	63.909	0.089	0.006	0.037	0.000	0.141	0.000	0.000	0.045	0.000
15 - Assemble pre-laminate	PLATool	10.608	74.517	0.089	0.000	0.028	0.000	0.141	8.833	0.000	1.518	0.000
16 - Lamination	Laminator	1.554	76.071	0.291	0.013	0.110	0.778	0.141	0.000	0.000	0.222	0.076
17 - Junction Box attachment	JBATool	5.429	81.500	0.023	0.006	0.016	0.259	0.141	4.207	0.000	0.777	0.000
18 - Framing	FrameTool	18.838	100.338	0.023	0.041	0.063	0.259	0.141	15.616	0.000	2.695	0.000
19 - Hi-pot test	HiPot	0.556	100.894	0.047	0.006	0.023	0.259	0.141	0.000	0.000	0.079	0.000
20 - Sun Soak	SSTool	0.557	101.451	0.047	0.007	0.024	0.259	0.141	0.000	0.000	0.080	0.000
21 - Module IV test	ModuleTester	0.737	102.188	0.168	0.004	0.059	0.259	0.141	0.000	0.000	0.105	0.102
22 - Sorting & Label	SLTool	0.610	102.798	0.093	0.000	0.030	0.259	0.140	0.000	0.000	0.087	0.000
23 - Packaging	Packaging	2.375	105.173	0.000	0.000	0.000	0.000	0.070	0.545	1.420	0.340	0.000
	Total Unit Cost :	105.173		18.896	2.109	8.883	7.520	4.571	47.243	1.420	14.531	

Report 5. Co-evaporation model: unit cost per step.

Process Step / Material Item	Item Cost * ($)		Annual Quantity Used		Annual Material Cost ($ x 1000)	Material Cost per Panel ($/Panel)	Fraction of Product Material Cost (%)
Starting Material, Bottom Glass	**3.3**	/ Panel	**732,673**	Panels	**2,417.8**	**3.594**	**27.63 %**
5.1 - Cu-Ga + In + Se deposition							
37 - Evap Cu	**29**	/ kg	**3,886,579**	g	**112.7**	**0.168**	**1.28 %**
38 - Evap In	**510.9**	/ kg	**5,653,206**	g	**2,888.2**	**4.293**	**33.00 %**
39 - Evap Ga	**387.4**	/ kg	**1,483,967**	g	**574.9**	**0.855**	**6.57 %**
40 - Evap Se	**125**	/ kg	**22,047,503**	g	**2,755.9**	**4.097**	**31.49 %**
					8,749.6	**13.006**	**100.00 %**

* Item cost includes inflation (if non-zero rate) and cost adjustment factors

Report 6. Co-evaporation model: material item costs.

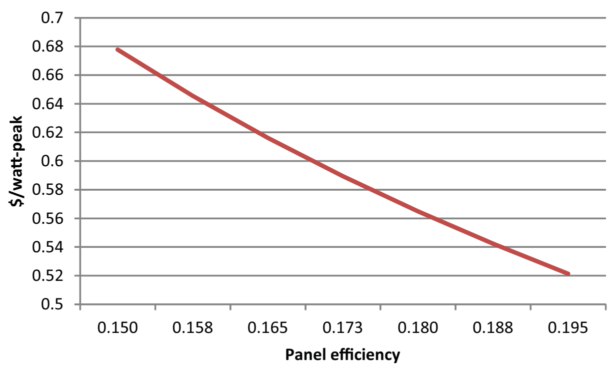

Figure 4. Panel efficiency sensitivity analysis.

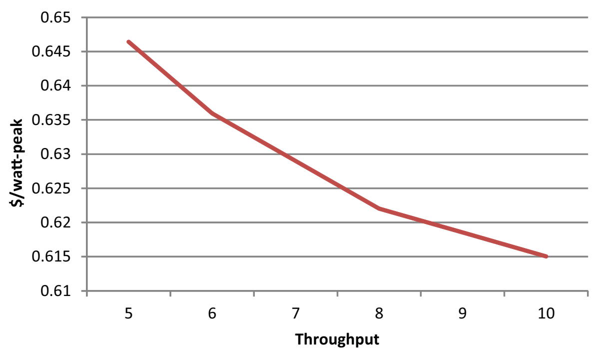

Figure 5. Selenization throughput sensitivity analysis.

consumption. Direct materials will be examined in more detail in Report 6, later in this paper. It should be noted that the co-evaporation step replaced two steps in the sputtering model. Those two steps exceeded $31. The significant difference is over $2.00 in additional equipment costs for the co-evaporation process.

Report 6 breaks down the material item costs, annual usage, annual costs and cost per panel. With regard to materials cost, the largest components for the co-evaporation step are the indium source at $4.29 per panel and the selenium source at $4.10. Together they represent almost 8% of the total panel manufacturing costs. Combined, the CIGS materials are $9.41/panel, or approximately 9% of the total panel cost. Much of this cost is associated with the efficiency of the co-evaporation process, where only 40% of the material consumed ends up on the panel in the case of Cu, In and Ga, and only 20% in the case of Se.

Sensitivity analyses

Both models were based on a module efficiency of 15%, which is approximately halfway between the Manz-reported 14% and the TSMC-reported 15.7% record. Since module efficiency has a major impact on the cost per watt-peak, Fig. 4 looks at efficiency from the starting point of 15% to near the small-scale record of approximately 20% for the sputtering model. In this example, each 1% improvement in panel efficiency decreases the cost per watt-peak by approximately $0.04.

Next, the impact of throughput improvements on the selenization furnace will be examined. Since 28 pieces of equipment are needed to meet the 100MW factory output, any improvement in throughput should yield a reasonable cost reduction. We could have also looked at reducing the equipment purchase price with the same relative results, but that is less likely as an outcome. Fig. 5 shows that doubling throughput from five to ten panels per hour decreases cost per watt-peak by nearly 5%. While that degree of increase in throughput may not be practical, the move from five to six panels per hour provides an overall cost reduction of approximately 1.6%. It should be noted that the baseline model called for 28 furnaces to provide excess capacity in case of equipment downtime. This sensitivity analysis removed that constraint and allowed the model to calculate the actual required amount of equipment. Equipment optimization will be discussed in more detail in the next section.

Lastly, one of the perceived major areas for improvement in the co-evaporation process will be looked at – the efficiency with which the CIGS materials are deposited on the panel. The baseline model used 40% material-use efficiency for copper-indium-gallium and 20% for selenium. As can be seen in Table 4 there is a modest cost benefit in increasing the deposition efficiency – between $0.005 and $0.01 for each 5% improvement in deposition efficiency. The amount of material used, even at lower efficiencies, is just a few grams per 1m^2 panel.

Other process options

While standard processes which have been in existence for some time were chosen, there are other options that

	Material-use efficiency (Cu-In-Ga, Se)					
	40%, 20%	45%, 25%	50%, 30%	55%, 35%	60%, 40%	90%, 90%
Cu - g/panel	5.50	4.89	4.40	4.00	3.67	2.44
In - g/panel	8.00	7.11	6.40	5.82	5.33	3.56
Ga - g/panel	2.10	1.87	1.68	1.53	1.40	0.93
Se - g/panel	31.20	24.96	20.80	17.83	15.60	6.93
$/watt-peak	$0.701	$0.692	$0.685	$0.680	$0.676	$0.660

Table 4. CIGS co-evaporation efficiency sensitivity analysis.

have the potential to reduce costs. One such example is to move from a framed to a frameless panel. The framing costs represent over $0.10/watt-peak; eliminating these costs would bring the total cost down to $0.573/watt-peak. Additionally, if the equipment set is optimized to allow for higher factory loading (higher reliability, better predictability of availability), the cost per watt-peak can be further reduced to $0.51.

Manz has reported further enhancements to the process, including the use of lasers for all patterning steps, edge delete and hole drill, which removes the CIGS pre-clean step as well as building the barrier into the Mo deposition, eliminating the SiO_2 deposition. Other improvements include a change in TCO materials, a reduction in CIGS materials usage through a linear source, the replacement of solder with silver glue, and the replacement of ethylene vinyl acetate (EVA) and butyl edge tape with thermoplastic material. As a result, Manz forecasts OPEX of below $0.50/watt-peak, even for a 14% efficiency module.

Conclusions

The PV industry has gone through immense changes in recent years, yet is still developing rapidly in many ways. While previous papers in this series have focused on c-Si manufacturing and assembly issues, this paper has looked at an alternative PV technology which holds the promise of superior energy generation in high ambient heat and high direct normal irradiance (DNI) locations, as well as offering competitive costs.

> "A series of lesser improvements is necessary for bringing the costs down to the $0.30/watt-peak level."

The models presented here are based on manufacturing costs on a watt-peak basis and indicate that fully burdened CIGS manufacturing costs are still above the sales price for many c-Si modules. The case study in this paper has shown that there is not likely to be just one major cost breakthrough for either of the CIGS manufacturing processes presented here but, rather, that a series of lesser improvements is necessary for bringing the costs down to the $0.30/watt-peak level, indicated as the potential for an optimized panel format.

It should be noted that cost per watt-peak was used as a convenient manufacturing metric, since the conditions of final installation are highly variable (and outside the scope of this paper). However, the author strongly suggests that all cost comparisons for the final installed equipment (utility scale, commercial/residential rooftop, etc.) be compared with metrics more suited to issues of system ownership (LCOE, TCOe). These metrics take into consideration actual energy production (site specific), annual efficiency degradation, balance of system (BOS) costs, installation, maintenance, etc.

References

[1] Solarthinfilms.com [http://www.solarthinfilms.com/active/en/home/photovoltaics/cigs_technology.html].

[2] Sinovoltaics.com [http://sinovoltaics.com/solar-basics/solar-cell-guide-part-2-thin-film-cdte-cigs-solar-cells/]

[3] U.S. Photovoltaic Manufacturing Consortium [http://www.uspvmc.org/technology_PVMC.html].

[4] Wright Williams & Kelly, Inc., Factory Commander® [http://www.wwk.com/productfc.html].

[5] Jimenez, D. 2009, "Cost of ownership and overall equipment efficiency: A photovoltaics perspective", *Photovoltaics International*, 6th edn, pp. 16–22.

[6] Wright Williams & Kelly, Inc., Factory Explorer® [http://www.wwk.com/productfx.html].

About the Author

David Jimenez is President of Wright Williams & Kelly, Inc. He has approximately 30 years of industry experience, including management positions with NV Philips and Ultratech Stepper. He holds a B.Sc. in chemical engineering from the University of California, Berkeley, and an MBA in Finance. For over 20 years he has been a facilitator in the SEMI-sponsored workshop "Understanding and Using Cost of Ownership".

Enquiries

Wright Williams & Kelly, Inc.
6200 Stoneridge Mall Road
3rd Floor
Pleasanton
CA 94588
USA

Tel: +1 925 399 6246
Email: david.jimenez@wwk.com

PV Modules

Trina Solar to supply 1.1 million solar modules to Copper Mountain 3

The 345MW Copper Mountain Solar 3 PV power plant project being built by AMEC in Boulder City, Nevada is to use 1.1 million PV modules supplied by Trina Solar. Trina Solar said it would start supplying 1,133,550 dual-rated, 72-cell PD14 solar modules in the fourth quarter of 2013, while the project is expected to be completed in the first quarter of 2015. The project will be owned and operated by Sempra U.S. Gas & Power. "Trina Solar is uniquely qualified to provide solar panels to this project," said Tom Dotson, vice president at AMEC. "Their modules' track-record of proven performance and their strong balance sheet made them an easy choice for Copper Mountain Solar 3." "The selection of Trina Solar for this record-breaking project is a strong endorsement of our capabilities in meeting the evolving demands of our customers in a maturing market," said Mark Mendenhall, president of Trina Solar Americas.


Source: Sempra U.S. Gas & Power, LLC

Trina Solar to supply 1.1 million solar modules to Copper Mountain 3.

Order Focus

JinkoSolar inks 23MW module deal for California solar farm

A deal to provide 23MW of PV modules has been agreed between PV manufacturer JinkoSolar and US firms Swinerton Builders and Clenera, for use in the construction of a solar farm in Fresno, northern California.

The ground mounted plant will be constructed for Westlands Solar Farms, a renewable energy company based in California formed through a partnership of companies located close to electricity transmission sub-stations.

Module deliveries are expected to be finished by Q4 2013. Expected completion date has not been announced. JinkoSolar's 300W 72-cell, high efficiency PV modules will be used and electricity generated sold to The Pacific Gas and Electric Company.

Solon supplies modules to 2.2MW roof project in Romania

Solon Energy has said it is to supply around 8,800 PV modules for a 2.2MW roof-mounted PV project in Bucharest, Romania.

The project, for logistics firm SC Atwar & TH Services SRL, is expected to be complete at the end of September this year.

Solon said that up to 15% of the 2.8MWh of power produced annually from the plant would be used to meet the needs of the logistics centre, while the remaining electricity produced would be fed into the grid and compensated using Green Certificates.

Canadian Solar lands Leeward Islands module contract

PV manufacturer Canadian Solar is to supply its modules to what will be the largest commercial PV project on the Leeward Islands of St Kitts & Nevis.

Anguilla-based installation firm Comet Solar will develop the 600kW project on behalf of SL Horsford, a trading, service and manufacturing company, spanning eight of the company's buildings

Chris Mason, Comet Solar's owner, said: "This project is our largest to date, with the challenge of having a remote location, a range of building types from steel buildings to concrete roofs and a mix of British and American electrical systems and voltages.

China Sunergy to supply 9.9MW of solar modules in Romania

Solar cell and module manufacturer China Sunergy has signed two contracts to supply 9.9MW of solar modules in Romania.

The contracts were with Bester Generacion, a Spain-based renewables EPC company, it will deploy China Sunergy's multi-crystalline modules for the two ground-mounted projects in Romania.

The modules will be supplied from Sunergy's Turkey plant, to Romania, in September 2013.

Chinese shrug off trade duties

Strong emerging market shipments boost Q2 fortunes for Trina Solar

Trina Solar said geographic diversification and pricing stabilisation helped it decrease losses and post stronger than expected shipments in Q2 2013.

The China-based manufacturer said increased emphasis on markets such as Japan, India and the US meant it exceeded its quarterly shipment guidance by 100MW and almost halved quarter-on-quarter losses from US$63.7 million to US$33.7 million.

Despite the EU-China trade dispute Trina reported "stable" shipments to the EU and strong growth in shipments to other areas of the globe.

Lightsource builds on Chinese inventory with 69.5MW Renesola deal

Lightsource Renewable Energy has penned a series of contracts with ReneSola that will see the Chinese manufacturer supply 69.5MW of modules to the UK developer.

The 300,000 modules will be used for 10 solar farm projects in the South West, Isle of Wight and Kent, as well as a number of undisclosed future projects – ranging from 20MW to 1MW in scale. The companies expect the 69.5MWp of capacity to generate enough clean electricity to power more than 23,000 households.

Certificates pave way for China Sunergy modules to enter French utility-scale market

Manufacturer China Sunergy (CSUN) has been awarded 'carbon footprint' certificates by the French engineering firm Solstyce that will allow its customers to enter the tender process for projects in France above the 250kW threshold.

Products from CSUN's recently opened Turkish manufacturing facility will now be eligible for use in large-scale solar farms in France. Manufacturing the modules in Turkey, using non-Chinese materials and components, allows CSUN to escape the tariffs and minimum pricing rules introduced by the European Commission.

NPD Solarbuzz: Yingli Green breaks industry shipment record

According to analysts NPD Solarbuzz, second quarter 2013 PV module shipments for the top 20 suppliers exceeded 5.8GW. The rise was led by Yingli Green Energy which saw shipments estimated to exceed 800MW and over 1GW for the first-half of the year, a new record for any PV module manufacturer.

Renesola is to supply 69.5MW of modules for Lightsource UK projects.

Source: Lightsource Renewable Energy

Efficiencies

Amonix beats own record with 35.9% CPV module efficiency

California-based concentrated PV (CPV) manufacturer Amonix claims to have beaten a record it set earlier this year by achieving a 35.9% efficiency rate for a CPV module.

The efficiency level, achieved in a National Renewable Energy Laboratory trial, supersedes the 34.9% average efficiency the company recorded in a similar test in April.

The trial was conducted under recently adopted International Electrotechnical Commission (IEC) test conditions for CPV of 1000 W/m2 and 25 degrees Celsius cell temperature, the first time NREL quantified the rating for a concentrator module at that temperature instead of operating temperature.

Winaico claims PV module efficiency victory in Australian desert

Taiwanese module manufacturer Winaico has claimed its panels achieved the highest efficiency by cost during trials at the Desert Knowledge Australia Solar Centre (DKASC). The testing centre provides live, real-time data on the output of the installed modules under harsh conditions including thin-film and crystalline panels from manufacturers including Q-Cells, Sanyo, REC and Trina.

The company claims its recent tests at DKASC have generated some of the best results with its modules 12% more cost efficient than its competitors.

Shakeout and restructuring

Komax pulls out of solar industry

Komax Group has announced it is pulling out of the solar industry by selling its module assembly equipment arm, Komax Solar.

Amonix has achieved 35.9% with one of its CPV modules.

Source: Amonix

Komax Group said the risk potential of Komax Solar was "not compatible" with the Group's objectives.

The company will continue to maintain machines it has already sold and affirmed its interest in finding a suitable buyer for the solar division.

Komax Solar cut jobs in June last year and again reduced its headcount by 50% in January this year, following a 90% drop in product orders, due to overcapacity and loss of customers.

Komax Solar makes up an estimated 3% of Komax Group's net sales. Komax Group has two other business units, Komax Wire, Komax MedTech, with most sales made in Europe.

Three Hareon directors step down following disappointing results

Three directors resigned from Chinese PV manufacturer Hareon in mid-August, three days after it announced a 19% drop in revenue for the first half of 2013 compared to last year.

On 10 August, the company announced first half losses for 2013 of RMB255 million (US$41.7 million) widening from RMB135 million (US$22.1 million) in the first half of 2012. Revenue was down 19% to RMB2.06 billion (US$336 million).

Meyer Burger sells module assembly line to UK start-up

UK-based PV manufacturing start-up, Sunsolar Energy, has placed an order with Meyer Burger for an automated and integrated module assembly line.

The order includes module lamination, cell connection, handling, performance testing and fast-track certification technologies with an initial annual production capacity of 35MW.

Meyer Burger said that the equipment was scheduled to be delivered by the end of September, 2013 with Sunsolar Energy beginning production in November 2013.

Company news

Photon Energy prepares IPO and expansion plans

Solar project developer, investor and manufacturer Photon Energy has announced it is assessing financing options ahead of a planned expansion and IPO in the first quarter of 2014.

The company is already listed on the New Connect segment of the Warsaw Stock Exchange but plans a full listing next year to coincide with a global expansion strategy.

Photon announced strong results for the second quarter with earnings before interest, taxes, depreciation and amortisation (EBITDA) up 32% compared to Q2 2012, to €2.5 million (US$3.3million).

The company said it would have returned to profitability had it not been for the 26% levy placed on Czech PV power plants.


Source: Canadian Solar

Canadian Solar and JA Solar raising funds worth US$96 million.

JA Solar and Canadian Solar raising funds

Both tier one PV module manufacturers, JA Solar and Canadian Solar, are raising funds to the tune of US$96 million and US$50 million respectively.

JA Solar said that it has entered into a Securities Purchase Agreement with a single institutional investor to buy 15,228,425 ordinary shares, US$0.0001 par value per share, of ordinary shares, represented by 3,045,685 American Depositary Shares at a price of US$7.88 per ADS.

The closing of the offering was expected to take place on or about August 16, 2013, according to the company and the funds used for 'general corporate purposes.'

Canadian Solar has taken the route of selling up to an aggregate of US$50.0 million of its common shares through an 'at-the-market equity offering programme', offered through Credit Suisse as the sales agent.

The funds are to be used for solar power project development expenses and working capital, the company said.

ReneSola posts 32.8% increase in sales on record shipment volume

Despite raising second quarter 2013 shipment guidance significantly, ReneSola exceeded the figure and reported record shipment volume of wafers and modules totalling 849.3MW.

The company previously expected total solar wafer and module shipments to be in the range of 760MW to 770MW, compared to its previously guided range of between 700MW to 720MW.

However, ReneSola guided third quarter solar wafer and module shipments to be in the same range as originally expected for the second quarter of 730MW to 750MW.


ReneSola saw record shipments in the second quarter of 2013.

Product Reviews

FLEXcon

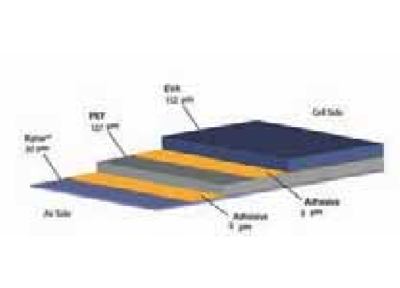

FLEXcon offer black backsheet for aesthetically demanding PV module markets

Product Outline: FLEXcon has expanded its solar module backsheet 'multiGUARD' offering with the addition of black/white and black/black products. The new, more aesthetically pleasing black backsheet products appeal to the high-end commercial market and a much greater portion of the residential market.

Problem: As PV installations are more commonly integrated into the design of commercial and residential projects. FLEXcon's expanded backsheet offering enhances the options for solar module manufacturers to produce solutions that tailor to the needs of a much broader market base.

Solution: FLEXcon's multiGUARD brand, a range of backsheets for photovoltaic modules are engineered to protect against moisture and humidity and provide superior partial discharge and high voltage insulation for proper functioning of the module. FLEXcon's line of backsheet products are designed to meet stringent industry standards and regulations.

Applications: C-Si solar cell backsheet protection.

Platform: Typically constructed in 12mm backsheet that offers advantages of Kynar material protection against harsh weather conditions. It features a polyester inner layer, which provides optimum electrical insulation and promotes ease of handling through the module manufacturing process, and an EVA layer which provides optimum adhesion to encapsulants. FLEXcon's existing white backsheet offering, which includes double fluoropolymer (TPT and KPK), single fluoropolymer (TPE and KPE) and non-fluoropolymer (PPE), is ideal for solar farms, commercial and residential installations.

Availability: Currently available.

Meyer Burger

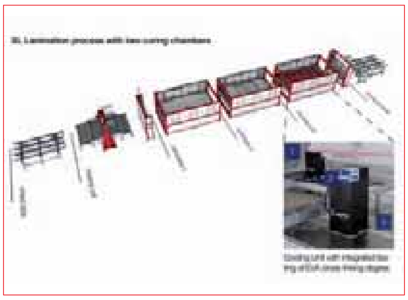

Meyer Burger and LayTec team on first fully integrated EVA cross-linking module production metrology solution

Product Outline: Meyer Burger and LayTec have collaborated to produce the world's first fully integrated EVA cross-linking metrology solution for PV module production lines.

Problem: Until recently, the guaranteed lifetime and long-term stability of a module was calculated by carrying out destructive off-line tests on less than 1% of the modules and then statistically extrapolating the results for end users.

Solution: The integrated EVA cross-linking metrology system is a streamlined solution for process optimization and yield enhancement in module manufacturing lines. The measurement heads are directly integrated into the cooling press of Meyer Burger laminators. They facilitate closed loop process control and 100% quality assurance of EVA lamination. The system fully replaces slow, error-prone and costly off-line analysis methods. By integrating original OEM technology into the non-destructive lamination process control, module manufacturers are able to undisputedly prove the long-term stability of 100% of their module production. Based on in-line and off-line X Link technology, certifiers can now refer to a non-destructive and repeatable standard method for line and fab certifications.

Applications: EVA lamination of PV modules.

Platform: Upgrade possible for NG and JT 3S Modultec laminators.

Availability: Currently available.

Engineered Material Systems

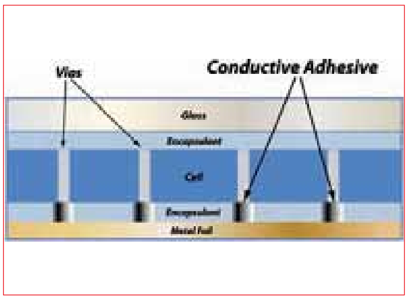

EMS offers lower-cost conductive adhesive for back contact sheet

Product Outline: Engineered Material Systems (EMS) has introduced its new DB-1588-2 low-cost conductive adhesive for back contact applications in crystalline silicon solar modules.

Problem: Conductive adhesive is required for metal wrap through (MWT) back contact solar cells to ensure correct bonding of the vias to the metal back contact sheet. Accurate and long-lasting adhesion is required, while minimizing process cycle-times to ensure correct contact.

Solution: DB-1588-2 is designed to make contact from vias or other conductors on the solar cells to the back contact sheet. The adhesive is stress absorbing to withstand the rigors of thermal cycling and features excellent conductive stability to back contact metallization during damp heat exposure. Additionally, the conductive adhesive is designed to cure through the encapsulant lamination and cure process. The material is claimed to be approximately 50% lower cost than standard silver-filled adhesives and is said to be significantly lower cost than its EMS DB-1588-1 product, currently used for manufacturing back contact solar modules.

Application: Conductive adhesive for vias and/or conductors for MWT solar cells.

Platform: The DB-1588-2 conductive adhesive is the latest addition to Engineered Conductive Materials' full line of conductive stringer attach adhesives, conductive adhesives for back contact crystalline silicon, thin-film and via fill applications as well as conductive grid inks for photovoltaic applications.

Availability: Currently available.

Quality makes all the difference

Nicole Nelles, **Max B. Koentopp** & **Sandra Scholz**, Hanwha Q CELLS GmbH, Thalheim, Germany

ABSTRACT

The aim of this paper is to shed some light on what difference the quality of a PV product makes to the customer and how much effort is required to deliver it. From the customer's point of view, the quality of a PV product is key to a worthwhile investment, since the value of a PV system is defined by its cost compared with its yield over the entire lifetime, or the levelized cost of electricity (LCOE). But while many manufacturers make more or less the same promises, in this paper a closer look is taken at what is really involved in living up to those promises. If quality is understood to be a fundamental attitude that is reflected in every single process along the entire value chain, only then will this eventually lead to high-quality products and services. The paper discusses in detail the principles, methods, tests and processes required to secure a superior quality brand.

Introduction

Quality makes all the difference. This axiom applies in particular to products which are expected to function and deliver constant performance over long periods. With a service life of 25 years or more, photovoltaic modules definitely belong to this category. Yet, in spite of this awareness, superior quality permits only a very slight increase in prices in the solar industry. When it comes to buying, the overriding argument continues to be the price, and brutal competition has driven this down to ruinous levels in recent years – proof of which is the constant consolidation in the sector. But why is this the case? From the customer's point of view, is it really right to base a decision to buy almost entirely on the initial investment?

Admittedly there are, at first sight, few reasons for buying a more expensive product: the visible differences between solar modules are very small. From a distance, or once incorporated into a larger system, modules hardly carry any weight in terms of their looks. And there are also very few differences when it comes to certification by external testing bodies: ISO certification and IEC testing are standard. What is more, many manufacturers make more or less the same promises: guaranteed performance for periods of 20 years or more, as well as apparent guarantees against potential-induced degradation (PID) and hot spots. But not everything that promises quality delivers on that promise, as becomes apparent by taking a second look at product quality, during which the customer should ask the following questions:

- Which manufacturer is able to prove that its PV products will actually do their job without problems for a full 25 years?

Figure 1. Quality is more than a product characteristic – it is a fundamental attitude.

- Are there tests which credibly underpin the promises made in the guarantee?
- What proofs of quality must manufacturers provide, and at what intervals, in order to retain their current certification?
- Are the standards comparable in different countries?
- Are products which have been mass produced selected for random testing, or does the manufacturer provide products of its own choosing for testing?
- What processes are used to effectively rule out hazards such as PID or hot spots?
- Does the manufacturer undertake internal quality testing and how often?
- Are processes also routinely tested for quality or is this limited to products?

"The demonstrable and sustainable quality of a product becomes an increasingly important factor in the purchasing decision."

No matter what the answers are to these questions, one thing is clear: the value of a PV system is measured by the levelized cost of electricity (LCOE). For this, the decisive factor is the yield over its entire lifetime, and, therefore, the constant and reliable performance of the system. Considered against this background, the demonstrable and sustainable quality of a product becomes an increasingly important factor in the purchasing decision. Even if the initial investment costs are higher, a better quality product can save the system operator a great deal of stress and unexpected financial losses. For this, 'product quality' is taken to mean 'meeting the maximum requirements that the customer has of the product'. In the case of PV products these requirements are, in particular, a long service life, a high level of safety, one hundred per cent reproducibility of the product characteristics and an elegant optical appearance (especially for mono products). An outstanding service quality, fast reaction times and a high level of reliability are also important for a good business relationship. From these customer requirements, a set of criteria for product characteristics and criteria for testing have been derived. But at Hanwha Q CELLS it is not just the products of which quality is demanded – and that is how it should be.

Quality as a fundamental attitude

Do you know of a company that is known for the quality of its products, but which does not place any value on the quality of its internal processes or on how colleagues deal with each other or on how it deals with its partners? In the authors' opinion such a contrast is not possible. Quality is rather a fundamental attitude, which either is valued through all levels and processes in a company or will not be found in its products. Furthermore, the theme of quality needs to be implemented at an organizational level throughout all areas and levels of the company. At Hanwha Q CELLS this is the task of the quality management (QM) team. This team drives forward the quality of current and future products through a certified quality management system, and supervises the entire value-added chain of production – from the inspection of all incoming raw, auxiliary and working materials, through the manufacture of solar cells and modules, to the creation of complete PV systems. Hanwha Q CELLS operates a tried and tested, certified, integrated management system that meets ISO 9001, ISO 14001, ISO 50001 and BS OHSAS 18001. The production workshops are ISO 9001, ISO 14001, ISO 50001 and BS OHSAS 18001 certified. For any PV company with an international production footprint it is also worth meeting high standards on an international scale. For this reason, Hanwha Q CELLS not only submits to audits by external certifying bodies, but continuously tests quality through internal cross audits. Likewise, the quality team is involved in product development from an early stage, so that it is possible to improve the standard of quality from generation to generation.

Quality right from the start

As well as enhancing performance and reducing production costs, improving the quality of products and manufacturing processes is a central aim in developing every new Hanwha Q CELLS product. That is precisely why the quality management team is involved in product development right from the start. This enables the introduction of quality targets early in the development, as well as the identification and remediation of discrepancies while still in the project stage.

Thus the actual development process itself is subject to Hanwha Q CELLS' philosophy of quality: in order to launch a new product, the product management must go through various levels, so-called 'gates', which include demonstrating that various quality tests have been passed and specific quality features met. A comprehensive analysis of possible failures and influences – failure modes and effects analysis (FMEA) – provides some guarantee that possible quality risks can be predicted at an early stage and avoided through optimizations of process, technology and/or product designs. In this way, risks can be thoroughly evaluated and minimized, especially in projects which are directly relevant to customers or to safety.

Standardized quality processes are also necessary with regard to internal quality assurance and customer service. So, for example, every new product-related document and every change to existing documents are subjected to a chain of approval by technical and expert auditors, before being automatically made available to all Hanwha Q CELLS' employees worldwide.

Every bit as important as the forecasts are subsequent evidence-based project evaluations and appraisals. At Hanwha Q CELLS, every project close-out meeting includes critical scrutiny of the project process in order to derive the maximum potential for improving process and product quality in every project.

An additional fixed quality checkpoint is the approval of every technical alteration by the change management team at Hanwha Q CELLS. The process of change is managed by the process change review board (PCRB) to guarantee a consistent method of proceeding and to ensure that changes to processes or products can be tracked. The PCRB is made up of colleagues from different sectors, and the quality management team is responsible for it. In addition to ruling on changes to products or processes, the committee makes decisions on quantitative, economic, safety and environmentally relevant aspects. The next level up from the PCRB is the quality board. In this committee, decisions are made on current requirements which involve higher goods values or are of broader scope. Thus it is ensured that the quality of processes and products is accorded the highest priority through all levels of processes and the hierarchy.

Supplier evaluation

Since 2005 Hanwha Q CELLS has established specific benchmarks

Dow Corning Corporation
Reliable Silicon Solutions for Solar PV

DOW CORNING

USA
Direct Dial: +1 989 496 7891
Toll Free: 866 562 5133
Belgium
Direct Dial: +32 64 511155
Toll Free: 0800 80525
Germany
Direct Dial: +49 611 237506
Toll Free: 0800 5250261
China
Direct Dial: +86 21 3899 7927
Toll Free: 4008807110
Email
solar.solutions@dowcorning.com
Web
dowcorning.com/solar
Year Founded
1943
Sales Volume
6.12 Billion USD
Employees
12,000 (worldwide)

Unleash the solar power of silicon

As the photovoltaic (PV) industry assumes an increasingly important role in meeting the world's energy needs, Dow Corning is committed to helping the industry increase the quality and durability of solar systems by unleashing the power of silicon.

Dow Corning delivers silicones, silicon-based technology and high-performance products that help create more reliable solar systems to increase kW/hour output and profitability.

A Growing Portfolio of Solutions

As a leading materials supplier to the PV industry, our goal is to help our customers grow through innovation and material solutions across the entire solar value chain. Our portfolio of solutions includes a wide range of options that improve the performance and durability of finished solar modules:

- Silicon feedstock
- Conductive adhesives, coatings and cell applications
- Silicone encapsulants
- Junction box adhesives and potting agents
- Silicone sealants and adhesives for module finishing
- Structural sealants for module installation

Investing in Partnerships

Our long-term commitment to sustainability and to providing solutions to the PV industry is demonstrated by major investments in Solar Solutions Application Centers around the world and by our support as a majority shareholder of the Hemlock Semiconductor Group, an important provider of polycrystalline silicon. Dow Corning's state-of-the-art PV module and solar cell applications centers enable close collaboration with leading industry players, tests and application development on site.

Built on more than 70 years of expertise, Dow Corning is a trusted partner to leading module manufacturers, collaborating to improve levelized cost of energy for solar power around the world.

You can learn more about Dow Corning Solar Solutions and view our virtual trade show at *dowcorning.com/solar* or e-mail *solar.solutions@dowcorning.com*.

against which suppliers are evaluated, and which are continually being developed through dialogue with its partners. If, during the evaluation of suppliers, the quality requirements are not met, urgent measures for improvement can be drawn up. Since 2008 the Hanwha Q CELLS Code of Conduct has obliged suppliers to meet internationally recognized standards, especially in the fields of quality, environmental protection and health and safety. To ensure that suppliers operate a quality management system that meets the standard set by ISO 9001 as well as other quality parameters, regular audits of suppliers are conducted. Requirements are also reflected in the internal purchasing guidelines at Hanwha Q CELLS. Changes made by suppliers to existing processes or intermediate products must be approved by the PCRB.

Incoming goods inspection

All raw, auxiliary or working materials that could affect the quality of the end product are subjected to a thorough inspection by Hanwha Q CELLS upon receipt. The content and structure of each inspection process are determined by how critical the material is to the quality of the end product. The scope of testing is generally defined by an acceptable quality limit (AQL) in accordance with DIN ISO 2859-1. Hanwha Q CELLS also works closely with its suppliers to continually improve their output inspections. In addition to this, specifications for quality assurance are agreed with suppliers; this enables faulty raw, auxiliary or working materials to effectively be controlled, claimed against and, particularly, to be minimized.

Production: quality on the line

In Hanwha Q CELLS' production plants for solar cells and modules at the company sites in Germany and Malaysia (cell production only), as well as at the company's certified contractors in Europe and Asia, all important factors that influence quality are monitored through 100% testing. The basis for this testing is a set of key parameters. In the event of deviation from Hanwha Q CELLS' target values, reaction plans are activated. This allows Hanwha Q CELLS to narrow down the root cause of the failure systematically and solve problems quickly.

"All important factors that influence quality are monitored through 100% testing."

For the fault analysis, the patented process TRA.Q is used, whereby every wafer is assigned a laser-engraved ID, which enables faults to be tracked individually, the sources to be identified and the underlying problem to be corrected. In addition to this, experts at Hanwha Q CELLS inspect and classify every cell according to optical and electrical parameters. For the inspection and classification, for both solar cells and modules, consistent calibration standards, verified by independent institutes, are used. Additionally, proprietary internally devised testing methods, such as the 100% hot-spot test, are in use throughout the company. A constant product quality is ensured through visual follow-up inspections.

And that is not enough – even the quality of the packaging is tested and optimized through regular random sampling. In this regard, close collaboration between all sectors involved, and particularly with customers, is very important, so that continual improvements can be made. In the development of the packaging it is important to strike the right balance between providing the best protection for the products and using packaging materials in a way that saves resources. To guarantee the protection of the cells and modules, the packaging materials are tested to international standards in independent testing laboratories. Transport and handling tests are also

Figure 2. Load testing at the Hanwha Q CELLS test centre.

carried out under real conditions, whereby product features before and after transportation or handling are compared.

Test centre for cells and modules

Covering an area of approximately 2300m^2 at the Thalheim site, Hanwha Q CELLS' test centre for solar modules is one of the biggest and most modern in the sector. This is evidenced by: sixteen climate chambers (damp-heat, thermal-cycling and humidity-freeze tests), with a capacity of 240 crystalline modules; seven light chambers, which can be used flexibly as UV or light soaking systems; two flasher lines, with an integrated electroluminescence imaging; and insulation measuring stations for dry insulation testing, hipot and wet leakage tests. During 2012 more than 4500 solar modules were tested in these flasher lines.

In addition to this, with two mechanical stress test machines (static/dynamic), a hail impact tester, a load testing capability, a hot-spot measuring station and three PID measuring stations, Hanwha Q CELLS regularly conducts a wide range of standard and special tests. Equipping the test centre with a range of other tests allows the execution of all the tests necessary for meeting IEC 61215 Ed. 2.0 and IEC 61730-2 Ed. 1.0 in house. It is therefore possible to achieve maximum security and flexibility in evaluating new combinations of materials, certifying new products and ensuring the high quality of Q CELLS products.

Hanwha Q CELLS' test centre is accredited by the Test Data Acceptance Program (TDAP) of the German VDE (Association for Electrical, Electronic and Information Technologies). This ensures that all results are verified by an independent third party, as well as speeding up certification and module development.

Test criteria for best products

To ensure the highest quality of Hanwha Q CELLS products, three basic principles for testing are adhered to: test hard, test continuously and test realistically.

Test hard

The IEC certification ensures a basic quality for PV modules, thereby setting a minimum standard (Fig. 4). Hanwha Q CELLS products, by contrast, must survive considerably tougher tests and are all certified 'VDE Quality Tested' – from cells to modules and all the way through to the standard block for large solar power plants, Q.MEGA. The VDE certification process sets much more demanding test criteria, which ensures the long-term performance of the products. For example, 'VDE Quality Tested' means that the test duration for standard damp-heat tests is increased from 1000 hours to 1500 hours, and the number of cycles for thermal cycling from 200 to 400. In addition to this, the number of test modules for the damp heat, thermal cycling and UV/thermal cycling/humidity freeze sequence is doubled from two to four in each case.

> "The VDE certification process sets much more demanding test criteria, which ensures the long-term performance of the products."

The dynamic stress test was introduced specifically for the VDE certificate. At the start of the UV/thermal cycling/ humidity freeze sequence, testers check the fracture behaviour of the solar cells within the module compound and thus increase the stress on the module. The subsequent ageing tests enable the long-term behaviour of the previously stressed modules to be predicted. The requirements are once more increased, since a module is only allowed to show a maximum performance loss of 5%

Figure 3. Testing must be hard, continuous and realistic in order to guarantee 25 years of quality performance.

HANWHA Q CELLS QUALITY REQUIREMENTS

REQUIRED TESTS	IEC CERTIFICATION	VDE Q.TESTED	INTERNAL TESTS
TEST FREQUENCY	once, only for initial certification	continuous sampling, quarterly monitoring	continuous sampling and monitoring
THERMAL CYCLING TEST (TC)	200 cycles	400 cycles	additional tests
DAMP HEAT TEST (DH)	1000 h	1500 h	additional tests
HUMIDITY FREEZE TEST (HF)	10 cycles	10 cycles	30 cycles
LOAD TEST	✓	dynamic load test before TC & HF	additional tests
HOT-SPOT TEST	✓	✓	100 % of cell production
EL TEST	certification module only	100 % of module production	100 % high resolution EL inspection
PID TEST	–	–	weekly production monitoring
USED SEAL	IEC	VDE Quality Tested ID 40032587	Q CELLS YIELD SECURITY ANTI PID TECHNOLOGY (APT) HOT-SPOT PROTECT (HSP) TRACEABLE QUALITY (TRA.Q™)

Q CELLS a Hanwha company

Figure 4. The quality test matrix for Hanwha Q CELLS products.

per test sequence. In comparison, the maximum performance degradation permitted for standard certification is 8%.

Test continuously

According to the criteria set down for IEC certification, for the certification process a product only has to pass the qualification test once with a specific number of test products. The products tested are often prototypes. In contrast to this, for the internal VDE Quality Tested certification, Hanwha Q CELLS products regularly undergo testing of randomly selected samples from mass production. As a result, deviations caused by production processes or by materials used can be promptly identified.

To closely monitor quality during production, Hanwha Q CELLS conducts not only in-line safety tests, but also supplementary in-line tests, as well as regular testing during production in order to test the cells and modules for hot spots, PID and so forth. Furthermore, at the end of production, the modules are checked for possible abnormalities with the aid of a 100% electroluminescence test. In addition to this, a specified percentage of the finished products are subjected to further insulation, ground continuity and reverse-current overload testing every day, with the aim of ruling out any safety problems. Only modules which are in perfect optical and electrical condition leave the production plants.

But it is not only Hanwha Q CELLS' internal tests that are continually being conducted. As a fixed element of the VDE Quality Tested seal, production is tested every quarter using randomly selected samples. This process includes – among other things – safety-related test measurements, such as hipot, wet leakage, reverse-current overload, hot-spot and ground continuity tests. Dynamic stress tests with subsequent thermal cycling and damp-heat tests are also a compulsory part of the testing. With the aid of these test sequences, production can be checked for consistent quality, possible deviations and faults. The results are reported to the VDE every quarter in order to retain the VDE Quality Tested seal.

Test realistically

Twenty-five years is a long time, and no PV product has so far been on the market long enough to test product quality through real-time testing. That is why testing methods which simulate as realistically as possible the stresses on products throughout their service life are being developed and employed. The comprehensive equipment in the Hanwha Q CELLS test centres allows more rigorous testing than is usual in the sector, and enables those results to be transferred, taking into account varying local conditions. For example, models developed using climate data are employed in order to translate the significance of the tests and testing procedures to realistic, location-dependent climatic conditions. This yields information about the degradation process or the appearance of various effects of ageing under a range of climatic conditions – whether in a temperate climate or in the desert, for example.

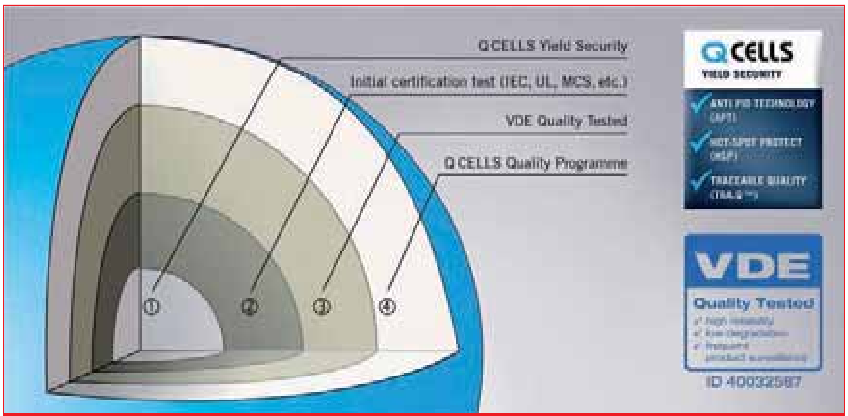

Figure 5. The four quality programmes operated by Hanwha Q CELLS.

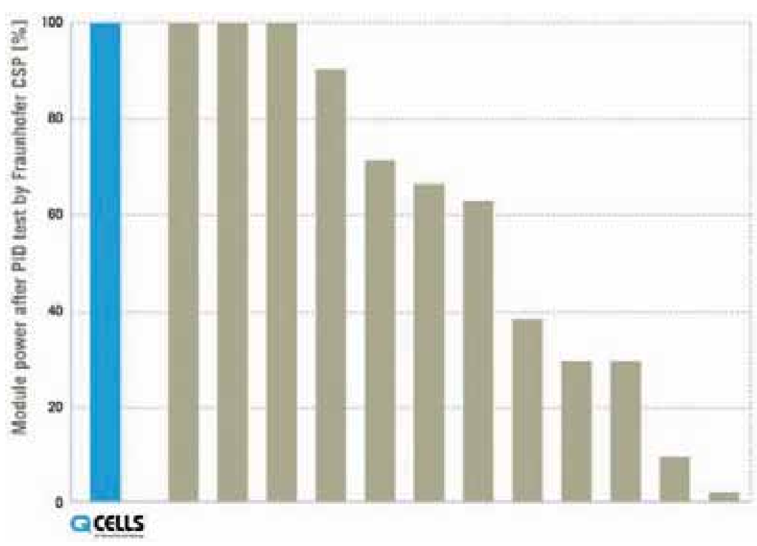

Figure 6. In May 2012 Fraunhofer CSP tested thirteen modules from brand manufacturers – nine of the modules failed.

Figure 7. A sign of above-average quality: the 'VDE Quality Tested' seal.

The four levels of quality at Hanwha Q CELLS

Before a product is worthy of using the name 'Q CELLS', it has to undergo and pass four independent quality programmes (Fig. 5):

1. Since 2011 the Q CELLS Yield Security has been the guarantee for reliable products from Hanwha Q CELLS. It combines guaranteed resistance to PID, security against hot spots and protection against the counterfeiting of the company's products.

2. The second layer comprises the international initial certification tests, for example in accordance with IEC, UL, MCS, JPEG and Kemco. These guarantee the electrical safety of the module and the safety of its construction in accordance with international standards.

3. The VDE Quality Tested programme (Fig. 7) exceeds the initial certification testing. Additionally, the quarterly re-testing guarantees consistent quality and product safety at all times.

4. The Hanwha Q CELLS internal quality programme ensures that all products meet the company's high safety requirements on a daily basis.

Quality as an international standard

To ensure that the Hanwha Q CELLS quality programme is implemented in external production plants, three essential tools have been introduced: on-site presence, Q-sampling and Q-monitoring (Fig. 8). The Hanwha Q CELLS quality control engineers visit the module conversion sites of the company's partners at regular intervals in order to ensure the quality and to improve it. For Q-sampling, the manufacturers must conduct regular random sampling tests and report the results to Hanwha Q CELLS. Finally, with Q-monitoring, random sampling tests on the conversions undertaken by partners are also regularly conducted in Hanwha Q CELLS' laboratories on site and in Thalheim.

Test the test

Hanwha Q CELLS' testing procedures are continually updated to optimize still further the standard of its testing methods. Good connections within the scientific community are maintained, and current developments as well as newly occurring faults in modules are always pursued. Thanks to its well-equipped test centres, Hanwha Q CELLS is then in a position to investigate and determine the causes. New test methods are developed in order to rapidly optimize processes and products and to eliminate occurrences of the fault in question. One example is the anti-PID technology (APT) test,

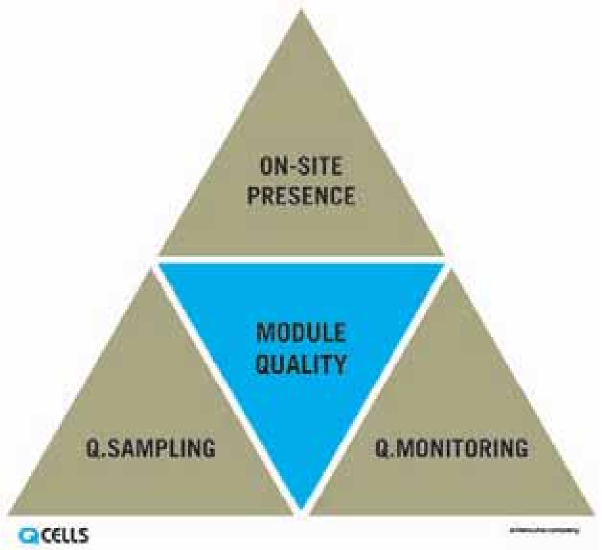

Figure 8. Tools to ensure that the internal quality programme is put into practice internationally.

which was developed in the Hanwha Q CELLS testing laboratory in 2009, to counteract PID. Since then this test has been further developed, so that it is now possible to test the PID resistance of cells during production and have conclusive results available within 48 hours.

Nobody's perfect

In the international PV market, the brand name Q CELLS stands for quality. And this is not the least of the reasons why the South Korean Hanwha Group decided to take over the company in 2012 and begin a bright future with Hanwha Q CELLS. But nobody is perfect, and complaints are occasionally received; in the ensuing process, the same attitude is taken as with the products – quality counts!

In the event of a complaint, customers contact the engineers in the complaints management department. Together with the customer, it is quickly decided what the best way to help will be: Is a plant visit required? Are test modules needed or does the available data suffice? If on-site measurement is necessary, Hanwha Q CELLS' field service team is available with its highly experienced technicians. They have been trained to test not only the modules, but also the whole plant with all its components. This service is provided for customers free of charge.

At the test centre it is then possible to carry out all the usual, and many additional, tests quickly and flexibly. If this is still not sufficient, there are links to independent institutes, such as the Fraunhofer Center for Silicon Photovoltaics in Halle, Germany. The cause of the problem is then determined using the eight disciplines (8D) problem-solving method, and the customer can be provided with a detailed 8D report if desired. If the analysis shows that the fault is covered by the guarantee, the customer will immediately be provided with a free replacement.

"Quality makes all the difference."

Conclusion

Quality is not just a sticker on a module or a promise made by a manufacturer. Quality is the result of a fundamental attitude and an immense effort, which runs through all levels and processes within a company and finally shows in the product. No less important is the financial and strategic basis on which a company makes the promises in its warranty at a time of constant consolidation in the solar industry. This makes the financial stability and sustainability of a company an integral part of quality from the customer's point of view. This very broad understanding of quality is the fundamental prerequisite for promoting customer satisfaction, and is an increasingly weighty argument to be considered when deciding which PV products to buy. For, at a time when solar electricity is partially achieving grid parity, and funding is being reduced, the importance of energy consumption, and hence of the yield of a PV system or the LCOE over the entire service life, is growing. A good-quality PV system is therefore one that comes from a financially secure company and on whose stable performance the customer can rely – for many years to come. Quality makes all the difference.

About the Authors

Dr. Nicole Nelles holds a Ph.D. in physics awarded by the Hamburg University of Technology (TUHH). She joined Hanwha Q CELLS in 2004, working as a project and process manager within the technology department, where she was responsible for projects including hot-spot protection and line support. She then advanced to the position of director of line technology in the production department. Since October 2011 she has been globally responsible for quality at Hanwha Q CELLS as vice president of quality management.

Dr. Max B. Koentopp received his Ph.D. in physics from the University of Karlsruhe (Karlsruhe Institute of Technology) in 2005, studying the simulation of electronic transport through molecular nanostructures. In 2009 he joined the R&D team of Hanwha Q CELLS as a project manager and simulation expert. As senior manager of the analysis and modelling group, he is currently responsible for module reliability testing, cell characterization, and device modelling and simulation.

Dr. Sandra Scholz received her Ph.D. in physics from the University of Freiberg in 2007, with a thesis topic of carbon distribution in solar silicon and its impact on electrical properties. She joined the R&D team of Hanwha Q CELLS as a process technologist in 2007. In 2008 she became a project manager for R&D crystallization, later advancing to senior manager in 2009, and then to expert quality engineer in 2012.

Enquiries

Jochen Endle
Hanwha Q CELLS GmbH
Sonnenallee 17–21
06766 Bitterfeld – Wolfen
Germany

Tel: +49 (0) 3494 6699-10121
Email: presse@q-cells.com
Website: www.q-cells.com

Compatibility of copper-electroplated cells with metal wrap-through module materials

Ian Bennett, **Bart Geerligs**, **Carol Olson** & **Maurice Goris**, Energy Research Centre of the Netherlands (ECN), Petten, The Netherlands

ABSTRACT

As part of the European FP7 R&D project 'Cu-PV', the compatibility of copper-electroplated metal wrap-through (MWT) cells with conductive adhesives has been investigated. The objectives of this project include to reduce, by the use of copper plating, the amount of silver utilized in cell manufacturing, and to demonstrate the compatibility of high-power n-type back-contact module technology with copper-plated cells. The overall goal is to reduce the impact on the environment of cell and module manufacture. MWT module technology as developed by ECN uses conductive adhesive to make the interconnection between cells and a conductive backsheet foil. These adhesives have been proved to result in very reliable modules in the case of cells with fired silver metallization. To determine the compatibility of conductive adhesive with copper-plated cells, component tests were performed, followed by the manufacture of modules with copper-plated cells and conductive adhesive interconnections. Climate chamber testing of these modules showed that the adhesive is compatible with the copper-plated cells. The next steps include further optimization of the plating process and additional testing at the module level.

Introduction

PV modules have an environmental impact, broadly speaking, via the embedded energy and scarcity of PV module material components, as well as an environmental impact in other fields (such as toxicity). The embedded energy is dominated (around 75%) by the silicon wafer (in the case of a crystalline silicon PV module); glass, EVA and the aluminium frame account for most of the remainder. Silver is the scarcest material used in crystalline silicon PV module manufacturing. Although embedded energy has the greatest environmental impact, there are also important contributions from silver, copper, aluminium and glass (Figs. 1 and 2).

The Cu-PV project [1] ('Cradle to cradle sustainable PV modules') is an R&D project in the European Union's Seventh Framework Programme on the topic of improving resource efficiency. It focuses on three key sustainability issues of current PV technology:

1. Reducing the energy demand in PV manufacturing, by developing high-power back-contact solar cell designs that use thinner wafers, i.e. less silicon.
2. Minimizing the use of critical materials, namely silver and lead.
3. Improving the recyclability of PV modules.

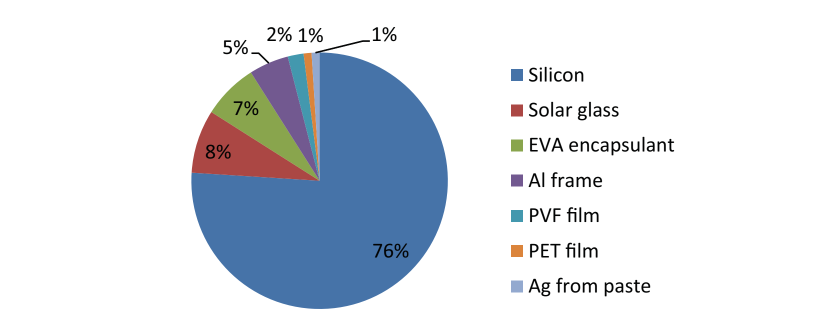

Figure 1. Embedded energy breakdown for a PV module containing crystalline silicon cells.

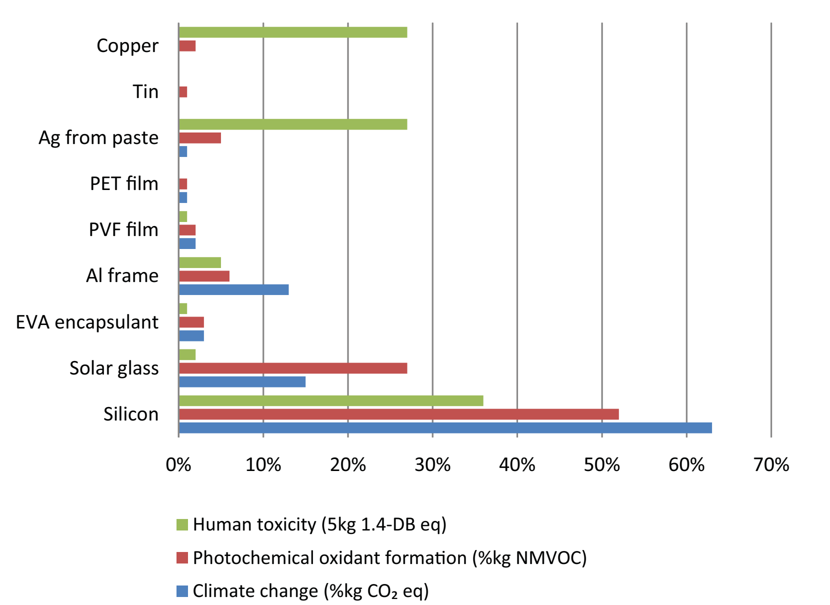

Figure 2. Environmental impact of silicon PV modules in terms of climate change and toxicity.

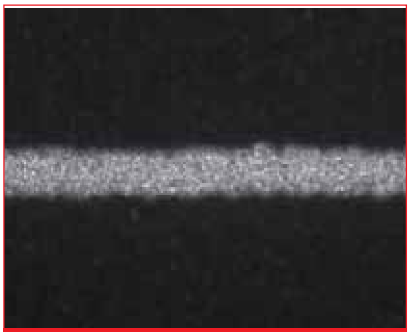

Figure 3. Seed and plated metallization finger with a width of 69µm.

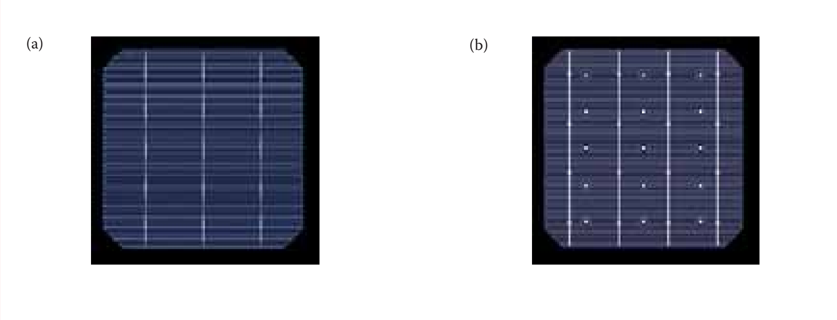

Figure 4. An nMWT cell design: (a) front-side grid; (b) rear-side contacts. The rear-side contacts are shown by the 4 × 4 pattern, and the front-side contacts (connected to the front-side grid through vias in the wafer) are shown by the 3 × 5 pattern.

Although Ag consumption in the manufacturing of solar cells has recently been significantly reduced for cost reasons, its use in solar cell metallization is still unsustainable in the longer term. The world's Ag reserves are sufficient for less than 25 years' mining of this metal at the current rate. Many options have been investigated for switching to non-Ag metallization of solar cells, most prominently physical vapour deposition (for back-contact cells) and copper plating, or a combination thereof.

> "The world's Ag reserves are sufficient for less than 25 years' mining of this metal at the current rate."

To make the transition from present fire-through metallization processes to copper plating as smooth as possible, one of the metallization methods under investigation in the Cu-PV project is seeding with a minimal amount of Ag metallization, followed by nickel–copper electroplating. Screen-printing technology cannot easily yield a significant reduction in Ag consumption for a seed pattern, as it does not have the ability to print very thin and very narrow lines. Thin lines are important for minimizing Ag consumption, whereas narrow lines are important for high efficiency (the Cu plating will widen the lines). In the Cu-PV project Ag seeding is therefore done by inkjet printing, which offers a contact resistance and recombination as good as that obtained using conventional Ag pastes, but with a much lower use of Ag and with significantly narrower lines. Seed patterns using 12mg Ag have so far been demonstrated, with 40µm-wide lines that could be electroplated without problems. A particular advantage is that bleeding of the seed lines is small, so that the plated lines do not contain much parasitic plated material at the edges (Fig. 3).

The current focus of the Cu-PV project is on high-efficiency n-type MWT cells [2, 3], with emitter contacts on the rear of the cell (Fig. 4). This means that rear-side junction isolation will be the centre of attention.

The first module tests in the project, however, as reported in this paper, were carried out on plated non-metal-wrap-through cells. Also, the seed grids in these first tests were made by screen printing rather than by inkjet printing (Fig. 5).

MWT module technology

MWT module technology as developed by ECN [5,6] makes use of a conductive backsheet foil in combination with a conductive adhesive, in contrast to the tabbing and stringing process used with H-pattern cells and modules. The conductive backsheet foil is made up of a copper–PET–PVF laminate, with the copper patterned to match the contact pattern on the rear of the cells. The conductive adhesive is chosen to have the correct printability, curing properties, and conductivity and flexibility after curing.

Manufacture is performed using a module line as developed by Eurotron. In this production line, the conductive foil is placed on a vacuum carrier, after which the conductive adhesive is stencil printed onto the foil at the position of the contact points on the cells. A layer of EVA is placed on the conductive backsheet foil. The EVA is perforated with holes at the positions of the conductive adhesive dots to ensure contact between the conductive adhesive and the cells. The cells are then arranged one by one on the conductive backsheet, with the cell only being touched once during the whole process. A second layer of encapsulant is then placed on the cells, followed by a glass sheet. This top layer of encapsulant is locally heated to tack the cells to the glass in order to prevent movement during lamination.

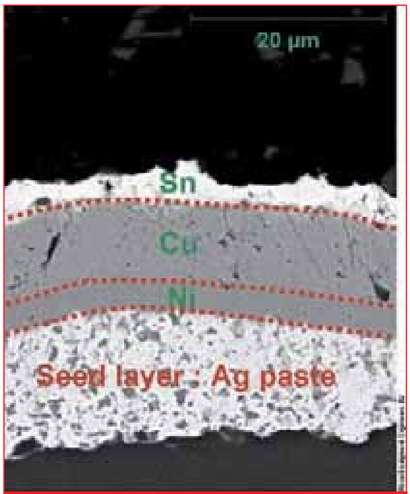

Figure 5. Seed and plate structure of the metallization as tested in this study [4]. The final layer was tin, silver or an organic solderability preservative (OSP). The OSP is also used on the conductive backsheet foils and so is known to be compatible with processing using conductive adhesive.

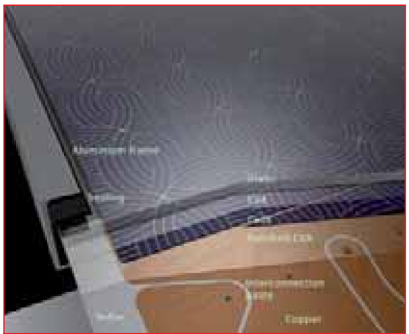

Figure 6. Cross section through an MWT module, showing the conductive backsheet with patterned metal layer, conductive adhesive dots (interconnection paste), the first sheet of EVA, MWT cells and other module materials.

The module stack is then inverted for the lamination process. During lamination, the encapsulant and adhesive are cured in a combined lamination and interconnection step.

There is no local heating as with soldering: the whole module is heated uniformly and the temperature is limited to the curing temperature of the adhesive and encapsulant (i.e. 150°C). This makes the process ideal for very thin cells as investigated in the Cu-PV project. A cross section of an MWT module is shown in Fig. 6.

Module manufacture with no cell breakage has been demonstrated in other projects [7,8] using cells with a thickness of less than 120µm. Climate chamber testing has been performed on MWT modules, resulting in less than 2% degradation in power output after 400 thermal cycles and 2000 hours of damp heat for cells with fired silver metallization and EVA as the encapsulant. With a thermoplastic encapsulant, a degradation of less than 1% in power output for the same test has been measured [9]. A number of production lines have been sold to module manufacturers, and commercial production of this type of module is expected to begin before the end of 2013. In this study, the suitability of the module technology and materials, particularly the conductive adhesives, in combination with copper-plated cells is investigated.

Component testing

The first stage in evaluating the compatibility of copper-plated cells with MWT module technology was to measure the contact resistance and adhesion strength between the adhesive and the copper plating on the cells and to compare this with the values for a cell with fired silver contacts. It is known that the adhesive in combination with a cell with fired silver metallization has a contact resistance low enough not to be dominant in the module performance, and an adhesion strength high enough to be able to survive module manufacture and thermal cycling up to 400 hours with limited degradation as mentioned above.

Contact resistance was measured using a transmission line method (TLM). A number of tin-coated copper tabs were stuck to the busbar of a copper-plated p-type cell using a conductive adhesive which had been proven in climate chamber testing with full-size modules. The cells were plated by Meco. A spacer was used between the tab and the cell to simulate the thickness of the EVA and adhesive found in an MWT module between the conductive backsheet foil and the cell. The adhesive dot was printed using a stencil, also with the aim of simulating the shape and volume of adhesive as used in the module. The resistance between the first tab and subsequent tabs was measured and plotted, allowing the contact resistance to be estimated by TLM analysis.

Copper-plating finish	90° peel strength [N]	180° shear strength [N]
OSP	0.5–1	30–40
Tin	0.3–1	21–33
Silver	0.3–1	9–24

Table 1. Peel strength and shear strength results for conductive adhesive contacts on copper-plated cells. The geometry of the adhesive dot in the MWT module makes the 90° peel test unsuitable for the assessment of adhesion strength. The shear test, however, is considered to be more representative of the stresses in an MWT module.

Three types of surface finish were used on the copper of the cell: a silver finish, a tin finish and an organic solderability preservative (OSP). This finish is needed to prevent corrosion of the copper on exposure to ambient conditions, which would result in an increased contact resistance. The contact resistance values of the three types of copper-plated cells were compared with the contact resistance measured for cells with fired silver contacts. The same samples were also used for adhesion testing. Peel testing at 90° was performed first; however, because of the dimension of the adhesive dots and the peel angle, very low values were obtained for the three copper-plated cell types as well as for the cell with fired silver contacts (Table 1). A second series of samples was subjected to a shear test, the results of which allowed the variations in adhesion strength between the different cells to be observed (Table 1). The shear test is considered to be more representative of the stresses seen in an MWT module. These stresses are caused by differences in thermal expansion coefficients between the different module materials and generally act in the plane of the backsheet, resulting in shear forces on the interconnections.

Contact resistance was found to be lowest for the copper-plated cells with a silver coating, followed by the copper-plated cells with a tin coating, and finally the OSP-finished cells. The value for the cells with the fired silver metallization was intermediate between the OSP- and silver-finished copper-plated cells. Despite the higher value, the contact resistance for the OSP-finished cell is nevertheless much lower than the calculated acceptance limit for contact resistance. A contact resistance of this magnitude will not have a noticeable effect on the performance of the module: for example, the contact resistance of the adhesive on an OSP backsheet foil is approximately 500µΩ, and it has also been calculated that this value will not dominate the series resistance in the module (well below 0.1% loss in fill factor). An OSP-finished cell is preferable because of cost and the use of OSP on the conductive backsheet foil. If both cell and foil have the same finish then compatibility with both surfaces can be engineered in one step. The shear test values show that the OSP-finished copper-plated cells have the highest adhesion in shear – higher even than that for the cells with fired silver metallization. This should result in a module that performs well in thermal-cycling tests.

“Contact resistance was found to be lowest for the copper-plated cells with a silver coating.”

Pseudo mini-module design and manufacture

After it had been confirmed that the conductive adhesive and copper-plated cells were compatible at the component level, single-cell mini-modules were manufactured for climate chamber testing. Since no copper-plated MWT cells were available at the time, the module design had to be adapted to allow the simulation of the adhesive contact in an MWT module by using an H-pattern cell. The front-side contact was made with tabs soldered to the busbars as for a standard H-pattern cell. The rear-side contacts were formed using a copper-based backsheet with adhesive dots printed on the copper to match the positions of the busbars on the rear of the cell (Fig. 7). Seven dots were printed for each of the three busbars. Holes corresponding to the

Figure 7. Image of a pseudo-MWT mini-module. The front-side interconnection is accomplished by soldering tabs to the busbars; the rear contact to a conductive backsheet is made by a conductive adhesive printed at the location of the busbars on the rear of the cell.

Figure 8. EL image of an H-pattern single-cell module with soldered front-side contact and MWT rear-side contact, showing cracking in the top left corner and finger interruptions at the edges of the cell.

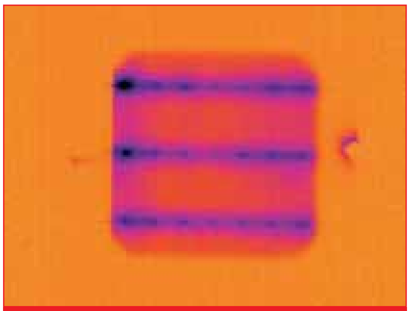

Figure 9. DLIT image of the same mini-module in Fig. 8, showing the position of the conductive adhesive interconnections between the cell and the conductive backsheet foil.

positions of the conductive adhesive dots were punched in an EVA sheet, and the sheet then placed over the dots. The cells were arranged on the EVA so as to make contact with the adhesive dots. A sheet of EVA and a glass plate were placed over the cells, and the stack was laminated to cure both the EVA and the conductive adhesive.

A total of four single-cell modules were manufactured. The performance of the modules was measured using a Pasan 3B flash tester (Table 2). Because of the non-optimized module design, the fill factors (*FF*) of the modules are not particularly high when compared with standard MWT modules, but were considered suitable for climate chamber testing.

Electroluminescence (EL) and thermography (DLIT – dark lock-in thermography) images were generated in order to evaluate the quality of the modules after manufacture. EL images (Fig. 8) reveal some cracking in the cell at the ends of the busbars, as well as finger interruptions on the front of the cell in several places at the edges; this is most likely caused by the soldering of the tabs. Thermography imaging (Fig. 9) shows the position of the conductive adhesive interconnections between the cell and the conductive backsheet foil.

Climate chamber testing

Initial climate chamber testing focused on thermal cycling. The aim of this was to confirm that the adhesion test results obtained during component testing could be translated into good performance. Because of differences in the thermal expansion coefficients of the various module materials, the conductive adhesive contacts between the cells and conductive backsheet foil will

Module code	I_{sc} [A]	V_{oc} [V]	*FF* [%]	Efficiency [%]
A1535	9.17	0.63	74.4	18.3
A1537	8.95	0.63	74.9	17.8
A1538	9.26	0.63	74.0	18.2
A1540 (control)	9.06	0.63	75.4	18.0

Table 2. *I-V* characteristics of modules manufactured using copper-plated H-pattern cells with MWT interconnections on the rear side and tabbing on the front side (before climate chamber testing).

Module code	ΔI_{sc} [%]	ΔV_{oc} [%]	ΔFF [%]	ΔEfficiency [%]	ΔPower [%]
A1535	0.29	0.93	–1.24	–1.68	–0.03
A1537	0.15	0.89	–0.52	–1.14	–0.51
A1538	0.34	0.90	–2.72	–3.14	–1.52
A1540 (control)	–0.16	1.23	0.80	0.19	1.87

Table 3. Changes in *I-V* characteristics of the modules after 100 thermal cycles, relative to their values at t = 0.

Module code	ΔI_{sc} [%]	ΔV_{oc} [%]	ΔFF [%]	ΔEfficiency [%]	ΔPower [%]
A1535	0.33	0.79	–2.46	–3.00	–1.37
A1537	1.05	0.57	0.48	0.43	2.11
A1538	4.54	0.91	–4.41	–0.82	0.84
A1540 (control)	–0.99	0.64	1.65	–0.37	1.30

Table 4. Changes in *I-V* characteristics of the modules after 200 thermal cycles, relative to their values at t = 0.

be stressed. Any degradation in the power output and fill factor of the module can be related to a loss of contact of the conductive adhesive with either the cell or the conductive backsheet.

> "Any degradation in the power output and fill factor of the module can be related to a loss of contact of the conductive adhesive with either the cell or the conductive backsheet."

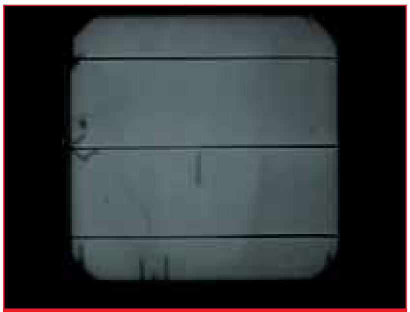

Figure 10. EL image of a single-cell module after 100 thermal cycles, showing little change relative to the module at t = 0. The module shows uniform illumination, indicating that the cell and interconnections are intact.

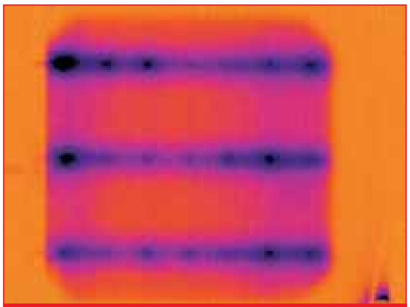

Figure 11. DLIT image of the same mini-module in Fig. 10, showing all contacts to the conductive backsheet foil intact, with little differences from the t = 0 image.

The thermal-cycling test is based on the test included in the IEC 61215 standard and is performed using a current corresponding to the applied I_{mpp}. This subjects the module to more stress in the form of additional heating, especially in areas of high resistivity, such as a failing contact. The total test time was 200 thermal cycles, but testing was interrupted at 100 cycles to allow characterization of the module, so that any degradation could be measured. Characterization of the module was performed by IV flash testing and EL and DLIT imaging, as was also done at t = 0. A total of three modules were subjected to this test, with one control module kept out of the climate chamber.

As seen in Table 3, a maximum of 1.5% reduction in power output was measured for one of the modules (A1538) after 100 thermal cycles. The other two modules showed smaller changes in power output. The reduction in power output for module A1538 could be accounted for by the 2.7% reduction in *FF*. EL and DLIT images (Figs. 10 and 11) of these modules show very little differences from the images made at t = 0. This shows that the interconnections and cells remained stable up to this point.

Table 4 shows that module A1537, showing a power loss after 100 cycles, now shows a power increase after 200 thermal cycles; moreover, the *FF* also no longer shows a decrease relative to the measurement at t = 0. One of the other modules (A1535) shows a loss of 1.4%; this can again be attributed to a 2.4% decrease in *FF*. The third module (A1538) shows no loss in power output, but does show a 4.4% reduction in fill-factor. As was the case for the measurements after 100 cycles, the EL and DLIT images are stable when compared with the images at t = 0, with no hot spots or areas not contributing to current generation.

The results show that, for the limited sample size tested in this experiment, interconnection between a copper-plated cell and a conductive backsheet gives rise to a reliable module. Some variation in power output was measured, but this was well within the limits as specified in IEC 61215 and was no larger than the variations seen in the control module. For module A1538, an *FF* loss of 4.4% was measured, which was close to the acceptable limit of 5%; no power loss, however, was measured, indicating that, in combination with the high current, the *FF* value may have been a measurement artefact. To determine whether this loss is significant or the result of a manufacturing or measurement error, the number of test samples would have to be expanded and the tests continued to 400 or 600 cycles.

Conclusions and further work

The component testing and climate chamber testing of the mini-modules shows that copper-plated cells are compatible with the MWT module concept and materials. In particular, the cells are compatible with contacting using a conductive adhesive. The contact resistance is similar to that seen in cells with fired silver metallization, as is the mechanical strength of the contact. In mini-modules the initial performance shows that a well-performing module can be produced using copper-plated cells.

> "Testing of the mini-modules shows that copper-plated cells are compatible with the MWT module concept and materials."

Thermal cycling to 200 cycles demonstrates little degradation in power output, comparable to the thermal-cycling results for an MWT module with cells having fired silver contacts. This shows that it is possible to manufacture reliable MWT modules with copper-plated cells in combination with a conductive adhesive and conductive backsheet foil.

Further work in the Cu-PV project will focus on the development of a high-power copper-plated n-type MWT cell and module. This will not only allow a direct comparison of copper-plated MWT cells and standard MWT cells (with fired silver metallization) and modules, but will also eliminate any negative effects of soldering tabs to the front side of the cell, a procedure that was necessary in the work discussed in this paper. The resulting modules will be subjected to additional climate chamber tests, including further thermal cycling and damp heat, as well as other tests stipulated in IEC 61215. Further work in the Cu-PV project in general will also focus on n-type copper-plated back-junction back-contact cells and modules, the reduction of the wafer thickness, and the evaluation and development of recycling strategies for PV modules.

References

[1] Cu-PV project [http://www.sustainablepv.eu/cu-pv].

[2] Guillevin, N. et al. 2012, "High-efficiency n-type Si metal-wrap-through cells from lab to fab", *Future Photovoltaics* (April).

[3] Guillevin, N. et al. 2012, "Development towards 20% efficient n-type Si MWT solar cells for low-cost industrial production", *Proc. SolarCon/CPTIC 2012*, Shanghai, China.

[4] Richard, D. 2011, "Technology in the waiting line", *Photon International* (July), pp. 198–205.

[5] de Jong, P.C. 2010, "Achievements and challenges in crystalline silicon back-contact module technology", *Photovoltaics International*, 7th edn, pp. 138–144.

[6] Eerenstein, W. et al. 2012, "Back contact module technology", *Proc. SolarCon/CPTIC 2012*, Shanghai, China.

[7] Bennett, I.J. et al. 2009, "World record module efficiency for large and thin mc-Si MWT cells", *Proc. 24th EU PVSEC*, Hamburg, Germany.

[8] Lamers, M.W.P.E. et al. 2010, "17.9% back-contacted mc-Si cells resulting in module efficiency of 17.0%", *Proc. 25th EU PVSEC*, Valencia, Spain.

[9] Rosca, V. et al. 2012, "Systematic reliability studies of back-contact photovoltaic modules", *Proc. SPIE*, San Diego, California, USA.

About the Authors

Ian Bennett is a researcher at ECN Solar and received a Ph.D. in materials science from the University of Bath. He has been working at ECN since 2006 as a member of the module technology and application group, where he has been involved in the development of MWT module technology and the application of new and novel module materials and module designs.

Bart Geerligs joined ECN Solar in 2000 and is currently a researcher. Since 2003 he has been involved in the development of n-base silicon solar cells, including silicon heterojunction technology, also occasionally carrying out scientific research in n-type doped silicon. He holds a Ph.D. from Delft University of Technology for research in nanoscale quantum electronic devices.

Carol Olson received a Ph.D. in physics from Imperial College, London, in 2003. After joining ECN in 2006, she carried out research in the areas of thin-film PV and characterization of silicon solar cells. Dr. Olson currently manages projects relating to life cycle assessment of photovoltaic products and processing lines, as well as those relating to sustainability of PV. She participates in the EPIA sustainability working group and in the IEA-PVPS Task 12 on PV environmental health and safety activities.

Maurice Goris is a chemical engineer and has worked at ECN since 1985. He has over 15 years' experience in research fields related to solar energy. For the past two years he has worked as a back-contact foil specialist on projects involving module cost reduction and alternative connection methods between MWT solar cells and back-contact foils.

Enquiries

ECN Solar Energy
Westerduinweg 3
1755 LE Petten
The Netherlands

Tel: +31 88 515 4709
Email: bennett@ecn.nl
Website: www.ecn.nl

Power Generation

108

109

White House fitted with solar panels

Solar panels are being fitted on the White House as part of an energy retrofit to improve the overall energy efficiency of the building. No details on the specification of the install or the companies involved have been revealed other than to confirm that they are "American-made" panels. Democratic President Jimmy Carter installed 32 solar thermal panels on the White House in the late 1970s; President Ronald Reagan then had the panels removed. The installation follows news that utility-scale solar power installations reached 3GW in the US, while residential solar installations hit an all-time high frequency with one installation every four minutes.

Solar panels being installed on the White House.

PV in emerging markets

Punjab government approves 700MW solar plan

Plans to develop 700MW of desert PV capacity in Punjab, Pakistan, have been approved.

The fourth meeting of the newly formed Energy Council of Punjab rubber-stamped plans for the Quaid-e-Azam solar park 'master plan' in August.

The Punjab government aims to install, from its own resources, a 700MW series of solar projects, according to Punjab chief minister Mian Shahbaz Sharif. It has set up a state-owned company, the Quaid-e-Azam Solar Power Co., to deliver the projects.

Rwanda's first grid connected solar project

Rwanda has announced the start of its first grid-connected solar project, also believed to the first of its kind in East Africa.

A power purchase agreement contract was signed with Gigawatt Global Rwanda as the Rwanda government prioritises energy production.

Gigawatt Global, a Dutch co-op that was established by the same American founders of Arava Power Company, will design, finance, maintain and operate the plant.

The plant is expected to be operating by June 2014 and is valued at an estimated US$23 million.

Rwanda is to get its first grid-connected solar installation.

Desertec France launched to help energy relations south to north to improve energy in Africa

The Desertec Foundation, the troubled non-profit organisation behind a push to generate export large volumes of renewable energy in developing countries, has launched Desertec France.

Contracts launching Desertec France were signed by Desertec Foundation president and co-founder Francis Petitjean, general director and co-founder Charles Ifrah, director of Desertec Foundation and fellow co-founder Thiemo Gropp and member of the executive board Oliver Steinmetz.

US PV news

California remains top US solar power generating state

Source: SolarCity

California remains top US solar power generating state.

California has installed 521MW of new PV in the last three months, making up a record 53% of all new PV installations in the US for the 2013 second quarter.

Finlay Colville, vice president at NPD Solarbuzz said California's installation rate "is a new record for PV added by any state in the US" continuing that California added "1.6GW in the past 12 months, with a further 1.1GW forecast for the second half of the year".

According to NPD Solarbuzz quarterly data analysis, the US added 978MW of PV in total in the second quarter of 2013. The record new installation rates are a 24% increase from the 788MW installed in the US in the first quarter of 2013.

The quarterly analysis also reveals that 72% of new installations were ground mounted and 28% rooftop. Utility-scale projects made up for 59% of installations and 41% residential and commercial.

Demand in the US PV market has been forecast to grow by 14%, with top solar installer states for the next quarter set to be Arizona and North Carolina, with a combined total of 400MW underway. A combined total of 500MW is scheduled for installation in New Jersey, New Mexico, New York and Texas.

Around 44GW of projects remain in the pipeline in the US, with over 2,300 projects generating 50kW or more.

Solar to be price competitive in western US by 2025: NREL

Solar and wind power could be price competitive with gas-fired plants in the west of the US by 2025, according to a new study by the National Renewable Energy Laboratory (NREL).

According to the research, Californian solar and wind in Wyoming will generate cheaper electricity than gas in 2025, the year when state-wide Renewable Portfolio Standards (RPS) expires.

The study concludes that the end of the RPS will drive renewable energy development into the most fertile areas. It predicts that areas with direct normal insolation of 7.5 kWh per metre squared a day will receive the most attention. Germany averages around 3kWh per metre squared a day.

Pentagon awards US$7 billion of solar contracts

The US Department of Defense (DoD) has awarded US$7 billion of contracts to 22 companies for the right to develop and sell solar energy to the US Army.

The winning companies include Gehrlicher US, Siemens and Sunpower.

Once projects are developed it is understood winning companies will bid against each other to supply solar power with the remainder of the ring-fenced US$7 billion available for purchasing.

The projects will be developed on land owned or under the jurisdiction of the DoD.

Source: Tepco

The Japanese government is looking to increase investment in clean energy infrastructure.

Technology and Information Progress

Thriving market Japan pushes for new power generation technology and storage

Japan's Ministry of Economics, Trade and Industry (METI), has requested an increase in the nation's clean energy budget of 62%, partly to help relieve bottlenecks of solar power projects.

METI released a series of budget requests in various fields, including two relating to the provision of renewable energy, which would require ¥46.2 billion yen (US$47.1 million) invested into the electrical grid system from an overall budget request for ¥198.1 billion yen (US$2 billion).

The document also discusses budgeting for assessment and research into various clean energy technologies including 'smart' energy saving integrated systems and lithium ion battery installation. The news comes as Bloomberg reports that in southern Japan, solar power projects are struggling to connect to the grid. Utility companies Chugoku Electric Power and Kyushu Electric Power each have less than 1GW of grid space remaining.

In April, Hokkaido Electric Power, based on the northern Japanese island of Hokkaido, revealed that as few as one in four solar power stations were being connected as scheduled due to overcapacity, with the grid unable to cope. Japan's grid system is split into 10 geographically divided regions, with different utility companies in different regions.

News

Kilowattsol to provide monthly UK irradiance anomaly data free of charge

Kilowattsol, a yield assessment provider for photovoltaic projects, is to provide monthly solar irradiance abnormality maps for the UK, following the launch of similar services in Germany, France and Spain in February 2013.

According to Kilowattsol, solar irradiance can frequently vary more than 40% above or below the mean figure for the month. The new monthly data, to be issued free of charge, aims to provide solar power plant owners and operators with better means to accurately calculate the outputs and performances of projects.

The company will provide maps of horizontal irradiation anomaly data for the preceding three months at the start of each month. A negative figure will indicate that irradiation was below the long-term average, while a positive figure will indicate that irradiation was above the average.

European subsidy cuts

Romania cuts green certificates

Romania made large cuts to its 'green certificates' (fixed price agreements for energy providers to buy solar power, in order to fulfil government quotas for renewably sourced energy). From the 1 July 2013, Romania cut certificates awarded per grid-fed renewable MW, from six certificates, to four, applicable for 15 years for plants up to 10MW.

Spain caps solar profits

Spain annoucned a cap on profits for solar investors of up to 5.5% of initial outlay has taken affect, despite the cap setting a lower percentage than interest rates, locking in losses.

Italy also announced renewable power generation reforms, with possible cuts to payment periods for renewable incentives from 20 years, 18 years.

Greek PV trade association pleas to prime minister

Greece's solar trade association, the Hellenic Association of Photovoltaic Companies (HELAPCO), has written an angry open letter to the Greek prime minister asking for support to help revive the country's PV industry.

Although Greece installed more PV plants in the first seven months of 2013 than in the whole of 2012, according to HEPALCO estimates, the industry has apparently lost one third of its jobs in the first half of 2013.

HELAPCO believes new restrictive policies will lead to further job losses and pleads for Prime Minister Antonis Samaris to listen to the association's recommendations.

The organisation argues that over 50,000 jobs have been created, either directly or indirectly, by the PV industry in Greece, while a further 14,000 companies have invested in solar parks and 38,000 residential customers have purchased PV installations.

Switzerland considers 40% tariff cut.

Switzerland considers 40% tariff cut

A petition with thousands of signatures calling for the protection of solar energy support in upcoming policy reforms has been delivered to the Swiss Federal councillor Doris Leuthard.

The 'Pro Solar' petition led by industry body Swissolar gathered more than 1,500 signatures over the weekend alone.

The petition was part of the 'Solar Wars' campaign, which uses references to the film series Star Wars to engage the public. The campaign included imposing Leuthard wielding a lightsaber onto a film poster distributed at the Locarno Film Festival.

The Swiss government is considering up to a 40% cut in solar tariffs.

Any changes or cuts decided will take effect from 1 January 2014.

The campaign claims that lobbying for oil, gas and nuclear is undermining opportunities for solar in the new energy strategy.

It also claims that energy users will lose money in the future without more renewables incentives that can help relieve energy dependency on international sources.

PV and development

Sunlabob to provide PV training in Kiribati

Laos-based Sunlabob Renewable Energy has been awarded a contract to provide training to PV engineers in the Pacific island state of Kiribati.

Funded by the European Development Fund, the company, which specialises in renewable energy provision in developing countries, will give instruction in on- and off-grid solar PV installation, operation and maintenance techniques.

The project follows Sunlabob winning another contract in Kiribati in early 2013 to supply equipment for a range of decentralised solar projects, including the installation of over 2,000 solar home systems and village solar 'mini-grids.'

Kiribati is said to be one of the least developed of the Pacific island states.

Seraphim donates off-grid systems to Tibetan primary schools

Seraphim Solar System, wafer cell and module producers, donated two 8KW off-grid PV solar systems, to two Tibetan primary schools.

The two schools in Pajiang village, Shigatse and Qudeng village of Litang county, Ganzi Tibetan Autonomous Prefecture of Sichuan Province, are far from infrastructure and transport including the national grid.

The two off grid systems will meet the basic electricity needs of schools, while books, clothes and stationary were also donated by Seraphim employees ready for the start of the new school term.

Hanwha's 'Happy Sunshine' campaign provides 30kW PV system for primary school in rural China

Hanwha Group's 'Happy Sunshine' campaign is to provide a 30kW distributed rooftop PV plant to Yuyangguan Town Hope Primary School, Wufeng County in Hubei province, China.

Hanwha Group has appointed Hanwha Solar One to design and build the installation, which is expected to be completed by November 2013. The 'Happy Sunshine' campaign was launched by Hanwha in partnership with CCCME and China Youth Development Foundation.

'Happy Sunshine' began in late 2011 and has pledged to provide PV systems at no cost in welfare or public facilities, aiming to provide over 500 different facilities over the next 10 years.

Source: Flickr/Nicolas Raymond

Sunlabob is to provide training for PV workers in Kiribati.

Product Reviews

AEG Power Solutions

The Protect PV.880 central inverter from AEG provides harsh environment protection

Product Outline: AEG Power Solutions (AEG PS) has launched the Protect PV.880 OD, a compact high efficiency central solar inverter for utility-scale applications on ground area installations in harsh outdoor environments.

Problem: With the majority of utility-scale PV power plants located in harsh environments around the globe, high-uptime and reliable performance of central inverters are essential for long-term project performance.

Solution: AEG PS' line of compact outdoor units for PV power stations supports between 500kWp and 1300kWp. Its integrated power stack PV core enables an input DC voltage of up to 1,000V and peak efficiencies of 98.7%. Designed for harsh outdoor applications, the new inverter supports a wide operating temperature range of -20°C to +50°C, while the light weight (1,850 kg) and small dimensions (2200 x 2,250 x 800 mm) raise the ease of transport, installation and service to new levels. All outdoor units comprise durable, external, weatherproof metal housings that meet the IP54 standard and can easily be mounted on concrete foundations. Designed for global use, the Protect PV outdoor systems fulfill all requirements in compliance with relevant national standards and guidelines.

Applications: PV power plants in harsh environments.

Platform: The Protect PV.880 design can be integrated in the turnkey container solution TKS-C 1600, enabling a total nominal AC output of 1600 kVA and connecting to a DC generation capacity of up to 2600 kWp.

Availability: Currently available.

Belectric

Belectric's 3.0 'MegaWattBlock' PV plant offers high grid stability

Product Outline: Belectric's new 3.0 MegaWattBlock is claimed to set new standards in solar power production. The power plant unit is designed to create electricity at the lowest possible levelized costs of electricity (LCOE). On a par with the functionality of large conventional power plants, the grid-stabilizing plant technology is designed to intelligently integrate renewable energy sources in existing power grids.

Problem: Regional public grids show many voltage deviations produced by different power loads. The dynamic reactive power control of the Power Conditioning Unit (PCU) stabilizes the public grid voltage - day and night and without solar irradiation. The PCU with its medium-voltage grid supply in outdoor construction enables optimum accessibility and easy maintenance of the system.

Solution: The 3.0 MegaWattBlock uses a maximum voltage of 1,500 Volt. Developed in co-operation with GE and PADCON, the 1,500 V inverter system reduces system and maintenance costs. A material-saving design is also built with the highest levels of quality and provides superior surface area efficiency, according to the company. The turnkey system uses an efficient, grid-stabilizing PCU with General Electric inverter technology, providing a claimed performance ratio of up to 85%.

Applications: Grid-tied PV power plants.

Platform: The specially developed PCU includes an intelligent power plant controlling system, the inverter system and the transformer. The inverter system was optimized for the use of thin-film module technologies and is characterized by the high level of system efficiency.

Availability: July 2013 onwards.

SMA

SMA's 'Compact MV Power Platform' reduces system costs and installation times

Product Outline: SMA Solar has introduced an improved, re-engineered version of its Medium-Voltage Power Platform. The new Compact MV Power Platform is an integrated, comprehensive power conversion solution for utility-scale PV plants in the North American market. It maximizes energy production while minimizing risk to EPCs, utilities and investors.

Problem: The current utility-scale solar market is showing increased demand for a more reliable, ready-to-use solution that will make investments worthwhile.

Solution: The Compact MV Power Platform is pre-engineered for simplified, faster installation and is designed for performance with a reduced levelized cost of energy due to simplified installation and superior energy production. Engineered for use with the Sunny Central CP-US, this NEC 2011-compliant solution is also fully NRTL listed, an industry first. Equipped with extensive grid management functions, it offers class-leading system efficiencies of more than 97.5% and provides an additional 10% power output at temperatures up to 25 C.

Applications: Available in 1.0MW to 1.8MW models, for utility-scale PV power plants.

Platform: The system-oriented design of the Compact MV Power Platform includes integrated AC Disconnects and optional DC Disconnect units. Its user-friendly customer interface and easy data monitoring enhance the simplified design.

Availability: Currently available in the US market.

Product Reviews

S:FLEX

S:FLEX designs flexible lightweight mounting system for flat rooftops

Product Outline: S:FLEX has introduced a lightweight, low ballast, client-customized, flat roof PV Solar mounting system, 'LEICHTmount.' Its lightweight, material-optimized design made of aluminum and stainless steel is suitable for all flat roofs and is custom-manufactured for each project.

Problem: Flat roofs with their different composites, skins, weight and wind loads, provide a variety of demands on PV mounting systems, which can limit choice of panel orientation and therefore yield potential.

Solution: LEICHTmount's variable row spacing and tilt angles between 0° and 35°, extendable base rails and individually customized projects with pre-assembled parts, guarantee a simple installation. In addition, it's adjustable to conform to unforeseen changes or obstructions on the roof. It provides absolute stability and uses precisely calculated, strong and even weight distribution. All standard 60 or 72 cell framed PV modules can be set in portrait or landscape and clamps are placed strictly according to the module manufacturer's specifications, so the risk of micro cracks is minimized.

Applications: Mounting system for flat roofed buildings providing flexible panel orientation.

Platform: In cooperation with one of the largest independent aluminum extruders, LEICHTmount was developed by a network of experienced engineers from Germany and NABCEP-certified PV installers in North America. RWDI wind tunnel tested and approved, it was engineered to meet all wind and snow load requirements even in earthquake and hurricane prone regions.

Availability: July 2013 onwards.

Fronius

Fronius PV string monitoring system provides yield loss protection

Product Outline: Fronius has introduced the String Control 250/30 string monitoring system, which ensures that photovoltaic systems with central inverters generate a dependable yield. Module strings can now be professionally monitored and their data compared. This early fault detection feature prevents loss of yield.

Problem: If a problem such as shading, module failure or broken or chafed cabling occurs in one or more strings, the relevant monitoring system informs the operator immediately. Loss of yield is thus prevented.

Solution: The Fronius String Control 250/30 DCD DF has been specifically developed to meet the requirements of central inverters. With a current carrying capacity of 250A and maximum input voltage of 1,000V, the Fronius string monitoring device is designed for the monitoring of photovoltaic systems that use Fronius Agilo inverters. Up to 30 module strings can all be connected together on one DC main line. With a separate DC power supply available as an option, the control system is also ideal for distances of more than 100m between the solar modules and the monitoring system.

Applications: Monitoring of photovoltaic systems that use Fronius Agilo inverters.

Platform: The integrated string fuses provide complete protection for the entire module array. The externally accessible DC disconnector ensures safe isolation of the PV generator from the inverter, enabling maintenance work. The monitoring system also has enough space for a DIN-rail mounted overvoltage protection module to be installed. An optional base for outdoor installations provides a stable and secure structure for all types of ground.

Availability: Currently available.

Scorpius Trackers

Scorpius Trackers Vader-xFP tracking system uses frictionless technology and no bearings

Product Outline: Scorpius Trackers claims to be the first company to have pioneered a frictionless pivot system that does not require bearings for free movement in solar tracking systems. The Vader-xFP tracking system is claimed to have zero wear and tear of mechanical parts.

Problem: The primary benefit of a tracking system is to allow the movement of PV modules in tandem with sun, thereby maximizing yield. However, limiting maintenance and yield loss is crucial for the lowest LCOE. Eliminating bearings in tracker systems could reduce costs and provide improved system performance over the lifetime of the system.

Solution: The Vader-xFP uses a 'no bearings, maintenance free, frictionless pivot' technology. The company claims there is no requirement of lubrication for life of the plant (>30 years) and that the system is completely immune to dust. Minimum power consumption of frictionless mechanism is claimed to be less than 0.1% of the generated power consumed for tracking a >1MW plant. The system also employs a backtracking algorithm that tries to minimize shading and maximize the angle between the panels.

Applications: Tracking system for utility-scale PV power plants.

Platform: Less force is required to move a tracker - which means that no external power source is required to move the panels, up to 150 KW can be moved using a 7Kg force. Typically, in 1 MW, 800-1000 of the xFPs will be required, accompanied by a lifetime replacement guarantee.

Availability: Currently available.

Product Reviews

IBM

IBM offers big data analytics and weather modelling to tackle intermittence issues of renewables

Product Outline: IBM has introduced an advanced power and weather modelling technology that will help utilities increase the reliability of renewable energy resources. The solution combines weather prediction and analytics to accurately forecast the availability solar PV energy.

Problem: Energy utilities around the world are employing a host of strategies to integrate new renewable energy resources into their operating systems in order to reach a baseline goal of a 25% renewable energy mix globally by 2025. Applying analytics and harnessing big data will allow utilities to tackle the intermittent nature of renewable energy and forecast power production from solar and wind.

Solution: The Hybrid Renewable Energy Forecaster (HyRef) represents advancements in weather modeling technology, stemming from innovations such as 'Deep Thunder.' Developed by IBM, Deep Thunder provides high-resolution, micro-forecasts for weather in a region - ranging from a metropolitan area up to an entire state - with calculations as fine as every square kilometer. When coupled with business data, it can help businesses and governments tailor services, change routes and deploy equipment-to minimize the effects of major weather events by reducing costs, improving service and even saving lives.

Applications: Utility-scale PV power plants.

Platform: The solution combines weather prediction and analytics to accurately forecast the availability of wind power and solar energy. This will enable utilities to integrate more renewable energy into the power grid, helping to reduce carbon emissions while significantly improving clean energy output for consumers and businesses.

Availability: Currently available.

SolarMax

The SolarMax 360 TS-SV central inverter provides PV plant flexibility and yield optimization

Product Outline: The SolarMax 360 TS-SV central inverter from Sputnik Engineering and the TS-SV Compact Station, with a rated output power of 720kW, are designed as a cost effective solution for large PV power plants. The 360TS-SV has a European efficiency of 97.4%.

Problem: : Central inverters with higher rated output power mean that PV plant designers and operators can employ fewer inverter stations resulting in reduced overall costs.

Solution: The SolarMax 360 TS-SV central inverter comes with an increased minimum input voltage and greater output voltage, enabling a rated output power which is 30kW higher than that of the 330TS-SV inverter. Two 360TS-SVs can be installed easily, in a time and cost effective manner, on site using the new TS-SV Compact Station whose weight is significantly lower than that of a conventional concrete station. In this specification a 720TS-SV Compact Station provides a rated output power of 720kW. However, the station is also available as 660TS-SV Compact Station with two 330TS-SV inverters and a rated output power of 660kW. Through the modular design of the TS-SV series, it is possible to control and monitor up to four inverters or 1.44MW via a control and operating unit (master control unit).

Applications: Utility-scale PV power plants.

Platform: The TS-SV Compact Station has a compact housing and is provided to the plant manufacturer as a turnkey solution. With a total weight of less than three tons, the TS-SV Compact Station is easy to install and transport.

Availability: Currently available.

Byson Electronics

Byson Electronics offers PV cable approved to TUV 1,500V/UL 2,000V

Product Outline: Byson Electronics announced its latest cable design has gained approval by TUV Rheinland – certified to 1,500V DC. This new TUV rating approval when combined with the existing UL 2,000V approval enables Byson Electronics to offer the world's first TUV 1,500V DC/UL 2,000V dual certified PV solar cable.

Problem: No dual approved TUV 1,500V/UL 2,000V PV solar cable was available to PV component manufacturers and EPC (engineering, procurement, and construction) firms around the world for installation, cable assemblies and interconnections.

Solution: Solution: Byson Electronics designed a cable construction which is fully tested and certified to TUV 1500V DC / UL2000V and incorporates a two layer electron beamed cross-linked halogen free compound with optimized copper conductor structures producing improved flexibility for easier installation; ammonia and ozone resistance: electrical and mechanical performance over a wide temperature range; and is compatible with all major PV connectors.

Applications: Large-scale utility and commercial PV installations

Platform: Byson Electronics also offers both standard and reduced diameter solar PV cables 600V & 1000V fully approved to UL & TUV or Dual.

Availability: Currently available.

Fab & Facilities

Materials

Cell Processing

Thin Film

PV Modules

Power Generation

Market Watch

The triple play: Achieving commercial benefits of PV and energy storage

John Merritt, Ideal Power, Spicewood, Texas, USA

ABSTRACT

Beyond lowering energy costs and demand charges, Superstorm Sandy demonstrated the frailty of centralized power generation. Building owners/operators throughout the Northeast in the USA are evaluating distributed power generation options for supporting building-critical loads during future grid outages. Those options (many of which also incorporate commercial-scale grid storage solutions) include on-site diesel generators, micro-turbines, fuel cells and solar PV systems. As electrical vehicle (EV) charging is added to the mix, the grid requirements and demand costs will further increase. This article will discuss specific value streams for integrating energy storage with PV for commercial buildings, and technologies – specifically, advanced power converters – that will enable those benefits to be achieved.

Introduction

Commercial buildings consume approximately 40% of the electrical energy produced in the USA, but the utility cost to building owners/operators is disproportionately high owing to punitive peak demand charges (kW) and peak demand rates (kWh). These charges and rates are rising, and the trend is unlikely to reverse in the near term because of the USA's ageing energy infrastructure and ever-growing energy appetite in the commercial and industrial sectors.

The peak demand charge is normally calculated as the highest peak demand during the monthly billing cycle, based on a 15-minute sample interval. Although the average commercial retail rate in the USA is \$0.10/kWh, the marginal cost of energy during these peak periods can be \$1.00/kWh or more, making demand reduction an attractive opportunity for saving costs. A commercial customer may have 30%, 40% or more of their monthly utility bill structures as peak demand charges.

"The first and most cost-effective strategy for reducing commercial energy costs begins with addressing energy efficiency *and* demand management."

The first step: reduce, measure and schedule loads

Before a commercial building adds solar and storage capabilities, the first and most cost-effective strategy for reducing commercial energy costs begins with addressing energy efficiency *and* demand management. Lighting as well as heating, ventilation and air conditioning (aka HVAC) upgrades are obvious choices, followed by the scheduling of heavy intermittent loads, such as large industrial motors and chillers when appropriate. Beyond such physical upgrades, energy management tools should be deployed for tracking and monitoring energy consumption in real time. Such tools are available from a number of companies, and are a critical component in the demand-reduction equation. Note that utilities often contract with large industrial and commercial customers in order to curtail load during peak demands: the compensation received generally justifies the cost of the management tools noted above.

The second step: deploy on-site energy generation

The remainder of this article will concentrate on the utilization of on-site generation resources, focusing specifically on the integration of PV and energy storage, and the related power conversion and management technologies required for delivering the highest value solution for demand reduction, and other high-value services.

Demand reduction

Adding on-site PV generation to a commercial building reduces utility energy (kWh) charges, but can have minimal effect on peak demand (kW) charges. Here is why: in the USA, summer peak demand occurs during the late afternoon, just when PV generation is declining rapidly. Commercial customers with large rooftop PV arrays will dramatically offset peak energy use (kWh), but may achieve no reduction in peak power (kW) demand. Adding storage to the PV array significantly improves this situation (Fig. 1).

Other value streams

While integrated PV and storage solutions can significantly reduce both energy (kWh) and peak demand (kW) utility charges, they may also bring

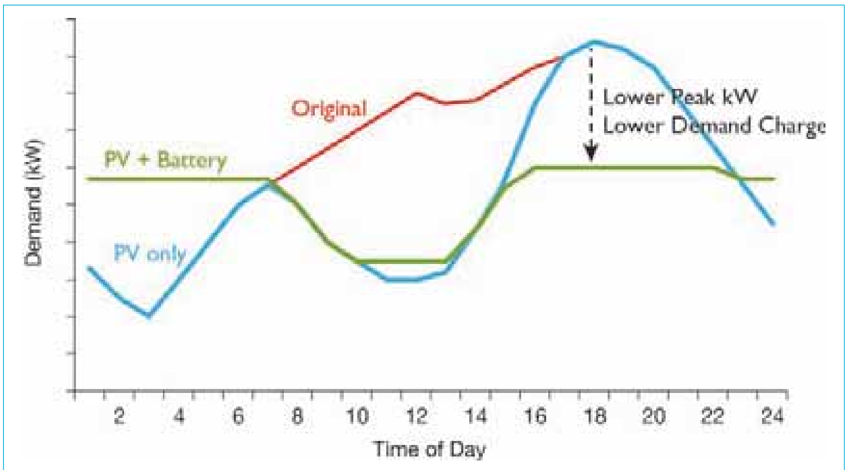

Figure 1. PV with storage delivers lower energy (kWh) and lower demand (kW) costs.

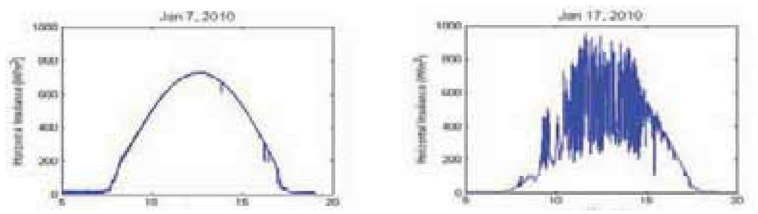

Figure 2. Impact of variable irradiance on power production.

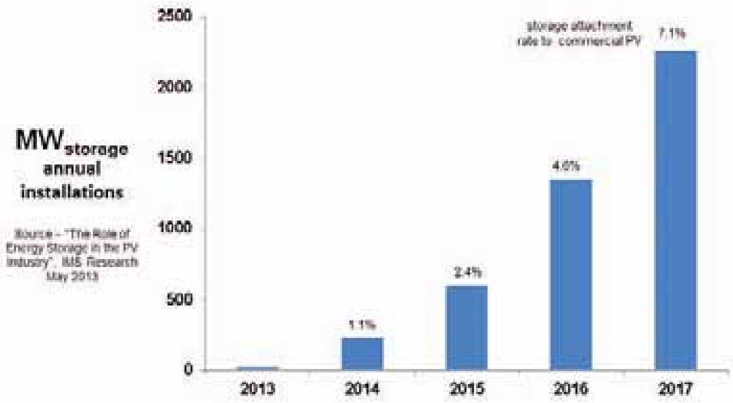

Source: IHS

Figure 3. Commercial storage with PV option.

additional value streams. One such stream is providing ancillary services support, including frequency regulation and reserve requirements, back to the utility operator. These create additional high-value revenue streams for the system owner/operator, which may be the building owner or a separate entity that finances the system and shares these benefits with the building owner.

During periods of highly variable irradiance, such PV with storage systems should also support a PV smoothing algorithm. Highly variable irradiance is the result of moving cloud cover, and the rapid swings in power output in PV arrays can disrupt grid quality, specifically in areas of high PV penetration. Irradiance and PV output power are highly correlated: as seen in Fig. 2, array power can drop more than 50% within seconds of a fast-moving/variable cloud event.

Although utilities have not yet monetized the value of smoothing, several national labs have modelled its impact, and generally agree that it facilitates deeper levels of PV penetration, while also improving grid quality relative to PV systems without integrated storage.

Last, but not least, these systems will eventually evolve to support building-critical loads during grid outages – a capability that today's PV inverters cannot support because of UL1741 anti-islanding requirements.

Triple-play systems

The value streams of integrated PV and storage solutions include:

- Managing and mitigating peak demand in order to reduce operating costs.
- Delivering high-value support services back to the grid operator to improve grid power quality and availability.
- Providing emergency backup of critical loads during grid outages.

This triple play of value streams improves return on investment (ROI), and facilitates cost-effective commercial-scale grid storage solutions.

Two major technical impediments have limited the practical deployment of these systems until very recently: 1) the high cost of batteries has limited the size and cost-effectiveness of the system; 2) the power conversion and power management systems have been costly and inflexible. These systems are – at best – described as single-function devices incapable of efficiently interleaving the AC and DC power flows in an integrated PV/storage system. Moreover, the power conversion equipment dedicated to critical-load support was bulky, heavy and expensive. As discussed below, these impediments are diminishing because of several factors.

> "It is now economically attractive to deploy integrated PV and commercial energy storage solutions for demand reduction alone."

The California opportunity

Continuing price reductions and efficiency improvements in battery systems mean that it is now economically attractive to deploy integrated PV and commercial energy storage solutions for demand reduction alone. As one might expect, the initial markets for these systems are areas where peak demand rates and demand charges for commercial buildings are significant.

In addition, a recently enacted Self-Generation Incentive Program (SGIP) in the State of California rebates up to 40% of the installed cost of battery storage systems. This incentive should accelerate market demand for commercial storage over the next few years. It is also likely that the SGIP will lead to similar incentive programmes in other states.

In California and New York, demand charges may exceed 30 to 40% of the monthly bill of commercial customers. Moreover, without local storage to 'buffer' the grid during EV charging, fast-charging providers could possibly have peak demand (kW) costs exceeding 70% of their monthly electric bill. The possibility of such a high instantaneous power requirement is frightening retailers and utilities alike.

Beyond California: lower costs and increased functionality open new markets

Grid storage battery costs, and projects integrating them, are forecast to drop appreciably over the next few years. This is fuelled in part by the cost reduction of batteries used in EVs, including plug-in hybrid electric and fully electric vehicles. There are additional opportunities to integrate used EV battery packs into storage applications. These 'second life' packs are those that would no longer meet vehicle power requirements (rapid discharge rates upon acceleration), but whose energy capabilities are more than adequate to support commercial storage applications as described above.

A study released in May 2013 by IHS/IMS Research [1] forecasts that an increasing percentage of commercial PV installations will also include grid storage (Fig. 3). This global market will begin in North America, and most likely in high peak demand charge utility jurisdictions such as California and New York. However, over the next few years as costs further decline, these same systems are expected to cost-effectively deliver a broader set of ancillary services as well as critical-load support, fulfilling a 'triple play' of value streams. Key to this enhanced functionality are flexible next-generation power conversion platforms.

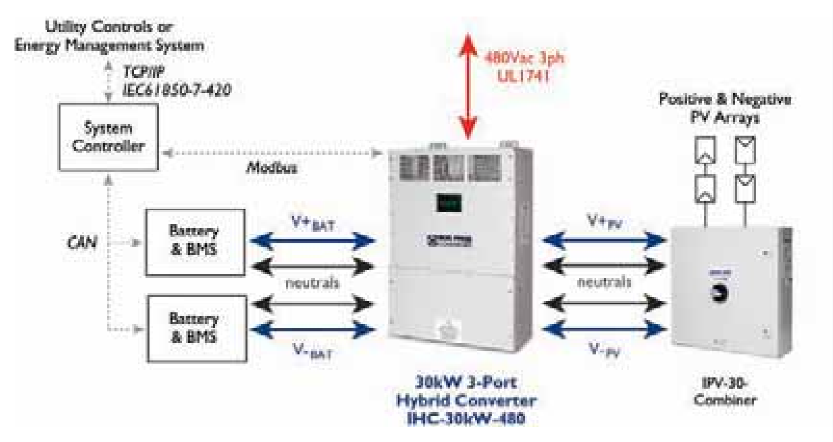

Figure 4. IHC-30kW-480 three-port hybrid converter.

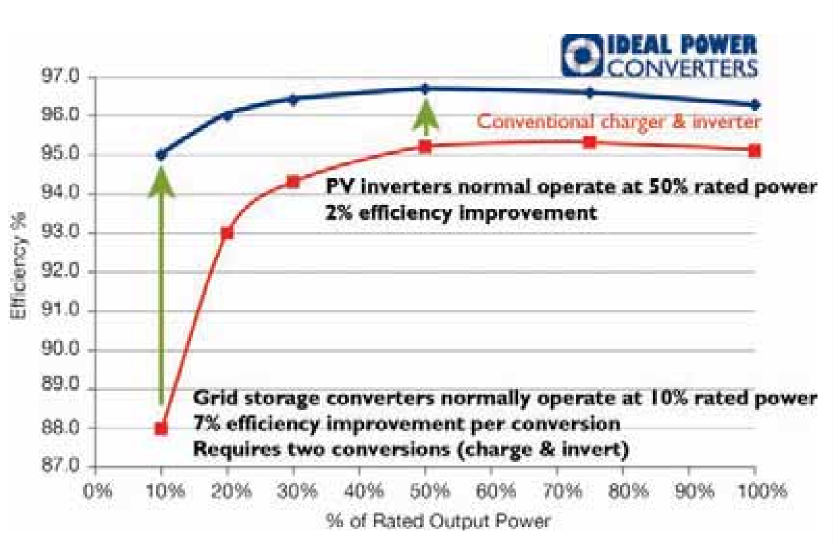

Figure 5. Efficiency of the hybrid converter.

Hybrid converters

Ideal Power's 30kW three-port hybrid converter is one example of new technologies being developed to combine the functionality of a PV inverter and battery converter together in a single hardware platform (Fig. 4). Equipped with two independent DC ports and an independent AC port, transferring power between any of the three ports, including interleaving power in real time, provides an efficient alternative to traditional AC grid-tied or DC bus-tied hybrid converters. There are considerable size and weight advantages relative to other solutions which typically require an external isolation transformer.

The size and weight advantages are principally derived from a novel and patented bidirectional and indirect power-switching topology, which ensures complete isolation between all power ports. Perhaps more importantly, this architecture is totally software driven, providing a significant degree of flexibility with regard to delivering new features and capabilities without changing or upgrading system hardware. This allows functionality to rapidly evolve and grow over time in response to changing applications and market needs.

"Conversion efficiency is more important in the hybrid scenario than with stand-alone PV applications."

Hybrid converter efficiency

Conversion efficiency (Fig. 5) is more important in the hybrid scenario than with stand-alone PV applications because multiple power conversion scenarios are required: summing PV and battery to the AC grid output, 'splitting' the PV output between battery and grid, charging the batteries from the AC grid, smoothing highly variable PV, and so forth. Conversion efficiency is particularly important at low power levels. PV inverters typically operate at 50–75% of rated power for five or six hours per day, whereas battery storage systems may operate at about 10% of rated power for 12+ hours per day. As a result, the 10% level is a very important system efficiency specification.

Hybrid converters will need to be highly efficient at all conversion tasks: interleaving, or splitting the power sources, and smoothing, as well as charging/discharging the storage array at low power levels. To fulfil broader market need, they should also be compatible with virtually all battery types, including lead-acid, lithium-ion, zinc-air and others.

Hybrid converter power ports

With their wide DC voltage operating range, and battery interface options, battery stacks may be connected as a bipolar array, enabling the support of 1000VDC stacks (±500VDC) in the Ideal Power hybrid converter. Unipolar and floating arrays should also be supported; however, there may be limits to maximum stack voltage in some applications.

When supporting batteries, the DC interface operates in current source mode, and multiple hybrid converters may be paralleled on the DC side to support charge/discharge power levels of greater than 30kW. This feature is specifically useful for larger commercial storage systems, and emerging applications such as EV fast charging, where fast-charge rates of 30kW, 60kW, 90kW and higher are required.

Ideal Power's hybrid converter features a 480VAC, three-phase AC grid inter-tie interface. Building larger systems is easily achieved by paralleling 'n' AC interfaces in a three-phase power panel, supporting designs of 120kW or larger, depending on application requirements.

Hybrid converter configuration, control and monitoring

Control and monitoring of power flow between PV, batteries and the grid is of critical importance. Ideal Power uses the SunSpec Alliance standard, an open standard developed for PV inverters, AC meters, combiner boxes, and other smart devices found in commercial and utility-scale PV arrays. The physical implementation of the Modbus port is RS-485, allowing multiple converters to be controlled on a single 'daisy-chained' communications cable.

Extending the SunSpec Alliance approach into energy storage will ensure that interfaces are open and familiar to a large community of embedded system design engineers, simplifying the development of external control algorithms and software. For our part, this interface is common between all Ideal Power products, further reducing the coding learning curve, which accelerates system design.

Hybrid converter roadmap

Future derivative versions of the hybrid converter are envisioned, including micro-grid compatibility, which can be utilized for supporting building-critical loads, and AC/AC/DC port models to support grid inter-tie of asynchronous distributed AC generators, including wind, diesel, natural gas combined heat and power (CHP) and other sources. The technology is also expected to eventually scale to larger power systems.

> "Systems that integrate PV with battery storage are becoming increasingly attractive to commercial building owners/operators."

Conclusion

Systems that integrate PV with battery storage are becoming increasingly attractive to commercial building owners/operators for a number of reasons. The advantages of reducing peak demand charges with PV-charged battery systems already bring significant value for commercial buildings that struggle with electric utility bills even after installation of a PV system. PV and battery systems also carry the potential for additional value streams, such as ancillary services to utilities and emergency backup for critical load during power outages. With increasing sales of EVs, integrated systems present an additional opportunity for providers of DC fast chargers to avoid exorbitantly high demand charges associated with the high spikes in demand from the EV charging points. As the price declines and battery efficiency continues to increase, advanced power converters that are able to efficiently convert power between the PV array, battery packs and the AC grid will play a central role in enabling these benefits.

Reference

IHS/IMS Research 2013, "The role of energy storage in the PV industry" [http://www.imsresearch.com/report/the_role_of_energy_storage_in_the_pv_industry_world_2013_edition&cat_id=198&type=LatestResearch].

About the Author

John Merritt has over 30 years of technical marketing experience spanning product marketing, product development, engineering, and project management in both high-tech and clean-tech companies. As Director of Applications Engineering at Ideal Power, John is responsible for pre- and post-sales technical support, including system engineering, design review and application fit, and product feedback.

Photovoltaics International

Advertisers & Web Index

To advertise within Photovoltaics International, please contact the sales department: Tel +44 (0) 20 7871 0122

Lack of Yingli Green's CapEx reveals scale of asset-lite fab operations

At the end of August 2013 the world's largest global solar PV module supplier, Yingli Green Energy, reported its second quarter earnings results and guided on expectations for the second half of 2013 and 2014.

The data mostly confirmed Yingli Green's clear status as the number one module supplier in the PV industry today. Just to get this into perspective, here are some stats from the latest NPD Solarbuzz Module Tracker Quarter report, based on Yingli's new updates:

- Yingli has shipped the most PV panels per quarter, every quarter, for the past six quarters going back to Q1 2012.
- During each of the past three quarters (Q4 2012, Q1 2013 and Q2 2013), Yingli has set a world record for quarterly shipments for a PV module supplier.
- Yingli has shipped almost 1GW more than any other PV module supplier in the trailing twelve months to end Q2 2013.
- Yingli's market share has reached 10% and is trending upwards

Records aside however, embedded in the results were some alarm bells. Not for Yingli but for companies that had been hoping to hear the words 'new CapEx', 'capacity expansion', 'new process flows', 'high efficiency upgrading', etc.

The news on CapEx is really bad if you have Yingli as a key customer. During the entire six-month period of the second half of 2013, CapEx (for a company with >2GW vertical integration) is only US$40 million. That's as close as you can get to maintenance-only.

But the more troubling news for PV equipment suppliers is that Yingli has now stated it can ship 4GW of modules in 2014 without having to add any new capacity.

Confused?

Well, first off, this fully contradicts some of the strange press releases and new stories in the past two weeks that claimed new PV capacity additions from the leading makers were imminent, and we should be expecting to see all the leading players adding lots of capacity in 2014.

And – it also squashes the odd claims that an equipment spending rebound is only a few months away and might get driven out of the Middle East or Latin America.

Neither of the above claims had any strong basis or analysis to support, but each got picked up on – maybe this is because people are still desperate for any positive news on new-capacity and new equipment spending.

The true explanation is that the PV industry is dominated by Chinese module suppliers today – more so than in the past. Chinese c-Si manufacturers have consistently operated in a part-fabless or asset-lite manner. Lately, leading Japanese module suppliers have adopted this approach also. During 2012 and 2013, the leading Chinese module suppliers have been able to increase the levels to which in-house and third-party capacity is adjusted to prevent inventory levels building up.

With more module share coming from China now, and as many Western competitors leave the industry or lose further market-share, the use of asset-lite operations is having a more profound impact on any company waiting for new capacity to be added.

Yingli Green is aiming for 4GW shipments with no CapEx

Other factors allowing Yingli to guide 4GW shipments with no-CapEx include:

- There is a 12GW virtual fab in China from tier 2 and tier 3 manufacturers with me-too capacity and limited access to overseas markets.
- The US demands non-China cells in modules.
- The leading suppliers are still posting negative operating margins. Saving costs everywhere is essential. CapEx can be avoided by using third-party capacity.
- Market-share gains (with overseas sales/marketing cost) outweighs adding new capacity.
- There is multi-gigawatt idled capacity at Suntech, LDK and elsewhere in China that could still be acquired at very low cost.

This all points to the equipment spending downturn lasting well into 2014, and perhaps the next meaningful new capacity is not going to arrive until 2015. Unless – of course – technology can rescue the industry and force every module supplier to perform significant line upgrades/process-flow changes in order to remain competitive. But without any technology roadmap being followed, this is highly unlikely to happen within the next 18 months.

This is a revised version of a blog that originally appeared on PV-Tech.org.

Finlay Colville is vice president of NPD Solarbuzz.

SOLAR ENERGY UK

REGISTER NOW FREE TO ATTEND!

The NEC, Birmingham, UK

8 – 10 OCTOBER 2013

THE UK'S LARGEST B2B EVENT FOR THE SOLAR INDUSTRY

DISCOVER:

- Live demonstrations and talks at our FREE-to-attend Practival PV feature area (sponsored by BayWa r.e.)
- 160+ exhibitors covering everything from PV and solar thermal systems, to whole building energy solutions, complimentary renewables, energy storage, heat pumps, smart grids, metering, cabling, anti-theft devices, training and lots more!

LEARN:

70+ expert speakers giving you valuable advice to help you grow your business:

Selling solar and gaining the competitive edge (free seminar)

- On message - dispelling myths and misconceptions of solar
- PV modules: From income generator to carbon saver – a new way of selling solar
- Diversifying your business – Up-skilling and integrating new technologies from heat pumps to biomass

Price-yield optimisation of the PV system (free seminar)

- Thinking ahead - component selection and balance of systems to maximise your ROI
- Rooftop PV performance update - design solutions, shading and efficiency
- Supply chain guarantees, warranties and contractual security

NETWORK:

Solar Power Portal Awards Gala Dinner (sponsored by Natural Sparx powered by Rexel Energy Solutions)
Celebrate and recognise best practice within the solar industry at an evening of dinner, drinks, live entertainment and celebration on 8 October, Hilton NEC. Hosted by Robert Llewellyn (Kryten, Red Dwarf), the Solar Power Portal Awards Gala Dinner will recognise the best in the UK solar industry.

Buy your award tickets today:
http://sppawards.solarenergyevents.com/awards-ceremony

UK.SOLARENERGYEVENTS.COM/REGISTER2013   **@_SolarEnergy**

Sponsors:

Antaris Solar, BayWa r.e. renewable energy, enphase energy, LDA Design, Omnik New Energy, vikram solar, Belectric, ET Towards Excellence, Natural Sparx, LG Life's Good, Schneider Electric